Structural Glaciological Evolution of Rapidly Receding Temperate Piedmont Glaciers: Implications for Debris Entrainment and Landform Development at Svínafellsjökull, Southeast Iceland.

AILSA GUILD

Structural Glaciological Evolution of Rapidly Receding Temperate Piedmont Glaciers: Implications for Debris Entrainment and Landform Development at Svínafellsjökull, Southeast Iceland.

Ailsa Guild

Department of Geography

Durham University

A thesis submitted in partial fulfilment of the requirements for the University of Durham for the degree of Doctor of Philosophy

2023

Structural Glaciological Evolution of Rapidly Receding Temperate Piedmont Glaciers: Implications for Debris Entrainment and Landform Development at Svínafellsjökull, Southeast Iceland.

Ailsa Guild

Abstract

Glacier recession in Iceland since the historical Little Ice Age maximum has brought about significant changes in the structure of all glacier snouts, particularly those of the south coast, because of their morphological switch from piedmont lobes to topographically constrained outlets. An exemplar is Svínafellsjökull, because its margin remained relatively stable between c. 1970 and 2000, when overall historical recession was dominated by downwasting. Since that time, it has undergone accelerated recession and pronounced thinning over an overdeepening. Recent research on ice cap piedmont lobes has highlighted variations on ice flow patterns related to the interaction between topographic controls and glacier structure as the glaciers respond to climate change and become more susceptible to recession into overdeepenings. This research provides a detailed understanding of the structural glaciological evolution and the implications for debris entrainment and landform development at Svínafellsjökull, Southeast Iceland. The structure of Svínafellsjökull has been impacted in recent years by a warming climate and this has initiated accelerated retreat of the glacier and pronounced thinning over an overdeepening. A debris transport process model for Svínafellsjökull and neighbouring Falljökull is proposed and incorporates various styles of debris-rich glacial ice formation, debris transfer pathways, and their glaciological controls. Changes in the structural configuration of the lower reaches of Svínafellsjökull, especially the development of radial crevasses, have impacted upon the landform record preserved within the glacier foreland. Geomorphological mapping of the foreland is presented and facilitates the development of more robust understanding of the spatially variable influence of structural glaciological and debris transfer processes on moraine construction since the Little Ice Age maximum.

Contents

List of figures

List of tables

List of abbreviations

ELA	Equilibrium line altitude
a.s.l.	Above sea level
AD	Anno Domini
LIA	Little Ice Age
LMI	National Land Survey of Iceland
NERC ARSF	Natural Environment Research Council Airborne Research and Survey Facility
LPS	Leica Photogrammetry Suite
UAV	Unmanned Aerial Vehicle
DEM	Digital Elevation Model
DSM	Digital Surface Model
C_{40}	Percentage of clasts with C/A axial ratios ≤0·4
RA	Percentage of clasts in very angular and angular grouping
AvR	Average roundness
VA	very angular
A	Angular
SA	Subangular
SR	Subrounded
R	Rounded
WR	Well-rounded
GSD	Ground sampled distance
NWZ	North-western zone
CZ	Central Zone
SEZ	South-eastern zone
SFD	Stratified solid ice facies
SFA	Stratified ice facies
SFB	Dispersed ice facies
S	Samples on ice 1-34
SM 1-14	Sample moraines 1-14
LiDAR	Light Detection and Ranging

Declaration and statement of copyright

I confirm that no part of the material presented in this thesis has previously been submitted by me or any other person for a degree in this or any other university. In all cases, where relevant, material from the work of others has been acknowledged.

Ailsa Guild

Department of Geography

Durham University

May 2023

Acknowledgements

Sincere thanks must go to my supervisors, Professors Emrys Phillips, Dave Evans, Dave Roberts and Dr Kay Smith for their time, expertise, and guidance throughout the last 7 years. Their insightful comments, patience and encouragement have contributed greatly to this project and the enthusiasm they have maintained while reading through manuscripts has been truly invaluable. Thanks must also go to Tessa Evans for always encouraging me, inviting me to visit and supporting me throughout this experience. Dave and Tessa have made my trips to Durham feel like a second home and I would like to thank them both. Also, Emrys, whom I wouldn't be here without, and cannot thank him enough for the opportunities and support he has given me throughout these past 7 years.

My thanks must also be extended to the British Geological Survey who have supported me financially throughout my 6 years of study through their British University Funding initiative (BUFI), and to Durham University's Geography department for funding conference attendances.

I would like to also take this opportunity to mention my colleagues at Dundee University, namely, Sue Dawson, Andrew Black and Wishart Mitchell, for their endless support.

Finally, I must thank my family and friends, without whom this would not have been achievable. My mum and sister, my partner- Willie, my gran, and the rest of my family, I thank you for all your support. However, a special thanks must go to my mum, without her constant encouragement I would be lost.

Dedication

I dedicate this thesis to my late grandad- William Davidson. Without his encouragement I would not have pursued this PhD and I can only hope that I have made him proud.

1 Introduction

1.1 Rationale

The structural and internal debris patterns of glaciers and ice sheets are strongly influenced by glacier motion and thereby are critical to understanding glacier dynamics (Benn and Evans, 2010; Hooke, 2019; Cuffey and Paterson, 2010; Jennings and Hambrey, 2021). Recent work on process glaciology has contributed to a substantial increase in our knowledge of glacial motion, but many questions still remain about flow, deformation rates and structural patterns within the ice. During the first half of the 20th century, advances in theoretical glacier physics and renewed interest in glacial structures stemmed from the formulation of flow laws for ice (e.g. Nye, 1953; Glen, 1995) and the application of these laws to glaciers (Nye, 1957). Since that time there have been numerous studies of deformation within glaciers (see Hambrey and Lawson, 2000 for a review). Many of these studies link structures within the glacier to known deformation rates (e.g. Allen *et al.*, 1960; Meier, 1960). However, the application of the structural geological concepts of progressive and cumulative deformation to glaciers are relatively rare (Maltman *et al.*, 2000). Where these studies have taken place (e.g. Rutter, 1965; Hambrey, 1977; Hambrey and Milnes, 1977; Hooke and Hudleston, 1978; Lawson *et al.*, 1994; Phillips *et al.*, 2013, 2014 and 2017; Dell *et al.*, 2019 and Jennings *et al.*, 2022) they have highlighted some potentially complex relationships concerning ice deformation in relation to the development of foliation, folds, crevasses and faulting.

Recent structural glaciological research has mainly been focused on the deformation structures developed within different glacier types, including polythermal and surging glaciers (Sharp, 1988; Sharp *et al.*, 1988; Lawson *et al.*, 1994; Lawson, 1996; Bennett *et al.*, 2000; Woodward *et al.*, 2002; Roberts *et al.*, 2009), and from a wide range of settings including Arctic (Hudleston and Hooke, 1980) and alpine glaciers (Allen *et al.*, 1960; Hambrey and Milnes, 1977; Glasser *et al.*, 2003; Goodsell *et al.*, 2005; Herbst *et al.*, 2006; Appleby *et al.*, 2010). This research has not

only contributed to our understanding of the structural evolution of these glaciers but has also provided important information on the mechanisms controlling their forward motion, highlighting the importance of deformation structures in controlling englacial sediment distribution. This approach has also been applied to the understanding of the structural response to active rapid retreat of glaciers in Southern Iceland (e.g. Phillips *et al.*, 2013, 2014 and 2017; Cook *et al.*, 2010 and Dell *et al.*, 2019). However, studies of the deformation and structural response occurring within the ice during stagnation and collapse are, in contrast, relatively rare (e.g. Glasser and Scambos, 2008; De Angelis and Skvarca, 2003; Scambos *et al.*, 2004). Chapter 3 of this thesis aims to address this knowledge gap.

Patterns developed in englacial debris have been the focus of long term glaciological and glacial geomorphological research. This has focused on debris incorporation, entrainment, modification, transport and deposition, and has informed our present understanding of both structural glaciology and glacial landform development (e.g. Hooke, 1973; Hudleston, 1976; Evans, 1989 and 2009). At the scale of a whole glacier system, glacial sediments can be examined using the concept of a debris cascade (Benn and Evans, 2010; Evans and Benn, 2014), whereby material can enter a glacier either supraglacially or subglacially. Debris that accumulates on the glacier surface can be incorporated into the main body of the glacier in two main ways: (1) burial by snow and ice; or (2) falling down crevasses or other holes in the glacier surface (e.g. moulins) where it can potentially be reworked and redistributed by englacial meltwater and/or reworking due to crevasses collapse/closure and the reconstitution of ice mélange at the base of icefalls (e.g. Swift *et al.*, 2018; Goodsell *et al.*, 2005).

Since the seminal research on debris-rich basal ice and its relationship to glacier flow on the Barnes Ice Cap by Hooke (1973), Hudleston (1980) and Hooke and Hudleston (1978), research has increasingly focused on the entrainment patterns and structural controls on debris transport in high-Arctic polythermal and cold-based glaciers (see Evans, 2009 and references therein). In particular, structural analysis of glacial sediment patterns has been effectively applied to a

number of valley glaciers in Svalbard (Bennett *et al.*, 1996; Hambrey *et al.*, 1996, 1999 and 2005). These studies have highlighted the importance of foliation, folding, and thrusting in controlling debris transport and distribution within polythermal and cold based glaciers, and how these processes can impact upon proglacial landform development (Jennings *et al.*, 2013). In contrast, there are comparatively few studies of such aspects associated with temperate valley glaciers (e.g. Drewry, 1972; Spedding and Evans, 2002; Evans, 2003; Goodsell *et al.*, 2005; Swift *et al.*, 2018), and of these the focus is mostly on the formation of certain debris-related glacial features (e.g. medial moraines; Boulton, 1967; Drewry, 1972; Anderson, 2000). Few studies have examined the relationship between debris distribution and ice structures (e.g. Goodsell *et al.,* 2005; Jennings *et al.*, 2014; Jennings *et al.*, 2021).

Although the effect of subglacial and ice-marginal deformation of glacial ice on debris incorporation has been well documented (see Evans 2018 and references therein), the role played by ice structures in determining landform morphology and the distribution of glacigenic sedimentary facies has been less widely researched and less nuanced (Shaw, 1977a and 1977b; Evans, 2009; Larson *et al.*, 2006; Cook *et al.,* 2010 ; Swift *et al.*, 2018), although typical glacial landsystems are being compiled for glaciation styles in which controlled moraines (see Evans, 2009) constitute a significant element. More widely, the concepts of landsystems and process-form models in glacial geomorphology are increasingly being established and improved through the utilisation of contemporary analogues (Eyles *et al.,* 1983; Evans, 2003, 2013), where ongoing process-form relationships can be clearly demonstrated (e.g. Boulton and Eyles, 1979; Krüger, 1987; Owen and Derbyshire, 1989; Evans and Rea, 1999, 2003; Kirkbride, 2000; Evans and Twigg, 2002; Evans *et al.,* 2015, 2016, 2017a, 2017b, 2018a and 2018b, 2019; Benediktsson *et al.*, 2008; Chandler *et al.*, 2020a, 2020b). The recently observed accelerated recession of glacier snouts around the world in response to increasing global temperatures, punctuated by occasional readvances and seasonal oscillations due to increased accumulation during colder winters, has facilitated a more systematic and quantitative analysis of glacial geomorphological processes on the forelands of glaciers of varying dynamics and morphologies. The lack of understanding

concerning the relationship between ice structures and landform morphology needs to be addressed to enable a complete understanding of glacial landsystems and the processes shaping these systems. This will facilitate the development of more robust palaeoglaciological models/interpretations of the landform and sedimentary record of Quaternary glacier-climate relations.

It is currently not fully understood how glaciers are responding to climatic changes. Retreating glacier margins are often considered to behave in two ways (Benn and Evans, 2010): (i) "active retreat" where the margin oscillates on an annual cycle. As retreat due to summer melt is partially offset by forward motion, a small readvance occurs during the cold winter months (e.g. Krüger, 1995; Marren, 2002; Evans and Twigg, 2002; Bennet *et al.*, 2010; Chandler *et al.*, 2020a,b): and (ii) "passive retreat" where the glacier is no longer moving and stagnates, retreating by in situ melting or "downwasting" (e.g. Schomacker *et al.*, 2014); in southern Iceland, this has been manifested as incremental stagnation (Eyles 1979; Bennett and Evans, 2012). Annual recessional moraines occur in front of all southern Icelandic glaciers e.g. Skaftafellsjökull (Chandler *et al.*, 2016a; Evans *et al.*, 2017a, 2019), Skálafellsjökull/ Heinabergsjökull (Sharp, 1984; Evans and Orton, 2015; Chandler 2016b), east Mýrdalsjökull (Krüger, 1995; Dugmore, 1987; Evans *et al.*, 2018 a), Lambatungnajökull (Bradwell, 2004), Breiðamerkurjökull/Fjallsjökull (Price, 1970; Evans and Twigg, 2002; Evans *et al.,* 2019; Chandler *et al.*, 2020a and 2020b, 2021); Flaajökull (Dabski *et al.*, 1988; Evans *et al.*, 2018b) and Falljökull/Virkisjökull (Bradwell *et al.*, 2013; Phillips *et al.*, 2013). The magnitudes of the fluctuations recorded by actively retreating margins such as these are strongly dependent on the glacier's mass balance, which is predominantly controlled by climatic factors, such as temperature and precipitation, averaged over time (e.g. Björnsson and Pálsson, 2008; Dell, *et al.*, 2017 Evans *et al.*, 2019).

The established view on the mechanics of movement of a non-surging valley glacier is that ice flows down the valley as a single 'plug flow' with the entire glacier body moving 'en-masse' (see

Benn and Evans, 2010 for overview). However, recent research on ice cap piedmont lobes (e.g. Phillips *et al.*, 2014, 2017) has highlighted some important variations on this large-scale ice flow pattern, apparently related to the interaction between topographic controls and glacier structure as glaciers respond to climatic changes, and in Iceland in particular become more susceptible to recession into overdeepenings (cf. Bennett *et al.*, 2010; Bennett and Evans, 2012; Cook and Swift, 2012). The role of such overdeepenings and the associated process of supercooling in the development of certain types of debris entrainment and englacial debris patterns (cf. Roberts *et al.*, 2002; Tweed *et al.*, 2005; Swift *et al.*, 2006; Cook *et al.*, 2007, 2010), as well as their role in deglacial landform development (cf. Larson *et al.*, 2006; Evans 2009; Bennett and Evans, 2012) has been recognised more recently and must be incorporated in any models of spatial and temporal change in structural glaciology and landsystem development.

1.2 Research questions, aims and objectives

The aim of this thesis is to:

Investigate structural responses of temperate maritime glaciers to the recent phase of accelerated retreat due to warming climate and, further, assess the implications of such responses for debris transfer through these glaciers and landform development at their retreating margins.

To achieve this aim, the thesis has the following objectives:

Objective 1: Structural glaciological mapping using a combination of aerial photographs and satellite imagery. These datasets are used to carry out the detailed analysis of a range of structures present within the ice (e.g. fractures, faults, banding, folds) with the results being used to investigate the changes in the structural architecture of the glacier over time and to quantify the resulting changes in aspects such as fracture density, length and orientation. Examination of deformation structures is also undertaken using ITS_LIVE data to establish

surface flow regimes and the changes that occur to these regimes through a period of changing climate.

Objective 2: Examination of debris transport pathways through the glacier using field-based detailed clast shape analysis on englacial debris bands. This facilitates the analysis of variable entrainment and structural controls on the incorporation and transport of debris in active temperate glacial systems influenced by overdeepenings and hence potentially characterized by supercooling.

Objective 3: Geomorphological landform mapping of the foreland of Svínafellsjökull. This investigates the spatial and temporal impacts of an actively retreating, structurally complex piedmont lobe on the landform imprint within its foreland, specifically the changing nature of longitudinal /radial crevasse development in the snout since the end of the Little Ice Age.

1.3 Study area

Located in southeast Iceland, Svínafellsjökull is one of a number of maritime glaciers (e.g. Skaftafellsjökull, Virkisjökull, Falljökull, Kviarjökull, Fjallsjökull) draining the Öræfajökull ice cap, which is located on the southern side of the much larger Vatnajökull ice cap (Figure 1.1a and 1.1b). Svínafellsjökull is c. 10 km long and < 2 km wide and descends from its accumulation zone via a steep icefall. Below the icefall, this ENE-WSW orientated glacier is confined within a steep sided valley, formed to the north by the mountains of Eystra-Hrútsfjall, Vestara-Hrútsfjall, Sveltiskarð and Hafrafell, and to the south by Svarthamrar (Figure 1.1b). A number of major rock falls from the slopes of Svarthamrar have resulted in the southern side of Svínafellsjökull being covered by a thick layer of debris, which has locally resulted in a marked reduction in surface ablation (Hannesdóttir *et al.*, 2015a and 2015b). The equilibrium line altitude (ELA) of Svínafellsjökull in 2010 was estimated to be 1060 ± 60 m above sea level (a.s.l.) and the amount of marginal retreat between 2007 and 2011 calculated as c. 0.8 km (Hannesdóttir *et al.*, 2015a and 2015b).

Where it emerges from its valley, Svínafellsjökull spreads radially to form an irregular fronted piedmont lobe confined within a series of arcuate terminal moraines, the largest and oldest (pre-1362 AD) of these being named Stóralda (Guðmundsson, 1998; Everest *et al.*, 2017). Two proglacial ice-contact lakes are presently located immediately adjacent to the snout on the northwest and southeast sides of the glacier. The lake waters penetrate into the heavily crevassed and indented glacier snout, and hence these lakes appear to be partly supraglacial (Figure 1.1c). Aerial photography reveals that the lakes initially formed as Svínafellsjökull retreated from its 1990s readvance limit and have been compounded by the large moraine amphitheatre. The up-ice side of this moraine complex forms the adverse slope along the south-western margin of an overdeepened subglacial basin, which is considered to underlie the margin of the glacier (Cook *et al.*, 2007, 2011a and 2011b). On-ice radar data published by Magnússon *et al.* (2012) reveals the presence of an elongate overdeepening up to 200 m deep, and mostly below present sea level, incised into the bedrock underlying the margin of Svínafellsjökull. This is thought to extend up-ice as a narrow channel which directly underlies the axis of the glacier (Figure 1.1c, Figure 1.2).

The ice-contact lakes formed because the proglacial drainage became impeded by the large and complex moraine amphitheatre composed of numerous superimposed end and recessional moraines. This complex of Neoglacial and historical Little Ice Age (LIA) moraines are dissected by six, large meltwater channels, all but two of which have been abandoned due to glacier downwasting, resulting in these earlier formed drainage systems becoming isolated from their meltwater source; the main drainage route is now occupied by the Svinafellsá, which drains from the southeast lake.

Marginal fluctuations at Svínafellsjökull from the Little Ice Age and through the early 21st Century have been studied in detail (e.g. Thórarinsson, 1943; Thompson, 1988; Sigurdsson, 1998; Hannesdóttir *et al.*, 2015a, 2015b). During the LIA the terminus of Svínafellsjökull coalesced with neighbouring Skaftafellsjökull and they remained joined until 1935, when the margins of the two glaciers eventually separated (Thórarinsson, 1943; Thompson, 1988; Evans *et al.,* 2019). Since decoupling, the overall retreat of Svínafellsjökull, totalling ~500 m, has been punctuated by several phases of readvance (Thompson, 1988). These fluctuations in the position of the ice margin have resulted in a suite of large, concentric, to occasionally sawtooth, moraines preserved on the surface of the foreland (Everest *et al.*, 2017; Chapter 4 of this thesis). Renewed glacier recession has occurred since c. 2000 AD and has been accelerating since 2010, accompanying a marked rise in mean global temperatures over this period. This recession has been accompanied by pronounced thinning of the terminal zone and the formation of dense longitudinal crevasse networks that give rise to indented radial pecten at the snout (Mottram and Benn, 2009; Phillips *et al.*, 2017; Dell *et al.*, 2019).

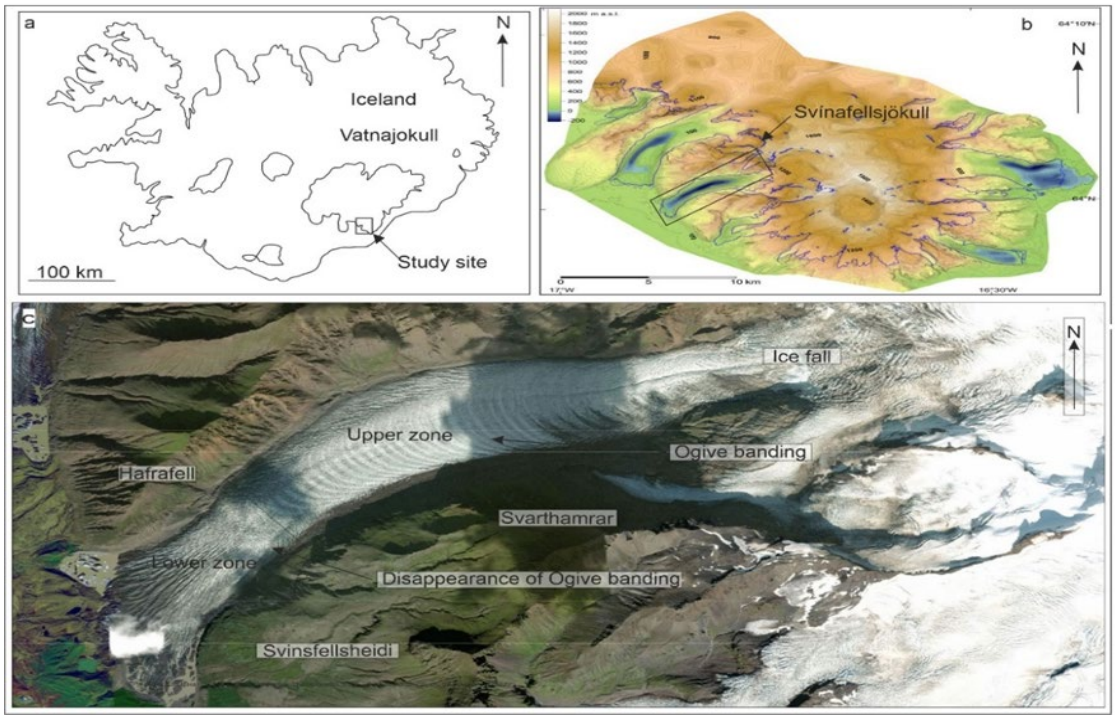

Figure 1.1: Location and characteristics of Svínafellsjökull: a) map showing the location of Svínafellsjökull, in southeast Iceland; b) Svínafellsjökull's overdeeping mapped by Magnusson et al. (2012) (outlined in the black box); c) aerial photo of Svínafellsjökull showing this east-southeast to west-southwest orientated glacier descending from its source area on Öræfajökull (map and aerial photograph sourced from Google Earth).

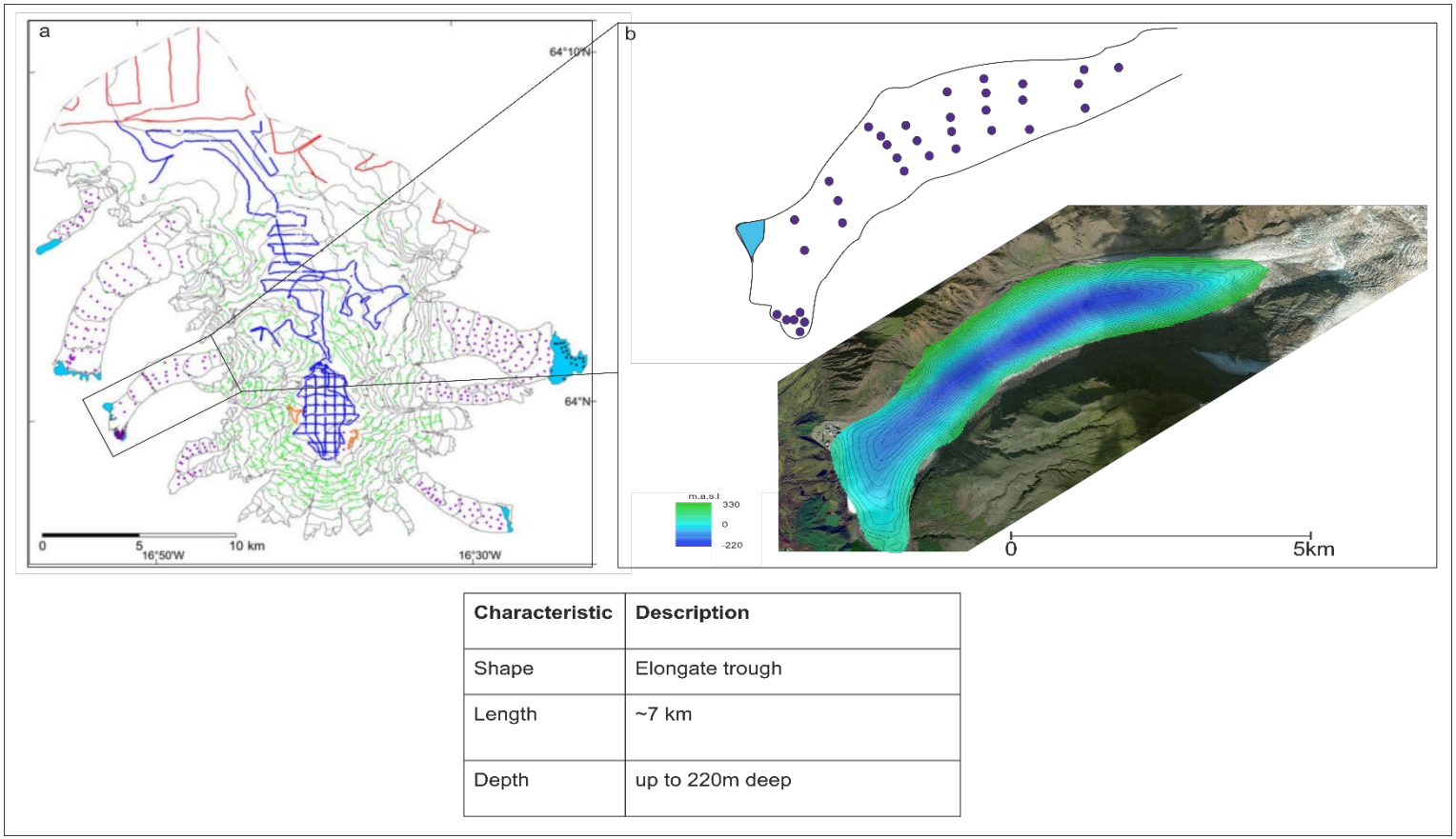

Characteristic	Description
Shape	Elongate trough
Length	~7 km
Depth	up to 220m deep

Figure 1.2 Svínafellsjökull's overdeeping mapped by Magnusson et al. (2012);a) RES lines 1991–1993 (red), 2009 (blue), 2012 (orange), RES point survey 1998–2006 (purple dots) and lake depth measurements 2006 (black dots). Green dots show points where thickness was estimated from a derived relation between thickness and surface slope (Figure 3). The figure only shows ice thickness estimates adopted in the making of the bedrock DEM (<20 m difference between the ice thickness obtained from our simple relation and the ice thickness derived by subtracting the final bedrock DEM from the LiDAR surface DEM); b) RES point survey 1998–2006 used to construct the DEM for Svínafellsjökull; table outlining key characteristics of the overdeepening.

1.4 Thesis structure

Each of the objectives listed are addressed in a series of research papers which form the basis of this thesis. Adapted versions of these papers have been/will be prepared for peer-reviewed journals. This chapter (Chapter 1) provides an overview and key aims of the research programme and now concludes with an overview of the following chapters:

Chapter 2 is entitled "Utilising a multidisciplinary approach for studying an evolving modern glacial landsystem: a case study from Southeast Iceland" and presents the techniques employed throughout this multi-disciplinary study. It also provides a critical review of the key literature related to: a) investigations of structural responses of glaciers to recent accelerated retreat into overdeepenings; and b) assessments of debris transfer and landform development implications of such glacial process-form regimes/landsystem.

Chapter 3 is entitled "The historical structural glaciology of the snout of Svínafellsjökull: Implications for ice dynamics of a piedmont lobe" and presents results of the detailed mapping of the structural glaciology of Svínafellsjökull. The results are used to investigate the glaciological changes in response to glacier retreat from a relatively unconfined piedmont lobe into a more confined valley, as well as the downwasting of the glacier snout into an overdeepening. In summary, the detailed results are used to determine the impacts on ice dynamics of a series of structural changes which occurred within the lowest part of the glacier terminus in response to retreat and thinning.

Chapter 4 is entitled "Ice structural and subglacial controls on the incorporation and transport of debris in active temperate glaciers, Svínafellsjökull and Falljökull, Southeast Iceland. This chapter provides a critical assessment of the hypothesis proposed by Swift *et al.* (2018) concerning the entrainment patterns of debris at Svínafellsjökull is undertaken using clast shape. Analysis was conducted on multiple samples consisting of 50 pebble/cobble sized clasts of a

similar lithology (massive basalt) collected from the moraines and subglacial landforms across the foreland, as well as samples collected from the surface of the glacier, where they emerged from different types of debris banding. A transport process model for Svínafellsjökull and Falljökull is developed and proposes debris-rich glacial ice formation processes, debris transport pathways, and their glaciological controls are presented.

Chapter 5 is entitled "Morphology and patterns of push moraine assemblages at Svínafellsjökull, southeast Iceland: insights into structural drivers of moraine development during glacial retreat" and investigates how the changes in the structural configuration of the lower reaches of Svínafellsjökull, especially the development of radial crevasses, have impacted upon the landform record preserved within the foreland of the glacier. Geomorphological mapping of the forefield is presented and reveals that the pre-Little Ice Age limits are arcuate in shape with the switch to a saw tooth pattern of moraine crests having occurred during the early 1990s (c.f. Everest *et al.*, 2017). This research demonstrates that the landform record within the foreland at Svínafellsjökull reflects changes in the structural architecture of the marginal zone of the glacier and has potential implications for the interpretation of the landform records preserved during deglaciation.

Chapter 6 draws together the main conclusions from each of the chapters to answer the aim of this thesis-"Investigate structural responses of temperate maritime glaciers to the recent phase of accelerated retreat due to warming climate and, further, assess the implications of such responses for debris transfer and landform development at their retreating margins". Suggestions for further work are given, along with the implications of this study.

2 Utilising a multidisciplinary approach for studying an evolving modern glacial landsystem: a case study from Southeast Iceland

2.1 Introduction

The research presented within this thesis uses a multidisciplinary approach to study the structural glaciology, debris entrainment and the history of landform development at Svínafellsjökull, Southeast Iceland from the 1950s to present day. The use of remotely sensed data, more specifically aerial photography, underpins this research.

Aerial photography has been routinely used in glaciology to map range of features at differing scales (e.g. banding, meltwater channels, fractures/crevasses, folds, banding etc.) on the surface of glaciers (e.g. Hambrey *et al.*, 2005; Goodsell *et al.*, 2005; Roberson, 2008; Roberts *et al.*, 2009; Phillips *et al.*, 2014, 2017; Dell *et al.*, 2019; Swift *et al.*, 2018; Jennings *et al.*, 2022). A seminal example of the application of aerial photography to understanding the internal structural architecture of glaciers is that of Hambrey *et al.* (1999) which investigated the structural glaciology of glaciers located along the west coast of Spitsbergen. They mapped a series of structures inferred to be longitudinal foliation and thrusts in the snout areas of Midre Lovenbreen and Finsterwalderbreen at a scale of 1:15 000 and 1:30 000, respectively, using vertical aerial photographs. The geographical (three-dimensional) orientation of these features (dip, strike and dip azimuth) was established on the ground. The resultant maps were used to examine the modes of debris entrainment and subsequent transfer in both surge and non-surge type glaciers. In another example, Goodsell *et al.* (2005) examined the structural glaciology of Haut Glacier d'Arolla using features traced from two overlapping black and white vertical aerial photographs taken from ~1000 m above the surface of the glacier. The criteria used by Goodsell *et al.* (2005) to establish the orientation, dimensions and cross-cutting relationships displayed between the structures within the Haut Glacier d'Arolla were later applied by Appleby *et al.* (2010) during their study of the Lower Fox glacier in New Zealand. Appleby *et al.* (2010) combined their mapping from aerial photographs with field data and ground penetrating radar to investigate the structural glaciology of this temperate glacier.

In contrast to using aerial photographs, Phillips *et al.* (2013) used a Digital Elevation Model to map the fractures exposed on the surface of Falljökull in southeast Iceland. This was combined with a ground penetrating radar survey, allowing a detailed model of the 3D structure of the glacier to be developed. Phillips *et al.* (2014) further developed this approach by using vertical aerial photographs, supplemented by field photographs and field survey data, to examine the same glacier and infer how a change in its structural evolution led to a marked reduction in the active length of the glacier during a phase of rapid retreat.

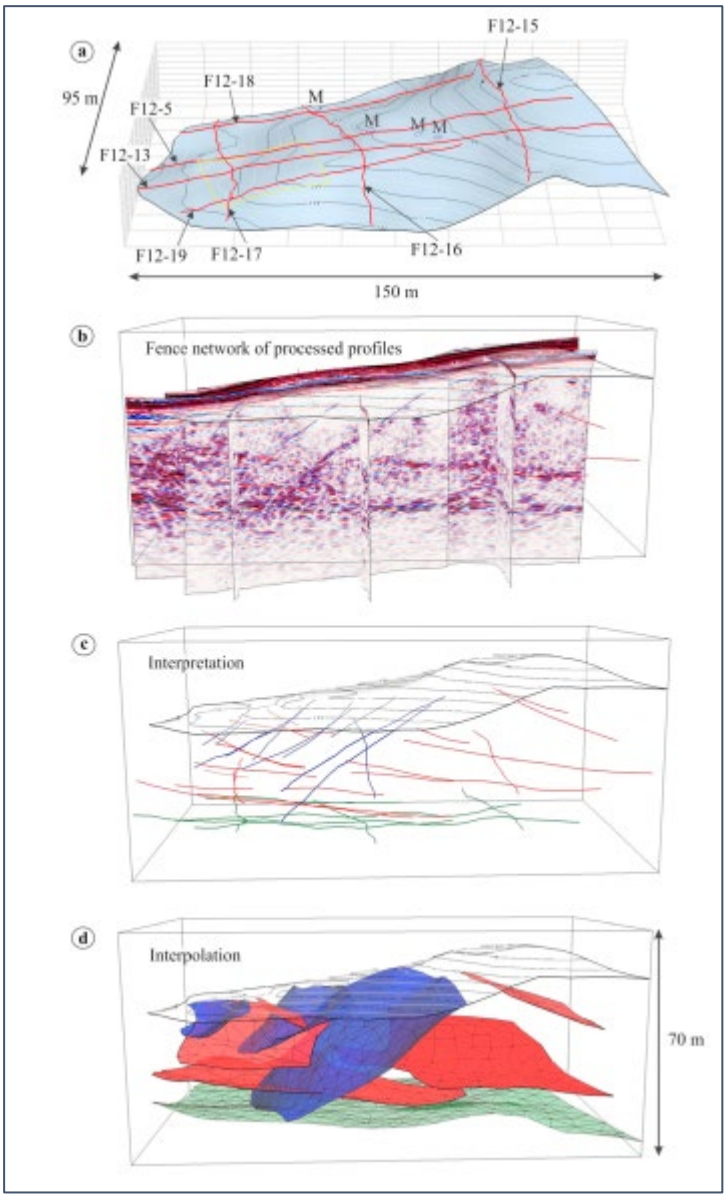

Figure 2.1 Methods used by Phillips et al. (2013) to develop a detailed model of the 3D structure of Falljökull (a) Position of GPR survey lines (red) on the clean ice margin of Falljökull. M denotes the position of the moulins; (b) Fence network of processed survey lines; (c) 3D image showing main reflectors picked from survey lines; (d) Interpolation of reflectors (combined with surface observations) to reveal interpreted internal glacier structure.

The use of remote sensing techniques for mapping the debris patterns within Icelandic glaciers has previously been undertaken, for example by Bennett *et al.* (2010) and Bennett and Evans (2012), who used digital photogrammetry alongside a digital elevation model to study glacier recession and landform development in the forefield of Kviárjökull, a debris-charged glacial landsystem characterized by an overdeepening. This approach was used to demonstrate that thick sequences of debris-charged basal ice/controlled moraine have a very low preservation potential. This approach also showed that ice-cored moraine complexes have the potential to develop into hummocky moraine belts in de-glaciated terrains. Bennett and Evans (2012) concluded that Kviárjökull is undergoing a process of incremental stagnation (sensu Eyles 1979) which involves the periodic switching from transport-dominant to ablation-dominant conditions (Kirkbride and Warren, 1999; Kirkbride 2000; Deline 2005).

Recent developments in the methods used to remotely map crevasses and debris patterns (e.g. Herzfeld and Zahner, 2001; Herzfeld *et al.*, 2004) have combined visible satellite imagery and aerial photos, including oblique aerial photos, to develop an automated algorithm for classifying crevasse fields. This geostatistical approach defined nine different types of glacier surface morphology, ranging from unstructured chaos to regularly spaced crevasses. Such an approach has utility for assessing changes in glacier dynamics through time, by analyzing historical satellite imagery to quantify changes in crevasse-related surface type. However, care must be taken using these approaches, because, although air- or water-filled crevasses are clearly visible as dark lines on the imagery, snow-filled crevasses are especially difficult to resolve against a snow-covered glacier surface (Colgan *et al.*, 2016). The research presented within this thesis has not used this approach, as there was no available satellite imagery of the same age as the aerial photographs or of a suitable resolution to carry out this type of analysis at Svínafellsjökull. Moreover, field-based observations made during this study, in combination with the use of Digital Elevation Models and aerial photography, have been used to “ground truth” any

observations from remotely sensed data, thereby eliminating some of the uncertainty inherent in maps/outputs derived from remotely sensed data alone.

2.2 Structural glaciology techniques

Recent advances in the quality and resolution of remotely sensed data, in particular aerial photography, LiDAR and satellite imagery, means that the structural architecture of glaciers can be analysed in far greater detail. The structural mapping and analysis of the pattern of the deformation structures (including fractures, faults, banding/layering) exposed on the surface of Svínafellsjökull was carried out using historical vertical aerial photographs, supplemented by field survey data acquired between May and September in 2016, 2017, 2018 and 2019. This approach has enabled the large-scale assessment of the spatial and temporal development of the structural architecture of this glacier. The approach has wide applicability to glaciers globally, as precise interpretation of glacier structures allows inferences to be made about how ice dynamics are changing over time, particularly in response to increasingly negative mass balances.

2.2.1 Structural mapping

The structural mapping and analysis of the pattern of large-scale deformation structures exposed on the surface of Svínafellsjökull (Chapter 3) was achieved using historical vertical aerial photographs, supplemented by field survey data and more detailed field-based UAV (Unmanned Aerial Vehicle) aerial photography. Digital scans of vertical analogue aerial photographs (National Land Survey of Iceland, LMI) for the years 1952, 1988 and 1992 were orthorectified using ArcGIS 10.3.1 software. For the analysis of the structures exposed in 2007 an image of the glacier taken by the UK National Environmental Research Council, Airborne Remote Sensing Facility (NERC ARSF) was orthorectified in Leica Photogrammetry Suite (LPS) and subsequently imported into ArcGIS 10.3.1. The ArcGIS 10.3.1 Esri World Image Basemap layer (Source: Esri, Maxar, Earthstar Geographics, and the GIS User Community) acquired in 2012 was used to undertake the complete structural map of the entire glacier. A clip of the Esri World Image

Basemap layer was used and projected into the same co-ordinate system (ISN, 1993 Lambert) as all other images.

The various sets of fractures and faults, as well as the banding identified on the surface of Svínafellsjökull, were digitised using ArcGIS at a scale of between 1:1000 and 1:1500, depending upon the resolution of the photographs. The orientation (strike) of individual fractures were calculated using a Python Script macro (Diaz Doce, 2014, unpublished) and the resultant dataset exported from ArcGIS and plotted on a series of rose diagrams using StereoStat by RockWorks™. Structure orientations were calculated using the Python Script by taking an average orientation of the nodes created when digitising the feature. The Python script used the georeferencing tool in ArcMap to georeferenced each node and took an average from the known georeferenced point.

Marked changes in the orientation, length and complexity of the main fracture sets exposed on the surface of the glacier were used to define a series of colour coded, structural domains (Chapter 3 Appendix 1-7) following the methodology used by Phillips *et al.* (2017) and Dell *et al.* (2019). It is understood that there is some degree of overlap at the domain boundaries, where fractures could be classified into either of the neighbouring domains. The use of domains is becoming increasingly used within structural glaciology in order to group together structures of the same characteristics (e.g. Glasser and Scambos, 2008; Glasser and Ghiglione, 2009; Phillips *et al.*, 2014, 2017; Dell *et al.*, 2019; Jennings *et al.*, 2022), thereby providing a clear visual representation of observed changes in the structure of the ice, which can then be used to investigate the nature of the deformation occurring within different parts of a glacier. The criteria used to define the domains used within this research is listed below:

Changes in:

- fracture length (changes of > 50 cm)
- fracture orientation (changes of > 90°) (using the Python Script for orientation)

- fracture morphology (open or closed, debris filled/ free fractures classified into different domains)

Each of the defined criteria is used in conjunction with one another. For example, structures may be classed into domains based on a combination of the criteria (e.g. change in length and morphology or change in orientation and length) however the factor in which the largest change occurs defines which domain it is placed within (for example- change in length of 60cm with an orientation change of 15°, would be classified in terms of fracture length change). If only one factor changes (e.g. orientation) then classification is based on this, however classifications are mostly based on a combination of factors relating to deformation styles (for example, as orientation changes more often than not fractures separate to form shorter crevasses, therefore both of these factors would be considered when classifying into domains).

This set criteria allows these structural domains to be reproduceable and allows the evolution of these domains over time. However, there is a degree of uncertainty around the boundaries of the domains and therefore the fracture orientations are crucial when classifying fractures into different domains at the boundaries. As stated, fracture orientation (strike) of individual fractures were calculated using a Python Script macro (Diaz Doce, 2014, unpublished). Due to the highly crevassed (open fractured) nature of the surface of Svínafellsjökull, field studies were restricted to the area close to the margin of the glacier. Field work undertaken between May and September 2016, 2017, 2018 and 2019 involved recording of the orientation (dip, strike, dip azimuth), sense and amount of offset (where applicable), and inter-relationships between the various sets of faults, fractures and foliations (banding) observed within the ice. The orientations of these planar structures were measured using a compass clinometer (corrected for magnetic declination of 11.5°) with the data displayed on a series of lower hemisphere stereographic projections and rose diagrams (Chapter 3, Appendix 1) using StereoStat by RockWorks®. The brittle deformation structures include both closed/tight fractures in which the walls are in contact, as well as open fractures (crevasses), allowing the structures to accommodate the

passage of meltwater and sediment. These vertical to moderately inclined fractures are the dominant structure observed within the glacier, confirming the evidence obtained during the mapping of the remotely sensed data, with these brittle deformation structures being observed penetrating up to several tens of meters into the ice. In the field, the light and dark coloured banding/layering identified on the surface of the glacier on the aerial photography is defined by the variation in the proportion of debris included in the ice (See chapter 3 for details). No obvious folding of this banding was observed in the field, confirming the apparent lack of ductile deformation structures on the aerial photography.

The detailed mapping of the structural architecture of the glacier, cross cutting 18elationnships and areas of overprinting were established and examined in detail for the years of 1952, 1988, 1992, 2007 and 2012, following the methods of Phillips *et al.* (2017). In 2007 and 2012 there was an increased structural complexity across the marginal area of the glacier, leading to an increase in the number of structural domains. These structural domains were grouped together in relation to similarities in structural complexity and orientations to form marginal zones (see Chapter 3, Appendix 1-7).

2.2.2 Fracture density mapping

Changes in fracture density within Svínafellsjökull (see Chapter 3) were calculated using a Python Script macro within ArcGIS 10.3.1™ developed specifically for this study. The merge tool within the ArcGIS toolbox was then used to combine (merge) all outputs of this script into a single shape file, enabling the construction of a fracture density map for the entire glacier (Chapter 3). Fracture densities were also calculated for each of the structural domains identified during the mapping of the structures exposed on the surface of the glacier. The resulting fracture density maps were used to distinguish areas where the ice has accommodated a relatively higher intensity of brittle deformation, with the presence of open fractures (crevasses) indicating areas where the ice is undergoing extension.

2.2.3 Ice surface elevation changes

Variations in ice surface elevation of Svínafellsjökull (see Chapter 3) have been calculated using the Arctic DEM dataset which is available from the Polar Geospatial Centre (https://www.pgc.umn.edu/) hosted by the University of Minnesota, which provides geospatial support, mapping, and GIS/remote sensing solutions to researchers working in the polar regions. The Arctic DEM data have a spatial resolution of 2 m and are downloaded as 17 km by 110 km strips (see Barr *et al.*, 2018). Once the Arctic DEM strip index, 2 m strips (DSMs) covering the area of Svínafellsjökull were downloaded, the changes in surface elevation of the glacier between 2012 and 2013 were calculated using the minus tool in the ArcGIS geoprocessing toolbox. The error associated with horizontal and vertical planes for the Arctic DEM data is 4 m. These comparisons were made for the period between 2012 and 2013 due to the restricted availability of the imagery within the Arctic DEM strip index.

2.2.4 Velocity mapping

The Inter-mission Time Series of Land Ice Velocity and Elevation (ITS_LIVE) project provides a globally comprehensive and temporally dense multi-sensor record of land ice velocity and elevation with low latency. Yearly and composite glacier velocities have been utilised, using the regional velocity mosaics feature, which are created from the synthesis of all scene-pair velocities to provide ice velocity maps for Svínafellsjökull for the years of 1986, 1992, 1995, 2012 and 2018 (see Chapter 3). Annual velocity maps are created by taking the error-weighted average of all image-pair velocity fields having a centre-date that falls within that calendar year. Netcdf files were downloaded from the web site (https://nsidc.org/apps/itslive/) and opened using ArcGIS 10.3.1. using the 'make netcdf raster' option. Band 'v' (velocity magnitude) was used as the main parameter when processing the netcdf file and the output is in the form of a raster layer with a resolution of 240 m.

To allow comparisons to be drawn, sample points were drawn at equal intervals down the centre axis of the glacier and converted to a vector line within ArcMap (the same vector line was used

for all maps to allow comparisons throughout different years). This allowed graphs to be constructed to show the changes in velocities from the ice fall to the margin for the years of 1986, 1992, 1995, 2012 and 2018 (chapter 3). The resulting velocity maps generated for Svínafellsjökull (Chapter 3) were then compared to the ice structure and fracture density maps constructed for the glacier in order to investigate how increased forward motion (higher velocity) was being accommodated by deformation within the ice.

2.3 Debris entrainment analysis

Boulton (1978) was the first to depict a relationship between the shapes of sedimentary clasts to different transport pathways through glaciers (also see Matthews and Petch, 1982; Benn, 1989; Evans, 1999; Swift *et al.*, 2018; Evans, 2010), he was also the first to compare the shape signature of the sediments between glaciers of different thermal regime. Boulton (1978) identified three transport paths: (1) a supraglacial pathway, where debris is introduced onto the glacier surface by rockfall or avalanching and remains on or near the glacier surface before being deposited on the foreland; (2) an englacial route, whereby material that is introduced onto the glacier surface within the accumulation area is transferred englacially until it melts out in the ablation area at the margin; and (3) material that is either transferred from a supraglacial to a subglacial position or that is eroded at the glacier bed. Boulton (1978) conceptualised the supraglacial and englacial pathways as undergoing passive or high-level transport and pathway 3 as active or low-level transport (also see Lukas *et al.*, 2013). Boulton (1978) demonstrated that angular and platy clasts tend to dominate in the former two categories (1, 2), whereas edge-rounded, abraded and blocky clasts characterise the latter (3).

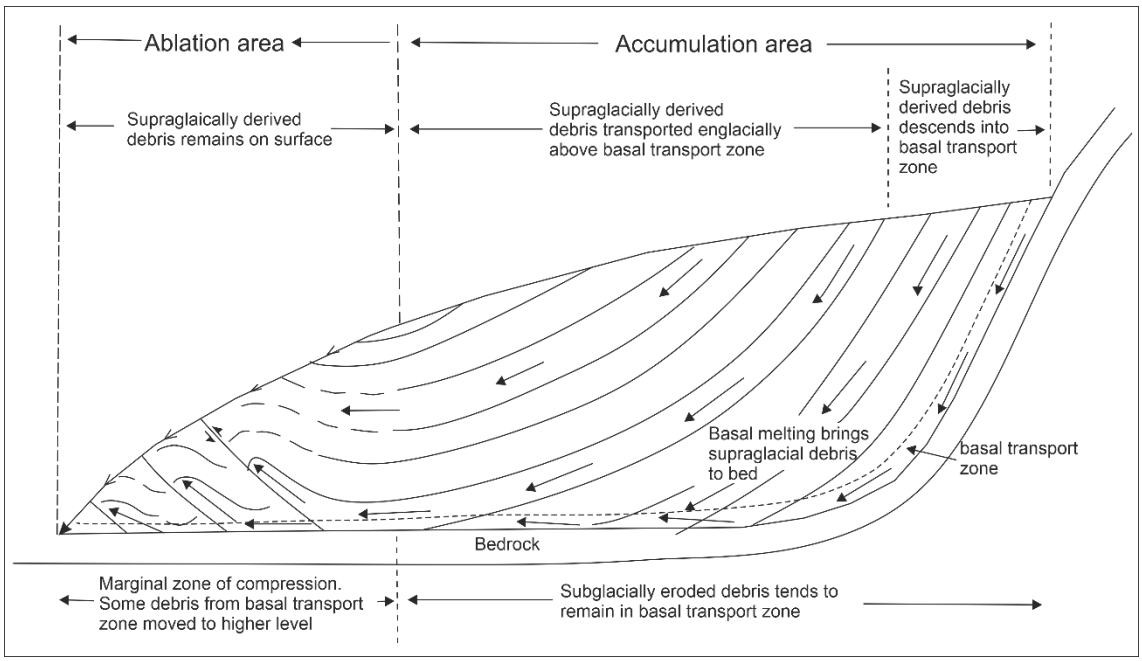

Figure 2.2 Transport paths identified by Boulton, (1978) of debris in a cirque or valley glacier derived from a headwall.

This theoretical separation has been confirmed and refined by a number of previous studies, who used measurements of clast shape to establish dominant transport pathways that contributed to the sediment budget of moraines (e.g. Weertman, 1961; Matthews and Petch, 1982; Sharp, 1982; Small, 1983; Matthews, 1987; Benn, 1989; Evans, 1989, 1999 and 2010; Shakesby, 1989; Benn, 1992; Hambrey *et al.*, 1997; Evans *et al.,* 2018a and 2018b) or to investigate the sedimentary dispersal processes operating across entire catchments (e.g. Ballantyne, 1982; Lukas *et al.*, 2013; Swift *et al.*, 2018). These published studies often used different statistical techniques to distinguish between different transport pathways, which often reduced the potential compatibility between different catchments (see Lukas *et al.*, 2013 for a discussion). Benn and Ballantyne (1993; 1994) provided a more widely uniform methodology, resulting in better comparability of results between catchments, leading to an increase in the number of clast shape studies subsequently published in the literature.

As an aid to visualising the variation in the data and provide a statistical interpretation of clast form Benn and Ballantyne (1993; 1994) recommended the use of ternary diagrams (first

introduced by Sneed and Folk, 1958). They also advocated using the percentage of very angular and angular clasts in a sample (Matthews, 1987) to differentiate between frost-weathered, angular clasts and those that have undergone subglacial edge-rounding (Lukas *et al.*, 2013). Instead of using sphericity and roundness plots (e.g. Boulton, 1978), Benn and Ballantyne (1994) demonstrated that plotting both RA (the percentage of angular and very angular clasts in a sample) and C_{40} indices (summary index for shape) in co-variance plots enables the effective differentiation between subglacially and supraglacially eroded clasts (Lukas *et al.*, 2013). The C_{40} index represents the percentage of samples with a c:a axial ratio of ≤ 0.4. Samples with low C_{40} value are dominated by clasts with higher c:a ratios. In other words, they are dominated by "blocky" clasts. To derive a C_{40}-index for a sample, involves the calculation of the c:a axial ratio for each clast, the identification of the number of values with a c:a axial ratio of ≤ 0.4, and then express this value as a percentage of the whole sample (i.e. 50 clasts). The RA index is the percentage of clasts in the same sample that are angular or very angular. Recently mechanically weathered material dominated by angular clasts displays high RA values. Material that has been transported by a glacier or a river for a significant distance generally has fewer angular clasts due to the greater degree of edge rounding while in traction (i.e. subglacial traction zone or fluvial bedload) and therefore has increasingly lower RA values in relation to the clast travel distance and/or the intensity of clast collisions.

This approach is now widely used to investigate sediment transport pathways in modern and formerly-glaciated mountain environments (e.g. Benn, 1992, 1995; Bennett *et al.*, 1997; Evans, 1999, 2010; Glasser *et al.*, 1999, 2006; Graham and Midgley, 2000; Benn, 2004; Goodsell *et al.*, 2005; Lukas, 2005, 2012 and 2013; Lukas and Benn, 2006; Lukas, *et al.,* 2007; Kellerer-Pirklbauer *et al.*, 2008; Mills *et al.*, 2009; Evans *et al.*, 2010, 2018a and 2018b; Cook *et al.*, 2010; Brook and Lukas, 2012). Consequently, it is used in this study to provide an assessment of debris transport pathways and entrainment at Svínafellsjökull (see Chapter 4). The analysis was conducted at samples sites which consisted of 50 pebble/cobble sized clasts of a similar lithology (massive basalt) collected from the moraines and subglacial landforms across the foreland, as well as

samples collected from the surface of the glacier where they emerged from different types of debris banding; the distribution of the sample sites is shown in Chapter 4. The size and form of the clasts were derived by measuring the length of the A (long), B (intermediate) and C (short) axes of the pebble/cobble and the roundness assessed using Powers chart (Powers, 1953). In addition to clast shape and roundness, the occurrence of striae on the surfaces of individual clasts was also noted, as this feature is considered to be diagnostic of subglacial transport in the glacial traction zone (Benn and Lukas, 2021). Statistical analysis of clast form was undertaken following the procedures outlined in Benn (2004, 2007) and Benn and Lukas (2021), whereby indexes of C_{40} (percentage of clasts with C/A axial ratios ≤0·4) and RA (percentage of clasts in VA (very angular) and A (angular) classes were calculated. Co-variance plots (specifically Type I plots of Lukas *et al.*, 2013 for basalt like lithologies) were compiled using C_{40} and RA values and roundness was further assessed by calculating an average roundness value using the procedure proposed by Spedding and Evans (2002) and refined by Evans (2010), who found that a value of average roundness can provide the most effective discrimination between clast forms. Following Evans (2010), the average roundness (AvR) was derived in this study by using the numerical values identified on the standard Powers gauge, whereby very angular (VA) = 0, angular (A) = 1, subangular (SA) = 2, subrounded (SR) = 3, rounded (R) = 4 and well-rounded (WR) = 5. The resulting clast morphology data were plotted on a series of binary and ternary diagrams (Chapter 4, Appendix 9-10) using Microsoft Excel. For comparisons, the Icelandic datasets for scree, subglacial till and glacifluvial deposits reported in Lukas *et al.* (2013) and Evans *et al.* (2018b) were used as control samples. An additional subglacial control sample was collected from a bedrock step exposed beneath the icefall of a neighbouring glacier, Falljökull, to facilitate comparisons with clasts entrained at bedrock steps below icefalls, a debris transport pathway identified as significant in debris banding development by Goodsell *et al.* (2005) and Swift *et al.* (2018) (see Chapter 4).

2.4 Geomorphological mapping

The approach of using aerial photography and remote sensing datasets coupled with field-based geomorphological investigations has been widely applied in the study of contemporary glaciated landscapes (e.g. Bennett *et al.*, 2010; Bradwell *et al.*, 2013; Reinardy *et al.*, 2013; Brynjólfsson *et al.*, 2014; Schomacker and Ingólfsson, 2014; Darvill *et al.*, 2014; Evans *et al.*, 2014, 2015, 2018a and 2018b and 2019; Jónsson *et al.*, 2014; Chandler *et al.,* 2016a, 2016b, 2020a, 2020b). This approach allows the production of detailed geomorphological maps that have been "ground truthed", thereby providing a degree of reliability in any subsequent interpretation of the landform evolution of the study area (see Chandler *et al.*, 2018).

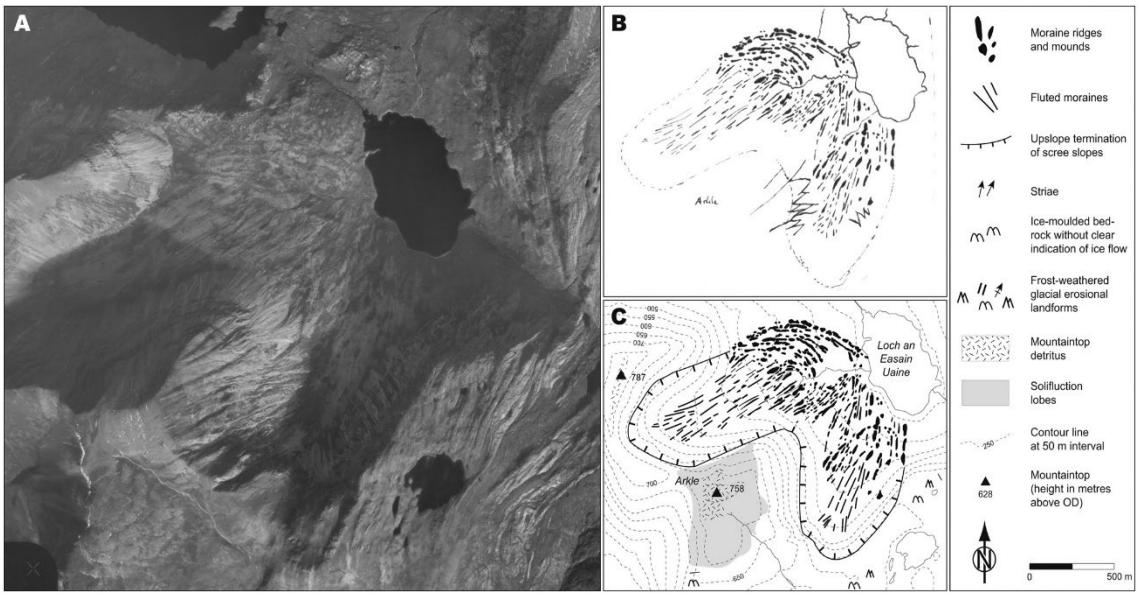

Figure 2.3 Taken from Chandler et al., (2018), an example of a study using multidisciplinary methods (A) aerial photograph at an average scale of ~1:25,000 (extract from photo 38 88 087; ©RCAHMS 1988); (B) scan of original overlay mapped through a stereoscope from (A), focusing on moraines, fluted moraines and the approximate upper limit of scree slopes as seen from the aerial photograph; (C) compiled, rectified geomorphological map, incorporating moraines and fluted moraines from (B) and additional data from field mapping, such as the exact upper limits of scree slopes, orientation of striae, solifluction lobes and mountaintop detritus.

The geomorphological features present within the foreland of Svínafellsjökull (see Chapter 5) were digitised at 1:1000 and 1:1500 scales in ArcMap 10.2 using high-resolution LiDAR generated by Johannesson *et al.* (2013). Air photographs for the years of 1952,1988, 1992 and 2007 and 2012 were also consulted when examining the foreland of Svínafellsjökull in order for

comparisons of landform characteristics. The scans of the photographs were obtained from the Icelandic survey company Loftmyndir ehf and have a resolution of 0.41 m ground sampled distance (GSD) per pixel. The initial interpretations of the landforms were "ground truthed" in the field (field surveys conducted in April, May, and September 2017, 2018, and 2019) to ensure reliability, with the detailed analysis and mapping of the landforms using the remote sensing data being conducted both prior to, and after the field investigations (see Chandler *et al.*, 2018 for full review of procedures). The final digitised features were then exported into CorelDRAW 2019 ™ for final editing and map production (Chapter 5, Appendix 12).

2.5 Summary

The range of techniques described in this chapter provide the basis of the multi-disciplinary approach used in this study to examine the structural glaciological evolution (Chapter 3), debris entrainment pathways (Chapter 4) and structural controls on process form relationships of moraine assemblages (Chapter 5) at Svínafellsjökull, Southeast Iceland and provide a better understanding of the spatially and temporally evolving landsystem. Although most of the above techniques are routinely utilised throughout glacial research, this study also features a new approach to the analysis of fracture density (Chapter 3), which can be applied more widely in order to understand structural changes on less accessible glaciers.

3 The historical structural glaciology of the snout of Svínafellsjökull: Implications for ice dynamics of a piedmont lobe

3.1 Introduction

The structural glaciology of terrestrial terminating glaciers undergoing rapid recession is typically less well known in comparison to marine terminating glaciers, which have received much attention in relation to their structural evolution in response to recent climate warming (e.g. Meier *et al.*, 1994; Pritchard and Vaughan, 2007; Glasser and Scambos, 2008). The established view on the movement of a non-surging valley glacier is that ice flows down the valley as a 'plug flow' with the glacier body moving en-masse (Benn and Evans, 2010). Recent research on ice cap piedmont lobes in Iceland (e.g. Phillips *et al.*, 2013, 2017; Dell *et al.*, 2019) has highlighted the important variations within these large-scale ice flow patterns related to the interaction between topographic controls and glacier structure as it responds to climate change. In southern Iceland in particular, glaciers have become more susceptible to recession and are retreating into marked overdeepenings within the underlying bed (cf. Bennett *et al.*, 2010; Bennett and Evans, 2012; Cook and Swift, 2012), accompanied by accelerated thinning. An overdeepening has been defined as a closed subglacial basin that under non-glacial conditions would form a lake and represents the location of maximum erosion during any one phase of glacier occupancy, thereby defining the approximate position of the long-term equilibrium line during a phase of glaciation. Once a snout recedes into this zone, continued melting can lead to the formation of an ice-marginal lake, leading to the glacier becoming susceptible to retreat due to calving (e.g. Boulton, 1996; Hallet, *et al.*, 1996). At the same time, accelerated thinning has brought about a noticeable change in snout crevasse patterns over time (e.g. Evans *et al.,* 2016, 2017 a, 2017b, 2019).

Recent work on process glaciology has contributed to a substantial increase in our knowledge of glacial motion, but a number of questions still remain around flow and resulting pattern and rate of deformation within the ice. During the first half of the 20th Century, advances in glaciological thinking and renewed interest in glacial structures stemmed from the formulation

of flow laws for ice (e.g. Nye, 1953; Glen, 1995) and the application of these laws to glaciers (Nye, 1957). Since that time there have been numerous studies of deformation within glaciers (for a review see Hambrey and Lawson, 2000; Colgan *et al.*, 2016). Many of these studies link structures within the glacier to known deformation rates (e.g. Allen *et al.*, 1960; Meier, 1960). However, the application of the structural geological concepts of progressive and cumulative deformation to glaciers are relatively rare (Maltman *et al.*, 2000). Where this application has taken place (e.g. Hambrey, 1977; Hambrey and Milnes, 1977; Hooke and Hudleston, 1978; Lawson *et al.*, 1994) relationships have been explored concerning ice deformation in relation to the development of foliation, folds, crevasses (fractures) and faulting.

Recent structural glaciological research has mainly focused on the structures developed within different glacier types from a wider range of settings, including polythermal, surging (Sharp, 1988; Sharp *et al.*, 1988; Lawson *et al.*, 1994; Lawson, 1996; Bennett *et al.*, 2000; Woodward *et al.*, 2002; Roberts *et al.,* 2009), Arctic (Huddleston and Hooke, 1980) and alpine glaciers (Allen *et al.*, 1960; Hambrey and Milnes, 1977; Glasser *et al.*, 2003; Goodsell *et al.*, 2005; Herbst *et al.*, 2006; Appleby *et al.*, 2010). This research has not only contributed to our understanding of the structural evolution of these glaciers, but has also outlined the mechanisms controlling their forward movement and highlighted the importance of deformation structures in controlling englacial sediment distribution. This is being increasingly applied to the understanding of the active rapid retreat of glaciers in Southern Iceland, where studies have highlighted the deformation and structural response by the ice during downwasting into overdeepenings and complex substrate topographies (e.g. Phillips *et al.*, 2013, 2014, 2017; Cook *et al.*, 2010 a and b; Swift *et al.*, 2018; Dell *et al.*, 2019).

Generally, valley and piedmont glaciers in mid-latitude settings appear to be responding to historical climate warming in two ways: (i) “active retreat”, where the margin oscillates on an annual cycle and retreat due to summer melt is partially offset by a small readvance during the cold winter months, thereby giving rise to the construction of annual recessional push moraines (e.g. Krüger, 1994; Evans and Twigg, 2002; Benn and Evans, 2010); and (ii) “passive retreat”,

where debris-charged parts of glacier margins are no longer moving forward and therefore retreat by in situ melting or downwasting (e.g. Kjaer and Krüger, 2001) or by incremental stagnation (cf. Eyles, 1979; Bennett and Evans, 2012). Annual recessional moraines occur in front of numerous Icelandic glaciers (e.g. Price, 1970; Gordon and Sharp, 1983; Boulton, 1986b; Krüger, 1994; Evans and Twigg, 2002; Bradwell, 2004; Bradwell *et al.*, 2013; Phillips *et al.*, 2014) and the spatial and temporal changes in their morphology have been linked to switches in style of structural glaciology concomitant with glacier responses to rapid climate warming (Chandler *et al.*, 2015). Additionally, push moraine construction in some locations has changed from annual to sub-annual in nature where recessional moraines are being constructed and/or pre-existing recessional features overridden by minor phases of readvance during the summer months (Chandler *et al.*, 2016a, 2016b, 2020a, 2020b), which has also been observed at Svínafellsjökull (Chapter 4).

Typical of the southern Iceland piedmont lobes, in terms of the glacier-climate interactions and snout changes briefly outlined above, Svínafellsjökull constitutes a prime location for assessing spatial and temporal changes in its structural glaciology, as these changes have been captured on repeat remotely sensed imagery (aerial photography and satellite imagery). Over the period 1970-2000, the position of the margin of Svínafellsjökull was relatively stable (Hannesdóttir *et al.*, 2015a), with retreat being dominated by downwasting, leading to a lowering of its surface rather than the lateral retreat of its margin. Since 2000, recession of Svínafellsjökull, like many other Icelandic glaciers (Sigurðsson, 1998; Evans *et al.*, 1999a; Sigurðsson *et al.*, 2007; Einarsson and Sigurðsson, 2015), has been occurring at an accelerated rate, and there has been a pronounced thinning of its terminal zone. Previous research at Svínafellsjökull has largely focused upon the glacial landform history preserved in its foreland (Everest *et al.*, 2017) and the glaciological processes (specifically supercooling) occurring beneath its margin (e.g. Cook *et al.*, 2007, 2011a and 2011b). However, very little is known about how the glaciological structure of this glacier has evolved in response to the changes in its mass balance and morphology driven by recent climate warming. This chapter seeks to address this knowledge gap by utilising

structural mapping based on historical aerial photographs, combined with detailed analysis of the changes in the fracture density and elevation of the glacier. These results are combined to investigate the evolution of the internal structure of valley glaciers in response to changes driven by climatic warming. The methods utilised within this study can be applied to valley glaciers worldwide to provide a better understanding of the internal glacial responses to climate change as well as the processes governing the imprinting of structural changes on the features within glacier forelands.

3.2 Study area and Geological setting

Located in southeast Iceland, Svínafellsjökull is one of several maritime glaciers draining the Öræfajökull ice cap, which is located on the southern side of the much larger Vatnajökull ice cap (Figure 3.1a). Svínafellsjökull is c. 10 km long and < 2 km wide and descends from its accumulation zone via a steep icefall. Below the icefall, this ENE-WSW orientated glacier is confined within a steep sided valley, formed to the north by the mountains of Eystra-Hrútsfjall, Vestara-Hrútsfjall, Sveltiskarð and Hafrafell, and to the south by Svarthamrar (Figure 3.1b). Several major rock falls from the slopes of Svarthamrar have resulted in the southern side of Svínafellsjökull becoming covered by a thick layer of debris, which has locally resulted in a reduction in surface ablation. Swift *et al.* (2018) also observed spreads of debris on the surface within the terminus zone that appear to be from subglacial sources which they interpret as being released (melted out) from thrusts where they intersect with the glacier surface. The equilibrium line altitude (ELA) of Svínafellsjökull in 2010 was estimated to be 1060 ± 60 m above sea level (a.s.l.) and the amount of marginal retreat between 2007 and 2011 calculated as c. 0.8 km (Hannesdóttir *et al.*, 2015a).

Where it emerges from its valley, Svínafellsjökull spreads radially to form an irregular fronted piedmont lobe confined within a series of arcuate terminal moraines, the largest and oldest (pre-1362 AD) being named Stóralda (Guðmundsson, 1998; Everest *et al.*, 2017) (Figure 3.1c and 3.1d). Two proglacial ice-contact lakes are presently located immediately adjacent to the snout

on the northwest and southeast margins of Svínafellsjökull. The lake waters penetrate the heavily crevassed and indented glacier snout, and hence the lakes appear to be partly supraglacial. Aerial photography reveals that these lakes have initially formed as the glacier has retreated from its 1990s readvance limit and have been compounded (dammed) by the large moraine amphitheatre. The up-ice side of this prominent moraine complex forms an adverse slope on the south-western margin of an overdeepened subglacial basin, which is considered to underlie the margin of the glacier (Cook *et al.*, 2007, 2011a and 2011b). On-ice radar data published by Magnússon *et al.* (2012) reveal the presence of an elongate overdeepened linear trough up to 200 m deep, and mostly below present sea level, incised into the bedrock underlying the margin of Svínafellsjökull. This trough is considered to extend up-ice forming a narrow channel directly underlying the axis of the glacier (Figure 3.1e).

The ice-contact lakes formed due to the proglacial drainage being impeded by a large moraine amphitheatre which is composed of several moraines superimposed on top of one another as the glacier repeatedly reoccupied this limit. This complex of Neoglacial and historical Little Ice Age moraines is dissected by six large meltwater channels, all but two of which have been abandoned due to glacier downwasting; the main drainage route is now occupied by the Svinafellsá, which drains from the southeast lake. During field work in April 2017, there was an observed fall (over an estimated period of around 24 hours) in the water-level of the largest lake on the north-western side of the glacier, leaving small icebergs and brash-ice stranded on the shallow proximal moraine slopes. Although this lake has previously drained through one of three breaches in the moraine amphitheatre on the western foreland, it now only drains through this breach when the lake reaches its maximum level. Consequently, it is considered that the periodic drainage of the enclosed/isolated lake occurs as a result of meltwater being able to drain either through and/or beneath the ice.

Marginal fluctuations at Svínafellsjökull have been studied in detail throughout the Little Ice age (LIA) and early 21st Century (e.g. Sigurdsson, 1998; Thompson, 1988; Thórarinsson, 1943;

Hannesdóttir *et al.*, 2015a, 2015b). During the LIA, the terminus of Svínafellsjökull coalesced with neighbouring Skaftafellsjökull and they remained joined until 1935, when the margins of the two glaciers eventually separated (Thórarinsson, 1943; Thompson, 1988). Since decoupling, the overall retreat of Svínafellsjökull, totalling around ~500 m, has been punctuated by several phases of readvance (Thompson, 1988). These fluctuations in the position of the ice-front have resulted in a suite of large, concentric, to occasionally sawtooth, moraines on the foreland (Everest *et al.*, 2017; Chapter 5) (Figure 3.1c and d). Renewed glacier recession has occurred since c. 2000 and has been accelerating since 2010. This recession has been accompanied by pronounced thinning of the terminal zone and the formation of dense longitudinal crevasse networks that give rise to indented radial pecten at the snout (Mottram and Benn, 2009; Phillips *et al.*, 2017; Dell *et al.*, 2019). The complex lower marginal zone of Svínafellsjökull forms the focus of this chapter.

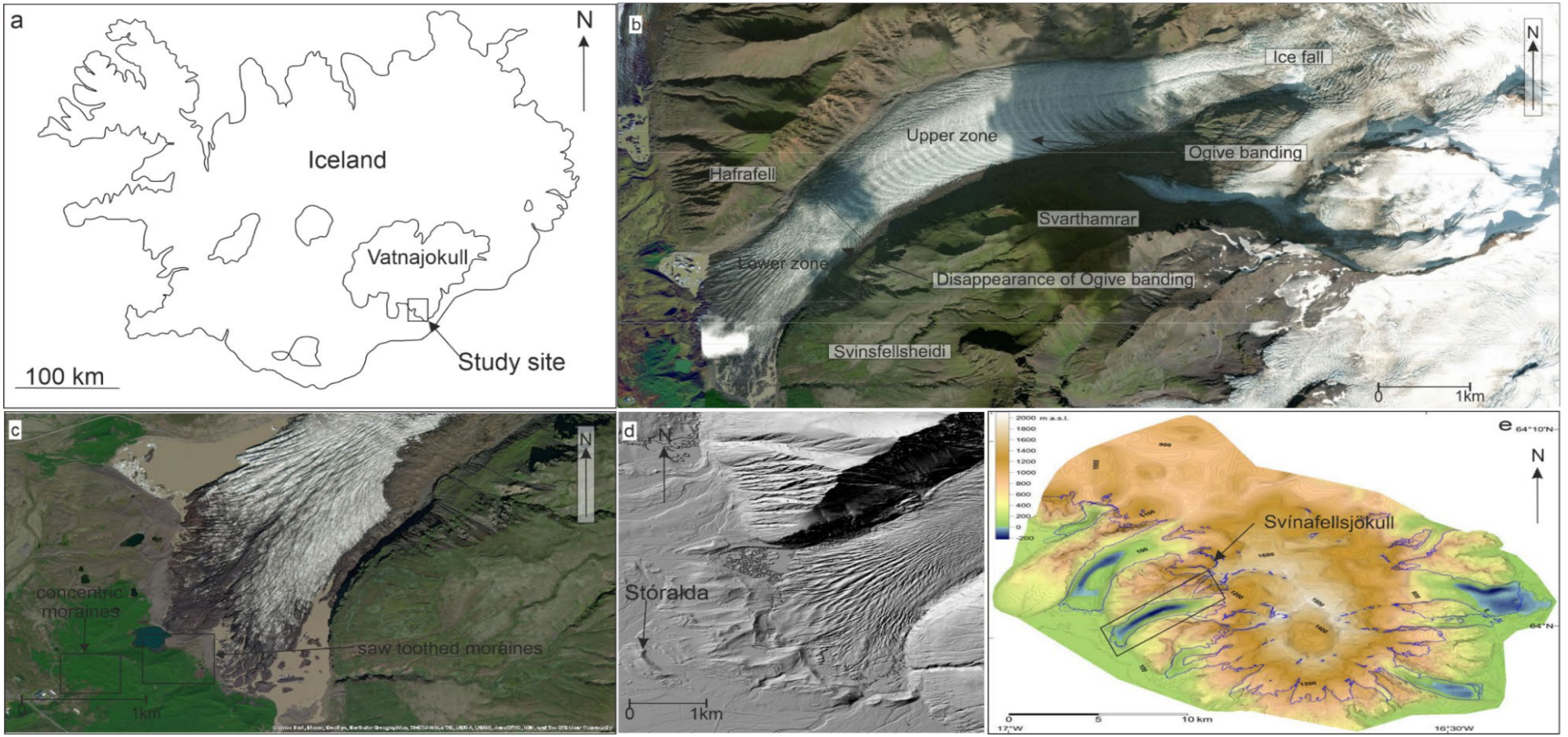

Figure 3.1: Location and characteristics of Svínafellsjökull: a) map showing the location of Svínafellsjökull, in southeast Iceland (adapted from Cook, et al. 2010); b) aerial photo of Svínafellsjökull showing this east-southeast to west-southwest orientated glacier descending from its source area on Öræfajökull (map and aerial photograph sourced from Google Earth); c) marginal area of Svínafellsjökull; d) LiDAR Imagery of the marginal area of Svínafellsjökull generated by Johannesson et al. (2013); e) Svínafellsjökull' s overdeeping mapped by Magnusson et al. (2012) (outlined by the black box).

3.3 Methods

In order to achieve a complete understanding of the evolution and changes in glaciological structures on Svínafellsjökull, a multi-disciplinary approach was adopted for analysing aerial imagery captured at various times over the period of 1952-2012 (see Chapter 2). The structural mapping and analysis of the pattern of large-scale deformation structures (including fractures, faults, banding/layering) exposed on the surface of Svínafellsjökull was carried out using historical vertical aerial photographs, supplemented by field survey data to "ground truth" this mapping. This approach has enabled the larger scale assessment of the spatial and temporal development of the glaciers' structural architecture.

Due to the highly crevassed (open fractured) nature of the surface of Svínafellsjökull, field studies were restricted to the area close to the margin of the glacier. Field work undertaken between May and September 2016, 2017, 2018 and 2019 has revealed that dominant deformation structures within the glacier are moderately inclined to sub-vertical fractures (Figure 3.2 a and b), which were observed penetrating up to several tens of meters into the ice; no obvious folding of the banding/layering (ogives), defined by the variation in the volume/amount of debris included in the ice (Figure 3.2c), has been observed (Figure 3.2). This on-ice survey involved the recording of the orientation (dip, strike, dip azimuth), sense and amount of offset (where applicable), and inter-relationships between the various sets of faults, fractures and foliations (banding); these data are presented later in this chapter. The fractures, as well as the banding identified on the surface of Svínafellsjökull, were digitised using ArcGIS at a scale of between 1:1000 and 1:1500, see Chapter 2 section 2.2.1 for further details.

Figure 3.2: Field photographs of Svínafellsjökull: a) panoramic photograph of dominant structures. Photo taken looking southwest; b) Dominant structures looking west; c) field photograph of central marginal zone, showing supraglacial ponding and dominant structures.

3.4 An Overview of The Structural Architecture of Svínafellsjökull

Detailed mapping of the structures exposed on the surface of Svínafellsjökull using the aerial photography and satellite imagery acquired between 1952 and 2012 has enabled the sub-division of the glacier into a series of structural domains for each year (see Figure 3.3, Appendix 1, Figure 3.5, Figure 3.6, Figure 3.7). These domains are distinguished by marked changes in the orientation, spacing and number of fracture sets observed on the glacier surface (for method see Chapter 2) and reflect changes in the stress field within the ice and depict the resulting changes in the style and relative intensity of deformation being accommodated across the glacier.

This approach has revealed that the overall structural architecture of Svínafellsjökull can be divided into two main zones (Figure 3.4a) : 1) an extensive (5.5 km long) upper zone extending from the icefall to within 2 km of the snout and which exhibits a relatively simple down ice radiating/fan-shaped fracture pattern, a locally well-developed network of supraglacial meltwater channels, prominent light and dark coloured ogive banding (Figure 3.4b) and; 2) a structurally more complex lower, 2.2 km long zone occupying the marginal, lower reaches of the glacier (Figure 3.4c). The icefall which feeds ice from the accumulation zone to Svínafellsjökull is structurally complex with the domains identified within this part of the glacier (Domains 12 to 16; Figure 3.3, Appendix 1) being characterised by a series of short, arcuate to irregular crevasses which are typically orientated transverse to direction of flow. The predominantly open nature of the fractures (crevasses) within the ice fall is consistent with these structures having formed as a result of the ice-flow-parallel extension of the glacier as it descends from the accumulation zone (see Figure 3.1b).

Immediately below the ice fall the structure of the ice within Domain 12 and the up-ice part of Domain 9 (Figure 3.3, Appendix 1) is characterised by poorly developed, irregular transverse to flow-parallel fractures. Unlike the other domains identified within the rest of Svínafellsjökull, the lack of a coherent structural pattern to the fractures may reflect the disorganised/disrupted nature of the ice after it has descended the icefall. However, the clearly well-developed radiating/fanlike to flow-parallel pattern of fractures which characterised much of the upper part of Svínafellsjökull (e.g. Domains 9 and 18; Figure 3.3, Appendix 1) indicates that the disruption to the glacier caused by deformation within the icefall is quickly lost and the ice begins to flow as a single coherent plug-flow. This area of the glacier is also characterised by the presence of the ogive banding with the convex down-ice shape of the bands indicating that this foliation dips at a low to moderate angle up-ice (Figure 3.3, Appendix 1). In addition, the detailed mapping of Svínafellsjökull reveals that the ogive banding is largely developed along the broad axial zone of the glacier, with this banding being either absent or overprinted by fractures developed close to its margins. This is most clearly apparent along the northern margin (Domain

10) where the ice would have been undergoing a combination of lateral shearing and longitudinal compression imposed as the glacier moves passed the steep valley side (Sharp *et al.*, 1988; Benn and Evans, 2010; Phillips *et al.*, 2017).

Rather than being a simple piedmont lobe with an associated splaying, fan-shaped crevasse pattern formed in response to a combination of the forward motion and lateral spreading of the ice (Sharp *et al.*, 1988; Benn and Evans, 2010; Colgan *et al.*, 2016), the structurally lower part of Svínafellsjökull (Figures 3.3 and 3.4c) comprises three approximately NE to SW-trending elongate, lobate areas which directly reflect the marked changes in the structural architecture within this part of the glacier (see below) (Figure 3.4c, Figure 3.6 Figure 3.7, Figure 3.10, Figure 3.11, Figure 3.12 and Figure 3.13).

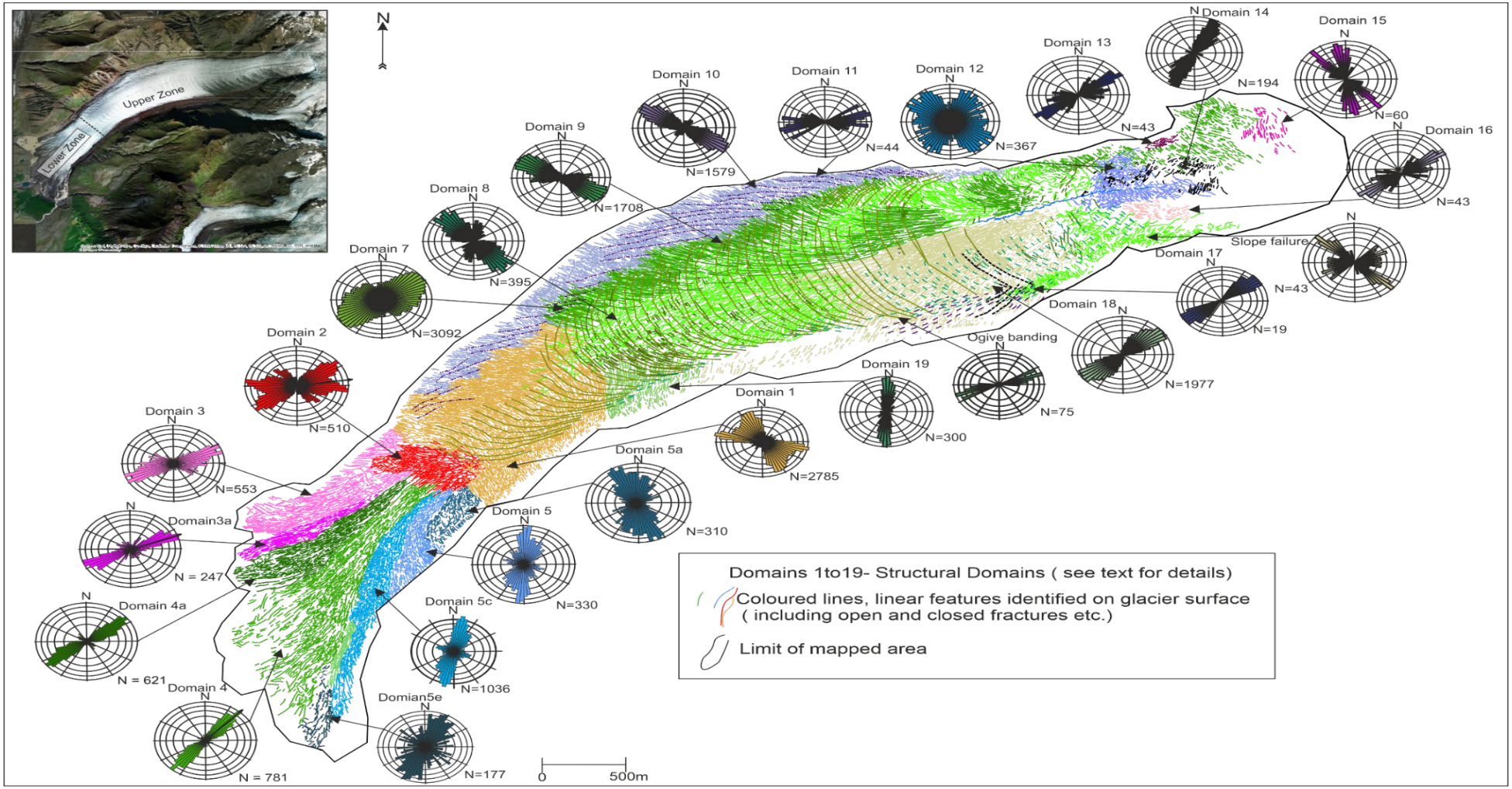

Figure 3.3: Structural map of Svínafellsjökull for the year of 2012 with associated rose diagrams and inset image showing the upper and lower zone classifications of the glacier.

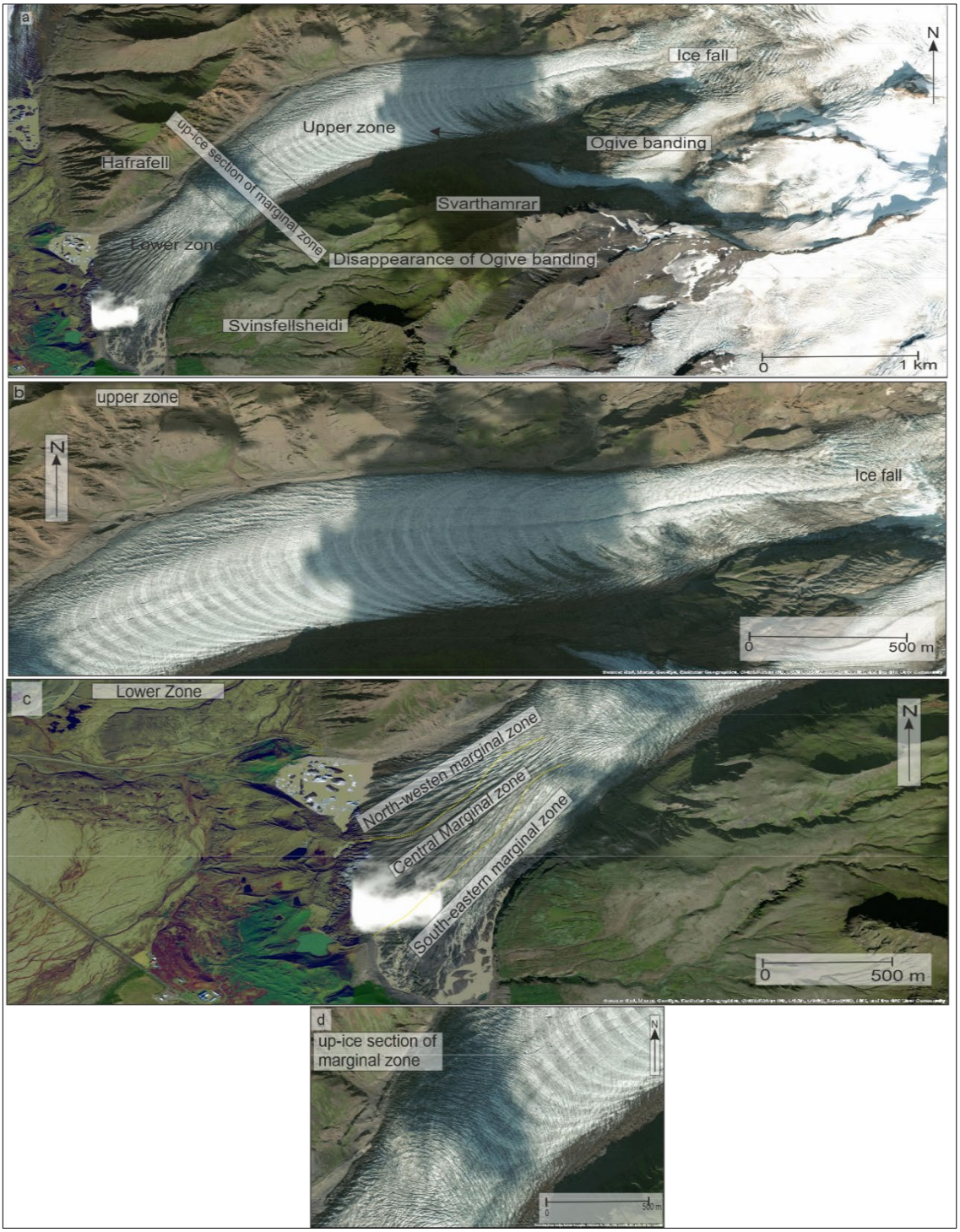

Figure 3.4: Sections of the glacier: a) aerial photo of Svínafellsjökull showing this east-southeast to west-southwest orientated glacier descending from its source area on Öræfajökull (map and aerial photograph sourced from Google Earth); b) upper zone of Svínafellsjökull. (Aerial photograph sourced from Google Earth); c) The north-western (NWZ), central (CZ) and south-eastern (SEZ) zones within the lower part of Svínafellsjökull; d) up- ice section of the marginal zone of Svínafellsjökull.

Internally the individual marginal zones exhibit different fracture patterns, potentially reflecting changes in the style and relative age of deformation being accommodated across the ice. These changes may result from a variation in the effects of compression and lateral shear stresses at different times (temporal) and locations (spatial) within the snout. The typical crevasse patterns widely documented at the lateral margins of glaciers are characterised by hook-shaped fractures associated with the effects of lateral shear stresses resulting from the frictional drag caused as the glacier moves past the valley sides (e.g. Nye, 1952; Colgan *et al.*, 2016). However, at Svínafellsjökull the up-ice sections of the NWZ and SEZ (2.5-3.5 km from the terminus) terminate in a c. 1 km long domain (Domain 1) characterised by concave, down-ice dipping, open fractures (crevasses) which can be traced laterally across the entire width of the glacier (Figure 3.4d). The three zones, the north-western (NWZ), central (CZ) and south-eastern (SEZ) zones within the lower part of Svínafellsjökull, which form the structurally complex lower part of the glacier, all appear to originate and extend from the southern side of Domain 1, with the northern end of the CZ being marked by a relatively narrow (4.7 m wide), roughly elliptical area (Domain 2) of highly fractured ice. Domain 2 is located at the southern end of the narrow, overdeepened trough which underlies the axis of the glacier (Figure 3.5) (Magnusson *et al.*, 2012). The remainder of the lower part of Svínafellsjökull directly overlies the adverse slope formed by the up-ice side of the moraine amphitheatre and coinciding with the shallowing of the overdeepening towards the glacier margin.

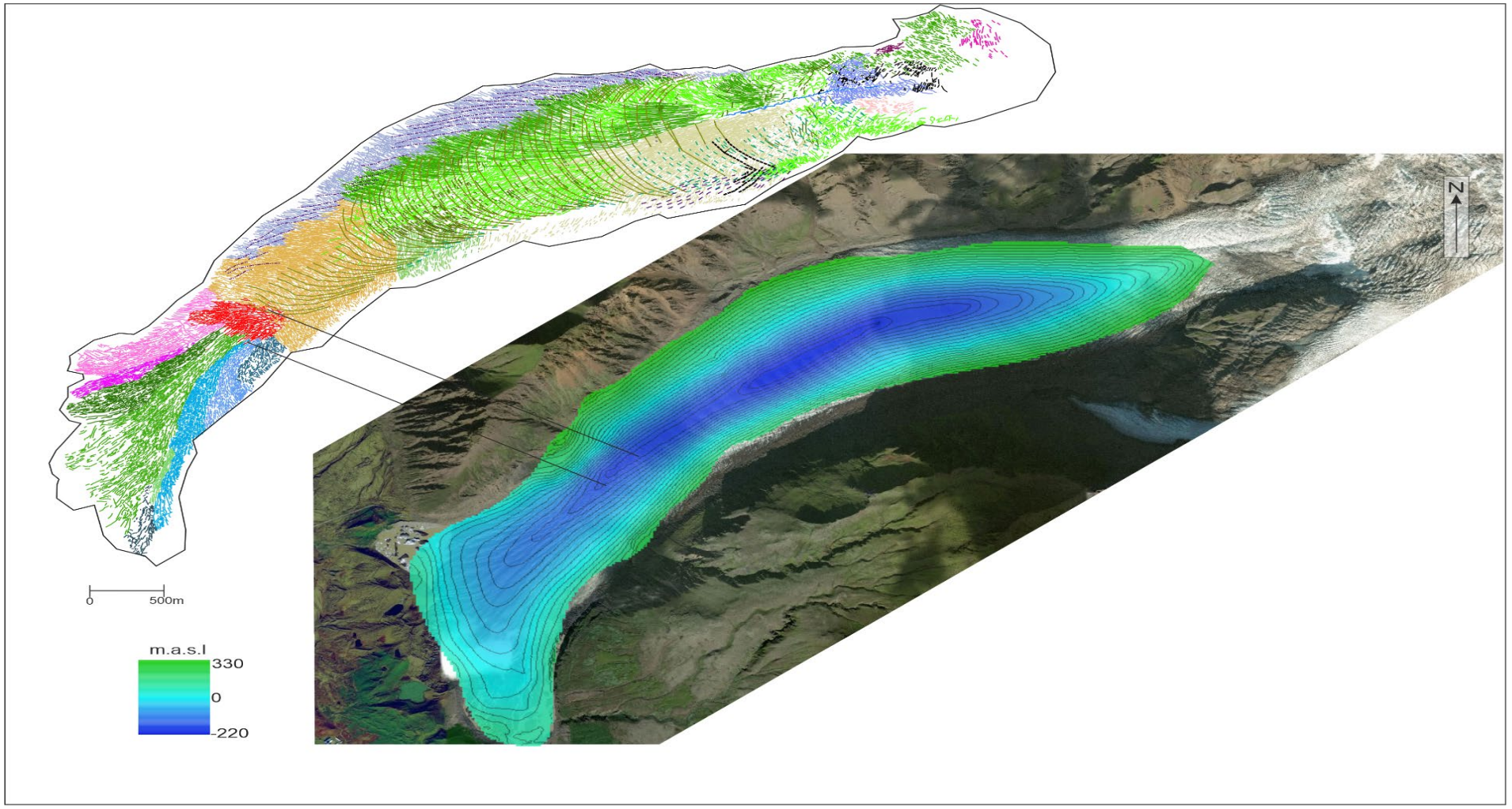

Figure 3.5: Comparison of the 2012 Structural map to a clip of the DEM used by Magnússon et al. (2012). Aerial photograph was taken from the Esri World Image Basemap layer (Source: Esri, Maxar, Earthstar Geographics, and the GIS User Community).

3.5 Evolution of the structure of the marginal area of Svínafellsjökull between 1952 and 2012

Examination of the structural maps of Svínafellsjökull during the period of 1952 to 2012 (Figure 3.6, Appendix 2) has revealed that the multi-lobate structure of the margin is most pronounced between 2007 and 2012. However, this structural architecture appears to have begun to develop in 1992 and was characterised by the development of a large area of en-echelon crevasses (Figure 3.6, Appendix 2) and increased structural complexity of the lower zone (compare maps in Figure 3.6, Appendix 2).

In detail, the lower part of Svínafellsjökull can be divided into three approximately east-west-trending areas which have been distinguished based upon the differences in the structural architecture of the ice (Figure 3.7) as follows : (i) a c. 0.5 km wide north- western zone (NWZ) occurring immediately adjacent to the north-western margin of the glacier, dominated by Domains 3 and 3a; (ii) ; a wedge-shaped central zone (CZ) (c. 2 to 0.5 km wide) which narrows up-glacier and dominates the lower part of the glacier and comprises Domains 4, 4a, 4b, 4c and 4d; and (iii) a south-eastern zone (SEZ) forming a 0.5 to 1 km wide zone along the southern margin of the glacier and comprises of Domains 5, 5a, 5b and 5c, with the addition of Domain 5e in 2012 (Figure 3.7b).

Domains 1 and 2 located in the up-ice section of the marginal zone do not exhibit any structural changes throughout the period of 1952- 2012 (Figure 3.6, Appendix 2). Domain 2 is characterised by an area of highly fractured ice, with the complex array of crevasses (see rose diagram on Figure 3.3, Appendix 1) resulting in the distinctive “elephant skin” appearance of the surface of the glacier (Figure 3.8d). The structures within Domain 2 appear chaotic in nature and comprise of relatively short, open fractures which truncate one another (Figure 3.8d). Domain 1 dominates the up-ice part of the marginal zone of Svínafellsjökull and is characterised by down-ice dipping crevasses and the loss/overprinting of the ogive banding, which is clearly visible on the surface in the upper zone of the glacier (Figure 3.8a and b). The steeply down-ice dipping

and open nature of the dominant fracture set within this domain is consistent with these structures having formed as a result of extensional deformation of the ice, which effected the entire width of the glacier. Domains 1 and 2 clearly mark a significant structural change within the glacier, from the "plug flow" characteristics in the upper zone, to a structurally more complex pattern of deformation within the marginal zone (Figures 3.3, 3.4a, 3.5 and 3.8c). It should also be noted that the well-developed ogive bands observed in the upper part of the glacier (Figure 3.8c) are absent within the Domains 1 and 2 (Figure 3.8b), consistent with the deformation in the lower part of Svínafellsjökull having overprinted this earlier formed foliation. Furthermore, the absence of any significant change in the structural architecture of Domains 1 and 2 on the aerial photography are considered to indicate that the style of deformation occurring within the ice within this part of Svínafellsjökull remained relatively consistent throughout the period 1952 to 2012. This has led to the conjecture that Domains 1 and 2 represent a "transition zone" between the coherent "plug flow" which dominates the upper part of the glacier and the structurally more complex marginal zone of the glacier.

Changes in the position of the margin of Svínafellsjökull are shown in Figure 3.9, which clearly highlights the fact that its position has been relatively stable between 1954 and 2016, with only minor fluctuations highlighting the overall pattern of retreat, punctuated by a minor readvance in 1992 (blue line on Figure 3.9). This figure also highlights that up to 1992 the shape of the margin was non-indented. However, after 1992 the shape of the margin has become progressively more complex (indented). This can be seen between 2007 (yellow line on Figure 3.9) and 2016 (pink line on Figure 3.9). This change clearly reflects the increasing influence of longitudinal crevasses (open fractures) on the ice margin morphology, associated with increased surface ablation (melting) during the progressive retreat of the glacier since the mid-1990's re-advance. Also, the northern (NWZ) and southern (SEZ) marginal zones of the glacier exhibit the most obvious retreat between 1992 and 2016 (Figure 3.9), with the position of the middle section of the glacier margin remaining relatively stable. Mapping of the position of the margin of Svínafellsjökull has revealed that there was a minor re-advance of this central part (CZ) of the

glacier between 2007 and 2012, with the increased volume of ice reaching the glacier snout leading to a closing of the open crevasses, reflected in the morphology of the margin becoming "smoother" and less indented (see Figure 3.9).

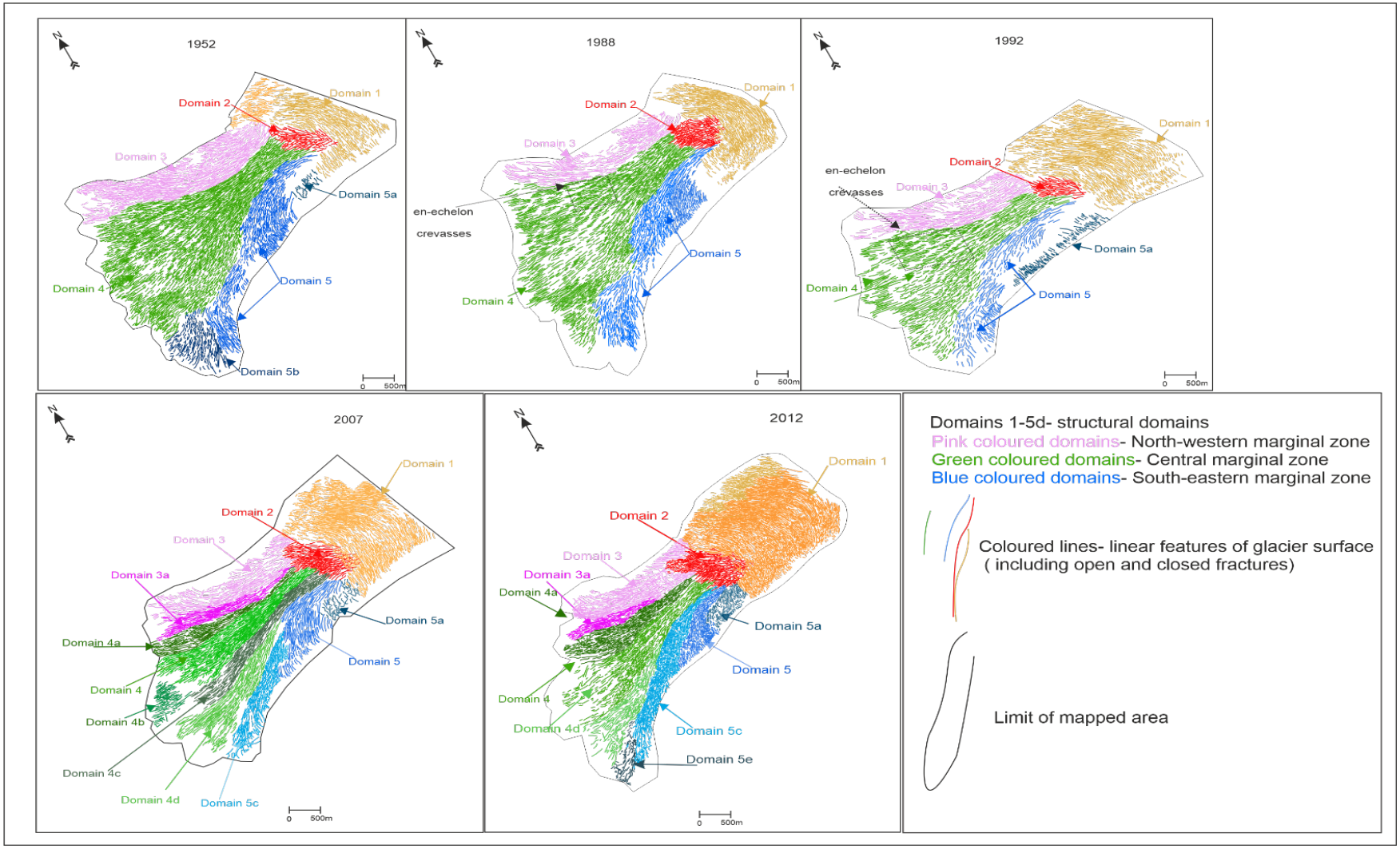

Figure 3.6: Structural maps of Svínafellsjökull for the years of 1954, 1988, 1992, 2007 and 2012).

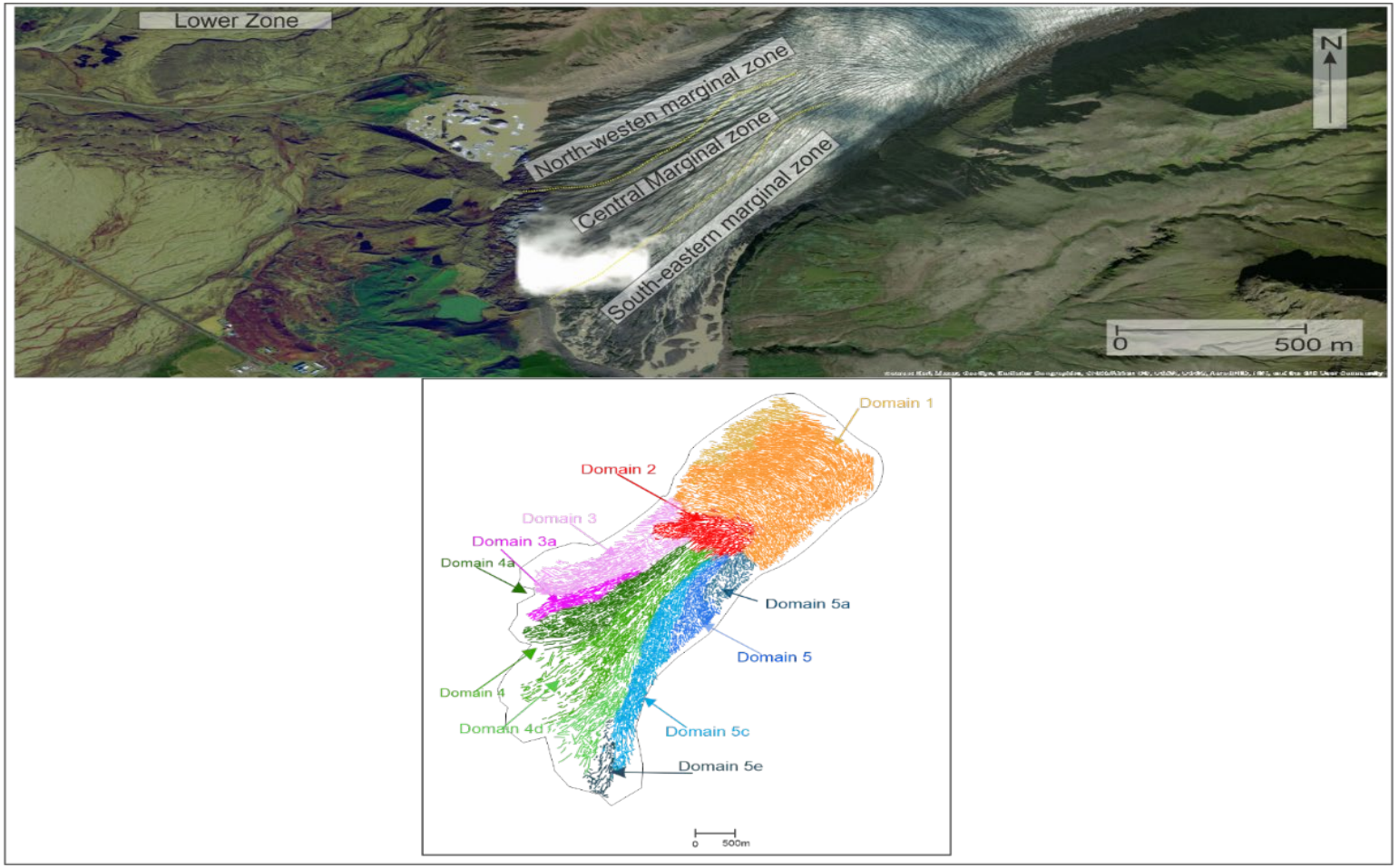

Figure 3.7: Svínafellsjökull marginal zones with associated structural map showing which domains fit within each marginal zone. Pink domains are associated to the north-western marginal zone, green domains are associated within the central marginal zone and the blue domains are located within the south-eastern marginal zone.

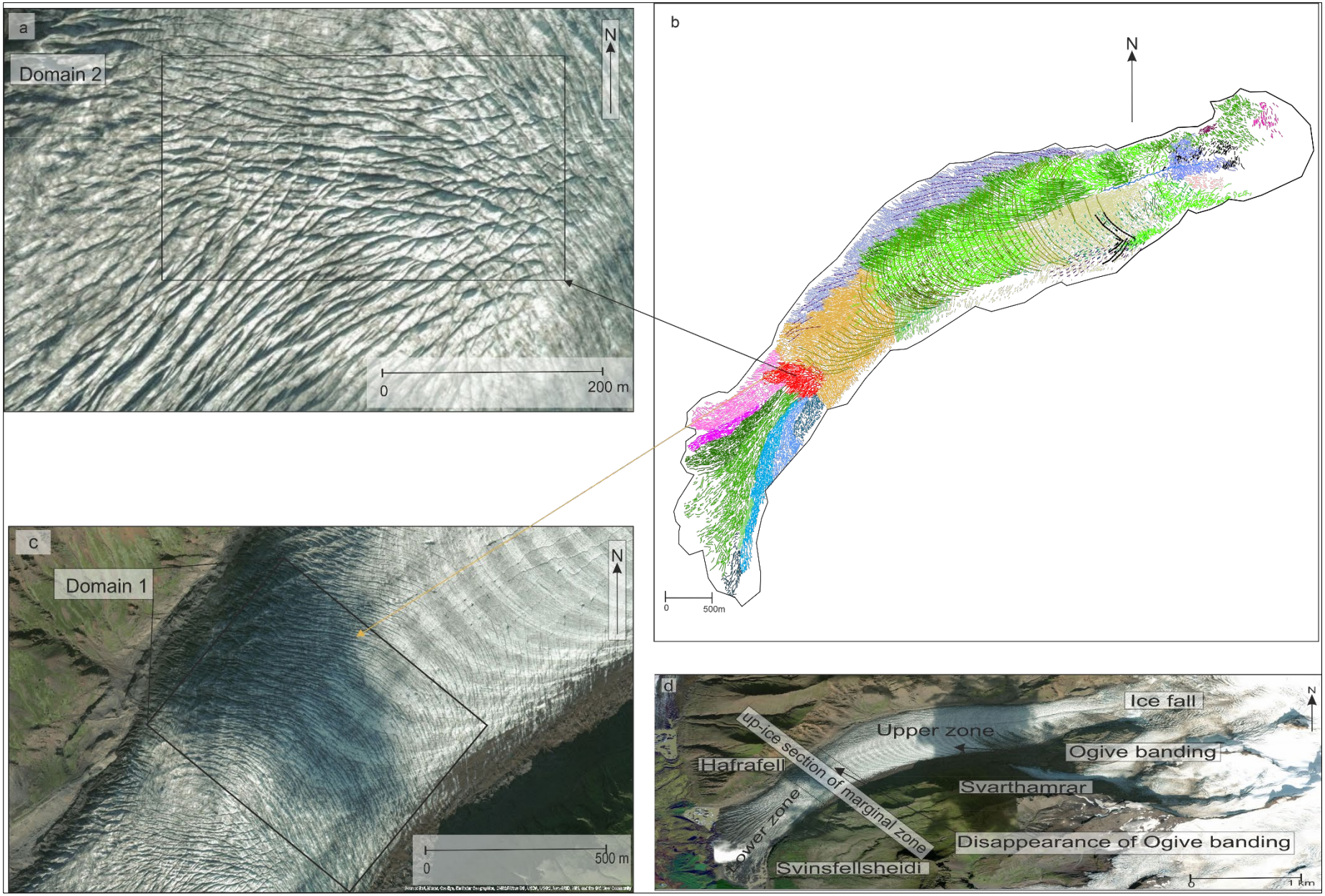

Figure 3.8: Locations of structural Domains 1 and 2: a) aerial photograph of Domain 1; b) 2012 structural map showing red domain is Domain 2 and orange domain is Domain 1; c) aerial photograph of Domain; d). aerial photography depicting the location of Domains 1 and 2 in relation to the full glacier.

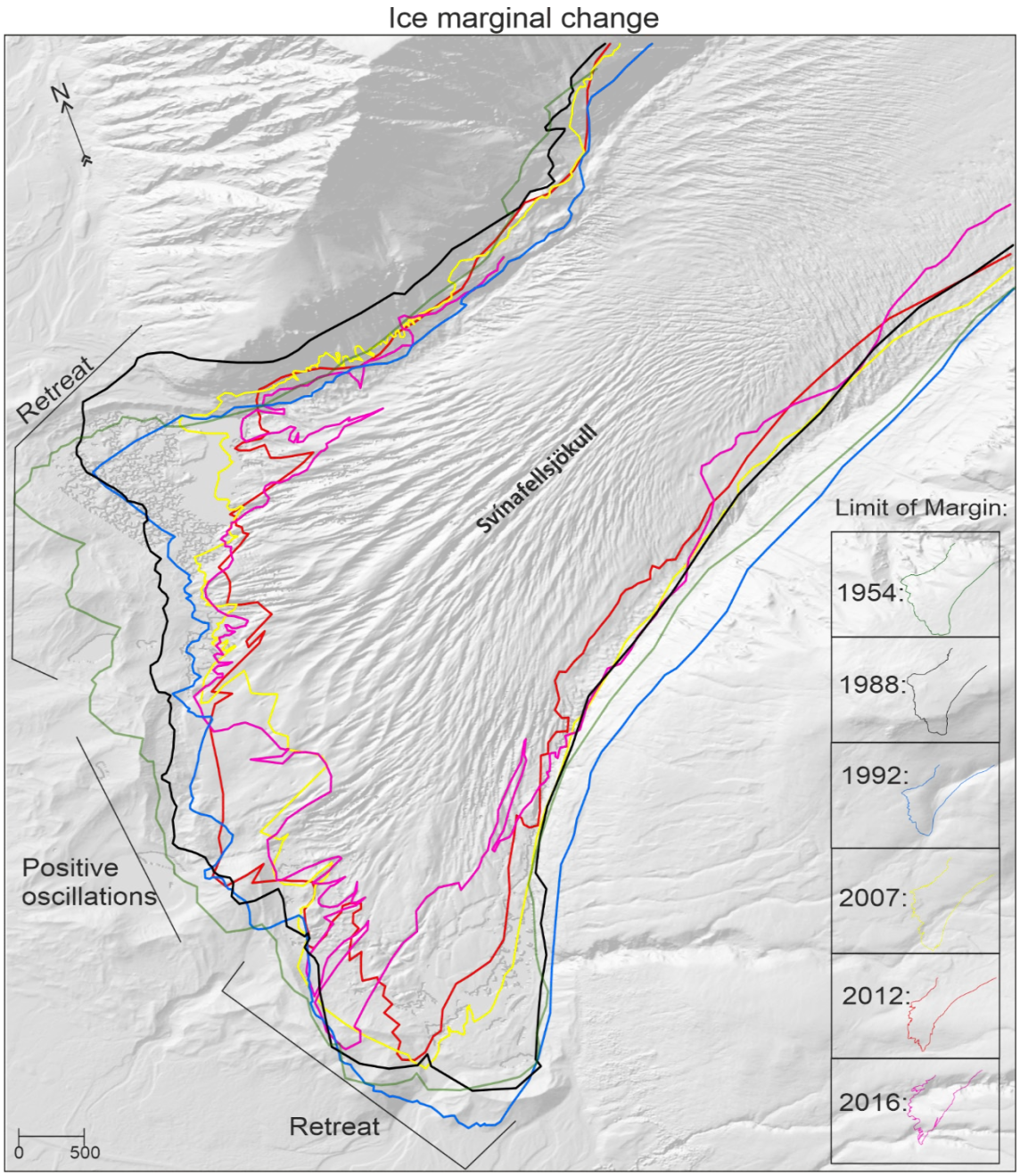

Figure 3.9: The changing position and morphology of the margin of Svínafellsjökull for the years of 1954, 1988, 1992, 2007, 2012 and 2016.

The morphology of the lower zone of Svínafellsjökull in 1952 is consistent with a single radially flowing piedmont lobe, characterised by a splaying crevasse pattern formed in response to a combination of the forward motion and lateral spreading of the ice (Sharp, 1988; Benn and Evans, 2010; Colgan *et al.*, 2016). This piedmont lobe can be divided into a total of 7 structural domains (Domains 1, 2, 3, 4, 5, 5a and 5b; Figures 3.10). Ogive banding was restricted to the

southern margin of the glacier in Domains 5 and 5b and can also be seen in the upper part of Domain 4 (Figure 3.10c, Appendix 3). In 1988 the lower zone of Svínafellsjökull still displayed a splaying crevasse pattern, characteristic of a single radially flowing piedmont lobe (Figure 3.11, Appendix 4). However, in contrast to 1952, the structural architecture of the glacier in 1988 included discrete flow-parallel zones of differential shearing leading to the development of a number of strike-slip shear zones (compare Figure 3.10, Appendix 3 and Figure 3.11, Appendix 4). These shear zones are preferentially and most clearly developed on the northern side of Domain 4 (Figure 3.11, Appendix 4) where their margins can be seen to rotate from approximately E-W adjacent to the boundary with Domain 3 (located to the north), to a more northeast-southwest orientation towards the centre of Domain 4 (insets a and b on Figure 3.11, Appendix 4). Short, curved to arcuate fractures within the shear zones form discreet bands of en-echelon crevasses (tension fissures) which record a consistent dextral (top to right) sense of shear (inset Figure 3.11, Appendix 4). The geometry of these tension fissures is consistent with an overall change in the direction of flow from westwards adjacent to the boundary between Domains 3 and 4, to an overall southerly flow direction in the central and southern parts of Svínafellsjökull. This more southern direction of flow may correspond to the formation of the distinct, elongate to lobate nature of the margin on the southern side of the glacier in 1988 (Figure 3.11, Appendix 4) and which remained a prominent feature of this part of the margin of Svínafellsjökull in 1992 (Figure 3.12, Appendix 5). The dextral shear zones observed on the structural map derived from the 1988 image of the glacier, have been recognised over a much wider area (Domains 3 and 4) of the surface of Svínafellsjökull in 1992 (Figure 3.12, Appendix 5). This more complex pattern of linear to lenticular shear zones (inset (a) on Figure 3.12, Appendix 5) may have developed in response to more extensive deformation within the marginal zone of the glacier during the minor readvance recorded in the early 1990's.

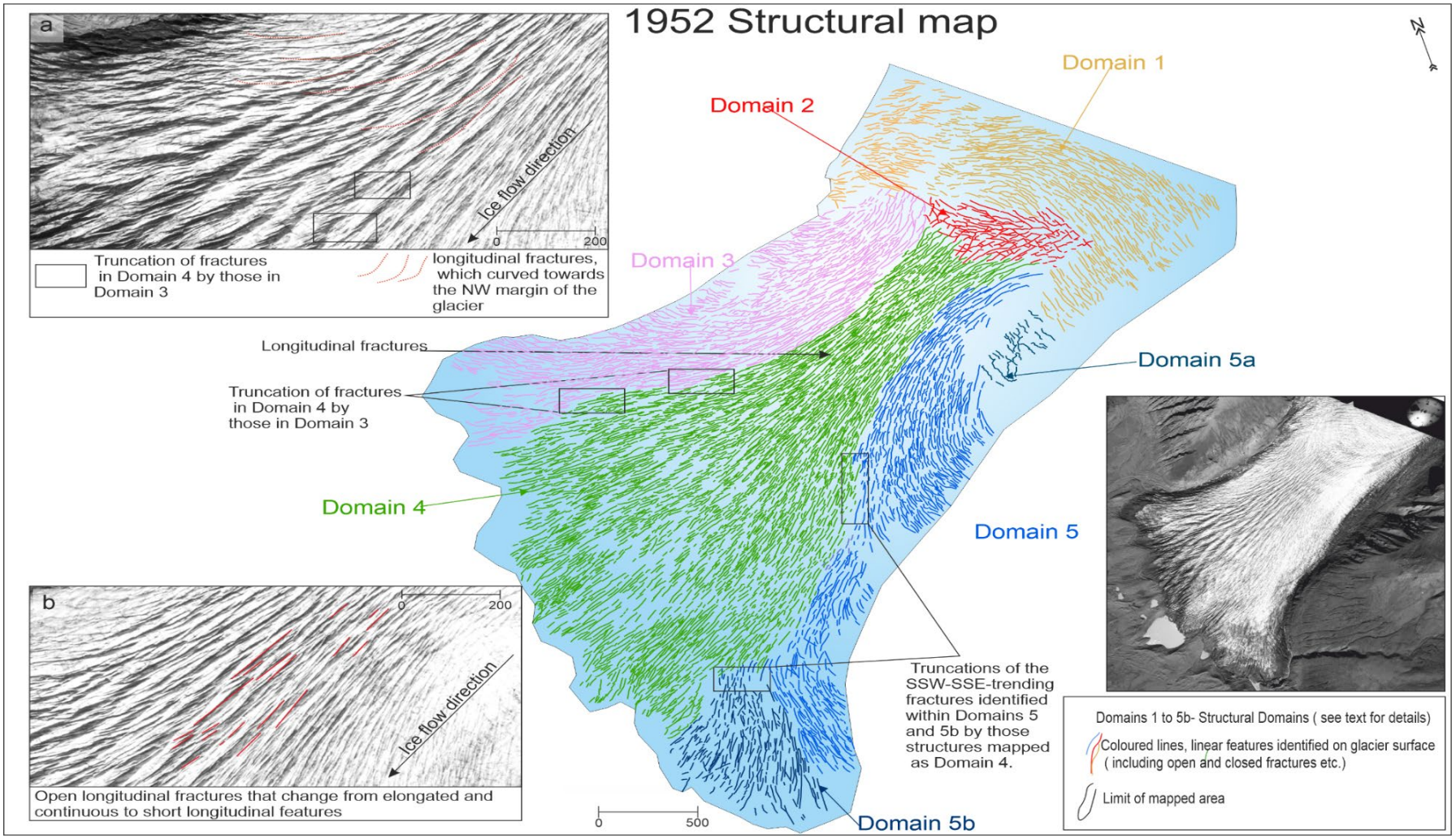

Figure 3.10: 1952 Structural map of Svínafellsjökull. Structural domains are depicted by different colours. The structural map was constructed using the 1952 aerial photography acquired from LMI. Inset a: Aerial photograph of structures in Domains 3 and 4. Inset b: Aerial photograph of structures in Domain 4.

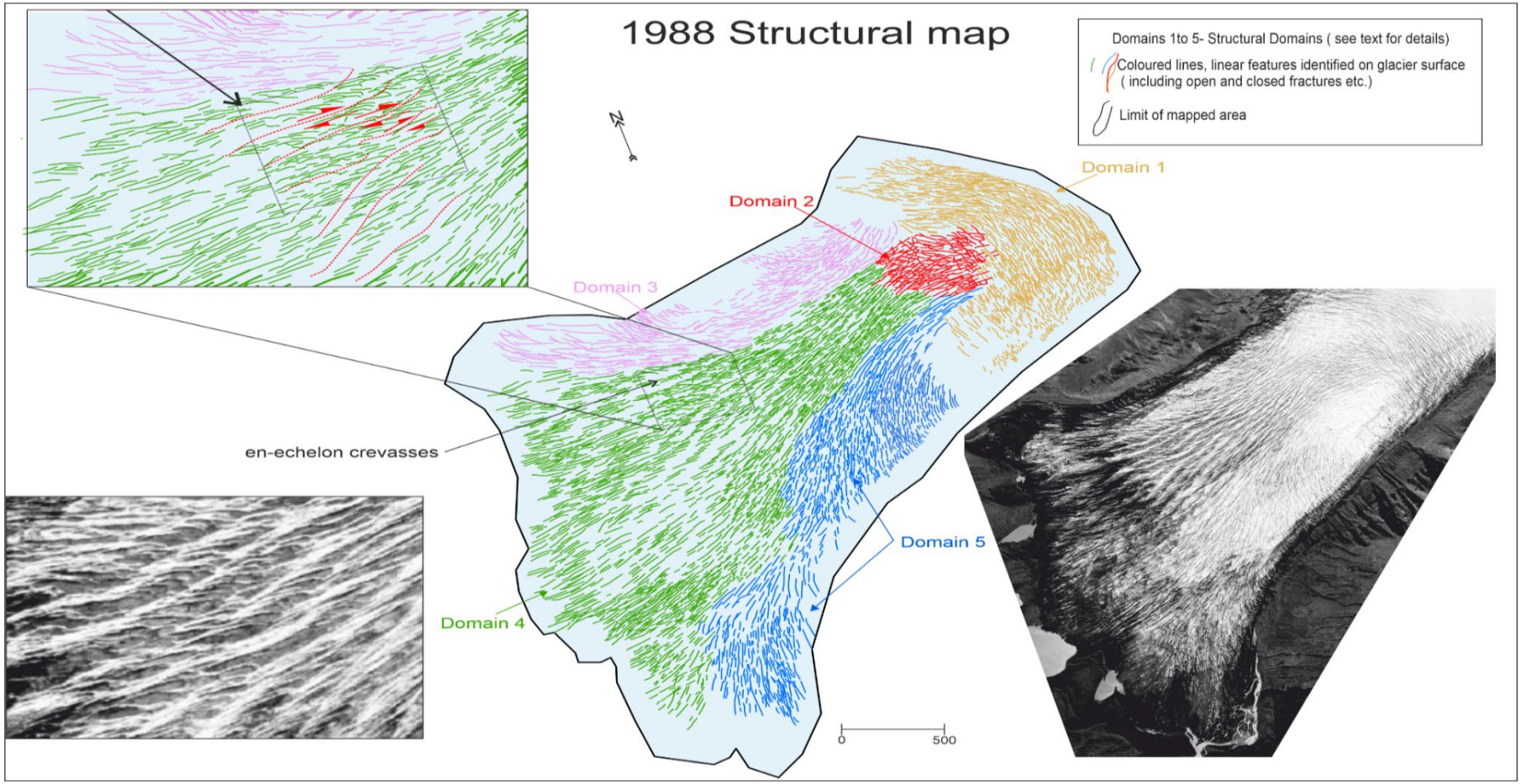

Figure 3.11: 1988 Structural map of Svínafellsjökull. Structural domains are depicted by different colours. Dashed box indicates an area of en-echelon crevasses. The structural map was constructed using the 1988 aerial photography acquired from LMI. Inset a: en-echelon crevasses. Inset a: Diagram of Shear zone b: Aerial photograph showing area of en-echelon crevasses. Inset c: Aerial photograph of areas of truncated structures.

In contrast to the roughly semi-circular nature of the glacier margin in the period between 1952 and 1992 (Figure 3.12, Appendix 5), the margin of Svínafellsjökull in 2007 (Figure 3.13, Appendix 6, also see Figure 3.9) has a distinct trilobate form. The more complex shape of the margin is considered to reflect a change in the internal architecture of the glacier and the presence/development of the 3 distinctive marginal zones within the ice. The leading edges of these three NE to SW-trending zones displayed numerous marked re-entrants or pecten (see Figure 3.9) which can be clearly related to the opening of the major longitudinal fractures (crevasses) within the ice (cf. Evans *et al.*, 2016). This relationship is most apparent/well-developed at the margin of the Northwestern Zone (yellow 2007 line on Figure 3.9 and inset on Figure 3.13, Appendix 6).

The trilobate structure of the lower zone of Svínafellsjökull first identified in 2007 becomes increasingly pronounced in 2012 (Figure 3.14, Appendix 7), accompanied by an increase in the indented nature of the glacier margin within both the Northwestern Zone and Central Zone (grey line on Figure 3.9). This increasingly indented nature of the margin of Svínafellsjökull between 2007 and 2016 (Figure 3.9) is thought to reflect preferential melting and erosion along the flow-parallel longitudinal fractures during the downwasting and retreat of the glacier. This process may have also enhanced the highly fractured appearance of the surface of the glacier shown in Figures 3.2 and 3.15a.

The historical changes in the structural architecture of the snout of Svínafellsjökull during period of 1952-2012 are described in detail below.

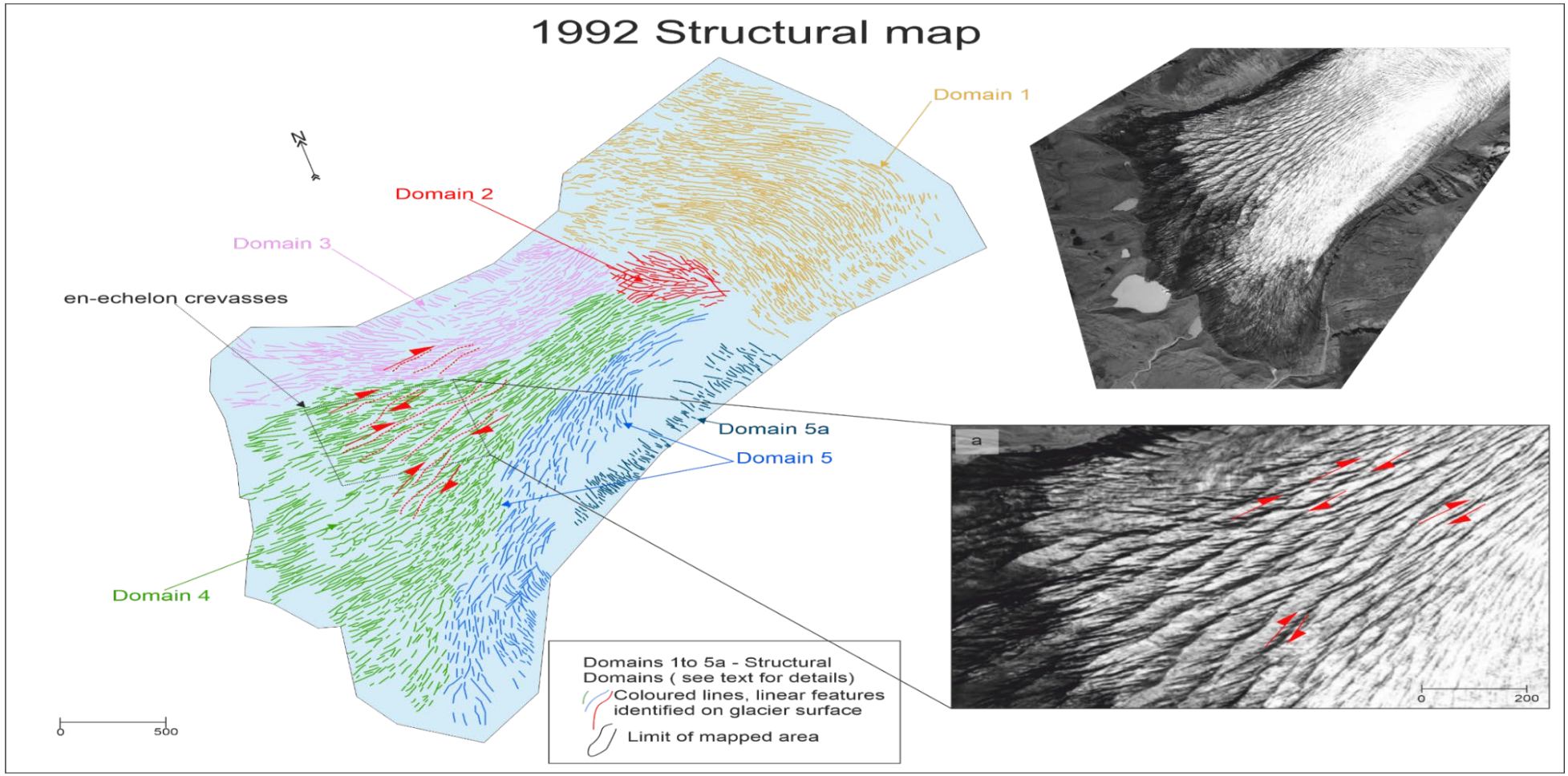

Figure 3.12: 1992 Structural map of Svínafellsjökull. Structural domains are depicted by different colours. Dashed box indicates an area of en-echelon crevasses. The structural map was constructed using the 1992 aerial photography acquired from LMI. Inset (a) aerial photograph showing area of en-echelon crevasses. Pink domains are the NWZ, green domains are the CZ and the blue domains are the SEZ.

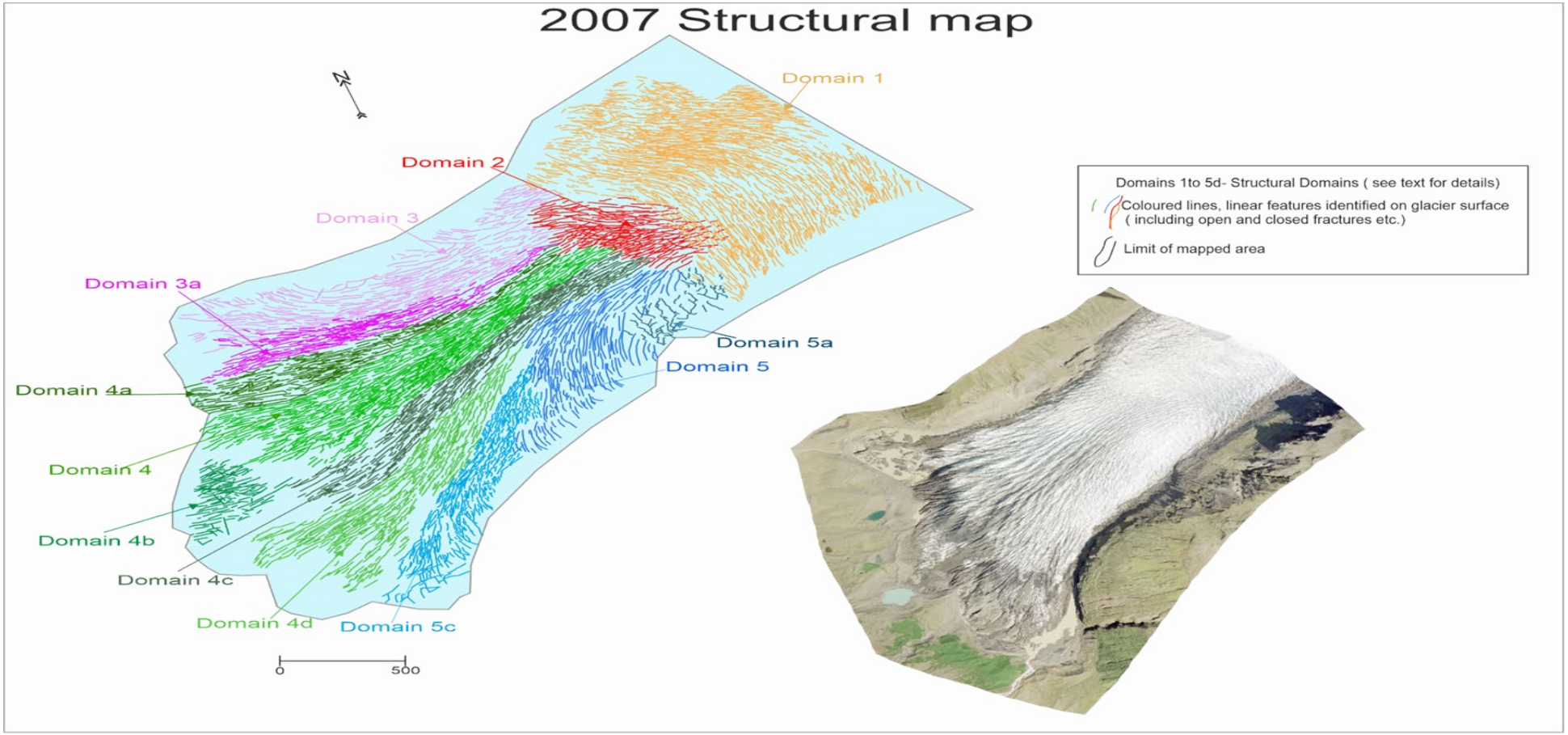

Figure 3.13: 2007 Structural map of Svínafellsjökull. Structural domains are depicted by different colours. The structural map was constructed using the NERC ASRF 2007 imagery. Pink domains are the NWZ, green domains are the CZ and the blue domains are the SEZ.

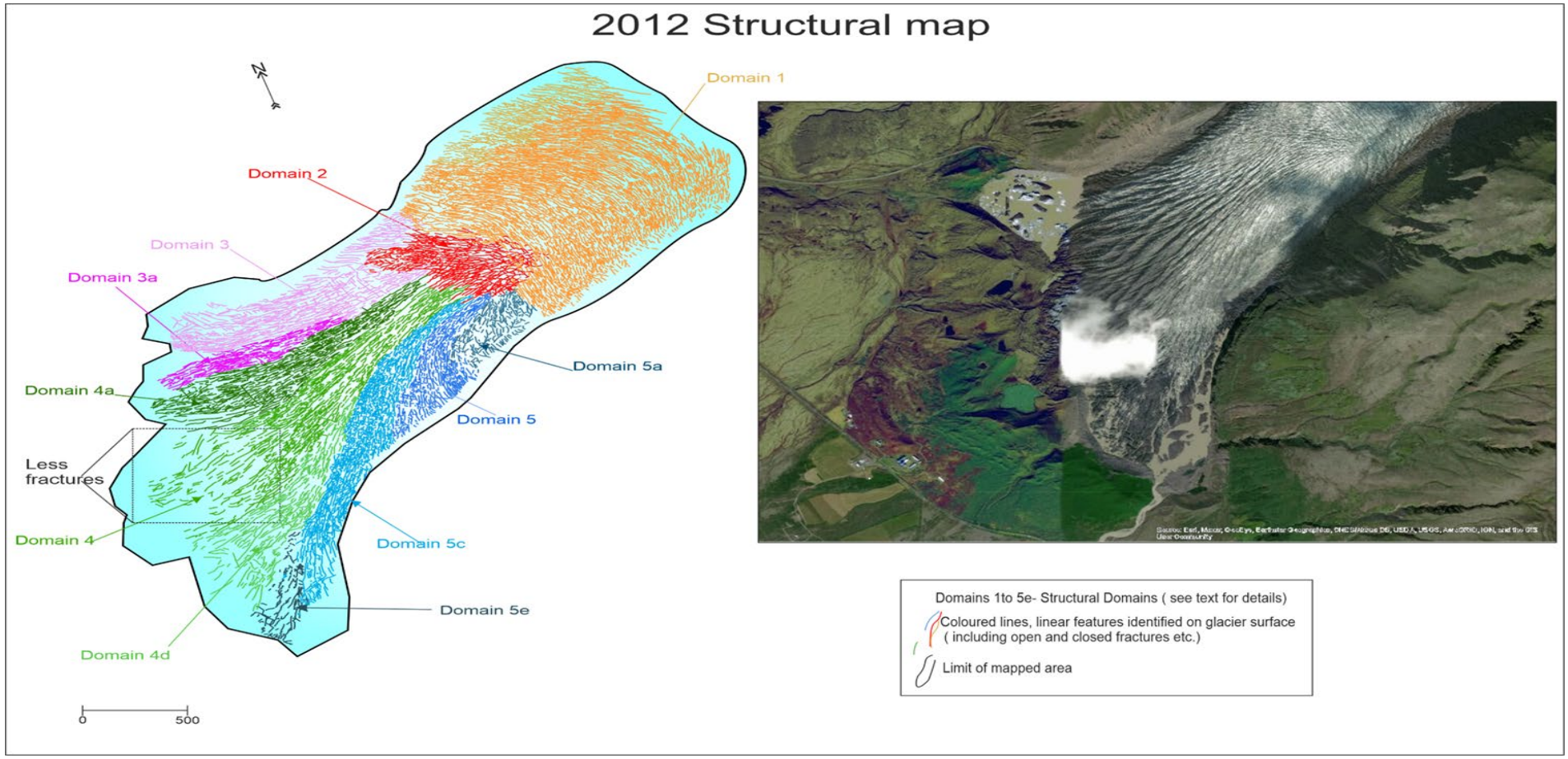

Figure 3.14: 2012 structural map of Svínafellsjökull. Structural domains are depicted by different colours. The structural map was constructed using the image which was taken from the Arc GIS Esri World Image Basemap layer (Source: Esri, Maxar, Earthstar Geographics, and the GIS User Community). Pink domains are the NWZ, green domains are the CZ and the blue domains are the SEZ.

3.5.1 North-western Zone (NWZ)

In 1952 the north-western zone of Svínafellsjökull was composed of a single structural domain (Domain 3; Figure 3.10, Appendix 3) and characterised by a curved to hook-shaped crevasse pattern. These open to closed fractures curve towards the northern margin of the glacier where they progressively become more NW-orientated and comprise of smaller (shorter/less laterally extensive) hook-shaped features (Domain 3, Figure 3.10, Appendix 3). This style of fracturing is considered to reflect deformation resulting from the lateral shear stresses (Sharp *et al.*, 1988; Benn and Evans, 2010; Colgan *et al.*, 2016) imposed on Svínafellsjökull as it flowed past the sub-vertical valley side. This pattern of crevasses adjacent to the north-western margin of Svínafellsjökull was also recognised in 1988 (Figure 3.11, Appendix 4), indicating that there had been very little change in the structural architecture of the NWZ in over 30 years.

In 1992, however, the structural complexity of the NE-SW trending NWZ began to change. At this time the NWZ can be subdivided into two domains (Domains 3 and 3a, Figure 3.12, Appendix 5) characterised by a series of laterally extensive, arcuate and approximately ENE-WSW-trending fractures that curved northwards towards the valley-side. Other changes in the structure of the lower zone in the period between 1988 and 1992 are an increase in the relative size of Domain 3. Importantly there is very little structural change within Domain 3 between 1952 and 2007, indicating that the ice within the northern zone may have been either static, very slow moving or under a uniform stress regime. The only addition in 2007 is the occurrence of a zone of westward curving longitudinal crevasses (Domain 3a, Figure 3.13, Appendix 6 and compare maps in Figure 3.6, Appendix 2) within the NWZ immediately adjacent to the boundary with Domain 4, which dominates the central zone (CZ).

Field observations in 2016 (Figure 3.15 a and b) revealed that in cross-section (approximately parallel to flow) the NWZ comprised an upper unit of clean (debris-free) ice overlying a much darker, relatively debris-rich unit, the latter representing a debris-rich basal ice facies. The traces

of the larger fractures within the upper clean ice facies are highlighted by the concentration of dark coloured debris. These fractures have been widened as a result of a combination of deformation of the ice at the retreating glacier margin and erosion by surface supraglacial runoff, with the debris being washed into these structures by the meltwater. The relatively debris-rich ice facies could be traced along the base of an ice-cliff and were well-exposed close to the northern side of the valley (Figure 3.15a). In detail this basal ice facies comprised alternating light (clean) and dark (debris-rich) bands, defining a gently to moderately up-ice dipping layering. The variation in dip of this banding, coupled with the presence of low-angle, cross-cutting relationships between the layers, suggest that the basal ice facies had been tectonically thickened as a result of low-angle, SE-directed thrusting (Hambrey and Lawson, 2020). Cook *et al.* (2007) have also identified stratified basal ice within this area at Svínafellsjökull (see chapter 4).

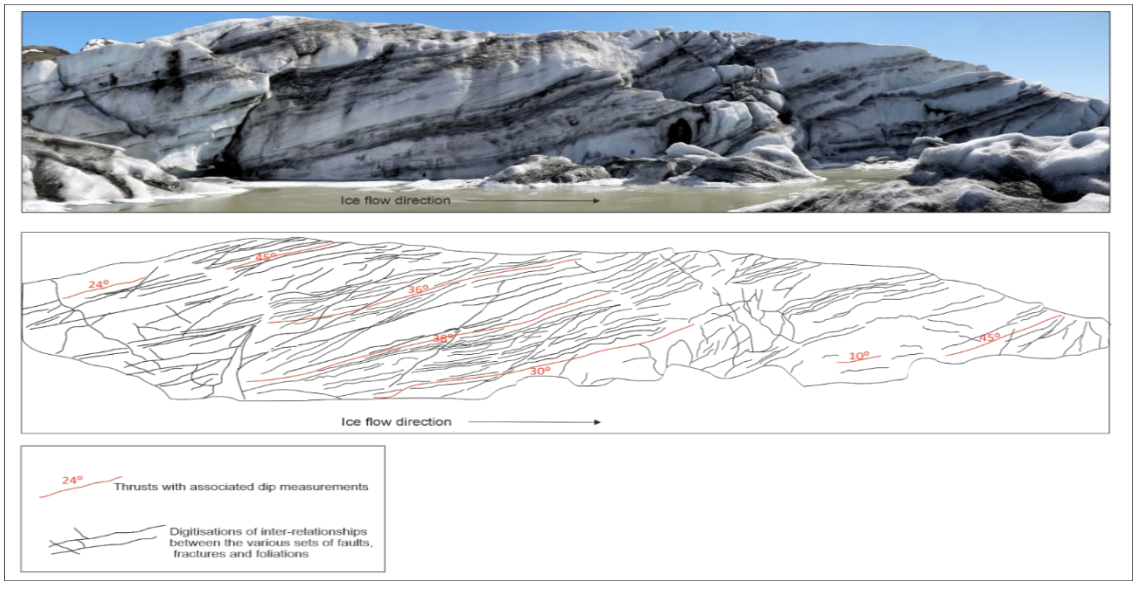

Figure 3.15: Field evidence of compressional flow at the margin of Svínafellsjökull. Top image taken at N:63.99724° W:16.87983°. Bottom image is digitisations of banding, and exposed deformation structures with associated dip measurements.

The structure of the NWZ in 2012 (Figure 3.14, Appendix 7) was characterised by a series of laterally extensive, arcuate, approximately ENE-WSW-trending longitudinal (flow-parallel) fractures (Domains 3 and 3a) which curved westwards near to the margin of the glacier, crudely

following the shape of the steep cliff-line forming the valley side. There is very little change within the NWZ between 2007 and 2012 (compare Figures 3.13, 3.14, Appendix 7 and maps within Figure 3.6. Appendix 2). The presence of icebergs within the lake is reflective of a periodic calving. As seen in the aerial photograph in Figure 3.14, (Appendix 7), the margin of the NWZ appears to dip beneath the surface of the proglacial lake at its margin and there is no obvious calving ice cliff. The large bergs present in the lake may have been formed due to the detachment of slab-like blocks of ice from under the surface of the lake, the latter being partially supraglacial in nature. The detached bergs would have floated to the surface due to the positive buoyancy of the ice. A distinctive, large V-shaped re-entrant in the margin of the NWZ appears to coincide with a marked increase in the intensity and/or density of the closely spaced longitudinal fractures within the ice that marked the boundary between Domains 8 and 10 (Figure 3.17a and b). The nature/structure of the boundary between the NWZ and CZ has not altered between 2007 (Figure 3.13, Appendix 6) and 2012 (Figure 3.14, Appendix 7) and is marked by a zone of well-developed S-shaped to sigmoidal tension fissures which recorded a dextral sense of shear (Figure 3.16c, see 3.16e for diagram of shear zones taken from Phillips *et al.*, 2017). The geometry of these shear zones is consistent with the westward flow of ice within the CZ at Svínafellsjökull.

Observations made during field seasons in 2017, 2018 and 2019 provide evidence for the periodic draining of the proglacial lake at the margin of the north-western zone, leaving icebergs stranded along the shoreline. During September 2018, 24 to 48 hours after a lake draining event, water was observed to be flowing back under the ice (Figure 3.15b). Observations by glacier tour guides suggest that periodic draining of this lake happens throughout the summer months each year and the periods between lake drainage events can be as short as 24 hours.

3.5.2 Central Marginal Zone (CZ)

In 1952 the central zone (Domain 4, Figure 3.10, Appendix 3) occupied the majority of the glacier margin, becoming narrower up-ice where it apparently originated from an area of highly

fractured ice represented by Domain 2. At this time, the structure of the CZ was characterised by flow-parallel longitudinal fractures orientated parallel to the central axis of the glacier. At the boundary between the CZ (Domain 4) and the NWZ (Domain 3) the cross-cutting relationships indicate that the longitudinal crevasses within Domain 4 are locally truncated by fractures defining the margin of Domain 3. The morphology of the open longitudinal fractures within the CZ changes from long (70 to 100 m), laterally extensive, relatively continuous fractures within the up-ice part of the Domain 4, to much shorter (20 to 15 m) features close to the glacier margin. Domain 4 is considered to be representative of the structure of the ice overlying the adverse slope formed by the moraine amphitheatre (Magnússon *et al.*, 2012), with the longitudinal fractures splaying outwards as Svínafellsjökull exited the confines of its valley and resulted in the formation of the piedmont lobe.

In 1988 the CZ of Svínafellsjökull still displayed this crevasse pattern, which is considered to be characteristic of a radially flowing piedmont lobe (Figure 3.11, Appendix 4). However, in contrast to 1952, the structural architecture of the glacier in 1988 included discrete flow-parallel zones of differential shearing leading to the development of a number of strike-slip shear zones (see inset on Figure 3.11, Appendix 4). These shear zones are defined by sigmoidal, en-echelon, open tension fissures recording a dextral sense of shear and are most clearly developed adjacent to its boundary with the NWZ. Importantly the traces of the tension fissures and the linear fractures defining the lateral margins of the shear zones indicates that they are very steeply dipping to subvertical. This may be used to suggest that strike-slip deformation occurring between subvertical flow-parallel crevasses may potentially be more common than previous structural glaciological studies have suggested; these have typically emphasised the role of thrusting associated with compressive flow within glaciers (e.g. Swift *et al.*, 2018). It is possible that strike-slip deformation occurring between flow-parallel longitudinal fractures/crevasses (e.g. Phillips *et al.*, 2017) may play a more significant role in glacier flow than previously thought (see below).

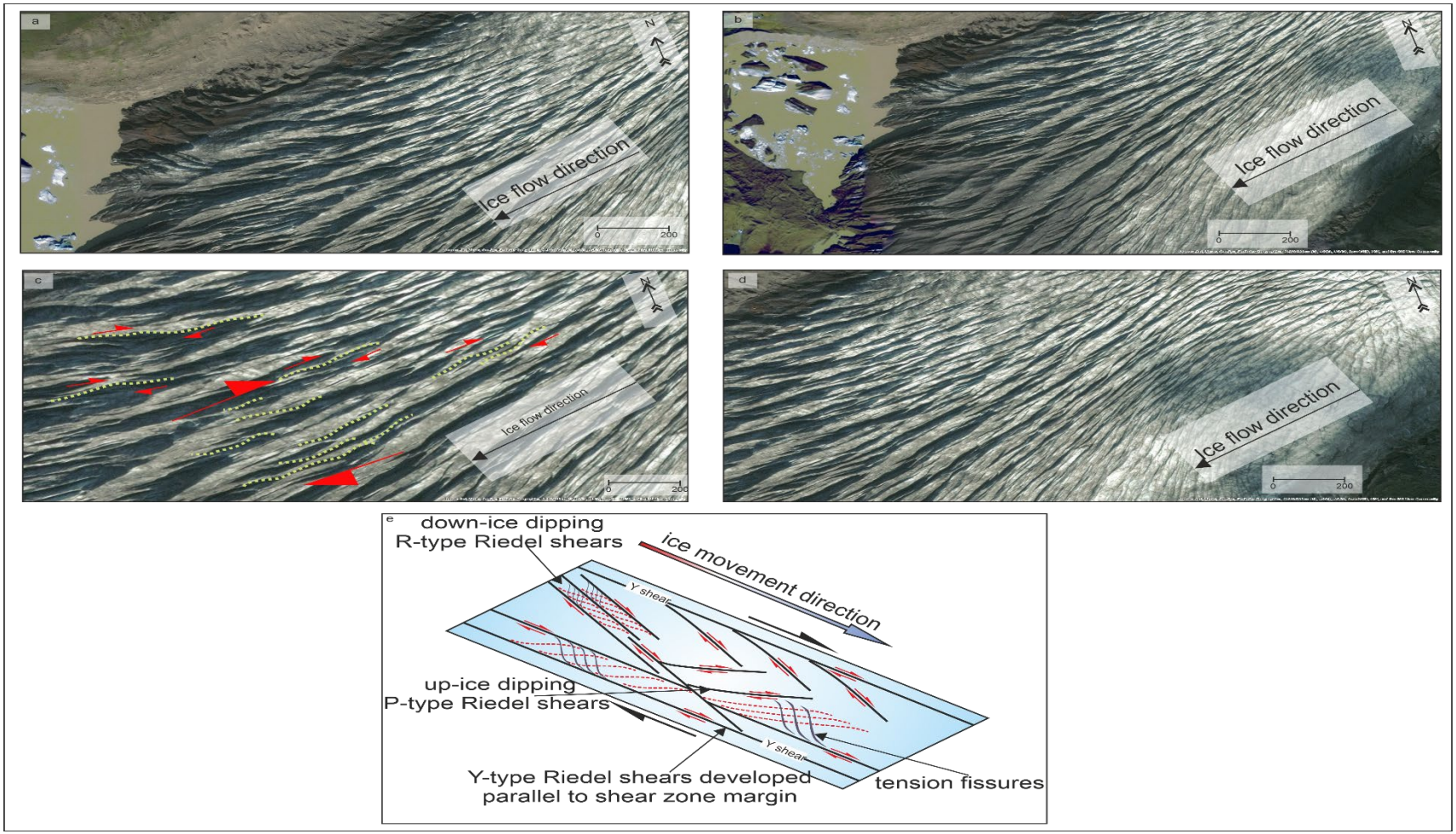

Figure 3.16 : Aerial photographs of structures on the ice; a) northern margin of Svínafellsjökull showing inlets exploited by proglacial lake; b) northern proglacial lake and central area of glacier; c) en-echelon structures apparent in 2007 and 2012; d) longitudinal crevasses within the central unit. (Aerial photograph sourced from Google Earth); e) a schematic figure showing the geometry of the various fractures related to strike slip/simple shear deformation including the various Riedel shears, taken from Phillips et al. (2017).

In 1952 the most intense fracturing occurred within the upper part of the CZ down-ice of Domain 2 (Figure 3.18) and in the lower reaches of the NWZ, close to the margin of Svínafellsjökull. The linear nature of the bands of higher fracture density (>12-13 fractures per 25 m^2) in these areas clearly indicates that deformation within the ice was largely being accommodated by the longitudinal, flow-parallel fracture sets, which dominate the structural architecture of both the CZ and NWZ. The fracture density map indicates that in 1952 deformation was focused towards the northern side of the glacier, with the lower fracture densities (typically below 7-9 fractures per 25 m^2) suggesting that the southern margin of Svínafellsjökull was relatively less "active". Furthermore, the area of more highly fractured actively deforming ice, narrows further up-ice, passing through Domain 2 and into a relatively small area of higher fracture densities (>13-14 fractures per 25 m^2) within Domain 1 (Figure 3.17). The area of increased fracturing within Domain 1 possibly reflects an increase in extensional deformation on the down-ice dipping crevasses caused as ice flowed into the lower reaches of Svínafellsjökull. Importantly the observed variation in fracture density, and thereby relative intensity of deformation within the ice, clearly indicates that in 1952, deformation within the lower part of Svínafellsjökull was concentrated towards the northern side of the glacier.

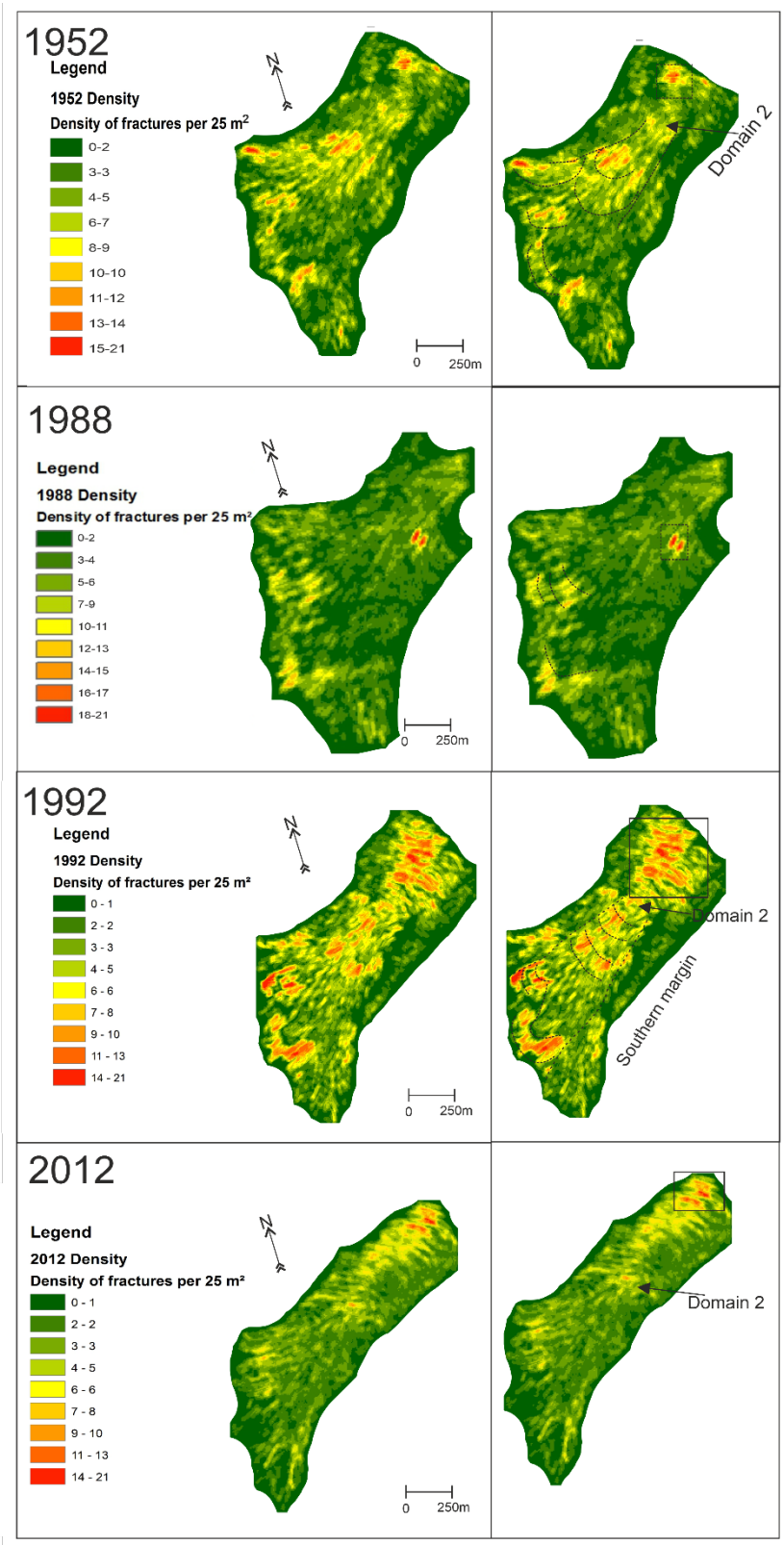

Figure 3.17: Fracture density maps calculated for the years 1952, 1988, 1992, 2007, and 2012. The variation in the density of factures can be used to highlight the changing spatial and temporal pattern of deformation within the ice. Maps on the right indicate interpretations which are discussed in the text.

In 1988 the wedge-shaped CZ (Figure 3.11, Appendix 4) continued to dominate the structure of the lower part of Svínafellsjökull. However, in contrast to 1952, the structures within this part of the glacier (Domain 4) include a set of well-developed en-echelon, sigmoidal (S-shaped) to hook-shaped tension fissures (Figures 3.11) which once again indicate that deformation within the CZ included a significant component of simple shear (Ramsay, 1963) accommodated by NE-SW-trending brittle-ductile shear zones. The dextral (right-lateral) sense of shear recorded by these shear zones is consistent with lateral shear (Sharp *et al.*, 1988; Benn and Evans, 2010; Colgan *et al.*, 2016) imposed by the relatively faster flow of ice within the central zone (Domain 4) relative to the apparently slower moving ice within the north-western zone (Domain 3) adjacent to the margin of the glacier. Importantly, in 1992 the area of dextral brittle-ductile shear within the CZ, indicated by well-developed open en-echelon (hook-shaped) crevasses, had increased (Figure 3.1, Appendix 5), with the geometry of these shear zones being consistent with ice flow towards the southwest. It is possible that the increase in the area of shear within the CZ between 1988 and 1992 is due to downwasting of the ice, revealing a deeper structural level within Svínafellsjökull close to its margin. However, in the early 1990's Svínafellsjökull was undergoing a period of minor readvance (Hannesdóttir *et al.*, 2015a and 2015b) with the observed increase in dextral shear occurring as the ice flowed up and spread laterally across the underlying adverse slope of the overdeepening.

In 1988 fracture densities across the entire surface of the lower part of Svínafellsjökull were low (typically < 5-6 fractures per 25 m^2; Figure 3.17). This suggests that flow-related deformation was at a minimum, or had possibly ceased, and that the lower reaches of the glacier may have entered a period of "quiescence" leading to increased downwasting and retreat. However, localised bands or areas of slightly more intense fracturing do occur close to the margin within the CZ (Domain 4). In marked contrast to 1988, in 1992 there is a significant increase in fracture density within Domains 1, 2 and the CZ (Domain 4). This can be attributed to a recorded readvance of Svínafellsjökull in the early 1990s (Hannesdóttir *et al.*, 2015a and 2015b), with increased deformation within the ice occurring as a result of higher rate of flow. The highest

fracture densities (14-21 fractures per 25 m^2) in 1992 occurred within the central part of Domain 1 and can be equated to increased extension on the down-ice dipping crevasses that characterise the structural architecture of this part of Svínafellsjökull. This extension occurs at the up-ice end of a crudely wedge-shaped area of relatively higher fracture densities corresponding to the CZ (Domain 4) (Figure 3.17c). Figure 3.17c also reveals the presence of an arcuate zone of highly fractured ice (density >11-13 fractures per 25 m^2) within the CZ immediately adjacent to the glacier margin. This feature is thought to potentially reflect thrusting of the ice as a result of compressional flow at the margin of Svinafellsjökull. Importantly, calculated fracture densities within the NWZ and SEZ were in typically much lower, consistent with the conclusion that these parts of the glacier were moving relatively slowly, or even static, and therefore accommodating very little, if any, deformation (see section 5).

In 2007 the CZ (Domain 4) appears to emanate/originate from the southern end of the overdeepened trough identified beneath the axis of Svínafellsjökull by Magnússon *et al.* (2012). Domains 4, 4a, 4b, 4c and 4d clearly indicate that the structure of the CZ was dominated by NW-SE-trending longitudinal, flow-parallel crevasses (Figure 3.13, Appendix 6) with the resulting radiating fracture pattern being consistent with the lateral spreading of Svínafellsjökull as it flowed out of the confines of its valley. More specifically, the boundary between the NWZ and CZ was marked by a zone of S-shaped tension fissures, which recorded a dextral (right-lateral) sense of shear. The geometry of this dextral shear zone indicates that it represents a significant structural boundary within the ice, with the sense of shear being consistent with the flow of ice within the CZ towards the southwest.

Detailed mapping of the structure of the CZ in 2007 has revealed that the spacing of the laterally extensive longitudinal fractures decreased up-ice, resulting in an apparent increase in the relative intensity of fracturing. Importantly the fracture sets identified in both the NWZ and SEZ (see below) are truncated against the dominant structures within the central part of the glacier, resulting in marked angular discontinuities between the dominant structural grain of each of the

marginal zones. These cross-cutting relationships are interpreted as the product of movement and/or flow within the CZ of the glacier that post-dates (i.e. is relatively younger) than that recorded by the deformation within the adjacent marginal zones. One potential explanation is that this relationship results from the CZ moving relatively faster than the NWZ zone and SEZ. Alternatively, the marginal zones may have ceased to move (i.e. they were static) and as a consequence the more recent flow has been preferentially focused along the central axis of the glacier. This could be related to a combination of a change in the volume of ice moving through the system, coupled with the thinning of the ice margin, changes in ice flux through the overdeepening and the impact(s) of bed topography on the pattern of flow/deformation within the thinning margin of the glacier as it retreats into the overdeepening.

This detailed analysis reveals that there was very little structural change within the CZ between 2007 and 2012 (compare Figures 3.13 and 3.14). Importantly structures within the CZ clearly truncate the fracture sets identified within both the NWZ and SEZ, indicating that the proposed preferential flow of ice along the axis of the glacier continued to impact the structural architecture of the margin at Svínafellsjökull. Although Domain 4d was recognisable as a broadly triangular-shaped area dominated by NW-SE-trending longitudinal fractures, the surface of this domain was largely obscured by debris. This debris is thought to be at least partially derived from the melt-out of a number of englacial eskers (Figure 3.18) (cf. Spedding and Evans, 2002; Bennett and Evans, 2012; also see Chapter 4). These eskers represent former englacial drainage channels that are thought to have facilitated the redistribution of debris initially deposited on the glacier surface by rock slope failures from the northern slopes of Svarthamrar (Chapter 4).

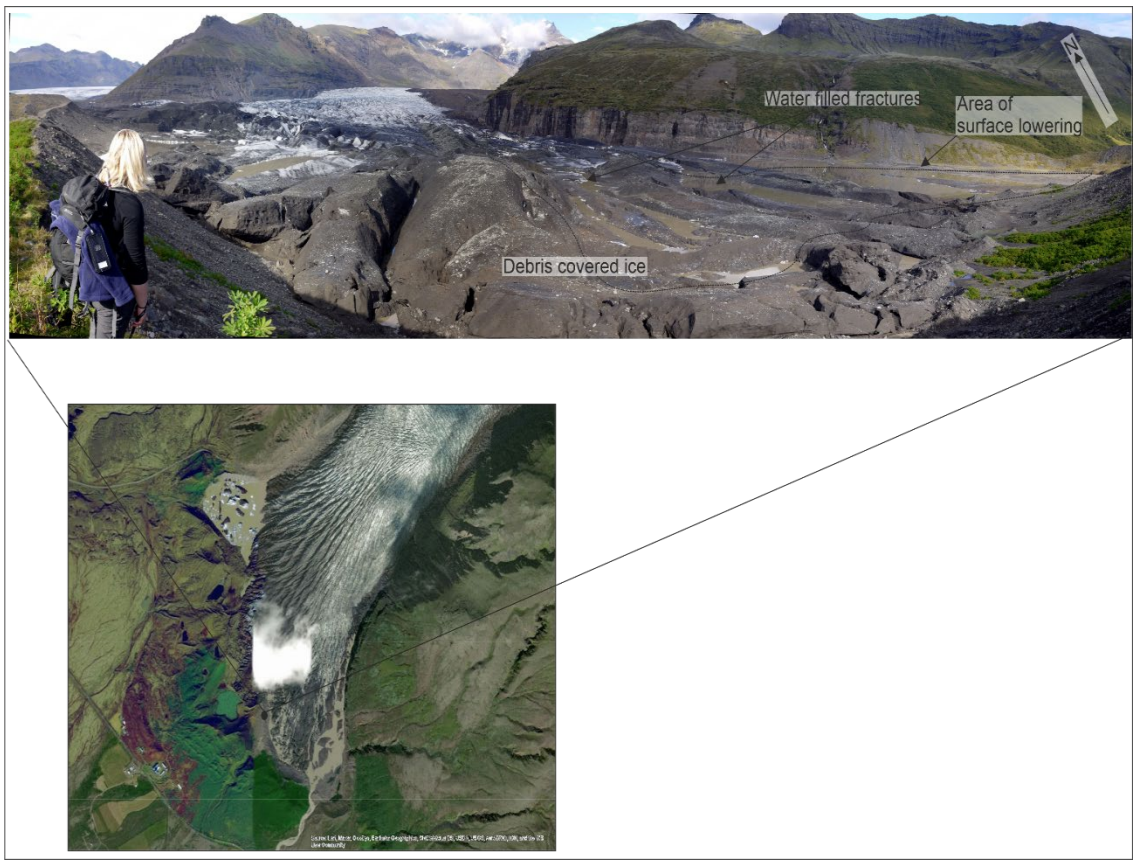

Figure 3.18: Panoramic view from the southern side of the glacier looking to the north.

Observations made during field work in August-September 2017 clearly demonstrate that the margin of the CZ was overriding a small-scale (c. 1 to 1.5 m high) push moraine composed of poorly sorted sands and gravels (Figure 3.19). This moraine is considered to have formed during the previous winter (2016-17) readvance/oscillation, consistent with an overall pattern of active glacial retreat. However, the continued forward motion and overriding of this recessional push moraine in August 2017 indicates that the CZ of Svínafellsjökull continued to move during the summer months. This observation is compatible with the proposal of Chandler *et al.* (2020a and 2020b) that push moraines in this part of Iceland have recently been constructed at a rate of more than one per year. In contrast to the highly fractured nature of Svínafellsjökull in 1992, the fracture density map for 2012 (Figure 3.17) clearly shows a marked decrease in fracture density (typically < 3 fractures per 25 m^2) which is considered to reflect a significant decrease

in deformation within the ice, possibly coinciding with a period of increased downwasting and retreat.

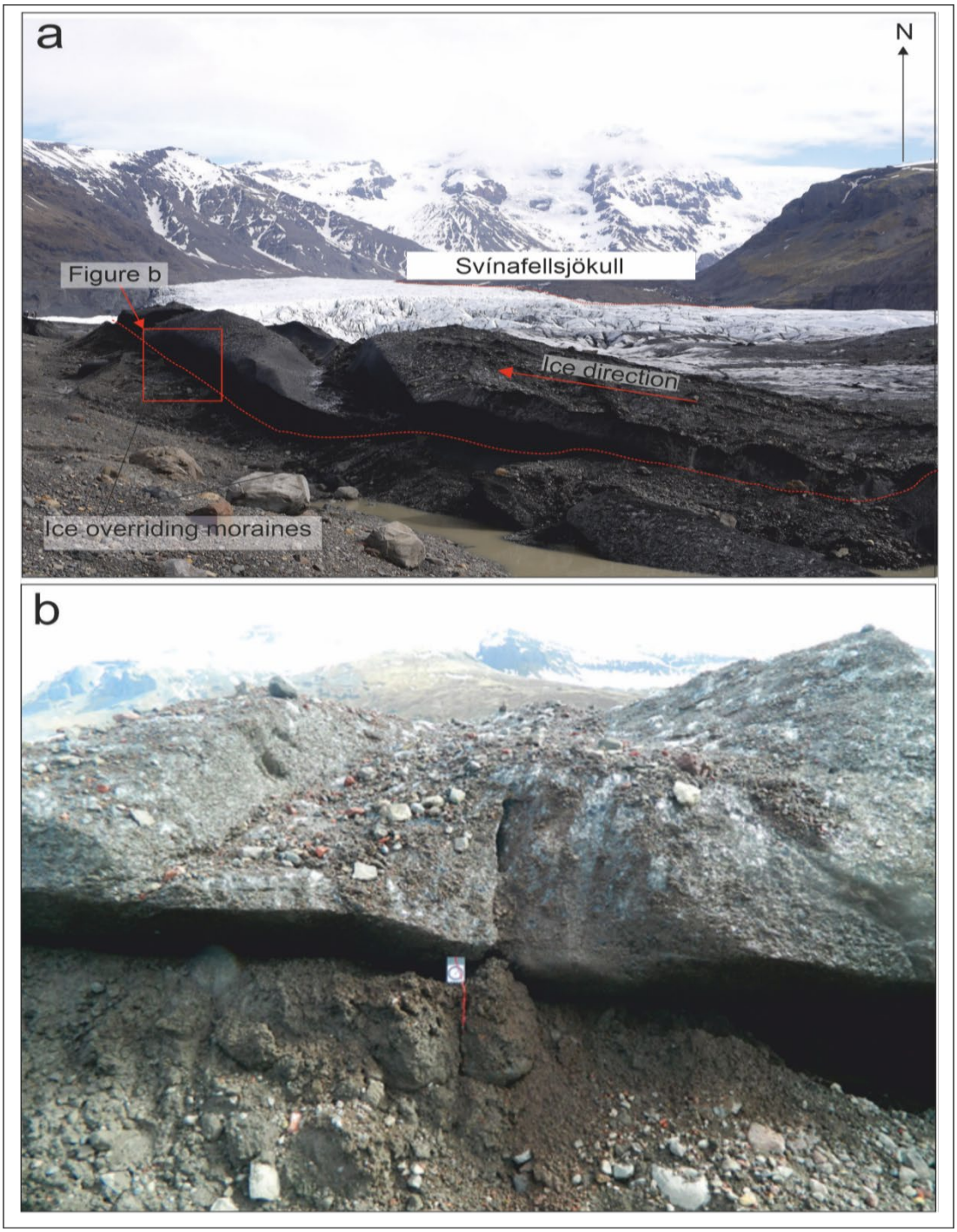

Figure 3.19: Field evidence for focused flow within the central lobe: a) photograph taken in August-September 2017 (looking north) showing the margin of the central lobe overriding a relatively substantial 1.5 to 2 m high recessional moraine. Also note the marked difference in the height of the glacier surface due to differential surface ablation resulting from the presence of rock slope failure debris on the surface of the ice, the margin of this supraglacial deposit is depicted by the red dashed line; b) photograph taken at location: N:63.98976° W:16.66784° showing a close up of the margin of the central lobe overriding the recessional moraine (compass for scale).

Further evidence of compressional flow leading to thrusting (low-angle reverse faulting) adjacent to the margin of the CZ of the glacier was observed in 2017 (Figure 3.16). This thrusting is thought to have occurred in response to compression within the marginal zone of Svínafellsjökull as it moved against the moderate to steeply dipping adverse slope on the up-ice side of the 1992 readvance moraine. Swift *et al.* (2018) argued that at Svínafellsjökull, thrusts result in the incorporation of 10 cm thick bands of stratified debris-rich basal ice into the glacier, substantially contributing to the transfer of subglacial material in the terminal zone. They state that the entrainment and transfer of this debris occurs by simple shear along the upper surface of debris bands and by strain-induced deformation of stratified glacier ice. They also found that debris within the thrust basal ice included striated, rounded to well-rounded clasts, which they concluded indicate that fluvial bedload deposited in subglacial channels was being entrained into the base of the ice and then incorporated into the overriding glacier as a result of thrusting.

3.5.3 South-eastern marginal zone (SEZ)

On the southern side of Svínafellsjökull, the structures mapped within the CZ (Domain 4) clearly truncate the SSW-SSE-trending fractures identified within the SEZ (Domains 5 and 5b; Figure 3.10-3.14, Appendix 3-7 and Figure 3.6, Appendix 2). Importantly, these cross-cutting relationships indicate that deformation within the ice on the southern side of the glacier occurred prior to fracturing of the ice within the CZ, thereby indicating that there are temporal as well as spatial changes in the deformation within the marginal zones of Svínafellsjökull.

The SEZ of the glacier defined by Domain 5 increased in width between 1952 and 1988 (compare Figures 3.10 and 3.11; also see Figure 3.6, Appendix 2). This increase in width of the SEZ was accompanied by the loss of Domains 5a and 5b by 1988, indicating the structural architecture of the southern margin of Svinafellsjökull had become much simpler. At this time the dominant structure in the SEZ (Domain 5; Figure 3.11, Appendix 4) is a set of arcuate, approximately SSE orientated fractures (see rose diagram on Figure 3.3, Appendix 1) which curve southwards towards the margin of the glacier. The geometry of these essentially hooked shaped fractures is

consistent with them having formed in response to lateral shear imposed on the ice as it flowed past the sub-vertical valley side (Sharp *et al.*, 1988; Benn and Evans, 2010; Colgan *et al.*, 2016). In 1992, however, the structural complexity of the SEZ had increased, with the formation of Domain 5a immediately adjacent to the southern margin of the glacier and characterised by short, approximately N-S-trending, transverse crevasses developed orthogonal (90°) to the valley side.

In 2007 the SEZ was once again characterised by an arcuate fracture pattern (Domain 5 Figure 3.13, Appendix 6), with the crevasses curving towards the south. In detail, however, the SEZ could be divided into three domains: (i) Domain 5a, displaying a chaotic fracture pattern, contrasting with 1992 when the fractures in this part of the glacier were relatively straight, transverse structures; (ii) the arcuate, hook-shaped fractures of Domain 5b; and (iii) the elongate Domain 5c defined by weakly curved to straight crevasses, with a locally more complex fracture pattern within the ice close to the margin. The more complex pattern of fracturing adjacent to the margin of the SEZ, represented by Domain 5c (Figure 3.13, Appendix 6), is likely to be related to localised deformation within the ice associated with increased buoyancy at this water terminating margin (see aerial photograph on Figure 3.13, Appendix 6). However, overall the structure of the SEZ (Domains 5, 5a, 5b and 5c) has remained largely unchanged since 1952, consistent with the interpretation that this part of the glacier is either very slow moving or essentially static, with the structures within Domain 5 preserving a pre-existing pattern of glacier flow. This interpretation is compatible with field observations of downwasting/collapse and widening water-filled crevasses and re-entrants within this part of the snout relating to this part of the glacier being under a uniform flow and stress regime.

The SEZ in 2012 was c. 2.2 km long and up to 540 m wide, being narrowest towards the east and widening to the west, where the surface of the glacier dipped gently beneath the surface of the supraglacial/proglacial lake drained by Svinafellsá (Figure 3.14, Appendix 7). The SEZ has been divided into four domains (Domains 5, 5a, 5c and 5e; Figure 3.14, Appendix 7) with the majority

of the zone displaying the same structural characteristics as in 2007 (compare Figures 3.13 and 3.14). However, the increase in the structural complexity at the margin of the SEZ (Domain 5e) where the ice enters the proglacial lake is consistent with the localised increase in the positive buoyancy of the ice associated with the growth of this lake. As there is no steep, calving margin to Svínafellsjökull at this water terminating margin, the large, apparently slab-like icebergs within the lake are thought to have been released from ice beneath the surface indicating that the lake is in fact partially supraglacial in nature.

3.5.4 Structural changes within Domain 2 between 1954 and 2012

As previously stated, Domain 2 does not alter in terms of its position on the glacier surface or its structural configuration, suggesting that it is a result of a discrete substrate feature. However, the size and complexity of the pattern of fractures within this domain do change over time. Figure 3.20 shows that Domain 2 occupied the smallest area on the ice (62,855 m^2) in 1952, and then increased considerably in size between 1952 and 1988 (95,079 m^2). It was at its largest in 2007, when it covered 135,241 m^2 of the glacier surface. Figure 3.20 also shows that the complex network of fractures within Domain 2 are all open (i.e. extensional) with this domain potentially representing an area of surface collapse or flow acceleration. This is supported by the majority of the area showing a negative elevation change. The increase in size of Doman 2 between 1957 and 2007 may indicate that the area of collapse was expanding. For this to occur it would require an accommodation space to form beneath Domain 2, or a change in ice thickness and flux. Alternatively, the accommodation space could have been created by the drainage of ponded meltwater below Domain 2; changing reservoir size over time could be controlled by a combination of variations in meltwater production, the amount of meltwater reaching the bed and changes in glacier discharge through the bed depression.

The slightly higher fracture density observed within Domain 2 (c. 9-10 fractures per 25 m^2) corresponds to the opening of the complex network of fractures characterising this domain and associated collapse of the ice.

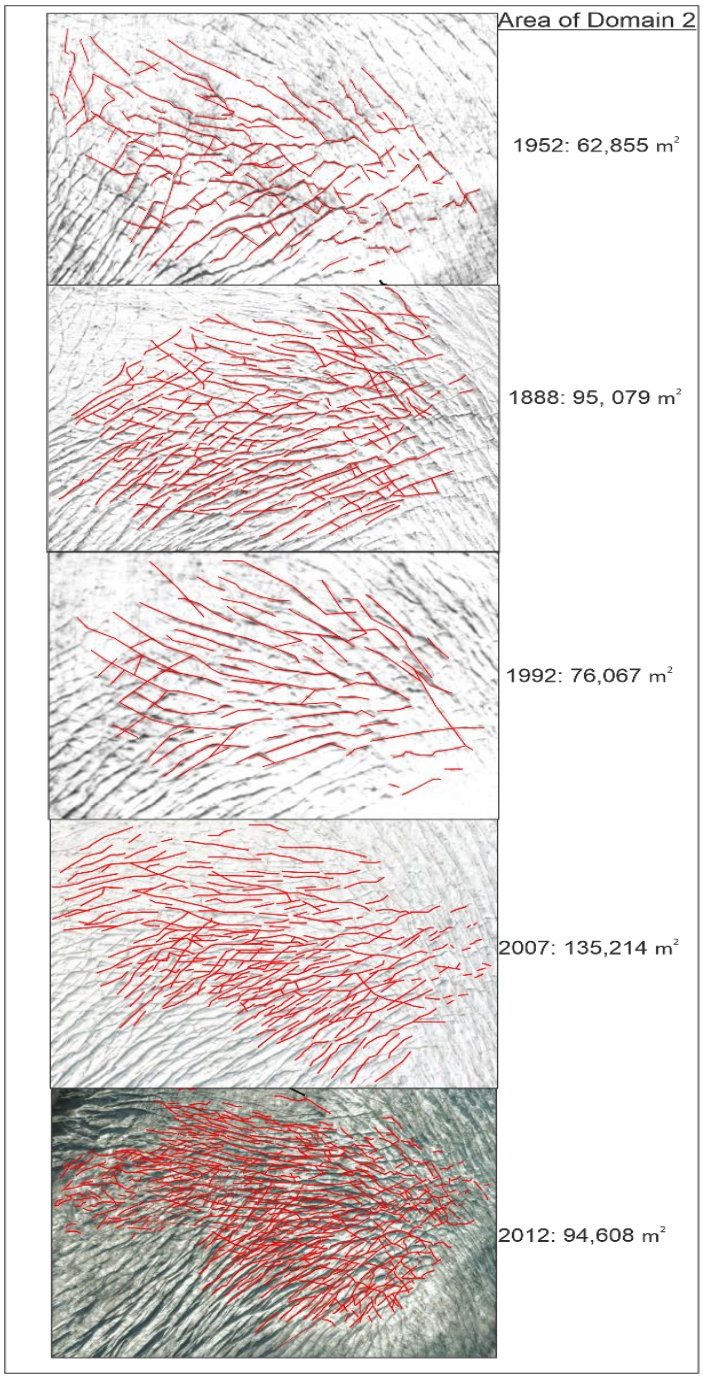

Figure 3.20: A series of aerial photographs showing the changes in the size of Domain 2 between 1952 and 2012.

3.6 Ice Surface Elevation Change

Ice surface elevation change analysis was limited to the years of 2013-2015 due to data availability (Figure 3.21). Overall, there is a calculated c. 28 m rise in surface elevation in this time period reflecting an increase in the volume of ice within the CZ (Domain 4) of Svínafellsjökull. The debris on the surface close to the margin of the glacier (see Figure 3.18) is likely, at least in part, to be responsible for the observed increase in elevation in this area due to an associated reduction in the rate of ablation. This agrees with Swift *et al.* (2018), who also identified a similar positive elevation change in this area of Svínafellsjökull. However, the linear, approximately E-W-trending bands of higher elevation (Figure 3.22) which occur parallel to the axis of the glacier clearly correspond to the upstanding "blades" of ice formed between the deep, open crevasses that mark the longitudinal fractures dominating the structure of the CZ (compare Figures 3.14 and 3.22 and 3.22). Figure 3.21 also highlights that, between 2013 and 2015, more ice is being drawn from the up-ice area (Domain 1), where there is negative elevation change (lowering of the surface), to the marginal zone of the glacier (area of positive elevation). This change from a relatively negative elevation to positive elevation corresponds to the area of the glacier occupied by Domain 2. However, it is important to also highlight that elevation increases could also reflect a decrease in subglacial water erosion (i.e., melting of ice from beneath).

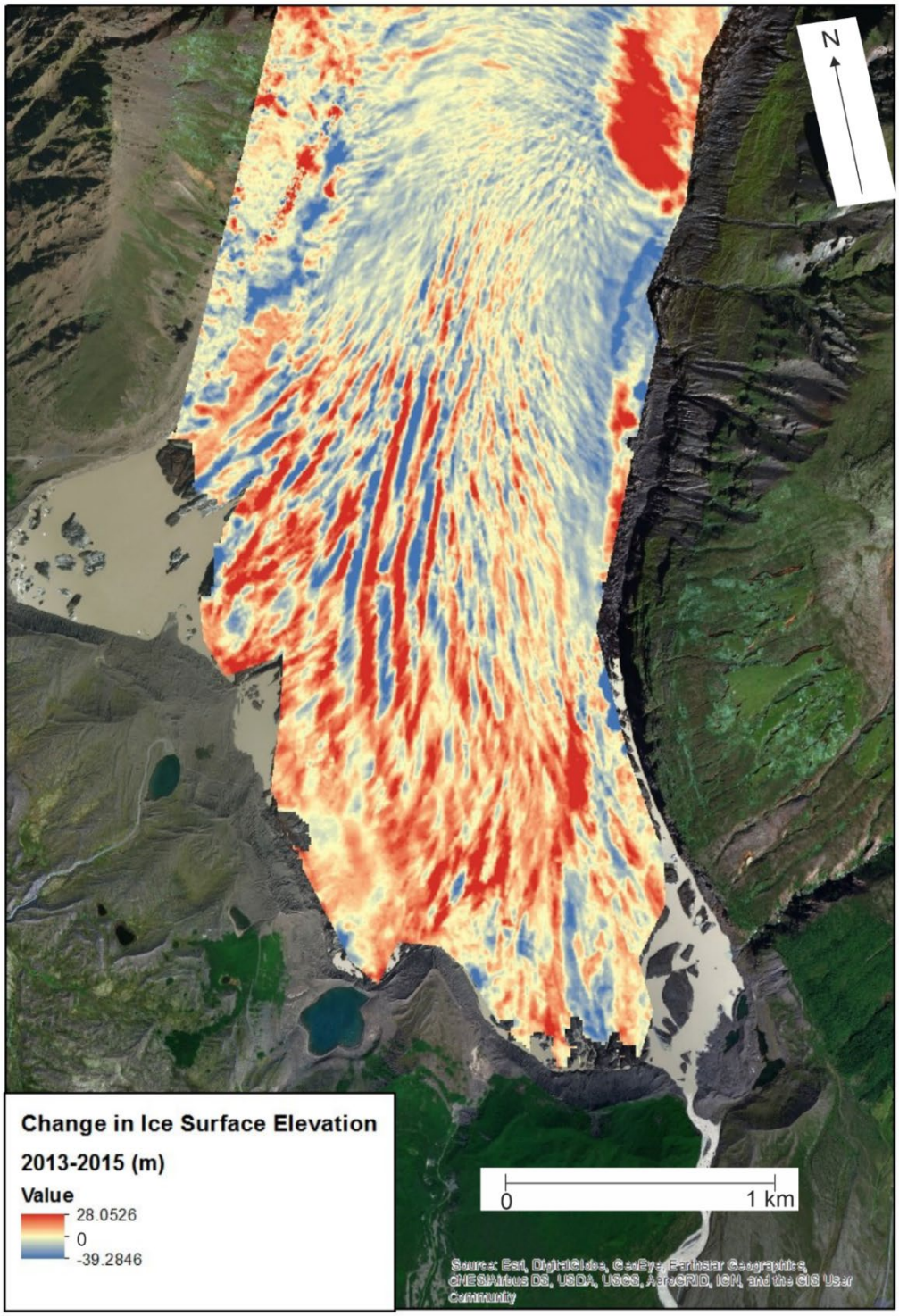

Figure 3.21: Changes in Ice surface elevation at Svínafellsjökull between 2013 and 2015.

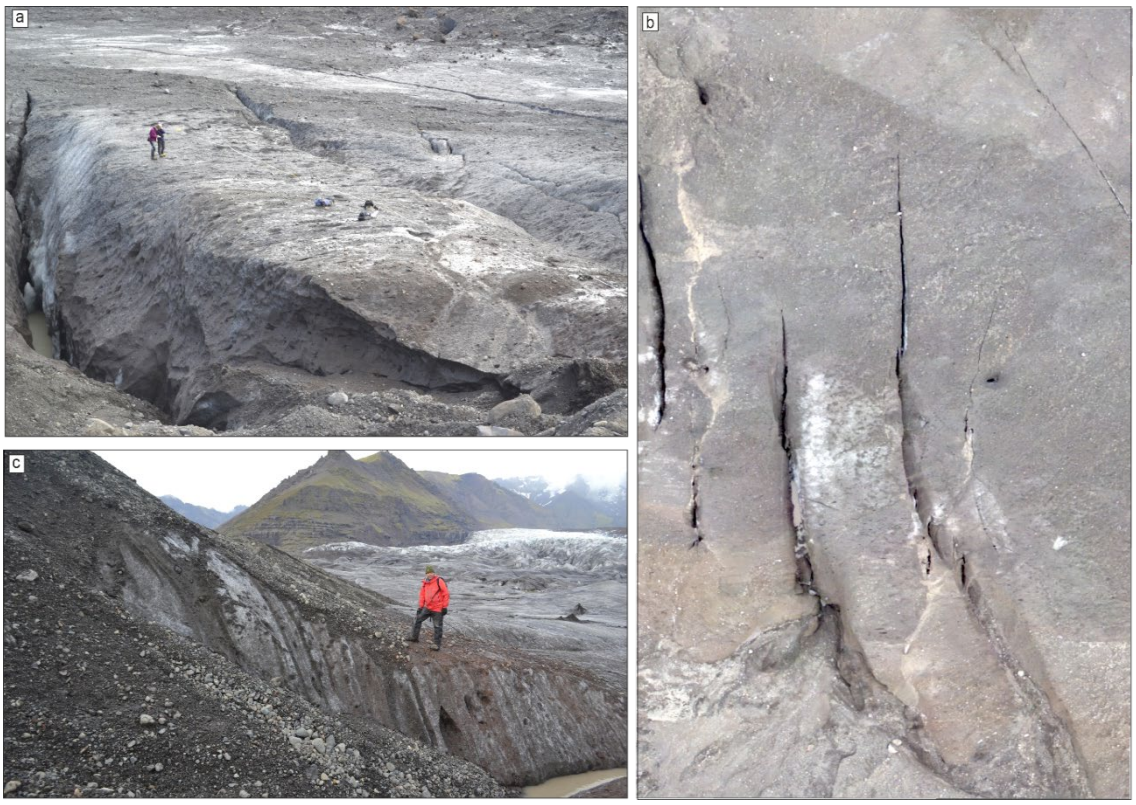

Figure 3.22: Open longitudinal fractures and intervening low-lying, flat-topped pecten observed at the margin of the central zone. Photographs taken at N:63.99648° W:16.87785°; a) View from margin of ice, looking south; b) oblique image of same area as shown in a; c) view looking northeast, showing open thrusting at margin.

3.7 Glacier velocities

Velocity data for Svínafellsjökull were generated for the period between 1986 and 2016 using auto-RIFT (Gardner *et al.*, 2018) and provided by the NASA MEaSUREs ITS_LIVE project (Gardner *et al.*, 2018). The resulting velocity maps for 1986, 1992, 1995, 2012 and 2016 are shown in Figure 3.23 and clearly highlight the persistent higher rate of flow (c. 1400 m yr^{-1}) in the vicinity of the steep ice-fall which feeds ice to Svínafellsjökull from its accumulation zone on Öræfajökull (see Figure 3.1). In 1986, high velocities can be seen to characterise the majority of the glacier surface, consistent with Svínafellsjökull actively moving as a coherent plug flow throughout most of its length. The much lower velocities at the glaciers' lateral margins are a result of the lateral frictional drag imposed where the ice comes into contact with the steep slopes of Eystra-Hrútsfjall, Vestara-Hrútsfjall, Sveltiskarð and Hafrafell. An area of lower velocity (88-49m yr-1)

within 0.5 km of the glacier snout, indicates that ice was decelerating at its terminus, potentially leading to compressional flow and the associated thrusting.

In contrast to 1986, in the period from 1992 and 2016 the surface velocities of Svínafellsjökull were considerably lower (c. 100 m yr^{-1}), with the only area of higher rates of flow in the lower reaches of the glacier corresponding to Domains 1 and 2. However, by 1995 the area of higher flow velocity in the lower part of the glacier had dissipated and the rate of flow at the snout had fallen significantly (40-50 m yr^{-1}). This cannot be reconciled with the observation that Svínafellsjökull underwent a period of readvance during the early 1990's, however this may indicate a period of quiescence after the readvance or could be an isolated area of higher velocity on the surface of the glacier in 1992. In 2012 a small area of relatively higher velocity (160-200 m yr^{-1}) had once again developed in the lower reaches of Svínafellsjökull, corresponding again to an observed increase in fracture density and extensional deformation within Domain 1. Also noted is a very small area of elevated velocity corresponding to the dextral shear zone marking the boundaries between Domains 4 (CZ) and 3 (NWZ), which developed between 1988 and 1992. By 2016 this area of higher flow velocity had apparently propagated both up and down-ice with an associated increase in velocity at the snout (~140 m yr^{-1}); the latter probably corresponds with the observed increase in surface elevation during the period 2013 to 2015. A very faint, narrow corridor of slightly high velocities (>140 m yr-1) can be seen extending up-ice, occurring immediately above the axial trough within the bedrock surface identified by Magnusson *et al.* (2012).

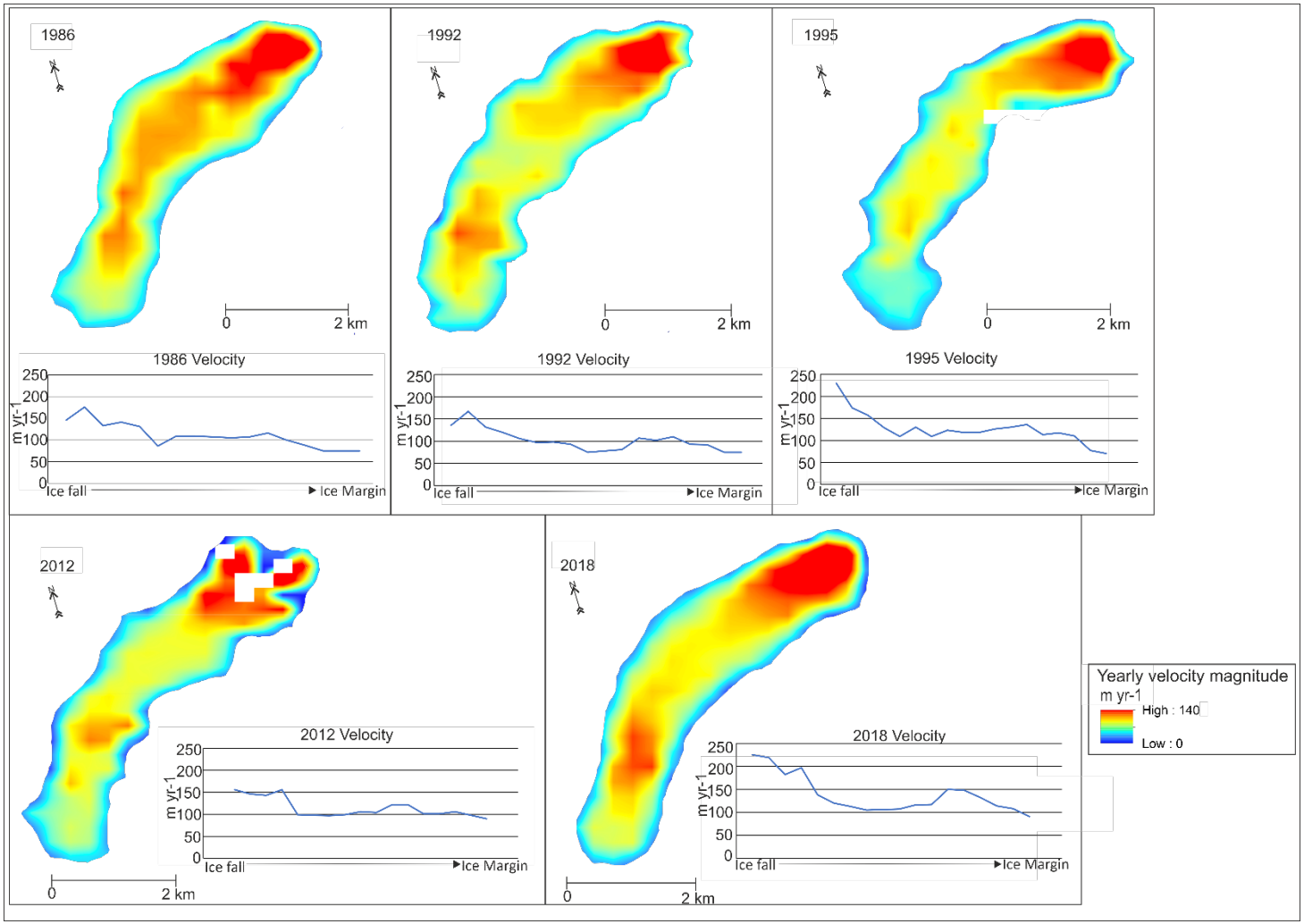

Figure 3.23: Annual ice velocity maps for Svínafellsjökull calculated using the NASA MEaSUREs ITS_LIVE project (Gardner et al., 2019). These surface velocity maps show the changing pattern of ice flow for the years of 1986, 1992, 1995, 2012 and 2018. Associated graphs show velocity changes through the centre line of glacier for each year.

3.8 Interpretation of the structural evolution of Svínafellsjökull

The regular view of the movement of a non-surging valley glacier is that ice flows as a single 'plug flow', with the entire glacier body moving en-masse down valley (Benn and Evans, 2010). Although initial results suggest that the structure of the upper part of Svínafellsjökull does indeed reflect this style of flow, the complex cross-cutting relationships of the splaying crevasses found in its piedmont lobe do not conform to the simple radiating crevasse pattern typically associated with such glacier morphologies (Sharp *et al.*, 1988; Benn and Evans, 2010; Colgan *et al.*, 2016).

The change from the more conventional structural architecture in the upper part of Svínafellsjökull to a structurally more complex multi-lobate morphology towards its margin is thought to initiate within Domain 1. These open, down-ice dipping fractures occur across the entire width of the glacier and indicate that the ice is undergoing significant extension parallel to flow. It is possible that these crevasses represent the surface expression of a series of closely spaced, down-ice dipping extensional (normal) faults which formed within <300 m of the structurally more complex marginal zone of the glacier. Consequently, these structures can be used to demonstrate that the glacier immediately up-ice of the structurally complex marginal zone is undergoing extension and possible thinning. This may possibly reflect the failure of the marginal zone into the overdeepening. In effect the structurally complex marginal zone is acting like an extensional failure mass, with the transverse down-ice dipping fractures charting the up-ice migration/propagation of the headwall of this system. The overdeepening in the bedrock surface underlying the marginal zone of the glacier would provide the accommodation space for the failed snout ice. There is also potential for ponding of subglacial meltwater in this overdeepened area beneath the ice which would have promoted the destabilisation of the overlying ice mass observed within Domain 2.

Despite these characteristics, the up-ice terminations of the three marginal zones, which characterise deformation in the lower part of the glacier, are all "rooted" into an area underlying the highly fractured ice (Domain 2) located on the down-ice side of this zone of extensional flow (Domain 1). This area corresponds to the loss of the ogive banding within the glacier that had been present up-ice in Domain 1. Initial results suggest that Domain 2 represents an area of instability or constriction within the ice which occurs immediately above the down-ice opening of the narrow axial trough within the bed of Svínafellsjökull (Magnusson *et al.*, 2012). This conclusion is compatible with the fact that this area of highly fractured ice occurs in exactly the same position and does not move up or down ice, but rather changes in size and shape between 1952 and 2012. This is thought to reflect an increase in the cause of the instability/constraint underlying this part of the glacier, possibly accentuated by the overall thinning of the ice and the increasing influence of the bed topography on its internal structure. This is also shown in the velocity data, as in each velocity map, Domain 2 is characterised by higher velocities compared to the surrounding ice. One possible underlying cause for the higher velocities in this area could be related to the concentration of subglacial drainage or even ponding of meltwater within this part of the overdeepened trough. This ponding could be due to the increased collapse associated with periodic draining of the subglacially stored meltwater and/or an increase in basal sliding. Alternatively, Domain 2 could represent the surface expression of a topographic constraint within the bed (i.e. the trough identified by Magnusson *et al.*, 2012) which, as the glacier progressively thinned, caused the increased funnelling of the ice through this constriction, resulting in preferential concentration of flow along the central axis of the glacier (Domain 4; Figure 3.24). The detailed mapping of the structure of the marginal zone of Svínafellsjökull presented here clearly indicates that this is not a recent phenomenon but has been established for at least the past 10 to 15 years. Consequently, it is unlikely that changes in the structures within Domain 2 is associated solely with the thinning of the ice during the recent period of accelerated retreat.

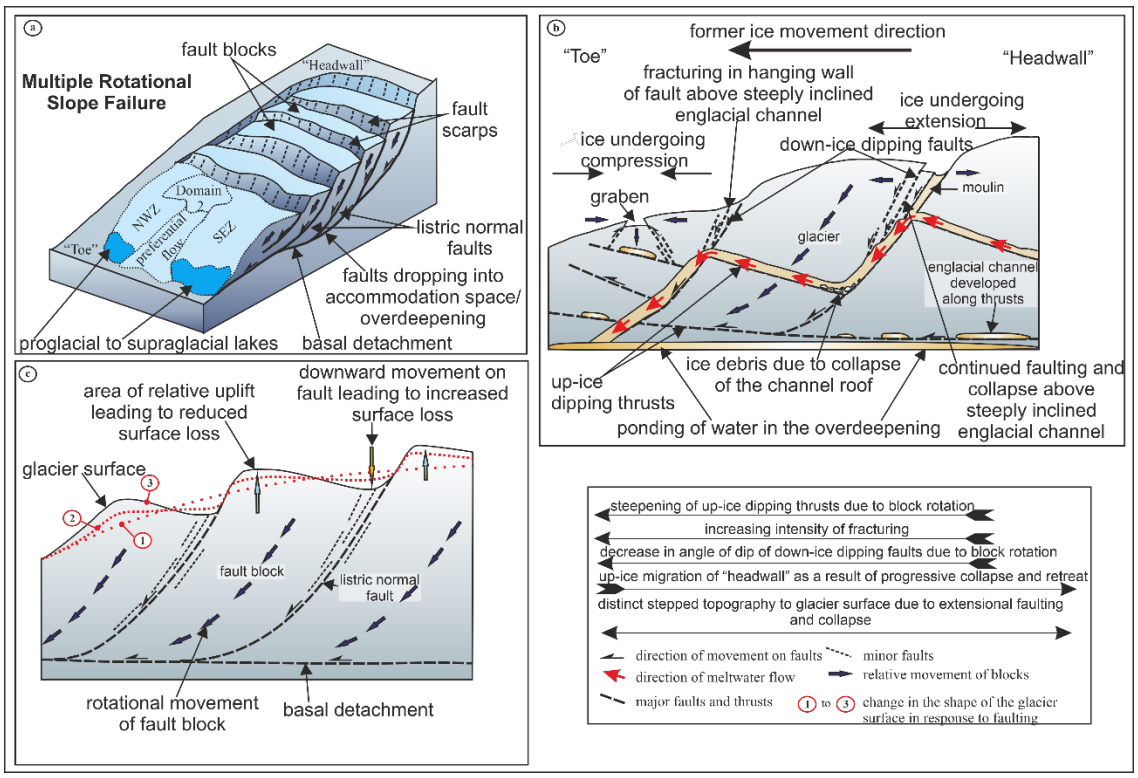

Figure 3.24: (a) Conceptual model for the collapse of ice in response to multiple rotational failure; (b) Schematic cross section through the ice at the margin showing the relationships between faulting, the pattern of englacial drainage, and ponding development during the ice-margin collapse; (c) Schematic cross section through the clean ice showing the potential relationship between faulting and changes in the surface of the glacier. Adapted from Phillips et al. (2013).

These down glacier structural changes impart on the marginal zone of Svínafellsjökull three lobate-fronted marginal zones which developed in the late 1990s, becoming firmly established within the snout of the glacier in the 2000s. The cross-cutting relationships displayed between these marginal zones and the occurrence of a large dextral shear zone separating the NWZ and CZ indicate that they are controlled by bed topography and areas of these units may be flowing independently of one another. Recent (2013-2015) increases in ice surface elevation between the developing crevasses indicate a period of readvance. Einarsson and Sigurðsson (2015) reported that Svínafellsjökull advanced by approximately 2 m at one of their two measurement sites in 2014. Field evidence (Figure 2.20) indicates that recent flow associated with this readvance has been focused within the CZ (Domain 4) and resulted not only in shearing between the main longitudinal (flow-parallel) crevasses which characterise this unit/domain, but also the overriding of the recently formed push moraine at its margin. This minor readvance is also

reflected in the 2018 velocity map by the higher velocities occurring along the centreline of the glacier. A similar phenomenon has been reported at Kviárjökull by Phillips *et al.* 2017 (cf. Swift and Jones, 2018), where pre-advance longitudinal or radial crevassing, in response to snout thinning and bed topographic controls, had produced discrete marginal zones/domains (more specifically individual ice splines), one of which became preferentially displaced over older push moraines on the foreland during a readvance. This may have happened twice at Svínafellsjökull, once in 2014 as described above, but also in 1970-1995, during the wider readvance that took place across south-eastern Iceland in the 1990s. Again, Einarsson and Sigurðsson (2015) reported that Svínafellsjökull advanced by 3 m between 1970 and 1995. This readvance may be reflected by the 1986 velocity map.

The changing sizes and structural characteristics of the individual marginal zones over time appears to be directly related to the thinning of Svínafellsjökull, but some shorter timescale developments such as shear zones possibly reflect changes in the volume of ice moving through the snout, more specifically during short phases of readvance. Comparisons of the structural maps for 1952, 1988 and 1992 indicate that the south-eastern marginal zone of the glacier became narrower. Its structural architecture appears to have remained the same for essentially 40 years, indicating that this part of the glacier is either very slow moving, static or in a phase of stable ice flux. This also can be said for the NWZ, which had not displayed any significant changes in its structure until 2007, when the narrow zone of closely spaced, longitudinal fractures characterising Domain 3a appeared. This domain may have formed as a result of deformation caused by lateral shear between the ice in the north-western marginal zone (Domain 3) and ice of the central marginal zone (Domain 4).

Significantly, in terms of landform development (see detail in Chapter 4), over the period 1952 to 2012, the glacier snout developed strong longitudinal crevassing and associated ice marginal pecten. Such changes have been identified at a number of sites around southern Iceland where they are manifest over longer periods of time in changes to push moraine morphology. Glacier

retreat since the Little Ice Age maximum has been recorded by recessional push moraines, initially created on an annual basis but more recently sub-annually (Boulton, 1986b; Evans and Twigg, 2002; Beedle *et al.*, 2009; Lukas, 2012; Chandler *et al.*, 2016a, 2016b, 2020a, 2020b; Evans *et al.*, 2017a, 2017b, 2019). Push moraine morphology has changed from more linear to increasingly sawtooth plan forms over time, and this has been associated also with progressively more till squeezing into ice-marginal pecten, so that moraines are now developing extreme sawtooth or hairpin plan forms (Chandler *et al.*, 2016a, 2016b, 2020a and 2020b; Evans *et al.*, 2016, 2017a, 2017b, 2019). These temporal changes in push moraine characteristics have been linked to two spatial changes in the structure of Svínafellsjökull: 1) snout thinning and a concomitant change in snout morphology towards a more divergent ice flow regime, thereby initiating stronger radial crevassing; and 2) a switch from well-drained foreland areas, on which snouts are coupled to proglacial streams draining over sandur fans, to increasingly poor ice-marginal drainage due to the uncovering of overdeepenings and recession inside large moraine amphitheatres, which is particularly well illustrated at Svínafellsjökull. Additionally, sawtooth moraine overprinting has developed more recently due to sub-annual moraine construction and short periods of ice-marginal readvance, the latter exemplified by the 1990s regional readvance event (Evans and Hiemstra, 2005; Sigurðsson *et al.*, 2007; Evans *et al.*, 2016, 2017a and 2017b). Observations presented here and at Kviárjökull by Phillips *et al.*, (2017) indicate that a similar but shorter readvance event in 2013-2015 (Einarsson and Sigurðsson, 2015) was recorded only locally in the moraine overprinting record, due to the preferential forward displacement of splines of snout ice whose shapes were pre-conditioned by radial crevasse construction during pre-advance snout thinning over an uneven subglacial topography. This interpretation potentially reconciles the alternative views of Phillips *et al.* (2017) and Swift and Jones (2018) on the potential for concentrated and pulsed axial flow in glacier snouts.

3.9 Conclusions

In summary, the results presented within this chapter demonstrate that, rather than displaying the structures of a simple piedmont lobe, the structural evolution of the lower reaches of this glacier is more complex. The combination of the data presented above has provided a greater insight into the spatial complexities of the evolution of the glacier snout. A multi-lobate structure in the margin occurs due to the focussing of recent flow associated with one or two re-advances within the central marginal zone, along with increases in snout thinning and a concomitant change in snout drainage. Snout thinning and passive retreat have accelerated in the 2000s and this multi-lobate style of flow became strongly established in 2007. Overall, historical mapping indicates that the structures of both the north-western and southern marginal areas of the glacier remained relatively unchanged between 1952 and 2012. This suggests that the north and south margins are largely static and that flow from the upper reaches of the glacier is being concentrated in the central unit. The change from a conventional "plug flow" mechanism in the upper reaches of Svínafellsjökull to this multi lobate structure is rooted in Domain 2, which is thought to be an area of instability, possibly related to the concentration of subglacial drainage or even ponding of meltwater within the overdeepened trough. From 1952-2012, Domain 2 has been accentuated by the overall thinning of the ice and the increasing influence of the bed topography on its internal structure. Furthermore, it is argued that the spatial complexities of the concentrated flow regime (within the central unit) are governed by the bed topography that underlies the glacier. The influence of this bed topography on the glacier's dynamic and structural regime appears to have increased throughout the study period, as the glacier has thinned due to recent climatic warming. The changes within the structural architecture of Svínafellsjökull between 1952 and 2012 clearly has had an impact on snout drainage. Significantly, in terms of landform development, over the period of mapping presented here, the glacier snout developed strong longitudinal crevassing and associated ice marginal pecten. Push moraines on the foreland of Svínafellsjökull are now developing with extreme sawtooth or

hairpin plan forms in response to its structural regime. This indicates that snout morphological changes and structural glaciological responses to climate warming can be clearly recorded in the push moraine characteristics over time.

4 Ice structural and subglacial controls on the incorporation and transport of debris in active temperate glaciers, Svínafellsjökull and Falljökull, Southeast Iceland

4.1 Introduction

Analysing sediment transfer pathways through glacial systems is essential to differentiating the various processes of bedrock erosion and sediment recycling beneath glaciers, yet sediment transfer at temperate glaciers with overdeepened beds, where subglacial fluvial sediment transport should be greatly limited by adverse slopes, remains relatively poorly understood (e.g. Alley *et al.*, 2003; Swift *et al.*, 2018; Swift *et al.*, 2021). Complex debris transfer processes in temperate overdeepened systems in Iceland are apparent in the nature of the deposits that comprise large frontal moraine systems, as well as the emergence of downwasting glacier snouts of supraglacial debris of mixed transport origin, thick debris-rich basal ice sequences, debris-lined englacial thrusts and englacial eskers (e.g. Spedding and Evans, 2002; Evans, 2009; Bennett and Evans, 2012; Swift *et al.*, 2006; 2018; Phillips *et al.*, 2017; Chandler *et al.*, 2020a and 2020b). Understanding the mechanisms involved in the entrainment and transfer of debris along these various pathways is essential to quantifying rates of subglacial erosion in active temperate glaciers and their role in longer term landscape change (e.g. Benn, 1992, 1995; Bennett *et al.*, 1997; Evans, 1999; Glasser *et al.*, 1999, 2006; Graham and Midgley, 2000; Etienne *et al.*, 2003; Alley *et al.*, 2003; Benn *et al.*, 2004; Goodsell *et al.*, 2005; Lukas *et al.*, 2005; Benn and Lukas, 2006; Lukas, 2007; Kellerer-Pirklbauer *et al.*, 2008; Mills *et al.*, 2009; Evans 2010; Evans *et al.*, 2010, 2018a and 2018b; Cook *et al.*, 2010; Swift, 2011a and 2011b; Bennett and Evans, 2012; Egholm *et al.*, 2012; Cook and Swift, 2012; Brook and Lukas 2012; Brook *et al.,* 2013; Swift *et al.*, 2018, 2021; Chandler *et al.*, 2020a, 2020b). In addition, glacial sedimentary deposits are key to understanding ice dynamics, thermal regime and, in turn, palaeoclimate in Quaternary and ancient glacial systems (e.g. Evans, 2009; Hambrey and Glasser, 2012).

Debris transfer within glacial systems occurs via a complex and varied range of pathways that reflect different entrainment sources and processes, referred to as the debris cascade by Benn

and Evans (2010; Figure 4.1). These pathways may include basal transport within till (e.g. Boulton, 1978; Clark, 1987; Alley *et al.*, 1997; Larsen *et al.*, 2004; Evans *et al.*, 2006; Hart *et al.*, 2011; Evans, 2018), basal ice layers (e.g. Lawson, 1979; Hubbard and Sharp, 1993; Sharp *et al.*, 1994; Knight, 1994; Knight *et al.*, 1994; Sugden *et al.*, 1987; Swift *et al.*, 2018) and/or englacial debris bands (e.g. Knight, 1987, 1994; Hubbard *et al.*, 2004; Swift *et al.*, 2006; 2018; 2021; Evans, 2009). The number and type of active pathways influences the overall capacity of sediment transport within a system, the volume of material being transported, and the sedimentological and geomorphological nature of resultant deposits and landforms, as demonstrated in Icelandic settings for example by Spedding and Evans, (2002), Evans *et al.* (2016, 2018a and 2018b), Swift *et al.* (2018, 2021) and Chandler *et al.* (2020a and 2020b).

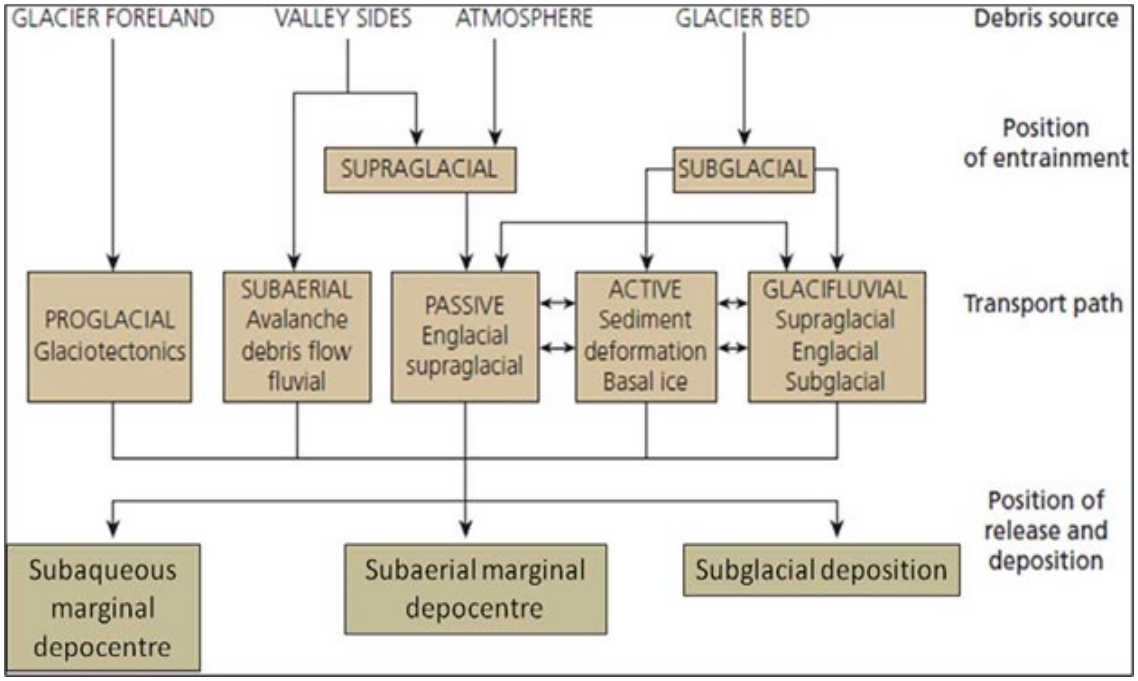

Figure 4.1: The debris cascade system (after Benn and Evans, (2010).

The prominence of subglacial till deposition in Icelandic temperate glacier systems is reflected in previous research (e.g. Boulton and Hindmarsh, 1987; Benn, 1995; Evans, 2000; Boulton *et al.*, 2001; Evans and Hiemstra, 2005; Evans *et al.*, 2016, 2018b). However, sedimentation directly from englacial transfer (cf. Eyles, 1979, 1983) has been scrutinised only relatively recently, for

example relating to the melt-out of debris-charged thrusts (Swift *et al.*, 2006, 2018), ice-walled channel fills/englacial eskers (Spedding and Evans, 2002; Bennett and Evans, 2012) and debris-rich basal ice facies (Swift *et al.*, 2006; Cook *et al.*, 2007, 2010, 2011a, 2011b; Waller *et al.*, 2021). Interpretations of large volumes of supraglacial and morainic debris being related directly to passive transport of extraglacial material, as promoted by Boulton and Eyles (1979) and Eyles (1983), have been tempered by subsequent investigations into debris-rich ice facies as cited above. Specifically, a large amount of fluvial material that has been detected in these englacial transport pathways has been attributed to deposition of fluvial bedload within and above terminal overdeepenings (cf. Spedding and Evans, 2002; Swift *et al.*, 2006; Swift *et al.*, 2018), whilst extensive exposures of debris-rich basal ice have been attributed to freeze-on of sediment-rich subglacial water as it ascends the adverse slopes of overdeepenings (Roberts *et al.*, 2002; Cook *et al.*, 2007, 2010; Larson *et al.*, 2010). Importantly, and indeed somewhat controversially, the latter hypothesis promotes supercooling (Lawson *et al.*, 1998; Evenson *et al.,* 1999; Roberts *et al.*, 2002) as a mechanism of debris entrainment and transfer in temperate glaciers, prompting some researchers to explain ancient hummocky moraine assemblages as supercooling landforms (Larson *et al.*, 2006). Benn and Evans (2010) have suggested that basal ice can have very high concentrations of debris content, up to 75% by volume in some cases.

The research reviewed above clearly demonstrates that a variety of debris entrainment, transfer and deposition processes operate in the debris cascade of Icelandic active temperate glaciers. Notions that any one pathway, for example supercooling (Roberts *et al.*, 2002) versus passive extraglacial (Eyles 1983), might dominate requires systematic testing (e.g. Spedding and Evans 2002; Swift *et al.*, 2006). In such a test, Swift *et al.* (2018) presented their analyses of debris derived from the basal ice facies at Svínafellsjökull and concluded that the overdeepened bed beneath the snout enhanced the transfer of locally high volumes of basal material of fluvial and subglacial origin in both englacial thrusts and basal ice facies created by regelation (supercooling; Figure 4.2).

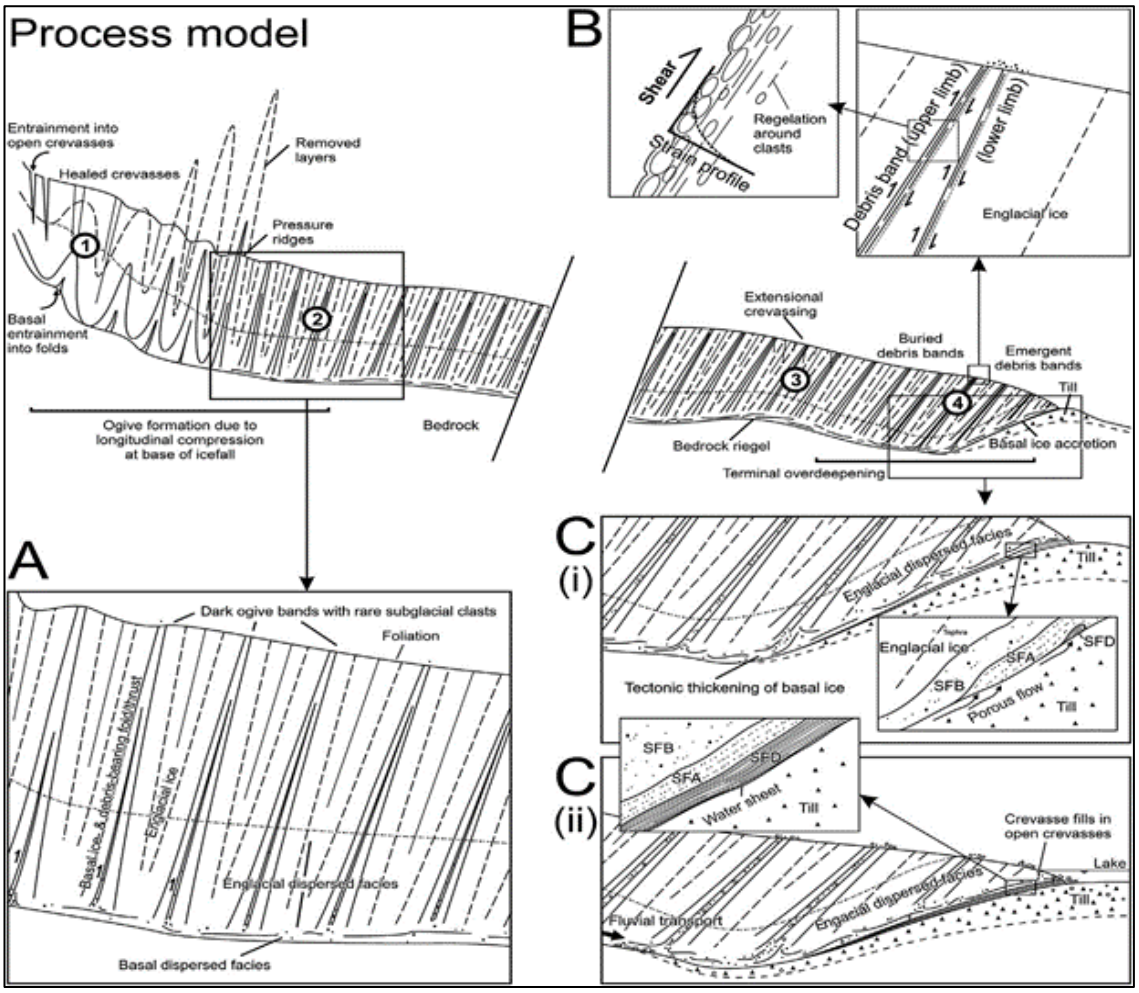

Figure 4.2: Process model proposed by Swift et al. (2018), illustrating the key proposed debris-rich glacial ice formation processes, debris transport pathways, and glaciological controls at Svinafellsjökull. 1. Entrainment into basal folds and surface crevasses at the ice fall. 2. Deformation below the ice fall further elevates basal material into dark-ogive bands (see detail in panel A). 3. Ice and subglacial water flow enters the terminal overdeepening. 4. Longitudinal flow compression produces thrusting along ogive-band foliation, whilst ablation reveals some closely spaced bands that may represent separate fold arms inherited from open folds formed at the base of the icefall (see detail in panel B). Steeper adverse slopes are less connected hydrologically and basal ice facies reflect near-closed refreezing conditions (panel Ci). Major axes of subglacial water flow are directed toward the deepest areas of overdeepening, where pressurisation of flow causes coarse material in fluvial transport to be deposited on the normal slope, which is then entrained into thrusts and basal ice. Shallower adverse slopes are more connected hydrologically and ice facies reflect more open water flow and refreezing conditions, including sheets, canals and channels (panel Cii). For key to facies codes see Table 4.1 and 4.2.

The varied hydraulic connectivity of the adverse slope, dictated by its steepness, creates either closed system (steep slope) or open system (shallow slope) refreezing, giving rise to various types of basal ice facies (see section 4.2 for details). Importantly, Swift *et al.* (2018) also recognise the role of englacial debris band formation (Forbes bands or ogives) at the base of the icefall, where both supraglacial and subglacial debris enters the englacial environment via crevasses and basal ice folds, respectively. Thrusting along the Forbes bands is proposed to be

an efficient debris transfer process (cf. Goodsell *et al.*, 2002; Swift *et al.*, 2006). However, detailed mapping of the surface structures of the glacier (Chapter 3) has revealed no obvious ductile folding within Svínafellsjökull, potentially questioning the validity of this model.

This study aims to test the Swift *et al.* (2018) debris cascade model depicted in Figure 4.2, through the analysis of clast shape data collected from the debris-rich ice facies in the marginal zone of Svínafellsjökull and from exposures through the basal ice at the foot of the icefall at neighbouring Falljökull. Additionally, clast shape data collected from the recent moraines constructed around the margin of Svínafellsjökull allow an assessment of the role of englacial transport pathways in the construction of recessional push moraines in terminal overdeepenings, thereby evaluating the applicability of alternative genetic models proposed by Cook *et al.*, (2011b; supercooling and melt-out) versus sub-marginal till squeezing/bulldozing (Price 1970; Sharp 1984), or indeed if some combination of processes operating on a spatio-temporal continuum is more appropriate (cf. Evans and Hiemstra, 2005; Evans *et al.*, 2018a, 2018b; Chandler *et al.*, 2020b; i.e. seasonally-driven sub-marginal till thickening). The key elements of the Swift *et al.* (2018) debris cascade model that this study aims to test are outlined below:

- Debris that has been incorporated through thrusting includes rounded and well-rounded clasts that are also striated, indicating that fluvial bedload is deposited as subglacial channels approach the overdeepening and then entrained along thrusts.At Svínafellsjokull there are a large number of active transport pathways present, and that mixing of debris between transport pathways is significant.
- The overall entrainment pathways are influenced very strongly by the presence of a terminal overdeepening, which promotes deposition of sediment from subglacial fluvial transport pathways, inhibits the flushing of subglacial sediment by fluvial processes.
- Entrainment of debris into basal folds and surface crevasses at the ice fall and deformation below the ice fall further elevates basal material into dark-ogive bands.

4.2 Study site and previous research

The terminal zones of many temperate, non-surging glacier systems in southeast Iceland, notably Svínafellsjökull, Falljökull/Virkisjökull, Morsárjökull and Kvíárjköull (Figure 4.3), exhibit locally high supraglacial debris loads, exposures of debris-rich englacial and basal ice, and extensive and large arcuate frontal moraine systems (Bradwell, 2004; Bennett *et al.*, 2010; Everest *et al.*, 2017; Evans *et al.*, 2017b). Supraglacial and proglacial debris characteristics at these glaciers are indicative of mixed transport from diverse pathways, including glacifluvial and subglacial in addition to passive supraglacial (e.g. Spedding and Evans, 2002; Swift *et al.*, 2006; Bennett and Evans, 2012; Lukas *et al.*, 2013; Swift *et al.*, 2018). This indicates a strong subglacial-to-supraglacial sediment flux over their overdeepenings. For these reasons, the glacier snouts of Svínafellsjökull and Falljökull, both fed by the Öræfajökull ice cap, were selected for data collection. The selection of Svínafellsjökull is predicated by its previous employment in studies on debris transfer processes, especially glaciohydraulic supercooling (Tweed *et al.*, 2005; Cook *et al.*, 2007, 2010), but a lack of safe access to icefall debris bands at that location necessitated the use of the excellent exposures at the base of the icefall at Falljökull.

Svínafellsjökull and Virkisjökull-Falljökull drain the southwestern flank of the Öræfajökull ice-cap. These steep glaciers descend from their combined source area at over 1500 m above sea level (asl), to below 150 m asl within just 2 to 3 km, thereby forming steep icefalls which feed ice to the lower snouts. Below its icefall, the tongue of Svínafellsjökull (Figure 4.3b) occupies an overdeepened basin situated behind an arcuate frontal moraine complex comprising overprinted recessional push moraines (Everest *et al.*, 2017, Chapter 5). The terminus position overall has not changed significantly since 1945 and is presently situated on the adverse slope of the large frontal moraine complex, giving rise to the damming of a series of minor proglacial, ice-contact lakes. The subglacial topography of Svínafellsjökull has been derived from a radar survey undertaken by Magnússon *et al.* (2012) (See Figure 3.5, Chapter 3) and comprises an elongate overdeepening extending down to ~320 m. Falljökull and its neighbour Virkisjökull have

retreated from a similar topographic setting, but recent accelerated collapse over their overdeepening, concomitant with proglacial lake expansion (Phillips *et al.*, 2013, 2014), has resulted in a steepened snout profile where Falljökull descends over a major bedrock step; this has enabled access to the base of the icefall, where the structural glaciological impacts of the steeper bed topography can be observed.

Glacier surface structures on Svínafellsjökull have been mapped in detail and are presented in Chapter 3. Generally, there is an arcuate, transverse crevasse pattern between 2.5 and 3.5 km from the terminus. Down glacier of this, the transverse crevasses are replaced by radial, approximately flow-parallel crevassing that extends to the terminus. The ice front is characterised by strongly developed pecten due to the radial crevassing. Ogive (Forbes) banding, although clearly developed on the upper reaches of the glacier, is not apparent on the lower snout, although two foliation types have been observed by Swift *et al.* (2018): Type 1 being a relatively distinct but intermittent cross-glacier, arcuate foliation; and Type 2 being a less distinct arcuate transverse foliation apparent only in the centre and true left of the lower 0.5-1.0 km of the glacier terminus.

At Svínafellsjökull (Figure 4.3b), debris-rich basal ice facies have been documented in detail by Cook *et al.* (2007, 2010, 2011a and 2011b) and Swift *et al.* (2018). Those investigations adopted the basal ice facies classification scheme of Lawson (1979; cf. Hubbard and Sharp, 1989; Knight, 1997; Hubbard *et al.*, 2009), identifying in particular debris-rich stratified and dispersed facies basal ice. Debris concentrations of debris-rich basal ice at Svínafellsjökull are shown in Table 1 as debris concentration (% in ice). Cook *et al.* (2007, 2011a) and Swift *et al.* (2018) deploy a hybrid approach to basal ice facies characteristic identification (Lawson, 1979; Hubbard and Sharp, 1989; Knight, 1997; Hubbard *et al.*, 2009). This study adopts the same hybrid approach used by Cook *et al.* (2007) and Swift *et al.* (2018), as while there are more recent schemes such as described by Hubbard *et al*. (2009) this hybrid approach has been applied before at the same location (Svínafellsjökull) and allows direct comparisons.

The stratified facies found at Svínafellsjökull have been examined in detail by Cook *et al.* (2007, 2011a; Table 4.1), who attribute their formation to the tectonic thickening of regelation ice and, in the southern part of the glacier terminus, to freeze-on of water and sediment as a result of glaciohydraulic supercooling. They also identified five distinct subfacies of stratified basal ice at Svínafellsjökull, only three of which were found to be consistent with supercooling: "subfacies A", formed by regelation; "subfacies C" formed by freeze-on of supercooled water; and "subfacies E", which resembles the herringbone facies of Knight and Knight (2005), who created such characteristics by freezing supercooled water under laboratory conditions. Swift *et al.* (2018) highlighted that these subfacies accounted for 42% of the stratified facies exposed at Svínafellsjökull and an estimated 83% of the debris flux from the stratified facies overall.

The dispersed facies are found in metres-thick exposures at the terminus in direct contact with the till substrate, although it is occasionally found to be underlain by the more debris-rich and visibly layered stratified facies (Swift *et al.*, 2018). An additional "stratified-solid" facies is recognised by Cook *et al.* (2010) and Swift *et al.* (2018), who classify the typical basal ice facies at Svínafellsjökull as SFD (stratified solid), SFA (stratified) and SFB (dispersed; Figure 4.2, Table 4.2). Also significant are debris bands that resemble stratified ice but contain a wider range of grain sizes and clast shapes, which Swift *et al.* (2018) classify as debris-charged thrusts (Figure 4.2).

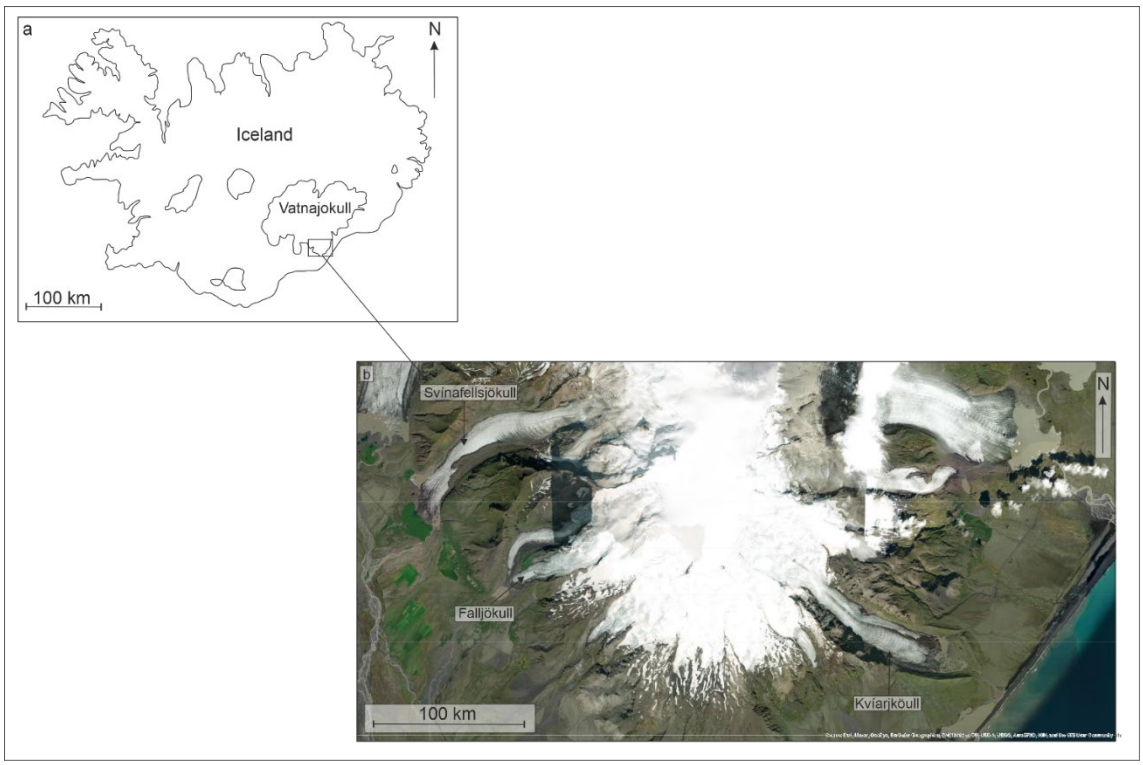

Figure 4.3: Locations of glaciers relevant to this chapter: a) map of Iceland showing study area; b) aerial image of the study area, showing the glaciers draining the Öræfajökull ice-cap and caldera (Image from Esri World Image Basemap layer (Source: Esri, Maxar, Earthstar Geographics, and the GIS User Community).

4.3 Methods

In order to describe and interpret the ice types from where clast samples were collected (Appendix 8), the scheme of Swift *et al.* (2018) and Cook *et al.* (2011a) was employed. Using both Tables 4.1 and 4.2, SFD, SFA and SFB basal ice facies were identified along with debris bands that resemble stratified ice but contain a wider range of grain sizes and clast shapes, which Swift *et al.* (2018) classify as debris-charged thrusts. Little to no evidence of thrusting (deformation) was recorded in association with these debris bands.

Clast shape analysis was undertaken on the debris-rich ice facies in the marginal zone of Svínafellsjökull and from exposures through the basal ice at the foot of the icefall at neighbouring Falljökull. Clast shape analysis was also undertaken on the moraines being formed at the glacier margin at Svínafellsjökull. This analysis involved the sampling of 50 pebble/cobble sized clasts of a similar lithology (massive basalt) per site.

The size and form of the clasts were derived by measuring the length of the A (long), B (intermediate) and C (short) axes of the pebble/cobble and the roundness assessed using a Powers roundness chart (Powers, 1953). In addition to clast shape and roundness, the occurrence of striae on the surfaces of individual clasts was also noted, as this feature is considered to be diagnostic of subglacial transport in the glacial traction zone (Kruger, 1979; Sharp, 1982; Lukas and Benn, 2021).

Statistical analysis of clast form was undertaken following the procedures outlined in Benn (2004, 2007) and Lukas and Benn (2021) (see Chapter 2), whereby indexes of C_{40} (percentage of clasts with C/A axial ratios ≤0·4) and RA (percentage of clasts in VA (very angular) and A (angular) classes) were calculated. Co-variance plots (specifically Type I plots of Lukas *et al.* (2013) for basalt like lithologies) were compiled using C_{40} and *RA* values. Roundness was further assessed by calculating an average roundness value using the procedure proposed by Spedding and Evans (2002) and refined by Evans (2010), who found that a value of average roundness can provide an effective discrimination between clast forms. Following Evans (2010), the average roundness (AvR) was derived in this study by using the numerical values identified on the standard Powers gauge, whereby very angular (VA) = 0, angular (A) = 1, subangular (SA) = 2, subrounded (SR) = 3, rounded (R) = 4 and well-rounded (WR) = 5. The resulting clast morphology data were plotted on a series of binary and ternary diagrams using Microsoft Excel.

For comparisons, the Icelandic datasets for scree, subglacial till and glacifluvial deposits reported in Lukas *et al.* (2013) and Evans *et al.* (2018b) were used as control samples and their envelopes included on all covariance plots (Figure 4.4). An additional subglacial control sample was collected from a bedrock step exposed beneath the icefall of Falljökull, to facilitate comparisons with clasts entrained at bedrock steps below icefalls, a debris transport pathway identified as significant in debris banding development by Goodsell *et al.* (2002, 2005) and Swift *et al.* (2006, 2018) (See Appendices 8,9 and 10).

The individual data points were further processed in ArcGIS in order to contour the clast shape characteristics and identify spatial patterns within and between the debris-rich basal ice facies and sub-marginal push moraines. The IDW geospatial tool was used to create rasters and then to contour the resultant raster layers to produce spatial patterns in C_{40}, RA, RWR and AvR, following procedures outlined in Evans (2010).

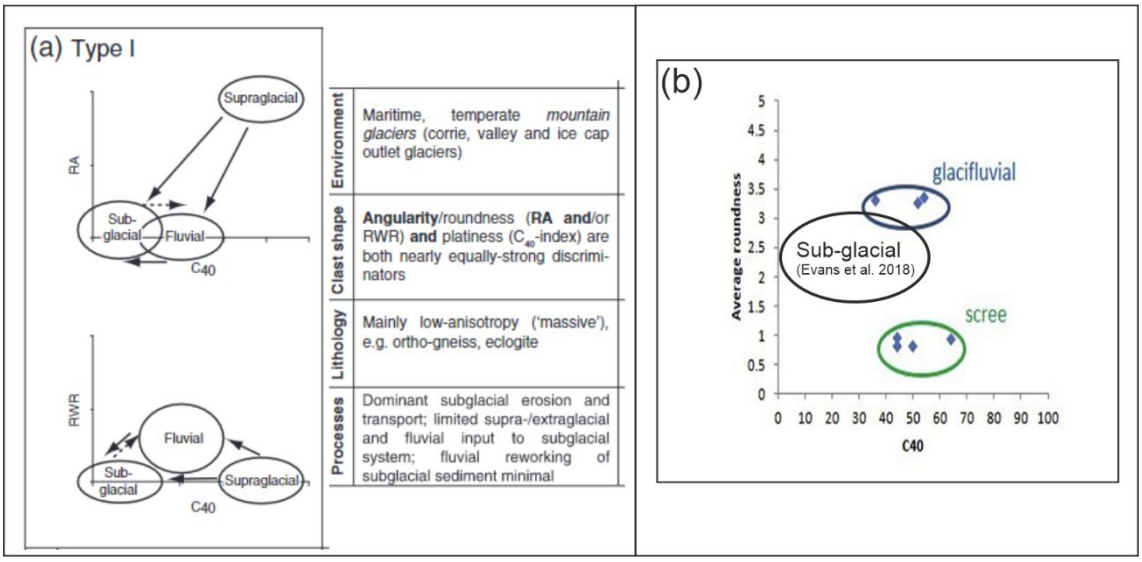

Figure 4.4: Existing clast form co-variance plots used for comparisons with data in this study: a) "Type 1" co-variance plot of Lukas et al. (2013) for low anisotropy basalt clast lithologies; b) co-variance plots for C_{40} and AvR data based on Evans et al. (2018b) for massive basalt lithologies.

Sub-facies	Unit thickness (m)	Physical character	Mean crystal diameter (cm)	Debris concentration (% in ice)	Sediment texture (G ¼ % gravel, S ¼ % sand, M ¼ % mud)	Descriptive equivalence	Field Photograph of Ice facies (taken from Cook *et al.*, 2007)
Basal ice facies							
A	0.12–2.0	Alternating debris-rich and debris poor laminations. Debris laminations comprise sub centimetre debris aggregates and centimetre-scale clasts.	1.871.4	5.771.7	Muddy sandy gravel: coarse sand	Laminated facies of Hubbard and Sharp (1995): closely spaced polymodal debris laminae 0.1–1mm thick separated by clean, bubble-free ice.	
B	0.02–1.75	Dispersed particles, debris aggregates and sub-centimetre clasts within clean ice matrix.	2.270.9	3.775.9	Gravelly muddy sand: medium sand	Clear facies of Sharp *et al.* (1994): scattered coarse clasts and grit particles within bubble-poor ice. Dispersed facies of Hubbard and Sharp (1995): bubble-free, dispersed polymodal debris, crude layering.	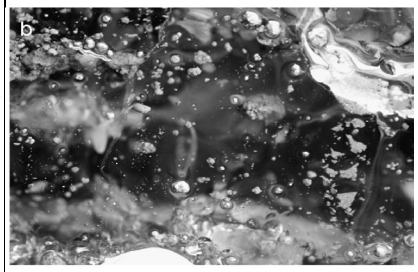
C	0.2–1.9	Angular and 'spidery'-shaped debris aggregates within clean ice matrix. Occasional but rare spherical bubbles.	0.470.5	27.6711.3	Gravelly mud very: fine sand	Suspended facies of Lawson (1979): suspended particles and aggregates without orientation, silt-dominated sediment.	

D	0.02–0.2	Frozen debris with only interstitial ice. Usually occurs as lenses or bands within sub-facies C or E.	Interstitial ice	80.873.2	Gravelly muddy sand: medium sand	Solid facies of Lawson (1979), Knight (1987) or Hubbard and Sharp (1995): sediment-supported matrix with interstitial ice, polymodal debris.	
E	0.2–4.0	Sediment and crystals depict 'herringbone-like' texture. Usually found as homogenous units or with lenses of sub-facies D.	0.570.2	36.678.3	Slightly gravelly mud: fine silt	Herringbone facies of Knight and Knight (2005): distinctive herringbone structure of interlocking crystals marked by intracrystalline bubble and debris lineation's.	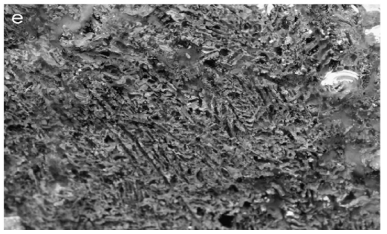
Vent ice facies Frazil ice	N/A	Interlocking platy or lozenge shaped crystals often found aggregating as flocs in supercooled subglacial discharge. Flocs are porous in nature.	Approximately 1.1	3.271.4	Gravelly muddy sand fine sand	Frazil ice of Evenson *et al.* (1999): individual lozenge-shaped crystals or crystal aggregates (flocs). Flocs may include trapped debris as sediment laden waters pass through them.	
Anchor ice	N/A	Relatively clean ice growing around the rims of supercooled discharge vents. Angular debris aggregates and spherical bubbles are common.	2.971.1	2.371.8	Slightly gravelly sandy Mud: very coarse silt	Anchor ice of Evenson *et al.* (1999): form around the rim of discharge vents. May be metres thick with crude stratification depicted by ice grain size differences and debris content.	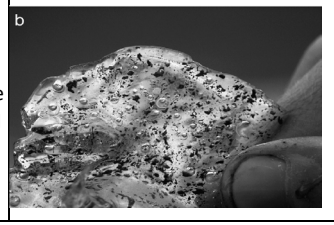

Table 4-1: Summary of the physical properties of basal ice facies and ice facies produced by glaciohydraulic supercooling, adapted from Cook et al., 2007 and cook et al., 2011a.

Facies	Survey 1	Survey 2	Survey 3	Facies code
Englacial	Large crystal (mean 3.8 cm diameter) bubble-rich ice containing dispersed debris and <0.1% debris by volume (volume insufficient for particle size analysis). Pervasive up glacier dipping transverse foliation. Healed crevasse structures dipped more steeply than foliation and contained little or no debris. Some angular aggregates and clasts up to 3 mm diameter of non-basal origin (survey 1).			N/A
Dispersed	Large crystal (mean 2.9 cm diameter) ice containing dispersed debris (<0.1 to 3% by volume; mean 0.8 ± 1.3%) comprising isolated particles and aggregates of silt to medium or coarse sand of 3 to 7 mm diameter. Generally massive and structureless though with occasional debris-rich planes (see Cook *et al.* 2011a). Isolated sub-angular and faceted sub-cm to cm diameter clasts of apparently basal origin.			SFB
Stratified	Medium crystal (0.5 to 3 cm diameter) ice, 0.1 to 3.2% debris by volume (mean 1.0 ± 0.8%), with mm-thick debris-rich and clean ice layers (though latter up to 3 cm thick). Debris layers comprise aggregates of silt/clay to granule gravel up to 4 mm diameter. Isolated faceted angular to rounded clasts up to 4 cm diameter.	Not present.	As survey 1.	SFA
Stratified	Tight folds of cm to 10s cm thick bands of small crystal (sub-cm diameter) ice within stratified ice (above), 29.4 to 49.0% debris by volume with mm-thick debris-rich laminae comprising sand to granule gravel and sub-cm clean ice layers < 3 cm long. Faceted and striated clasts up to 4.5 cm diameter.	Not present.	As survey 1 but extensive up to metre thick exposures of gently rippled sub-horizontal mm to cm thick debris-rich and clean-ice laminae, poor sorting (debris-rich laminae comprised silt/clay to granule gravel), 37.3% debris by volume· numerous sub-rounded to rounded clasts, some up to 25 cm diameter, sparse angular clasts. Occasional cm-scale displacement of laminae on up glacier dipping shear planes.	SFD
Crevasse fill	Not present.	Diffusely laminated, small crystal (sub-cm diameter) ice, 0.3 to 2.7% debris by volume (mean 1.3 ± 1.1%), in narrow intensely deformed or sheared bands within dispersed ice (above), with texture qualitatively similar to nearby 'herringbone' crevasse-fill ice, 3.2 to 7.9% debris by volume.	As above but sub-vertical laminae with bifurcating N/A structure, weak sorting but mainly sand to granule gravel, 22.4 to 25.0% debris by volume· no clasts and no apparent displacement of laminae along shear planes. Also 'herringbone' ice, 13.2 to 22.8% debris by volume, with intricate branching laminae structures of silt and fine sand.	

Table 4-2: Characteristics and distribution of observed ice facies at Svínafellsjökull by Swift et al. (2018).

4.4 Results

4.4.1 Debris-rich basal ice facies

Thirty-four sample locations were established within the debris-rich basal ice facies in the marginal zone of Svínafellsjökull (Figure 4.5, Appendix 8). This enabled the shape analysis of 1700 individual clasts in foliation and sediment filled fractures in order to determine debris transport pathways and their possible relationships to ice facies types. Healed crevasse structures also visible in the debris-rich basal ice facies are more steeply dipping than the foliation but contained little or no debris for clast shape sampling.

Samples S1-S8 (Figure 4.6, Appendix 8 and 10) were taken at intervals dictated by ice facies changes along a 50 m long transect on the glacier surface where foliation and debris bands were inclined sub-vertically and therefore could be accessed by walking in an up-glacier direction (Figure 4.7). This enabled the compilation of a vertical sequence log employing the classification scheme of Swift *et al*. 2018 (Figure 4.8). The ice facies are characterised as SFB (Table 4.2) and display features that have been used by Sharp et al. (1994) to define the degree of clear facies, including scattered coarse clasts and grit particles within bubble-poor ice and dispersed facies of bubble-free ice including polymodal debris. Generally, the SFB was massive and structureless with occasional debris-rich foliae. Clast shape data from the transect reveal that the debris within the SFB is mostly striated (36-86%) and is either SA or SR (AvR = 2.18-2.66).

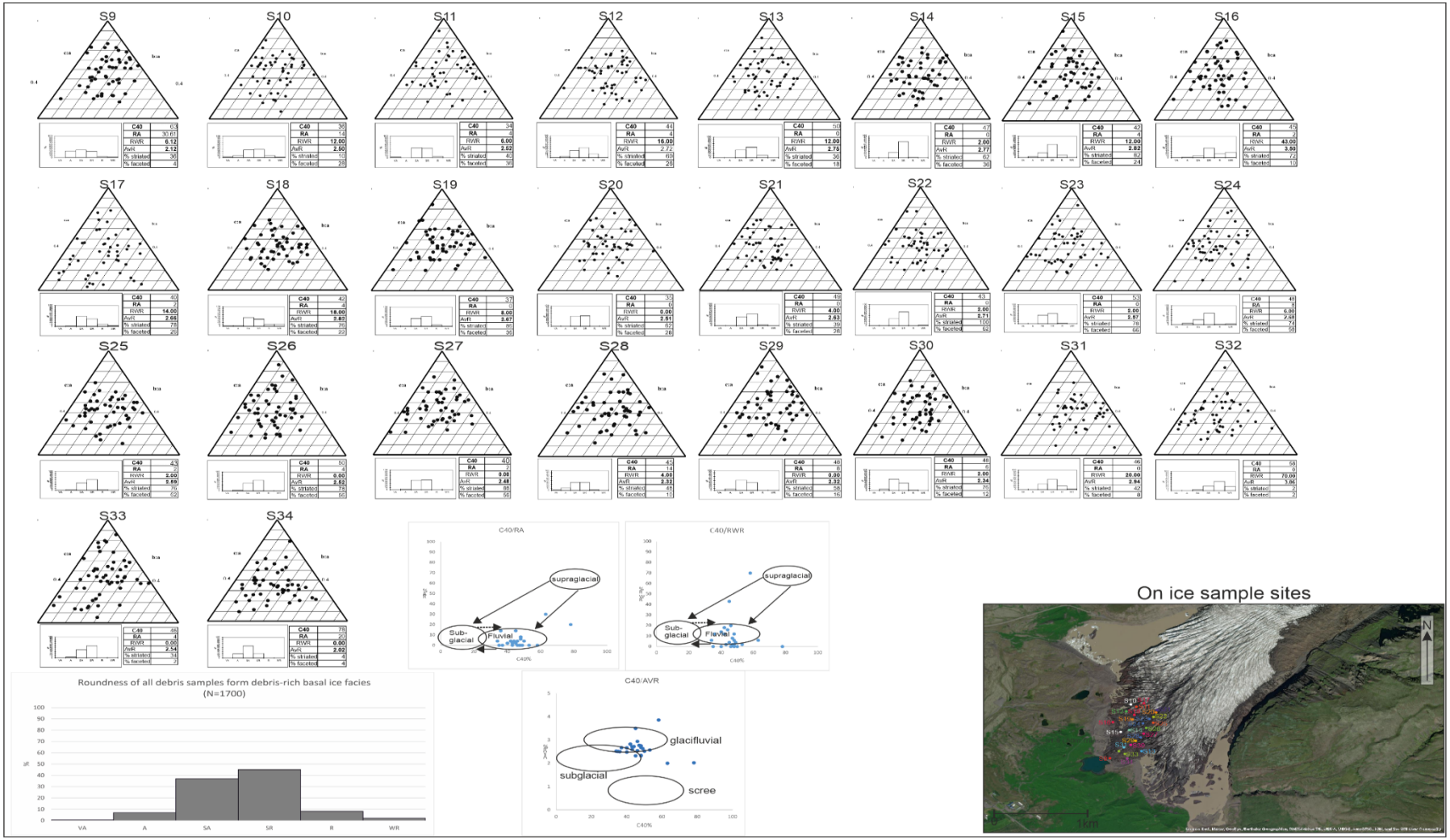

Figure 4.5: Clast morphology and co-variance data for debris-rich basal ice facies and sample locations at Svínafellsjökull. S1-34 are sample locations Esri World Image Basemap layer (Source: Esri, Maxar, Earthstar Geographics, and the GIS User Community). See Appendix 8.

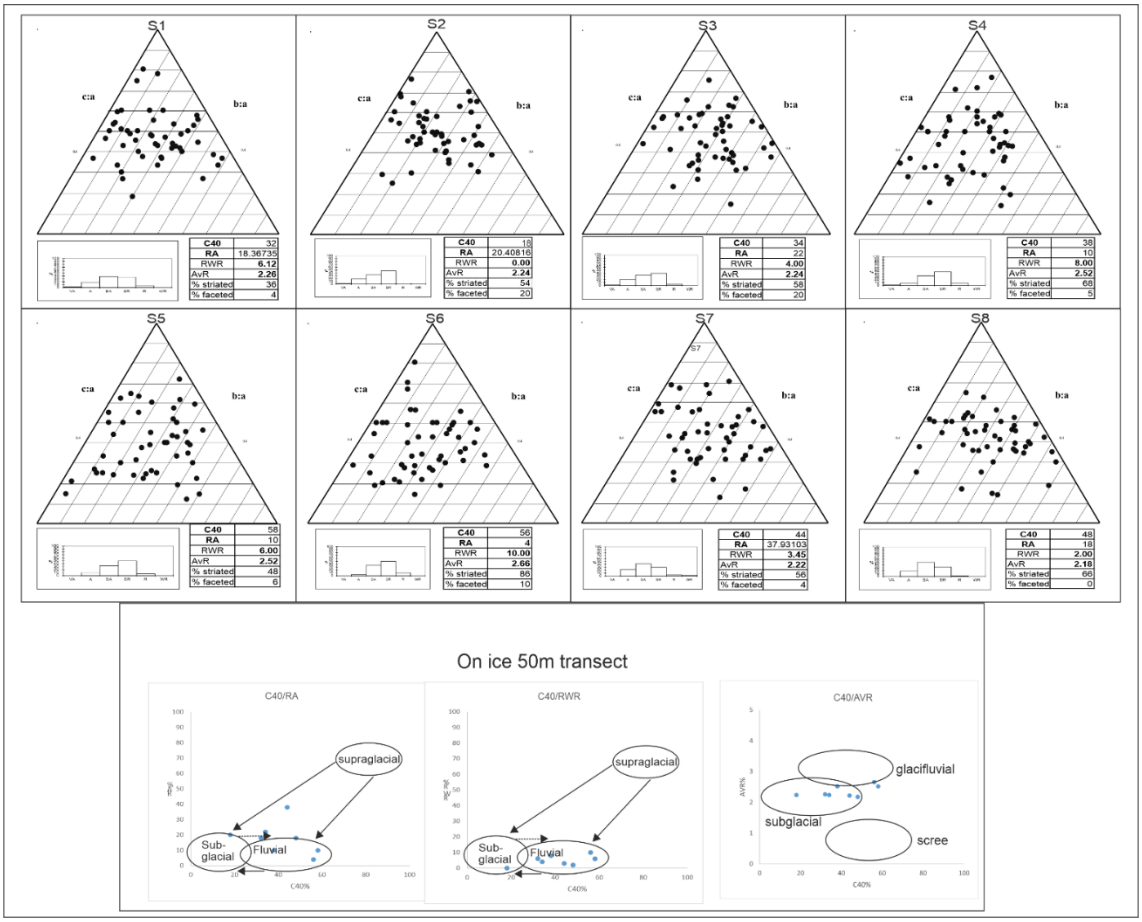

Figure 4.6: Clast morphology and covariance data for on ice samples S1-S8, a 50m transect on the glacier surface. Co-variance plots with envelopes shown based on control data from Lukas et al. (2013) and Evans et al. 2018.See Appendix 9

Figure 4.7: Field photographs of foliation and debris bands which were inclined sub-vertically and could be accessed by walking in an up-glacier direction.

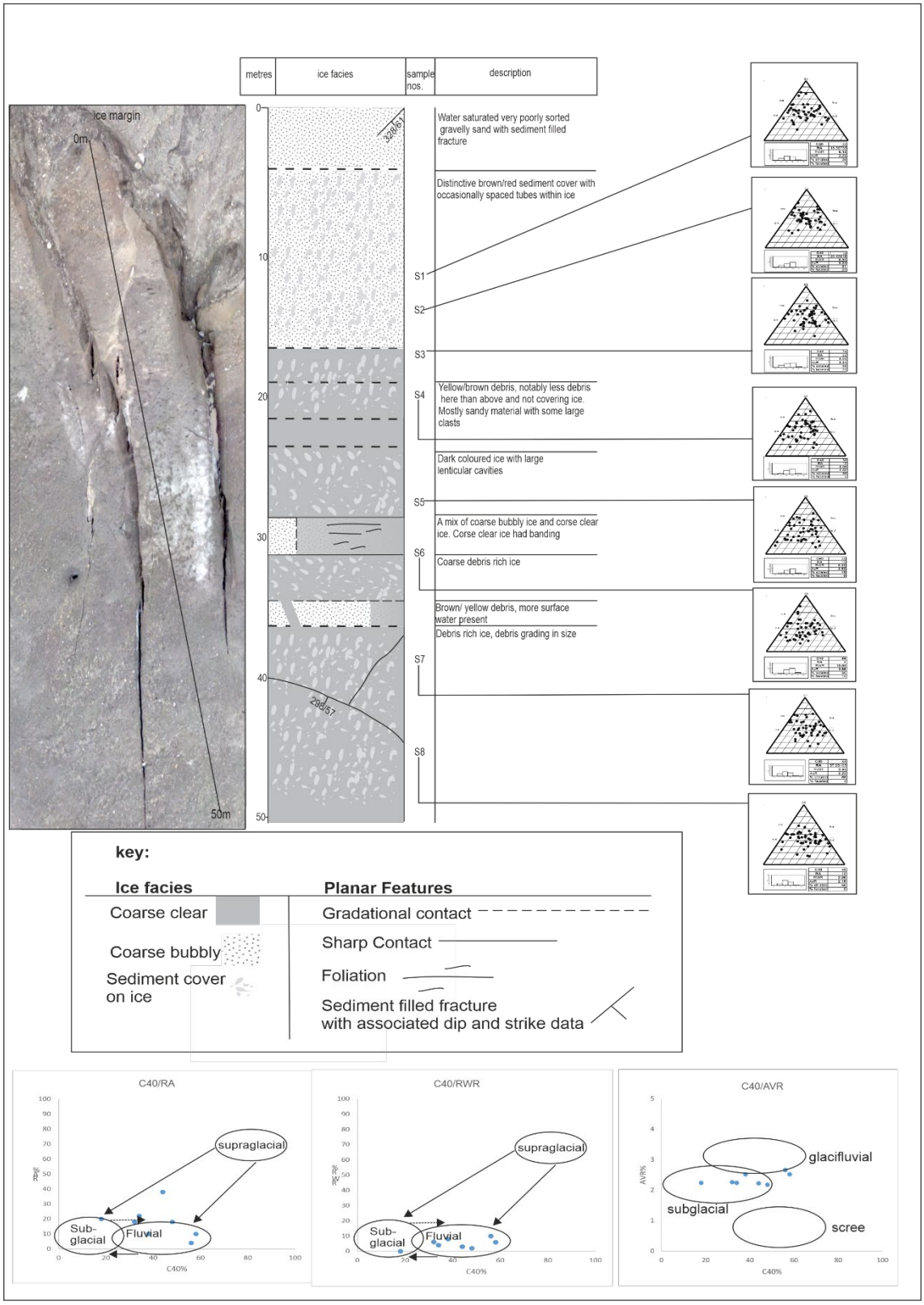

Figure 4.8: Log of ice facies and debris cover characteristics with associated UAV image (acquired in 2017) showing transect line. Sample locations are also marked on the transect with associated clast shape data plots and co-variance plots with envelopes shown based on control data. See Appendix 10 for clast shape data plots and co-variance plots.

Moving to another sample location, Sample (S9) (Figure 4.9a). This was obtained from stratified solid (SFD) basal ice facies that makes up the lower part of a vertical sequence, the middle and upper parts of which comprise SFB and SFA, with the whole sequence lying on a saturated till layer (Figure 4.9b). The SFD comprises of an ≤1 m thick exposure of alternating gently undulating, sub-horizontal mm to cm thick debris-rich and clean-ice laminae, with the debris-rich laminae displaying silt/clay to granule gravel with occasionally larger clasts up to 11 cm in diameter (Figure 4.9 b-d). Also visible is the localised cm-scale fault displacement of laminae. This sample contains angular (36%), sub angular (35%) and sub-rounded (28%) clasts with minor rounded and well-rounded components, 36% of which are striated. The striated clasts had a variety of rounding (Figure 4.9 a). The C_{40}/RA covariance plot (Figure 4.4 and 4.5) indicates a subglacial or glacifluvial signature for this sample.

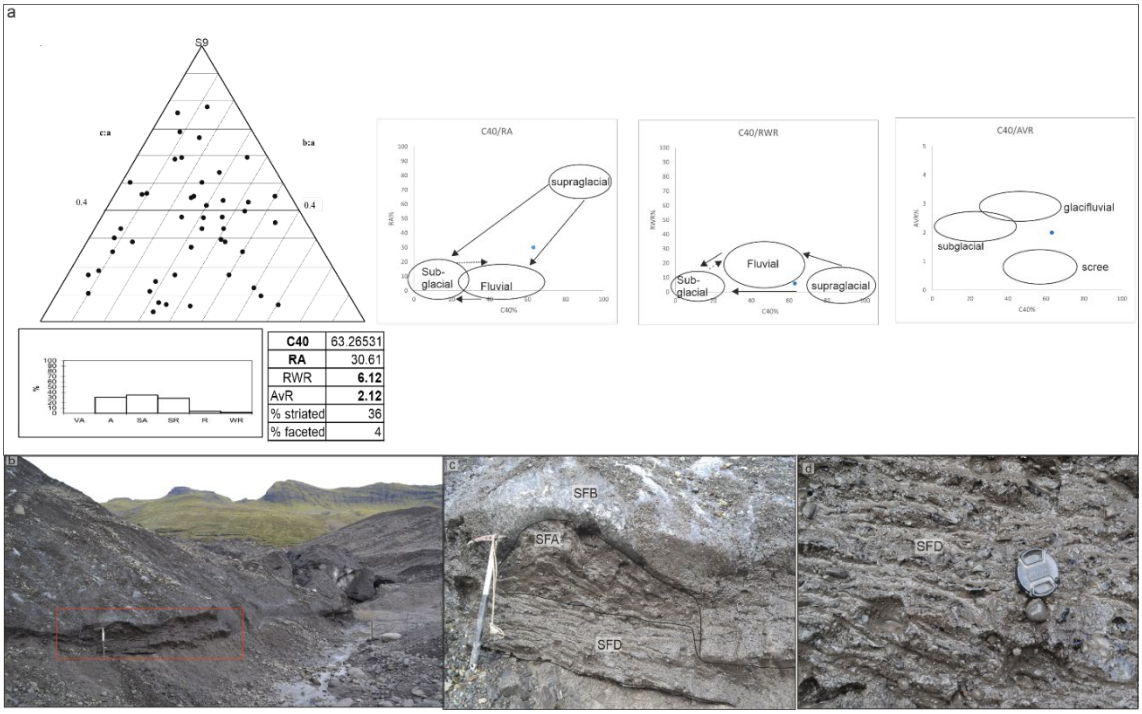

Figure 4.9: Clast shape data for sample S9 in stratified solid basal ice: a) clast form data and co-variance plots with envelopes shown based on control data from Lukas et al. (2013) and Evans et al. (2018b); b) sample site with red box showing sample location; c) details of basal ice layer; d) detailed image of SFD basal ice showing stratification layers and clast distribution.

Samples S10 and S12-34 (Appendix, 8, Figure 4.5) were taken at more random locations on the snout where debris concentrations facilitated clast extraction. The majority of these clasts were sub-angular (37%) or sub-rounded (45%) with a minor percentage of rounded (8%), angular (7%) and very angular 0.5%) clasts (Figure 4.5). The covariance plot shows that the clasts have subglacial characteristics when compared to control sample envelopes and this is verified by the fact that more than 50% of clasts in every sample are striated. Notably the majority of these striated clasts are from sub-rounded, or rounded clast populations. The variety of RA values (0-30%) within and between samples indicates that some relatively unmodified material is present.

4.4.2 Englacial stratified ice-debris dyke

A vertically inclined stratified debris band or dyke was also sampled within the marginal zone. This dyke comprised brown-grey sand and fine gravel (Figure 4.10b), was around 30 cm in width and could be traced laterally for around 15 m. The facies that made up the outer or lateral margins of the dyke was relatively clean with large ice crystals and displayed similar characteristics to anchor ice (see Table 4.1) potentially suggesting that the fracture accommodated several phases of fluid flow. The fill contained a high clast content comprising a range of grain sizes, but predominantly medium to coarse sand and gravel with a minor amount of silt and clay. The boundaries between the inner dyke fill and the relatively clean ice were sharp (red dashed lines on inset images in Figure 4.10). Notably, the dyke was partially open, with water present in what could be sigmoidal tension fissures. Larger clasts within the debris-rich ice were situated towards the boundary between the debris-rich and clean ice and smaller clasts towards the middle of the fill. This grading could reflect the changing velocity of the fluid (sediment and water) flowing into the open/active fracture during the formation of the dyke. Striations were present on 35% of the clasts sampled from the dyke fill, and clast roundness ranged from angular to sub-rounded (AvR = 2.52), with the majority being sub-angular and with a low RWR value of ~6%. The C_{40} and RA covariance indicates that the clasts have either fluvial or subglacial characteristics. These results provide evidence that the source of sediments being

released/transported by glaciers is complex and that the sedimentary components are polycyclic.

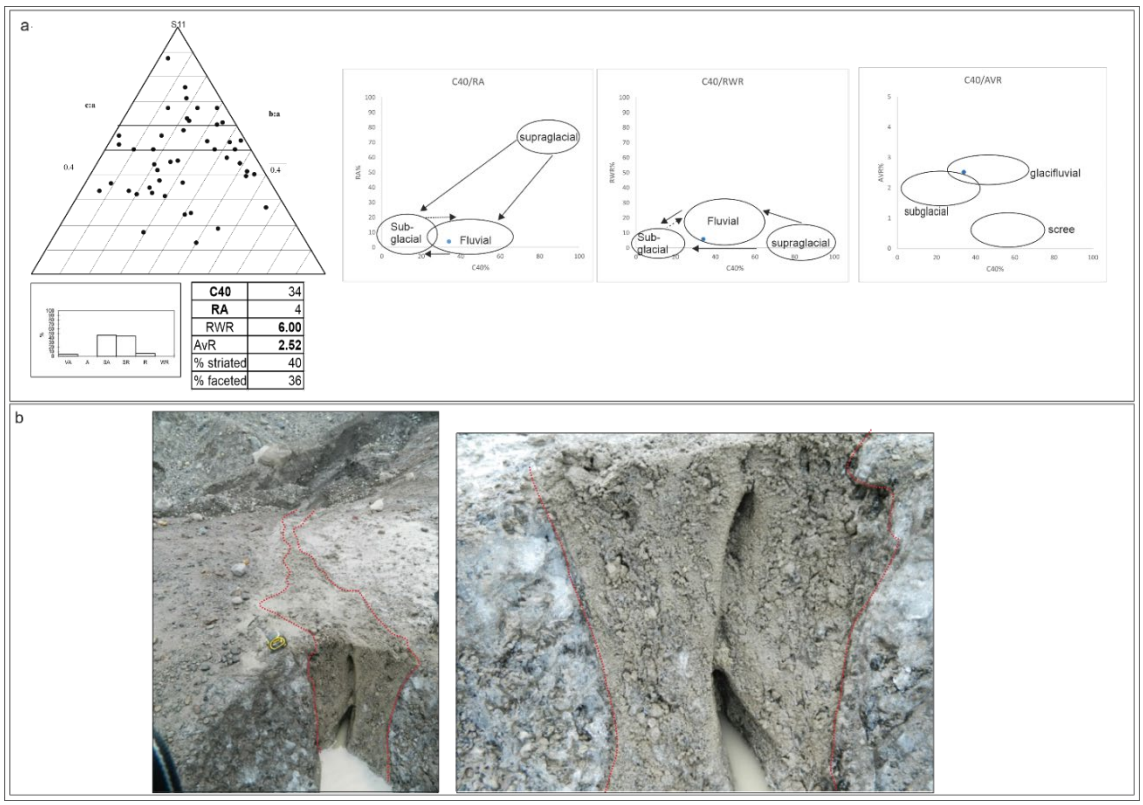

Figure 4.10: Clast shape data for sample S11: a) Clast shape data and co-variance plots with envelopes shown based on control data from Lukas et al. (2013) and Evans et al. (2018b); b) photographs for on-ice sample S11 (debris-rich dyke/englacial stratified ice).

4.4.3 Falljökull bedrock step

A sample of 30 clasts were collected from an exposure of basal ice overlying a bedrock step on the southern side of Falljökull (Figure 4.11, Appendix 11). The broad scale englacial stratification and structure of the ice here is highlighted as white dashed lines in Figure 4.12. This illustrates that there is not only clear stratification but there are traceable deformation structures at this sample location. The cross-cutting of the stratification in particular shows that thrusting is occurring and thrust planes are dipping up ice. These cross-cutting relationships between the thrusts can be used to indicate that there are at least two phases of thrusting. The basal ice stratigraphy at this location comprises a lowermost, debris-rich layered facies (SFA), overlain by dispersed facies ice (SFD) (Figure 4.13a-d). The facies contained brown-grey sediment and

contained layers of ‘clean’ (i.e. debris-free) ice between more debris-rich laminae. The ice contained a high clast content and alternating centimetre scale layers and lenses of both clean and debris-rich ice (Figure 4.13). Overall lamination thickness ranged from 5 to 20 cm (Figure 4.13b, c). Debris comprised a wide range of grain sizes, but mainly medium to coarse sand and granule gravel with a minor amount of silt and clay (Figure 4.13b and d). ‘Clean ice’ lenses were typically 1-5cm cm thick and contained isolated clasts (Figure 4.14) and pinched out laterally (Figures 4.13c and 4.14). The majority of the clasts within this debris-rich stratified basal ice were angular and sub-angular, with only 3% of these clasts showing striations. The clast shape data and C_{40}/RA plot in Figure 4.11 reveal a blocky, sub-angular sample indicative of subglacial in origin, although a small number (3%) of striated clasts and relatively high RA value of 20% reflects a relatively immature signature.

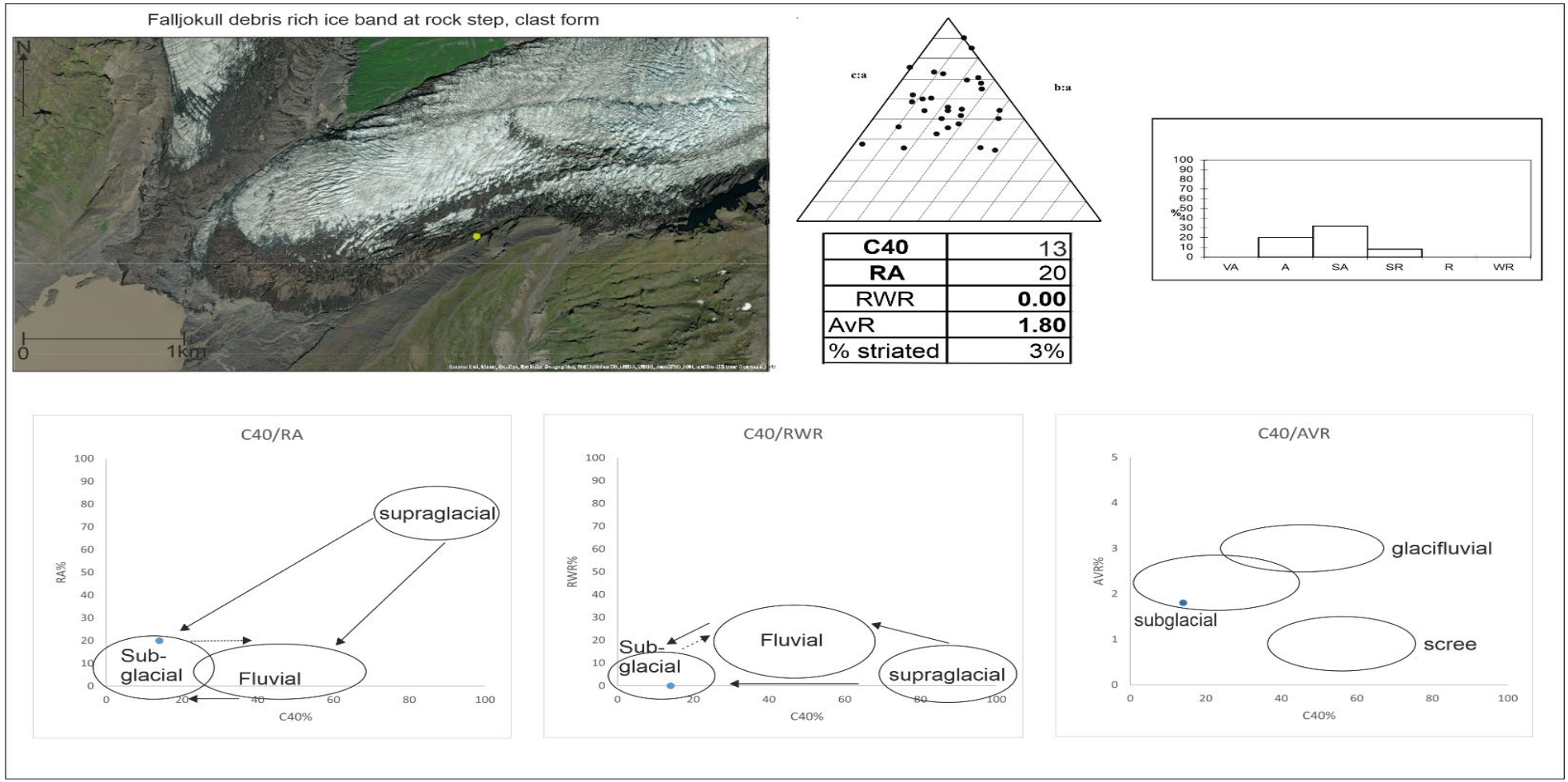

Figure 4.11: Clast shape data for sample collected from an exposure of basal ice at a bedrock step on the southern side of Falljökull. Co-variance plots with envelopes shown based on control data from Lukas et al. (2013) and Evans et al. (2018). See Appendix 10.

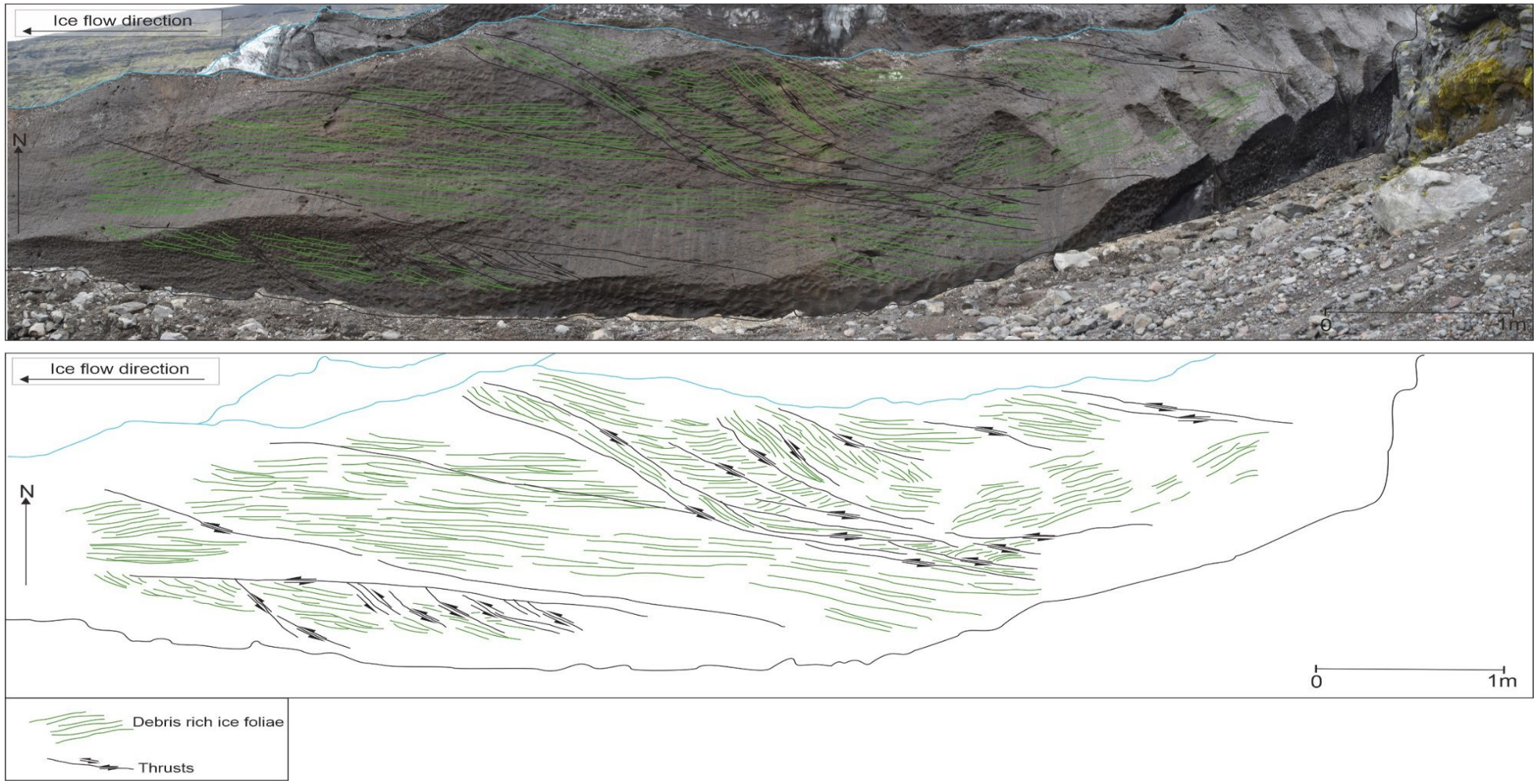

Figure 4.12: Overview of englacial structures and stratification above the bedrock step and at the base of the icefall at Falljökull. Green lines depict stratification and black lines depict thrusts.

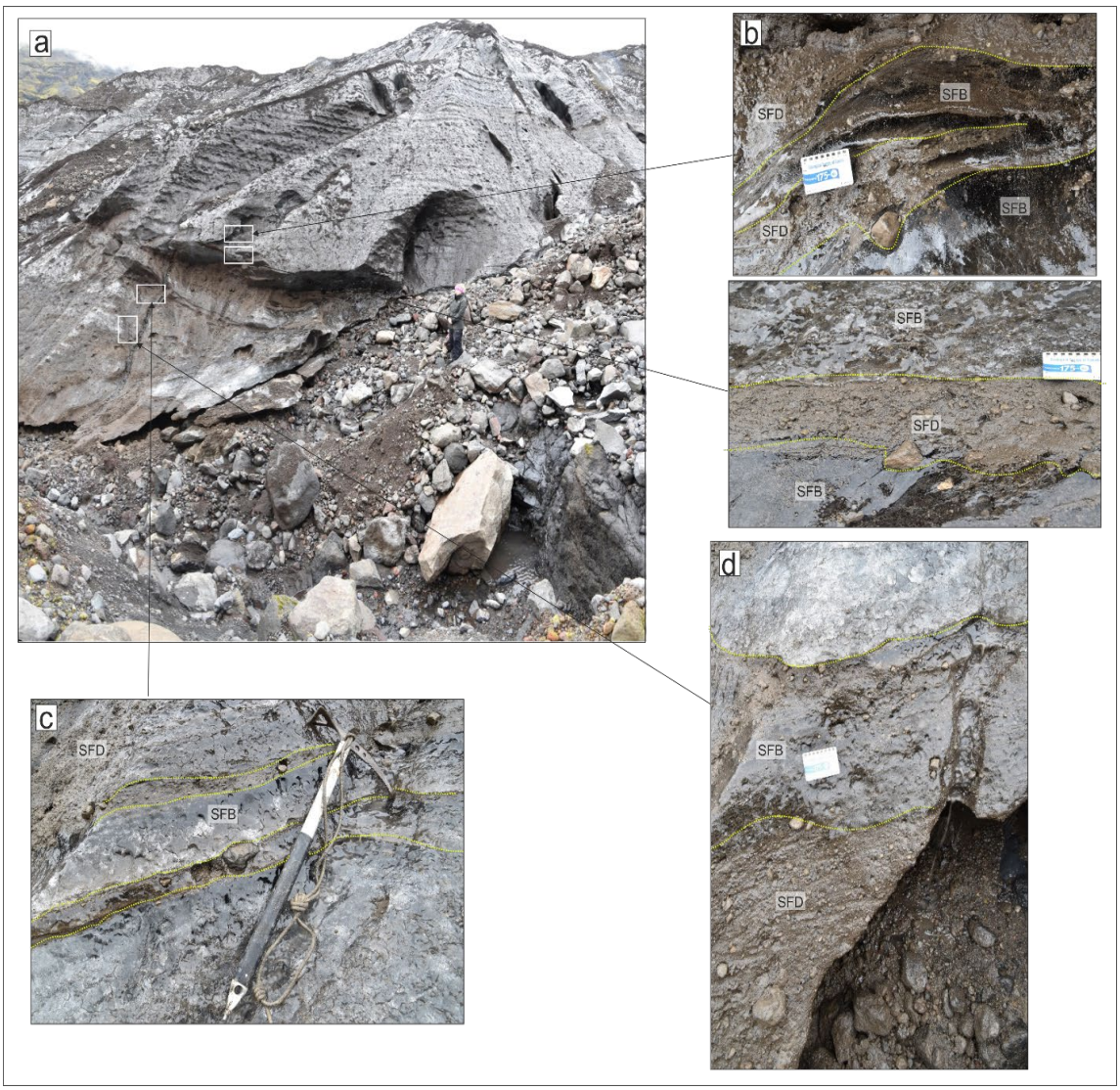

Figure 4.13: Field photographs of the Falljökull bedrock step and basal ice sample site: a) overview of sample site with white boxes showing the location of detailed images (person for scale); b) two images showing sediment banding in the ice (yellow dashed lines separate different debris bands); c) stratified ice with bands (depicted by the yellow dashed lines) of clean and debris-rich ice and enclosed clasts. Ice axe is approx. 40cm; d) stratification within the ice. SFB, SFD depict ice facies, classified using the scheme of Swift et al. (2018) and Cook et al. (2011a).

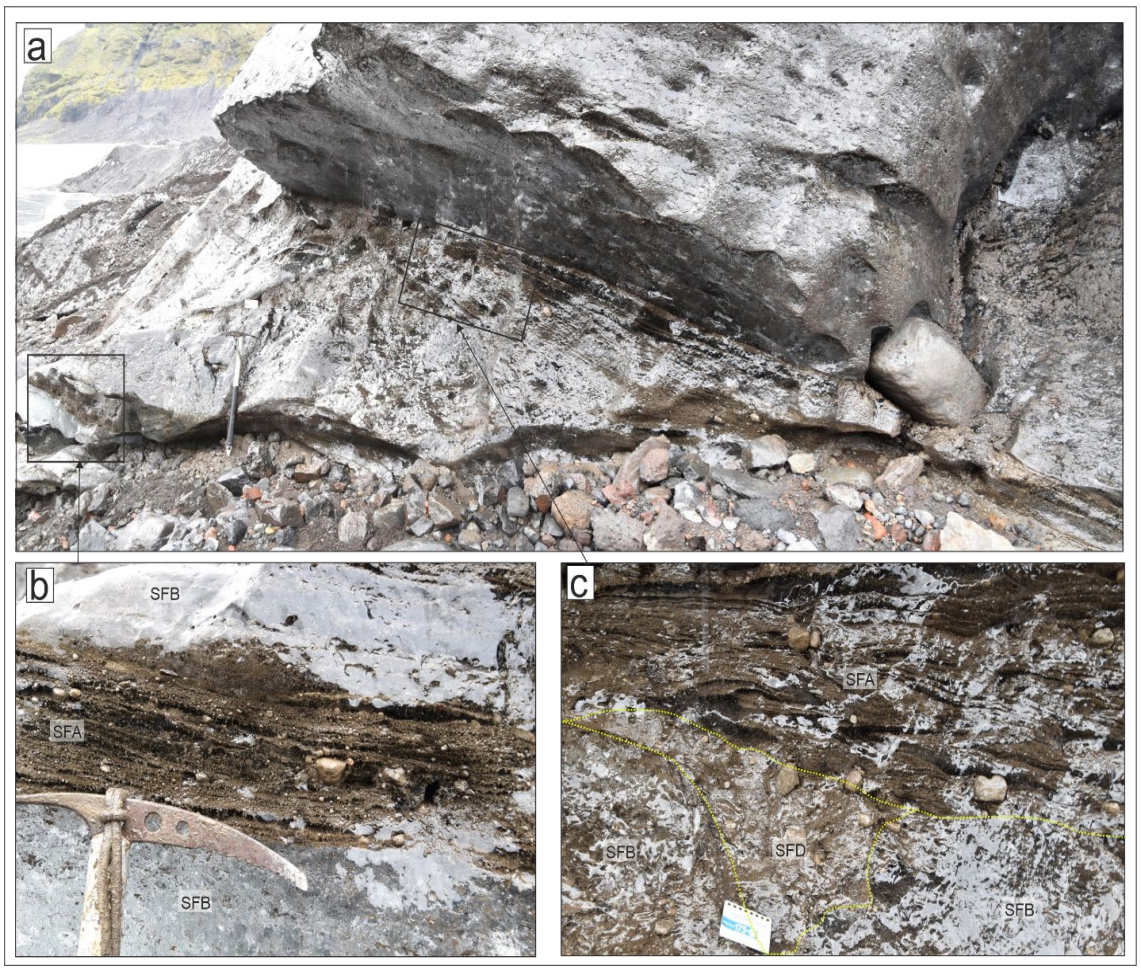

Figure 4.14: Details of the stratified ice facies at the Falljökull bedrock step: a) overall site image with black boxes showing detailed images; b) and c) stratified ice with labels SFB, SFD and SFA identifying ice facies classified using the scheme of Swift et al. 2018.

4.4.4 Contemporary sub-marginal push moraines and crevasse infill at Svínafellsjökull

Results from the 14-moraine sample (SM) locations (SM1-14, Figure 4.15, Appendix 8 and 11) recently formed at the snout of Svínafellsjökull demonstrate that the clasts are mostly sub-angular (60%) or sub-rounded (33%) with a small percentage of rounded clasts (4%). The C_{40}/RA plot indicates that these samples are characterised by clasts that display indicators of a glacifluvial transport pathway through the ice to the sub-marginal area, where moraine construction is occurring by bulldozing this sediment during periods of advance. Notably, twelve of the fourteen sample locations contain 50% or more striated clasts, indicative of their passage through the subglacial traction zone or that they represent striate bedrock plucked from the bed.

Sample moraine 5 (SM5) (Figure 4.16) was taken from a push moraine that was created during the winter months of 2017, and which was still in contact with the ice. The facies of this ice is SFD. The sediment contained within the moraine comprises brown to dark grey sediment, which was in most part fine sand and silt with isolated clasts. Clasts found within this push moraine range from sub-angular (52%) to sub rounded (40%), with a small amount of angular (2%) and rounded clasts (6%). The C_{40} (60%) and RA (2%) values indicate that samples have fluvial characteristics (see envelop on C_{40}/RA plot in Figure 4.15). Also notable is the large number of clasts that have striations (62 %) and are faceted (36 %). Sample SM7 is also from a push moraine that was still in contact with the marginal ice in 2017 (Figure 4.17). It also has the same brown-dark grey sediment colour, but with notably more clasts. The majority of these clasts are sub-angular (62%) and sub rounded (38%), with 54% displaying striations. Similar to sample moraine SM5, the clasts within this moraine display glacifluvial characteristics when their covariance plot is compared to control samples (Figures 4.15 and Figure 4.17). The sediment composition of the crevasse infill (SM6) was similar to that of the push moraines (Figure 4.18), however notably more water was present within the brown/grey sediment and less larger clasts were apparent. The clasts within the crevasse infill were mainly sub-angular (68%) and sub rounded (28%), with fluvial transportation characteristics (C_{40}-60%, RA-2%) (Figure 4.18). Notably 86 % of the clasts are striated, and 32 % are faceted with a AvR value of 2.30 this is of interest, as that the shape of the clasts is indicating that they are fluvial/glacifluvial but the high percentage of straited and faceted clasts would indicate a period of time being transported and/or residence time within a subglacial setting. This is a rather complex signature to interpret and possibly reflects the complexity of ice marginal sediments which are being overidden by the ice and incorporated into the push moraines and crevasse squeeze ridge.

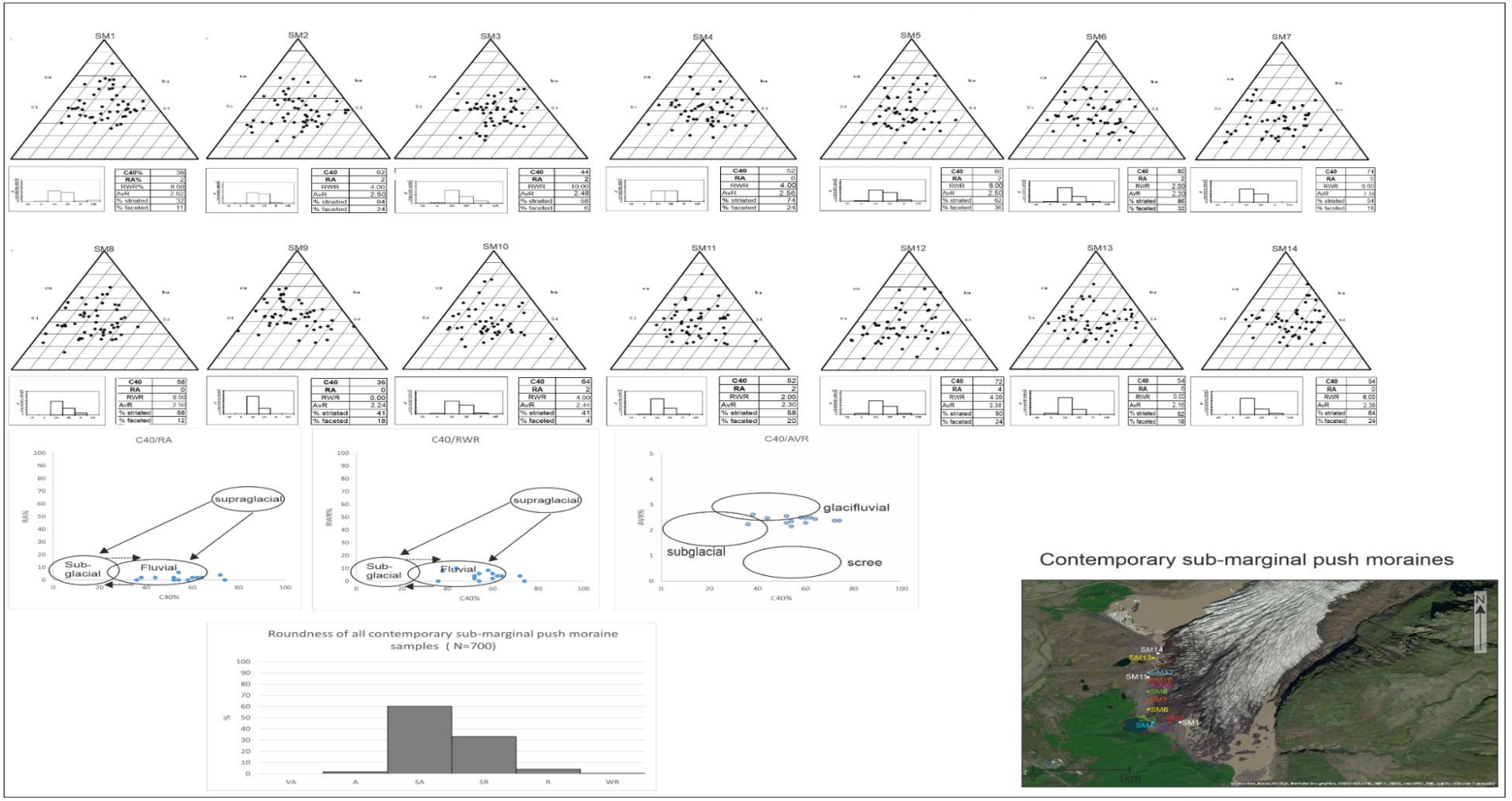

Figure 4.15: Clast shape data for samples taken from contemporary sub-marginal push moraines (SM 1-14). Background image from Esri World Image Basemap layer (Source: Esri, Maxar, Earthstar Geographics, and the GIS User Community). Co-variance plots with envelopes shown based on control data from Lukas et al. (2013) and Evans et al. (2018).

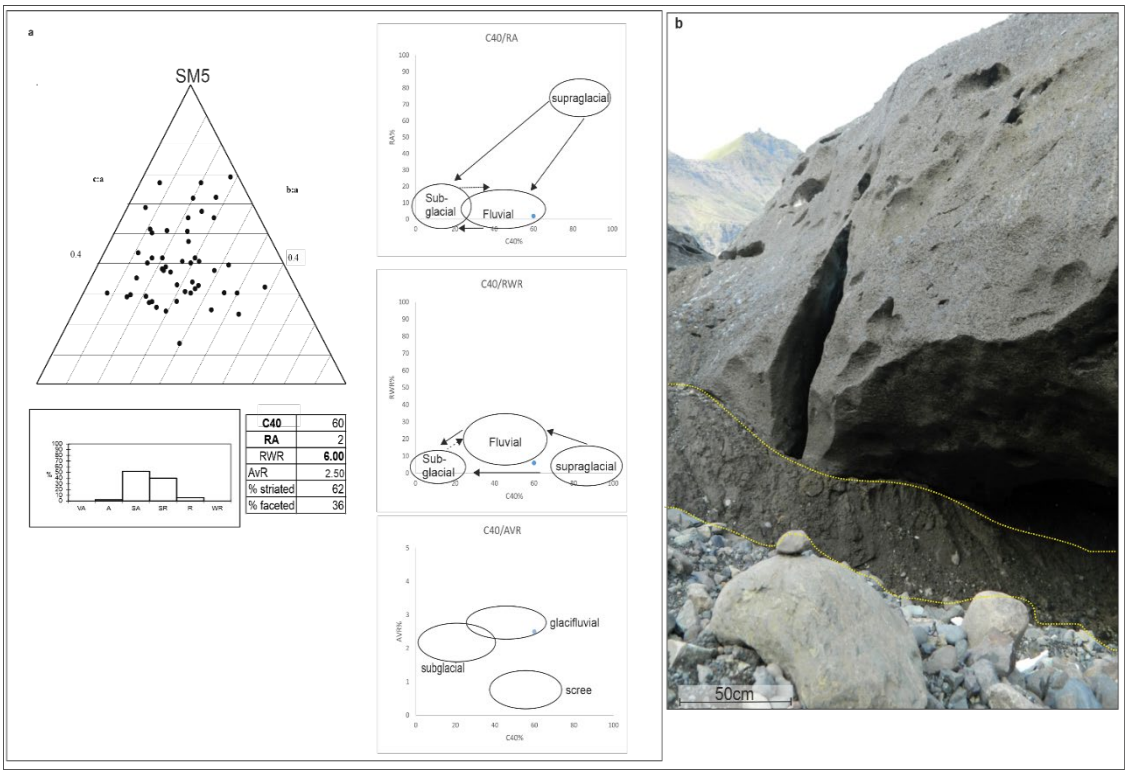

Figure 4.16: Sample site SM5: a) clast shape data and co-variance plots with envelopes shown based on control data from Lukas et al. (2013) and Evans et al. (2018b); b) field image of sample site, with yellow dashed line depicting the push moraine sample area.

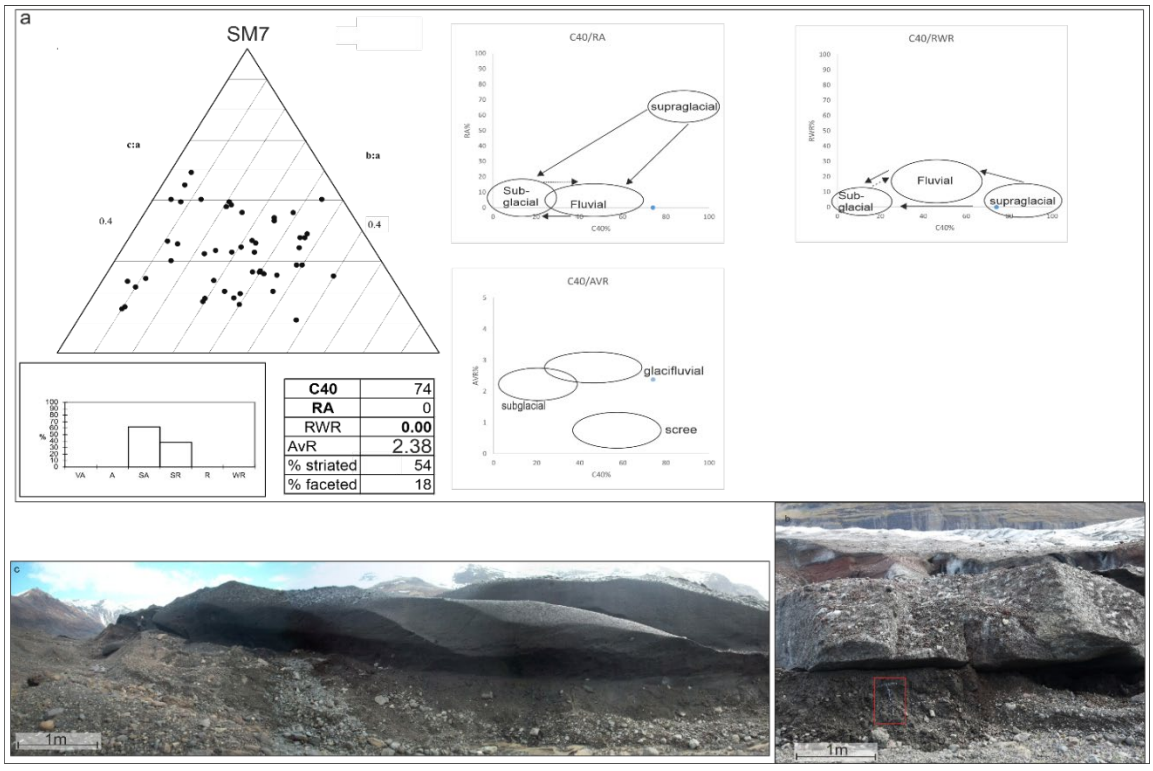

Figure 4.17: Sample site SM7: a) clast shape data and co-variance plots with envelopes shown based on control data from Lukas et al. (2013) and Evans et al. (2018b); b) and c) field images showing push moraine sample site (ice axe in b for scale).

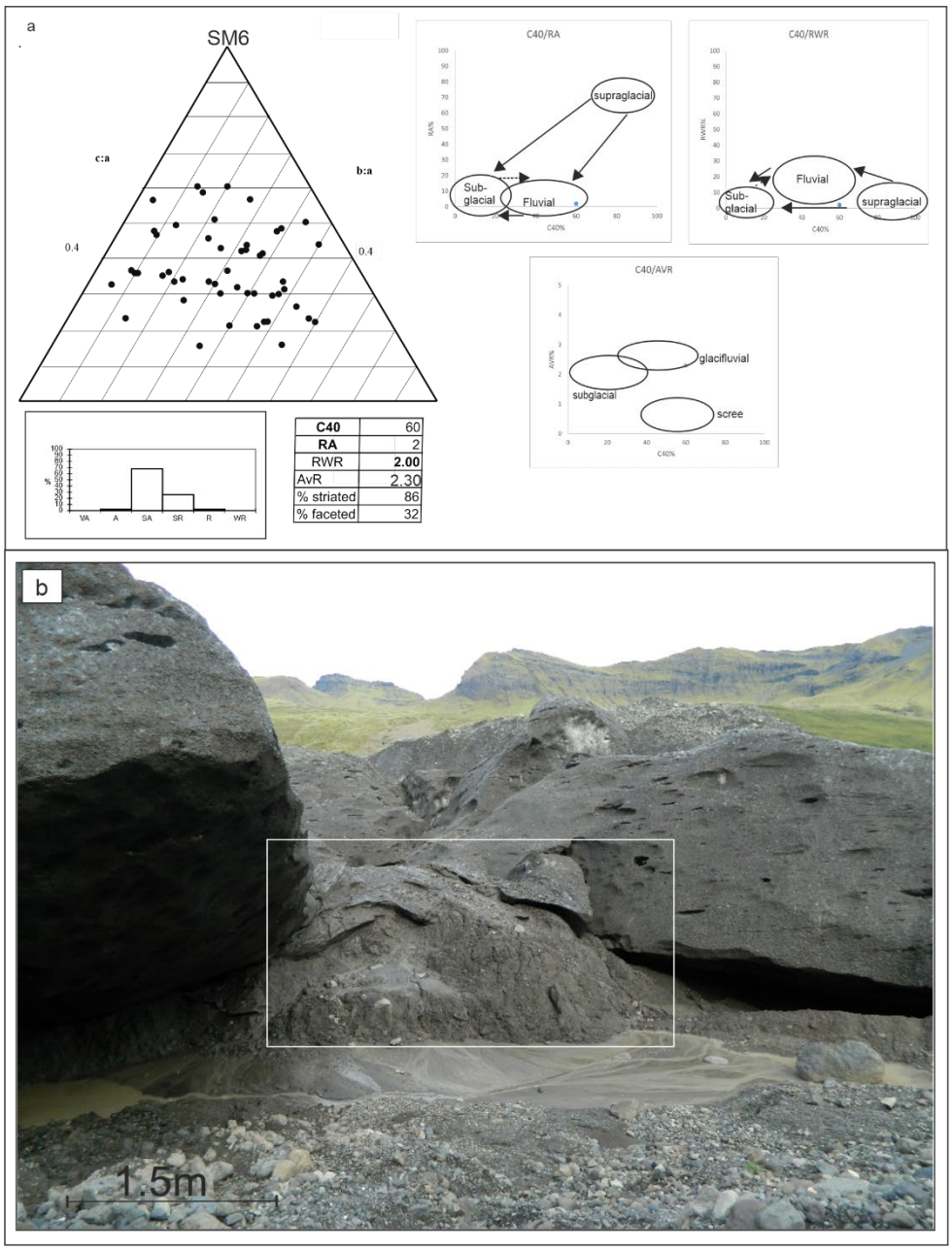

Figure 4.18: Ternary clast form diagrams and histograms of roundness with values for C_{40}, RA, RWR and average roundness (AvR). Abbreviations: VA very angular; A angular; SA sub angular; SR sub rounded; R rounded; WR well rounded; b) Field photograph of sample area SM6.

4.4.5 Spatial Patterns in Debris Characteristics

Contour maps of C_{40}, RA, RWR and average roundness (AvR) data highlight clear patterns in the debris transport pathways both on and off ice. The general trend highlighted by the basal ice facies and the englacial stratified ice (Figure 4.19) shows the occurrence of mutually exclusive concentrations of high RA versus RWR and AvR values. The pattern of C_{40} values displays a range

of relatively high and low concentrations that do not closely correlate with any of the other variables, despite previous studies on covariance identifying a strong correlation at least between C_{40} and RA (Benn and Ballantyne 1994). The bullseyes of high RWR, AvR and generally low overall values of RA, indicative of a predominance of subglacial and/or glacifluvial wear, indicate that: 1) passive, supraglacial transport has been negligible, with only one high RA cluster up to 43% occurring near the glacier margin; and 2) sediments derived from the bed or from meltwater networks (active transport), although dominant, have not been delivered and incorporated into basal ice facies uniformly across the glacier snout but rather occur in pockets within the ice, with an elongated zone of relatively high rounding being represented by two ellipsoid clusters on the western edge of the central glacier margin (Figure 4.19).

Based on the current spread of data points the initial interpretation is that the contour maps for the clast shape data for the contemporary sub-marginal push moraines (Figure 4.20) indicate that actively (subglacial) transported debris has been delivered to the glacier margin unevenly. The C_{40} data again have no clear correlations with other indices but the concentration of samples with high AvR and RWR ratios towards the southern end of the glacier is interpreted as indicating that a prominent transport pathway and depo-centre for subglacially and/or glacifluvially worn clasts occurs at the southern tip of the central glacier margin. This coincides with the on-ice cluster of relatively higher rounding (Figure 4.19), indicating a potential clear transport pathway from englacial stratified ice to proglacial push moraine emplacement. A similar linkage between on-ice and proglacial push moraines samples is apparent in RA values on the western edge of the central glacier margin.

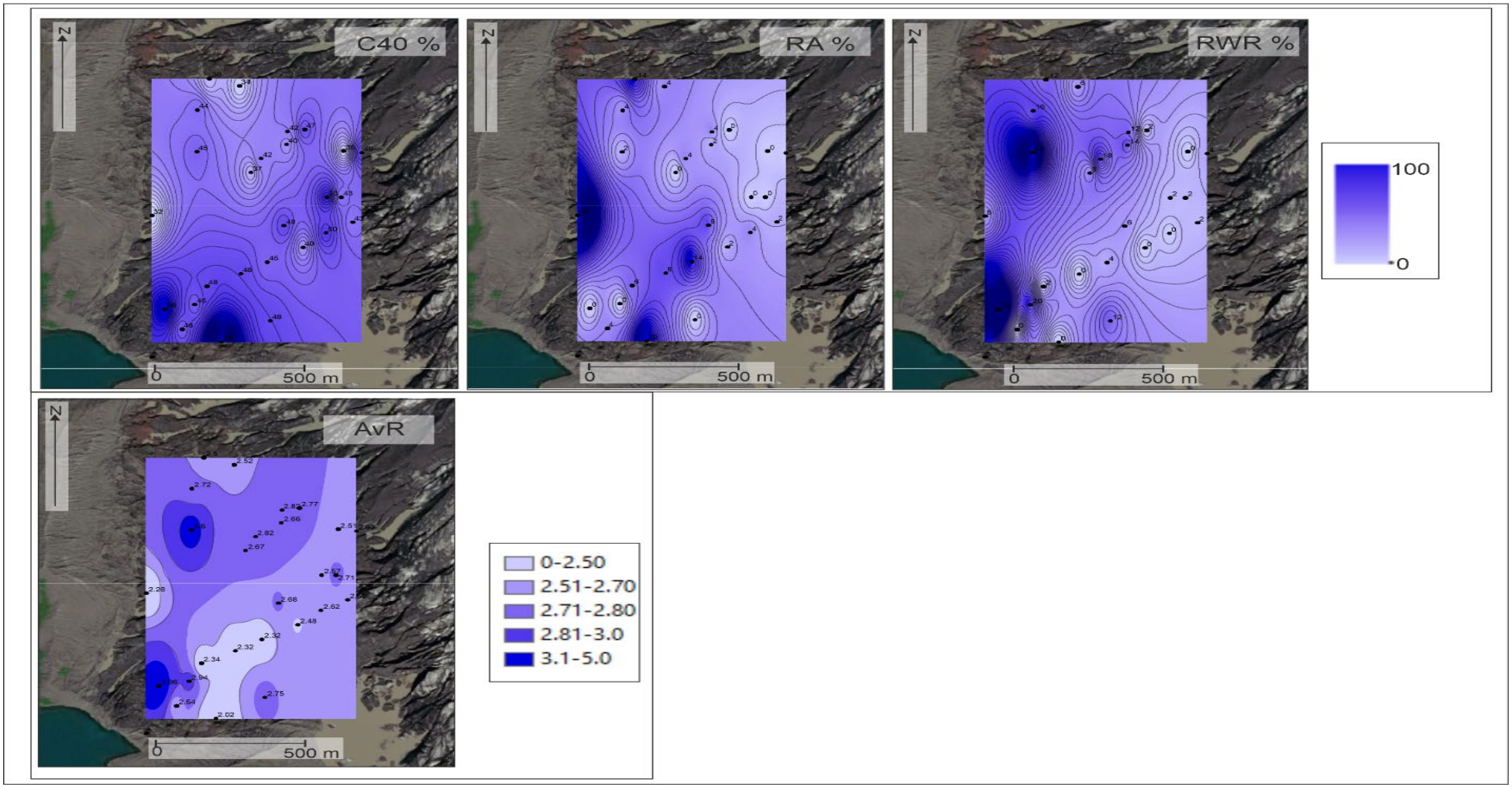

Figure 4.19: Contour maps of RA, C_{40}, AvR and RWR using data from the sampling points identified within debris-rich basal ice and englacial stratified ice on Svínafellsjökull.

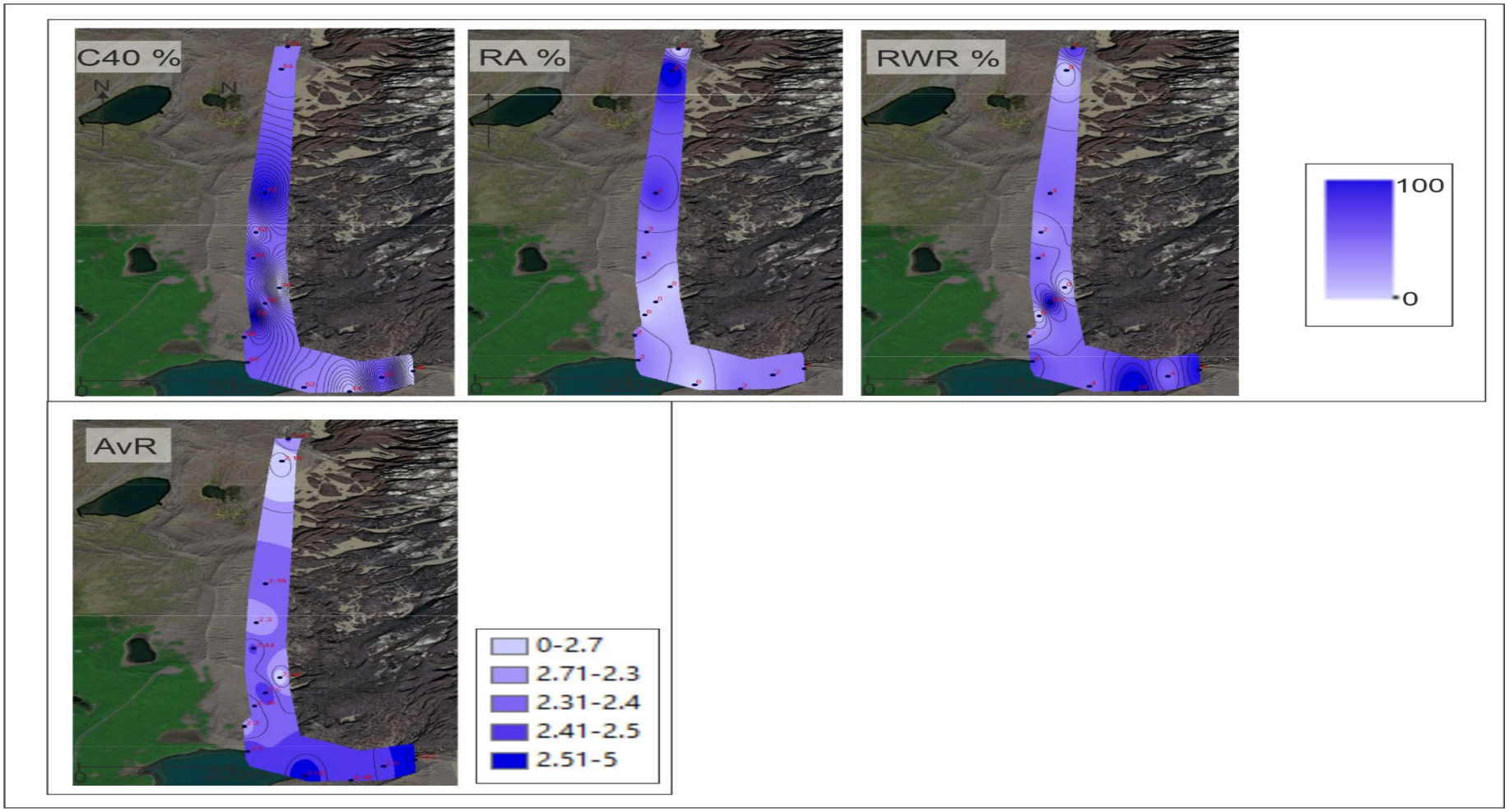

Figure 4.20: Contour maps of RA, C40, AvR and RWR using data from the sampling points identified within contemporary sub-marginal push moraines on the foreland of Svínafellsjökull.

4.5 Interpretations

In summary, the main ice facies identified above are SFA, SFB and SFD (Figure 4.21). Facies SFA exhibits the same characteristics described by Cook *et al.* (2011a) and Swift *et al.* (2018), which they describe as exhibiting medium ice crystal sizes of 0.5 to 3 cm diameter, with low debris by volume of 0.1 to 3.2% and comprising mm-thick, alternating debris-rich and clean ice layers. Debris layers within SFA comprise silt/clay to granule gravel up to around 4 mm diameter with isolated examples of faceted, angular to rounded clasts up to 4 cm diameter. These characteristics are compatible with a subglacial origin, likely by incremental freeze-on, as proposed by Swift *et al.* (2018) who concluded that some stratified (but not stratified solid (SFD)) ice is formed by regelation. They go on to state that freeze-on in this environment can occur by freezing of flowing water or through a combination of regelation infiltration and/or segregation ice formation (cf. Christoffersen and Tulaczyk, 2003; Christoffersen *et al.,* 2006). Evidence from this study supports this theory, specifically when analysing the englacial stratified ice-debris dyke.

Facies SFB is massive and structureless with occasional debris-rich foliae (Figure 4.21). The sediment texture from these facies is gravelly, mud-rich medium sand. Clast shape data reveal that the coarser debris within the SFB is mostly striated (36-86%) and is either sub-angular or sub-rounded (AvR = 2.18-2.66). Co-variance plots indicate that the clasts sampled within the SFB facies have subglacial and (glaci)fluvial characteristics (Figure 4.22) suggesting that the sediment within these facies includes a significant input to the englacial debris from basal till and from meltwater networks developed either at the ice-bed interface or as englacial tunnels.

Facies SFD, which is more extensive than the other two facies, is characterised by alternating, gently convolute and sub-horizontal, mm to cm thick debris-rich and clean-ice laminae. The debris-rich laminae display silt/clay to granule gravel with occasionally larger clasts up to 11 cm diameter (Figure 4.21). Clast forms in SFD are typically angular (36%), sub angular (35%) and sub-rounded (28%) with minor rounded and well-rounded components (AvR = 2.12), 36% of which

are striated. The covariance plot (Figure 4.22) indicates that these clast characteristics are indicative of short distance glacifluvial transport, likely representing the subglacial meltwater reworking of basal till prior to entrainment as englacial debris. This is consistent with the findings of Swift *et al.* (2018), which indicate that stratified solid facies debris has travelled a shorter distance in active transport than the diamictons found throughout their study. This facies was also considered by Cook *et al.* (2007, 2010) to be consistent with a supercooling origin due to the resemblance to the 'solid' facies of Lawson (1979), which has since been attributed to supercooling by Lawson *et al.* (1998). Cook *et al.*, (2007, 2010) observed this and other facies attributable to supercooling only in the southern region of the terminus of Svínafellsjökull, where they also found direct evidence of upwelling of supercooled subglacial waters.

With respect to debris entrainment processes at the base of ice falls (Figure 4.2), the basal ice stratigraphy at the Falljökull bedrock step comprises a lowermost, debris-rich layered facies (SFA), overlain by dispersed facies ice (SFD). The SFA facies contains brown-grey sediment and layers of 'clean' (i.e. debris-free) ice. Where debris-rich, the facies contains high clast contents and alternating centimetre scale layers and lenses of both clean and debris-rich ice. Overall lamination thickness ranged from 5 to 20 cm. Debris comprised a wide range of grain sizes, but mainly medium to coarse sand and granule gravel with a minor amount of silt and clay. 'Clean ice' lenses within the ice were typically 1-5cm thick and contained isolated clasts and pinched out laterally. The majority of the clasts within this debris-rich stratified basal ice were angular and sub-angular, with only 3% being striated. However, co-variance reveals that the clasts in the SFD facies here (red data point in Figure 4.22), in contrast to the glacifluvial trends in the SFD at Svínafellsjökull, have a clear subglacial signature. The occurrence of SFA and SFD facies with subglacial clasts at the base of the icefall, in addition to the repetition of stratified facies by overthrusting (Figure 4.12), is compatible with the model of ogive formation proposed by Swift *et al.* (2018), wherein debris is entrained into basal thrusts and elevated into englacial positions due to longitudinal compression (Figure 4.2). Regelation at the ice-bed interface in these settings is driven by strain heating and frictional melt due to increased ice flow velocities at the icefall.

Work by Phillips *et al.* (2013, 2014) at Falljökull highlights that surface velocities below an icefall can be around 72m yr^{-}1. This work also highlighted the operation of thrusts in the glacier and their role in transmitting water and debris both subglacial and englacially. Notably this research highlighted that these thrusts were reported as inactive and no longer under compression when they were being exploited as fluid pathways. Between September 2012 and April 2013, continued movement on a down-ice dipping normal fault led to the glacier surface being vertically offset by approximately 4 to 5 m (Phillips *et al.,* 2014). Field observations during this research also highlights that overpressurized englacial and/or subglacial meltwater formed a series of artesian upwellings or fountains along the glacier margin during the spring to early summer, indicating that the thrusts likely extend to the ice-bed interface and/or the englacial drainage was also pressurised.

Clast shape data collected from the debris-rich ice facies in the marginal zone of Svínafellsjökull indicates that basal to englacial debris-rich ice formation has involved entrainment of subglacial and glacifluvial material. Indeed, clast samples contain notable occurrences of well-rounded clasts, many of which are striated (cf. Swift *et al.,* 2018). The occurrence of such material in relatively thick sequences of debris-rich ice facies suggests that entrainment was likely not entirely due to regelation and/or supercooling but also could be attributed to elevation along englacial thrusts (Swift *et al.*, 2018). Thrusts may also cross-cut englacial meltwater drainage tunnels and crevasse infills (cf. the conduit fills of Spedding and Evans, 2002) and subglacial and glacifluvial material may be elevated through glacier ice by injection of high-pressure subglacial water into basal crevasses, especially during jökulhlaups (e.g. Bennett *et al.,* 2000; Roberts *et al.,* 2000; Ensminger *et al.*, 2001; Evans *et al.,* 2012, 2022; Lovell *et al.*, 2015). Such complex debris transfer pathways, have been inferred from supraglacial and proglacial clast analysis at other Icelandic glaciers, including Kvíarjökull (Spedding and Evans, 2002; Swift *et al.,* 2006), Tungnafellsjökull (Evans, 2010), Flaajökull (Lukas *et al.*, 2013) and Skaftafellsjökull (Evans *et al.,* 2018b).

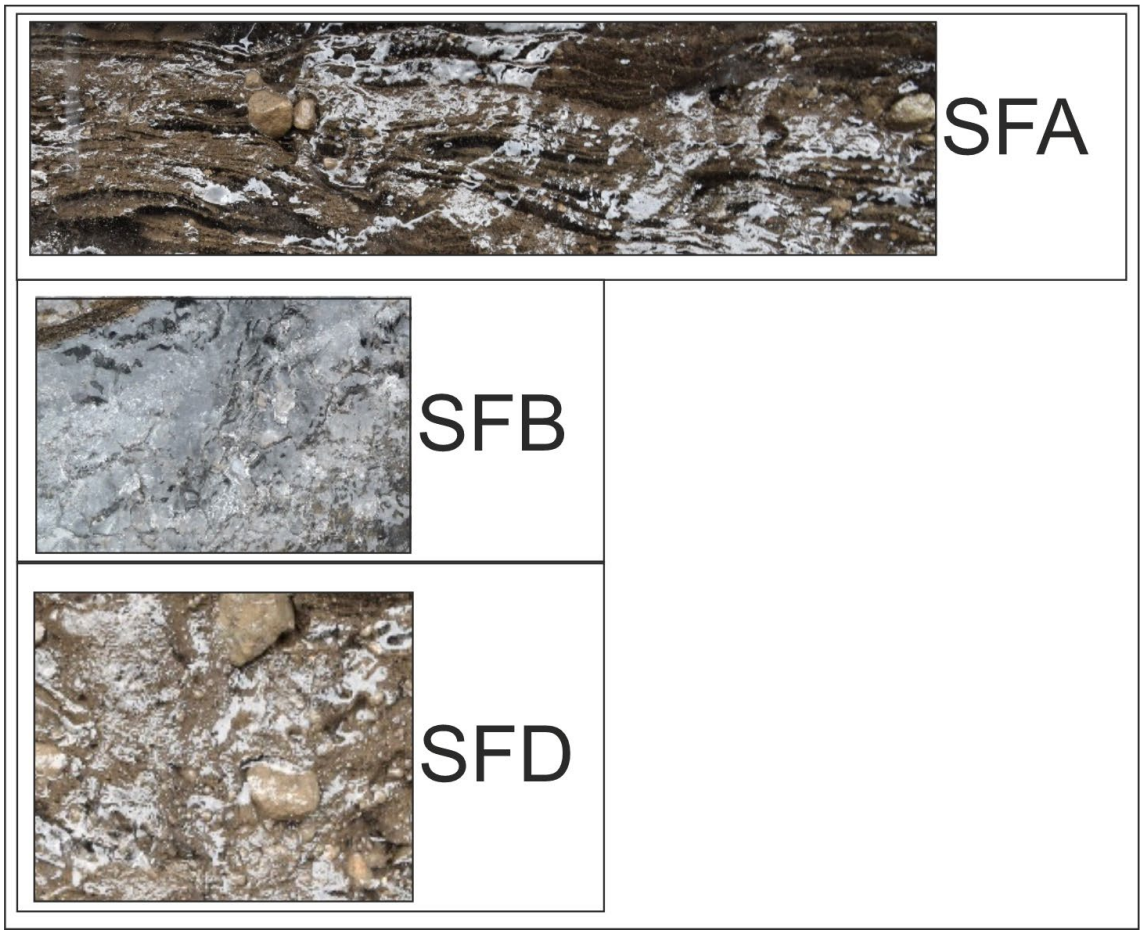

Figure 4.21: Field photographs of marginal Ice facies found at Svínafellsjökull.

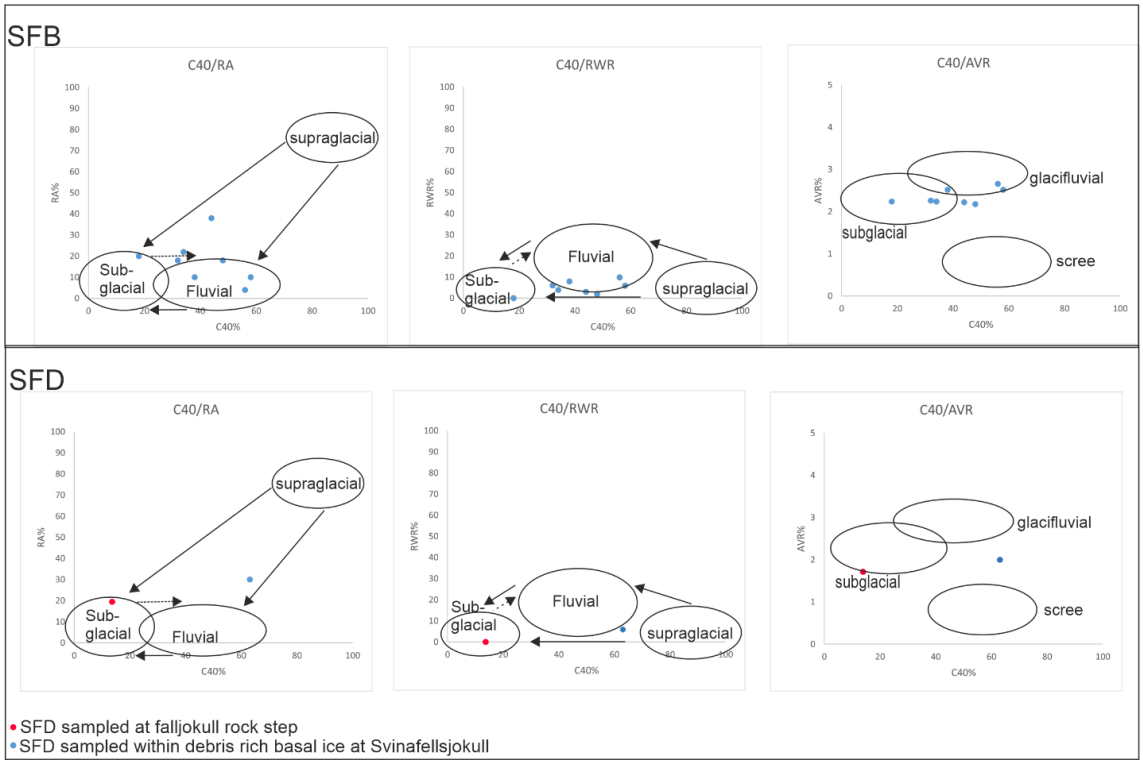

Figure 4.22: Co-variance plots of marginal ice facies found at Svínafellsjökull, and Falljökull bedrock step. Envelopes shown based on control data from Lukas et al. (2013) and Evans et al. (2018b).

The complex glacifluvial transfer of debris through glacier snouts as outlined above is likely reflected in the pattern of clast shape characteristics across the marginal area of Svínafellsjökull (Figure 4.19), as outlined in section 4.4.5. The contour bullseyes of high RWR, AvR and generally low overall values of RA are suggested to represent concentrations of debris emerging through the supraglacial melt-out of debris-rich ice facies containing clasts with subglacial and/or glacifluvial wear signatures. Such concentrations or clusters of subglacially and glacifluvially derived material are difficult to explain as regelation or supercooling products, as they indicate a point source rather than a more evenly spread entrainment pattern created at the ice-bed interface and then exposed across the snout through rising foliation (controlled moraine; Evans, 2009). Clusters of high RA values, on the other hand, can be explained by the passive transportation of extraglacial (i.e. rockfall) debris from their sporadic emplacement point higher up the glacier down to the snout without passing through the subglacial traction zone (avalanche type medial moraines of Eyles and Rogerson, 1978). The emergence in clusters of subglacially and glacifluvially derived debris via active transport indicates a point source or, more precisely, an elongated source zone, as demarcated by the two ellipsoid clusters of relatively high rounding on the western edge of the central glacier margin (Figure 4.19). This pattern cannot be easily explained as the product of regelation/supercooling and/or englacial thrusting of subglacial debris, but instead the result of entrainment and shearing of englacial tunnel deposits formed by lake decanting/drainage through the snout of the glacier. Evidence for this debris transport pathway has been presented in Chapter 3, where it was shown that a proglacial lake situated on the north-western margin of Svínafellsjökull periodically drains, leaving icebergs stranded along the shoreline. During September 2018, 24 to 48 hours after a lake draining event, water was observed to be flowing under the ice (See Chapter 3, Figure 3.15b). Observations by glacier tour guides suggest that periodic draining of this lake happens throughout the summer months each year and the periods between lake drainage events can be as short as 24 hours. This could offer an explanation as to why glacifluvial material is apparent in debris samples from the marginal

zone of Svínafellsjökull. Considerations must also be given to the factors that are controlling the location of the englacial channel. From Chapter 3, it can be seen that the structural architecture of the glacier is dominated by flow parallel, longitudinal fractures. Analysis indicates that these fractures accommodate strike slip movement which includes the formation of extensional shears as open crevasses on the surface (for example S11). Not only does this allow the sediment from rock falls to penetrate the ice, but also form open cavities which can transmit meltwater and sediment. The thermal expansion caused by the meltwater within these cavities can then contribute to the formation of the englacial channels through the ice which exploit the longitudinal fractures.

4.6 Discussion

4.6.1 Debris entrainment and transport processes at Svínafellsjökull and Falljökull

Debris bands are found in all glaciers regardless of morphology and thermal characteristics (e.g. Swift *et al.*, 2006; 2018; Hubbard *et al.*, 2004; Evans, 2009; Larson *et al.*, 2010; Lovell *et al.*, 2015) and thrusting is accepted as one possible explanation for their formation, or at least the replication of supraglacial controlled moraine initiated by a range of entrainment processes (e.g. Evans, 2009; Swift *et al.*, 2018; Jennings and Hambrey, 2021). However, as Evans, (2009) and Swift *et al.* (2018) have demonstrated, the debris transfer thrust mechanisms, the identification criteria for debris-charged thrusts, and the relative importance of thrusting compared to other debris entrainment processes remain subjects of significant debate (e.g. Weertman, 1961; Hooke and Hudleston, 1978; Woodward *et al.*, 2002, 2003; Glasser *et al.*, 2003; Hambrey *et al.*, 1996, 1999; Hubbard *et al.*, 2004; Lukas, 2005; Graham *et al.*, 2007; Evans 2009; Moore *et al.*, 2010). The debris entrainment and transfer model proposed by Swift *et al.* (2018) elucidates the processes of debris-rich glacier ice formation and debris transport for Svínafellsjökull, expanding on previous studies on active temperate glaciers more widely (e.g. Goodsell *et al.,* 2005; Swift *et al.*, 2006; Evans 2009; Bennett and Evans, 2012; Jennings *et al.*, 2014). The model also advocates large scale folding as being a method of incorporating sediment into the ice, however

very little folding was found within sample sites used within this project (for location of sample sites see Appendix 8).

In testing the Swift *et al.* (2018) model, this study has verified certain aspects of debris entrainment proposed therein, specifically the entrainment of subglacial debris via regelation and elevation along folds and thrusts at the base of icefalls. Swift *et al.* (2018) propose that, within the icefall, deformation causes supraglacial debris to become dispersed after entering supraglacial crevasses. At the base of the ice fall this debris imparts cross-glacier arcuate band-type ogive foliation (Forbes bands) that elevates basal ice and debris into basal folds, the upper limbs of which develop into thrusts (cf. Goodsell *et al.*, 2002; Swift *et al.*, 2006) (Figure 4.23). Rotation of ogive formation then occurs, due to internal deformation, and particularly high strain rates near the bed. This causes dispersed basal ice and debris to form a relatively thick dispersed facies basal ice layer (cf. Cook *et al.*, 2011a). However, the rate of flow at the bed is likely to be lower than that found within the glacier, due to the frictional drag at the base of the ice and along the walls of the valley. Therefore, it is more likely that the degree of rotation occurs within the main body of the glacier and this would result in a listric shape to the ogive bands. Swift *et al.* (2018) then states that deformation below the ice fall further elevates subglacial basal material into a thick sequence of debris bands whose characteristics reflect the specific nature of entrainment and cumulative mixing over time (Figure 4.23). Data obtained from the bedrock step at Falljökull in this study, most specifically the subglacial clast form characteristics, verifies this concept of elevation of basal debris. The occurrence of stratified basal ice at this location also provides insight into the exact process of entrainment, which according to the process-form regimes identified by Cook *et al.* (2011a) and Swift *et al.* (2018) is likely to be regelation.

Further down glacier, in the compressive zone of the snout, surface ablation slowly uncovers buried englacial structures, including those initiated at the base of the ice fall. Additionally, the process of debris band production here by supercooling (Swift *et al.,*2018) appears to be

augmented by the entrainment of subglacial and water-worked debris through the emplacement of englacial sediments in englacial drainage networks and hydrofractures, which are periodically opened during melt events and then closed by ice creep and annealing and subject to compressive ice flow, thrusting and folding (Figure 4.23). This is manifested at Svínafellsjökull by the ellipsoid clusters of high clast rounding on the western edge of the central glacier snout, thought to be the product of subglacial tunnel infilling that is being exposed at the snout after emplacement by periodic draining of a proglacial lake at the northwest snout margin. This also explains the delivery of more rounded clasts to the contemporary sub-marginal push moraines in this area of the foreland. It also provides an explanation for the lack of uniformity and snout wide delivery of such water-worked debris to basal ice facies, a trend previously identified by Spedding and Evans (2002) at nearby Kviárjökull and related there to the development of englacial tunnels bypassing the overdeepening.

Finally, when examining the structural maps within Chapter 3 a significant limitation of Swift *et al.* (2018) model is highlighted. The structural mapping presented within Chapter 3 do not reveal any evidence for large scale folding in the upper reaches of Svínafellsjökull, below the icefall, which is a key process in step 4 of Swift *et al.* (2018) model, see Figure 4.2. Also, on Figure 4.2 the dip of the developing Ogives is far steeper than the observed dip of this type of banding seen on the aerial photographs presented in Chapter 3. The aerial photographs show the geometry of the intersections of the ogive bands on the surface of the glacier and indicate that they dip at low to moderate angles up ice. However, very steeply inclined to subvertical bands as shown on Figure 4.2 would appear as straighter, less curved lines cutting straight across the glacier surface. Again, when linking the Swift *et al.* (2018) model to the structural maps found within Chapter 3, it can be concluded that thrusts within the marginal area of Svínafellsjökull are identified, however not all show evidence of debris being thrust into the ice. Hence, this process and supercooling may not be as widely developed as suggested by the Swift *et al.* (2018) model and could be occurring as localised and periodic in nature, which could be directly controlled by annual, decade or even centennial variations in subglacial hydrogeology.

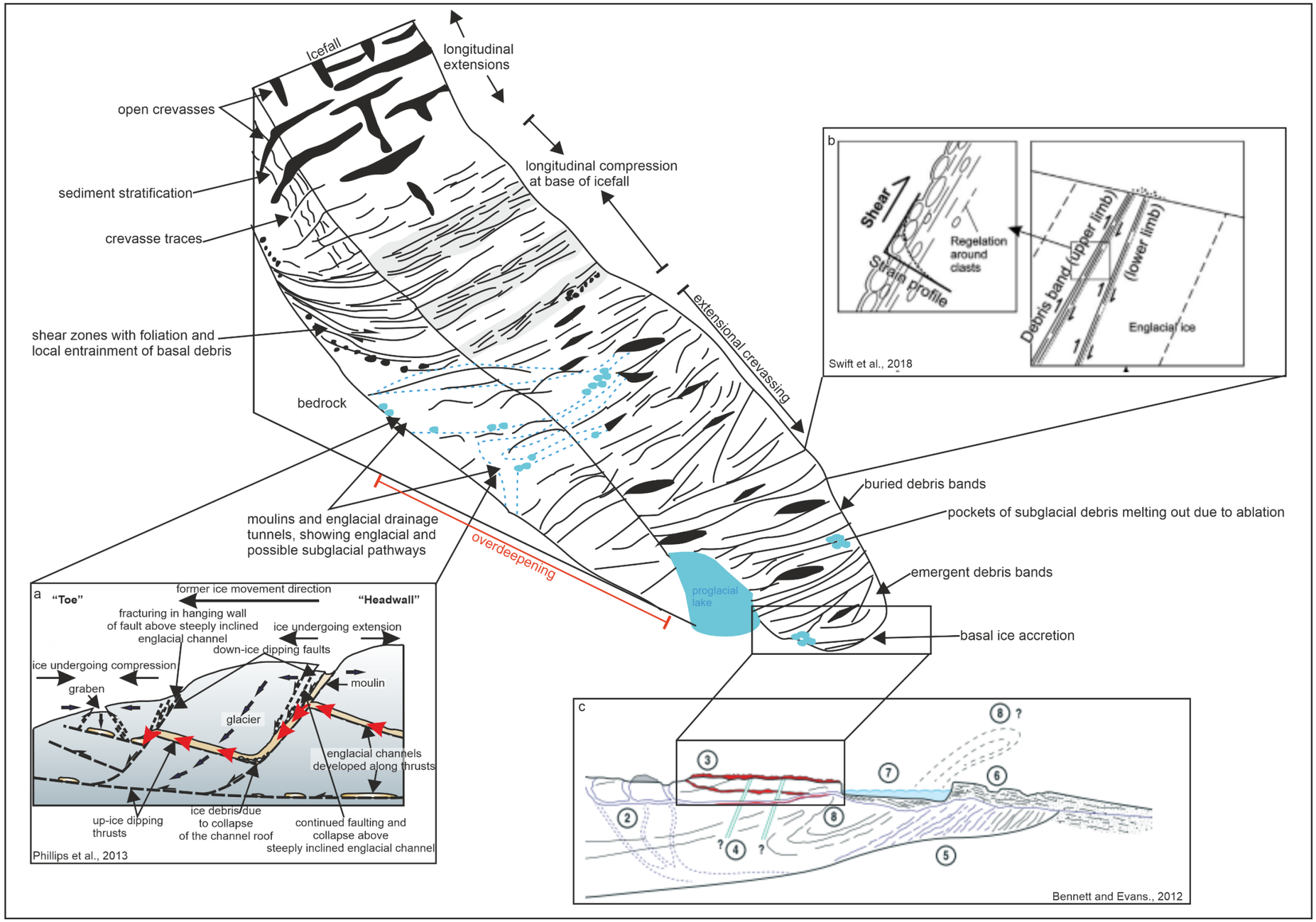

Figure 4.23 Schematic representation illustrating the key proposed debris-rich glacial ice formation processes, debris transport pathways, and glaciological controls (modified from Goodsell et al., 2002). Key areas of the schematic are; entrainment of debris into basal folds and surface crevasses at the ice fall, deformation below the ice fall further elevates basal material into dark-ogive bands (modified from Swift et al., 2018). Schematic cross section through the clean ice at the margin of Falljökull showing the relationships between faulting, the pattern of englacial drainage, and moulin development during the ice-margin collapse (panel a (Phillips et al., 2013)). Longitudinal flow compression produces thrusting along ogive-band foliation, whilst ablation reveals some closely spaced bands that may represent separate fold arms inherited from open folds formed at the base of the icefall (see detail in panel B, Swift et al., 2018). Ablation of the ice surface allows subglacial and englacial channel infill sediments to be uncovered in marginal sediments and on ice data in pockets relating to locations of channel infills. A cross profile through the glacier snout is presented from Bennett and Evans ., 2012, showing the hypothesized entrained debris patterns, ice structures and depositional styles (1 = rising folia transferring subglacial material entrained at the base of the icefall to produce controlled moraine; 2 = moulins and englacial drainage tunnels, showing englacial and possible subglacial pathways; 3 = eskers developed in englacial tunnels and exposed by ablation; 4 = clastic dykes presumably produced by hydrofracture filling; 5 = debris bands formed by supercooling; 6 = pitted outwash head; 7 = supraglacial lake with prograding deltaic sediment fed by englacial tunnel systems; 8 = folded foliae and debris bands with former continuation of folds prior to snout downwasting depicted by broken lines).

4.6.2 Recessional push moraines in terminal overdeepenings

An assessment of the role of englacial transport pathways in the construction of recessional push moraines in terminal overdeepenings can be made from the data obtained from the glacial foreland of Svínafellsjökull. This allows an evaluation of the applicability of alternative genetic models proposed by Cook *et al.* (2011b; supercooling and melt-out) versus sub-marginal till squeezing/bulldozing (Price 1970; Sharp 1984), or indeed if some combination of processes operating on a spatio-temporal continuum is more appropriate, such as seasonally-driven sub-marginal till thickening (cf. Evans and Hiemstra, 2005; Evans *et al.*, 2018a and 2018b; Chandler *et al.*, 2020b). Moreover the role of overdeepenings and the associated process of supercooling in the development of certain types of debris entrainment and englacial debris patterns (cf. Roberts *et al.*, 2002; Tweed *et al.*, 2005; Swift *et al.*, 2006; Cook *et al.*, 2007, 2010), as well as their role in deglacial landform development (cf. Larson *et al.,* 2006; Evans, 2009; Bennett and Evans, 2012) has been recognised more recently and must be incorporated in any models of spatial and temporal change in structural glaciology and landsystem development.

At Svínafellsjökull, research has been undertaken by Cook *et al.* (2011b) and Swift *et al.* (2018) to assess the extent to which regelation and glaciohydraulic supercooling are processes of basal ice formation and if they can be identified from ice-marginal sediments. The results indicate that sediments derived from the melting of basal regelation ice have a massive structure, a matrix which is dominated by coarse sand and a higher proportion of angular clasts than supercooled basal ice and associated sediments. Sediments derived from supercooled basal ice: (i) can be either massive or layered; (ii) tend to have a silt-dominated matrix; and (iii) contain a slightly higher proportion of rounded and well-rounded clasts than regelation basal ice. However, the morphology of the clasts is dependent upon the nature of the sediment within the bed. Results presented by Cool *et al*. (2011b) indicate that the distinctive sedimentary characteristics of basal ice produced by two different processes (glaciohydraulic supercooling and regelation) are preserved within ice-marginal sediments during basal ice melt out. However, Cook *et al.* (2011b)

also concluded that the large proportion of (glaci)fluvially rounded clasts found within supercooled basal ice is not always reflected in ice-marginal sediments and, hence, may not be a reliable indicator of supercooling. Indeed, they noted that, although there was a statistical difference between supercooled basal ice and basal regelation ice in terms of clast roundness, the same trend was not observed in ice-marginal sediments. Moreover, Spedding and Evans (2002) concluded that sub-rounded (i.e. water-worked) clasts are rare in supercooled ice. The significant variability in basal ice clast roundness makes the likelihood of a clast morphological signature of supercooling being present in ice-marginal sediments uncertain. Not only do Cook *et al.* (2011b) suggest that the subglacial supply of rounded clasts could be variable, Lawson *et al.* (1998) described concentrations of sorted gravels with rounded clasts within basal ice that they related to channel fills beneath the glacier; both scenarios are compatible with the spatial patterns of clast shape indices discovered in this study. The rounding of clasts could come from pre-existing glacial fluvial outwash that is overridden as the ice readvances and reworks the clasts enabling the incorporation of polycyclic rounded clasts into the basal ice.

As Cook *et al.* (2011b) have demonstrated, there are multiple factors involved in the formation of push moraines on the foreland of Svínafellsjökull. The range of clast shape characteristics reported by them and in this study also indicates a variety of glacial transport pathways to the sub-marginal zone. Hence, it is more appropriate to acknowledge a combination of processes operating on a spatio-temporal continuum around terminal overdeepenings and that sub-marginal entrainment via supercooling contributes only partially to moraine construction, specifically through the melt-out of debris-charged ice (cf. Evans and Hiemstra, 2005; Chandler *et al.*, 2020b). Such melt-out deposits (melt-out till) have been identified at a very localised scale by Evans *et al.* (2017 a, 2017b, 2018a and 2018b) on the foreland of Skaftafellsjökull, where restricted outcrops of pseudo-stratified diamicton are regarded as the rare products of melt-out from supercooled glacier ice that was visible in the form of controlled moraine (*sensu* Evans, 2009) at the glacier snout in the 1950s-1980s.

4.7 Conclusion

Highlighting and quantifying the potential complexity of glacial debris transfer pathways are critical to developing a full understanding of glacial debris cascades and their implications for glacial landsystem evolution and the Quaternary record. This research indicates that a large number of active transport pathways should be considered when examining valley glaciers, and that mixing of debris between transport pathways is significant. In summary, the data obtained through this study provides a transport process model for Svínafellsjökull and Falljökull. From the highlighted data trends from this research the key proposed debris-rich glacial ice formation processes, debris transport pathways, and their glaciological controls are:

1) entrainment of debris into basal folds and surface crevasses at the ice fall (shown by the data from Falljökull);
2) deformation below the ice fall further elevates basal material into dark-ogive bands and includes relationships between faulting and the pattern of englacial drainage during the ice-margin collapse;
3) longitudinal flow compression at the base of the ice fall produces thrusting along ogive-band foliation, whilst ablation reveals some closely spaced bands that may represent separate fold arms inherited from open folds formed at the base of the icefall;
4) ablation of the ice surface of the lower snout reveals subglacially entrained and englacial channel infill sediments, locally augmented by supercooling, the patterns of which reflect debris transfer processes and their influence in the development of ice-marginal sediments and landforms.

This research also supports the overall theory that debris entrainment is influenced very strongly by the presence of a terminal overdeepening, which promotes deposition of sediment from subglacial fluvial transport pathways, inhibits the flushing of subglacial sediment by fluvial processes, promotes the formation of thick sequences of basal ice that may be thickened by

flow along the adverse slope of an overdeepening, and promotes active transport of basal ice and debris to the glacier surface partly along thrust planes.

An assessment of the role of englacial transport pathways in the construction of recessional push moraines in terminal overdeepenings has been made from the data obtained from the glacial foreland of Svínafellsjökull. Alternative genetic models of push moraine formation have been considered and it is concluded that multiple processes are operating on a spatio-temporal continuum is the most appropriate explanation in the construction of recessional push moraines in terminal overdeepenings. This is supported by recent push moraine morphology at Svínafellsjökull changing from more linear to increasingly sawtooth plan form, and this has been associated also with progressively more till squeezing into ice-marginal pecten, so that moraines are now developing extreme sawtooth or hairpin plan forms (see Chapter 5).

5 Morphology and patterns of push moraine assemblages at Svínafellsjökull, southeast Iceland: insights into structural drivers of change in moraine development during glacial retreat.

5.1 Introduction

Assessing current glacial landsystem signatures along with their spatial and temporal evolution is important for developing process-based analogues that can be applied to deglaciated landscapes. Research into modern glacial environmental landsystems enables process-form regimes to be related to specific factors such as glaciological, environmental and topographic conditions (e.g. Evans and Twigg, 2002; Bennett and Evans, 2012; Schomacker *et al.*, 2014; Evans *et al.*, 2016a, 2017a, 2019a; Ewertowski *et al.*, 2019; Chandler *et al.*, 2020a). These landsystem models enable landform assemblages in ancient glacial landscapes to be used as proxies for factors such as palaeoglaciological and palaeoclimatic indicators (e.g. Evans *et al.*, 2014, 2020; Darvill *et al.*, 2017; Sutherland *et al.*, 2019; Chandler *et al.*, 2020a).

Outlet valley glaciers located in southeast Iceland are predominantly active temperate glaciers and their forelands are characterized by the diagnostic landsystem signature of recessional push/squeeze moraine sequences. Within these moraine sequences, individual moraines are constructed by the emplacement of submarginally deforming till wedges, typically on an annual or seasonal timescale but more recently sub-annually (see Chapter 4) (e.g. Price, 1969, 1970; Boulton, 1986b; Krüger, 1995; Evans and Twigg, 2002; Chandler *et al.*, 2016a; Evans *et al.*, 2018a; Chandler *et al.,* 2020a).

The temporal changes in push moraine sequences can be used to demonstrate the responses of locally diverse process-form relationships of individual temperate glaciers to rapid climate change. Generally, localised changes to glacial landsystem signatures (Evans, 2013) are triggered by two factors (Chandler *et al.*, 2020a): (i) climatically-driven glaciological changes; and/or (ii) topographically-controlled changes to the morphology and structural architecture of thinning glacier snouts. In recent years, active temperate outlet glaciers in Iceland, specifically on the

southeast coast, have exhibited both spatial and temporal changes in their landsystem signatures. Predominantly this has involved a switch from active temperate, oscillatory snout behaviour and concomitant annual push/squeeze moraine formation to large scale downwasting and calving in expanding proglacial lakes (e.g., Bennett *et al.*, 2010; Bennett and Evans, 2012; Bradwell *et al.*, 2013; Phillips *et al.*, 2014; Evans and Orton, 2015; Everest *et al.*, 2017; Chandler *et al.,* 2020a). This switch is partly due to accelerated climate warming since the late 20th century, but can also reflect topographically controlled changes in drainage conditions at the margins of glaciers (e.g. Evans *et al.*, 2016, 2017a, 2019; Chandler *et al.*, 2020a). Also, recession into substantial overdeepenings (cf. Magnússon *et al.*, 2012) or at ice-contact slopes of sandur fans (Kirkbride, 2000) has resulted in switches from unconfined, well-drained areas to constrained, relatively poorly drained settings (Chandler *et al.*, 2020a). Alternatively, changing environmental conditions and glacier retreat down an adverse, poorly drained slope have been recognised as contributing factors for the construction of sub-annual moraines at the southern margin of Skálafellsjökull (Chandler *et al.*, 2016a). These observations of diversity in process-form responses highlight the need for continued monitoring of individual temperate glaciers to assess the impact of ongoing climate change (Chandler *et al.*, 2020a).

This chapter investigates the evolution of push moraine assemblages at Svínafellsjökull, Southeast Iceland to establish the process-form regime of this rapidly receding active temperate glacier and to investigate any possible links between this process-form regime to changes in the structural glaciology of the snout.

5.2 Study area

Svínafellsjökull is an outlet glacier of the Öræfajökull ice cap (2110 m above sea level (a.s.l.), a partially isolated ice cap within Vatnajökull (Figure 5.1a) that feeds nine principal outlet glaciers. Svínafellsjökull is c.10 km long and <2 km wide, and flows from a relatively steep icefall, with its lower reaches characterised by generally low gradients (Figures 5.1 and 5.2). Where it emerges from its valley, Svínafellsjökull spreads radially to form an irregular fronted piedmont lobe

confined within a series of arcuate terminal moraines (Figure 5.2). The lake waters penetrate into the heavily crevassed and indented glacier snout, and hence these lakes appear to be partly supraglacial (Figure 5.1b). Aerial photography reveals that the lakes initially formed as Svínafellsjökull retreated from its 1990s readvance limit and have been impounded by the large moraine amphitheatre. Tephrochronological data from Thorarinsson (1956) indicated that soils on the outermost moraine, known as Stóralda, pre-dated the Ö1362 eruption and therefore most likely relate to a pre-historic (Neoglacial) advance of Svínafellsjökull (Everest *et al.*, 2017). Gudmundsson (1998) limited this glacial advance event more precisely to between 800 and 740 BP. Additional geomorphological evidence for earlier Holocene fluctuations of Svínafellsjökull has been removed by erosion by meltwater rivers, although subtle lateral limits may lie on the flanks of Svínafellsheiði (Everest *et al.*, 2017).

Marginal fluctuations at Svínafellsjökull have been studied in detail throughout the post Little Ice Age (LIA) period and early 21st Century (e.g. Thórarinsson, 1943; Thompson, 1988; Sigurdsson, 1998; Hannesdóttir *et al.*, 2015a, 2015b). During the LIA, the terminus of Svínafellsjökull coalesced with neighbouring Skaftafellsjökull and they remained joined until 1935, when the margins of the two glaciers eventually separated (Thórarinsson, 1943; Thompson, 1988). Since decoupling, the overall retreat of Svínafellsjökull, totalling around ~500 m, has been punctuated by several phases of readvance (Thompson, 1988). These fluctuations in the position of the ice front have resulted in a suite of large, concentric, to occasionally sawtooth, moraines on the foreland (Everest *et al.*, 2017). Renewed glacier recession has occurred since c. 2000 and has been accelerating since 2010. This recession has been accompanied by pronounced thinning of the terminal zone and the formation of dense longitudinal crevasse networks that give rise to indented radial pecten at the snout (Mottram and Benn, 2009; Phillips *et al.*, 2017; Dell *et al.*, 2019).

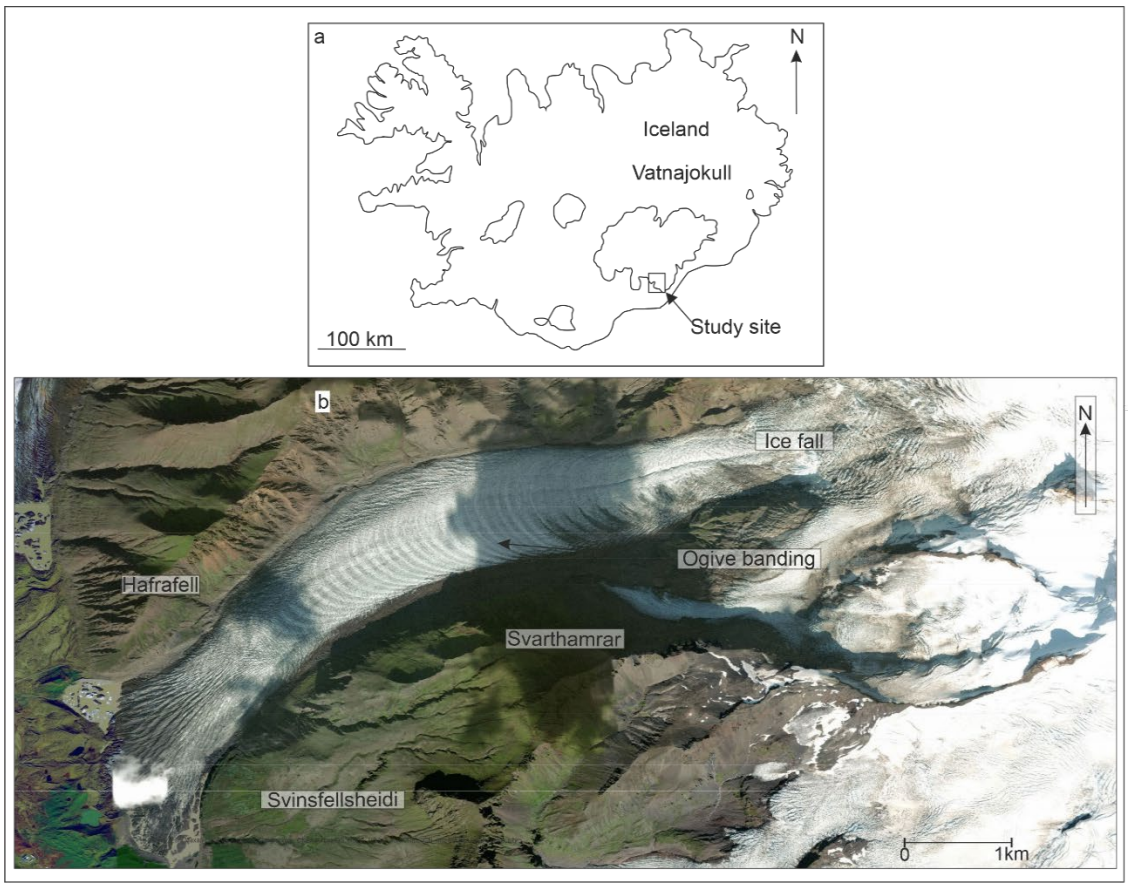

Figure 5.1: Location and characteristics of Svínafellsjökull: a) map showing the location of Svínafellsjökull, in southeast Iceland (Adapted from Cook, et al., 2010); b) aerial photo of Svínafellsjökull showing this east-southeast to west-southwest orientated glacier descending from its source area on Öræfajökull (map and aerial photograph sourced from Google Earth).

Figure 5.2: Field Photographs of typical moraines on the foreland of Svínafellsjökull: a) panoramic view looking southeast across the southern edge of the glacier snout, showing recent recessional push moraines lying inside the larger moraine amphitheatre to the right b) view looking southeast across the 1990s readvance moraine towards the older large moraine amphitheatre on the southern foreland; c) panoramic view looking southwest across the southern edge of the glacier snout, showing recent recessional push moraines (people for scale); d) recently formed push moraines on the southwestern margin, person for scale.

5.3 Methods

Geomorphological mapping of a range of glacial landforms present in the foreland of Svínafellsjökull was carried out using high-resolution LiDAR imagery generated by Johannesson *et al.* (2013; Figure 5.3). Aerial photographs for the years of 1952, 1988, 1992 and 2012 were also consulted when examining the foreland of Svínafellsjökull in order to facilitate comparisons of landform characteristics over time (Figure 5.4). The detailed geomorphological mapping was combined with field investigations conducted in April, May and September 2017, 2018 and 2019 to ground truth the desk-based analysis. The application of both field and desk-based techniques allows an holistic approach to geomorphological mapping (Chandler *et al.,* 2018) and has traditionally been utilised in Quaternary geology in the assessment of surface materials and landforms (e.g. Hodgson, 1984; Aylsworth and Shilts, 1989; Dredge and Cowan, 1989; Dyke *et al.,* 1992; Fulton *et al.,* 1995; Kleman *et al.,* 1997). On recently deglaciated forelands, especially in Iceland, such an approach also facilitates the surveying of historical landform development in the context of glacier behaviour and dynamics (e.g. Price, 1969; Evans and Twigg, 2002; Schomacker and Kjaer, 2007; Bennett *et al.,* 2010; Evans, 2013; Evans *et al.*, 2016, 2017b, 2018a, 2018b, 2019, Everest *et al.,* 2017; Chandler *et al.,* 2020a and 2020b; Guðmundsson and Evans, 2022).

Geomorphological features were digitised (see Chapter 2 for details) and the initial interpretations of the geomorphological features were confirmed in the field; to improve accuracy, examination of the remotely sensed data was conducted both prior to and after the field investigations. The first phase interpretation of field-based observations was combined to create the final map of the landforms on the foreland of Svínafellsjökull. Moraine ridges and small areas of subglacial flutings are mapped using their crestlines.

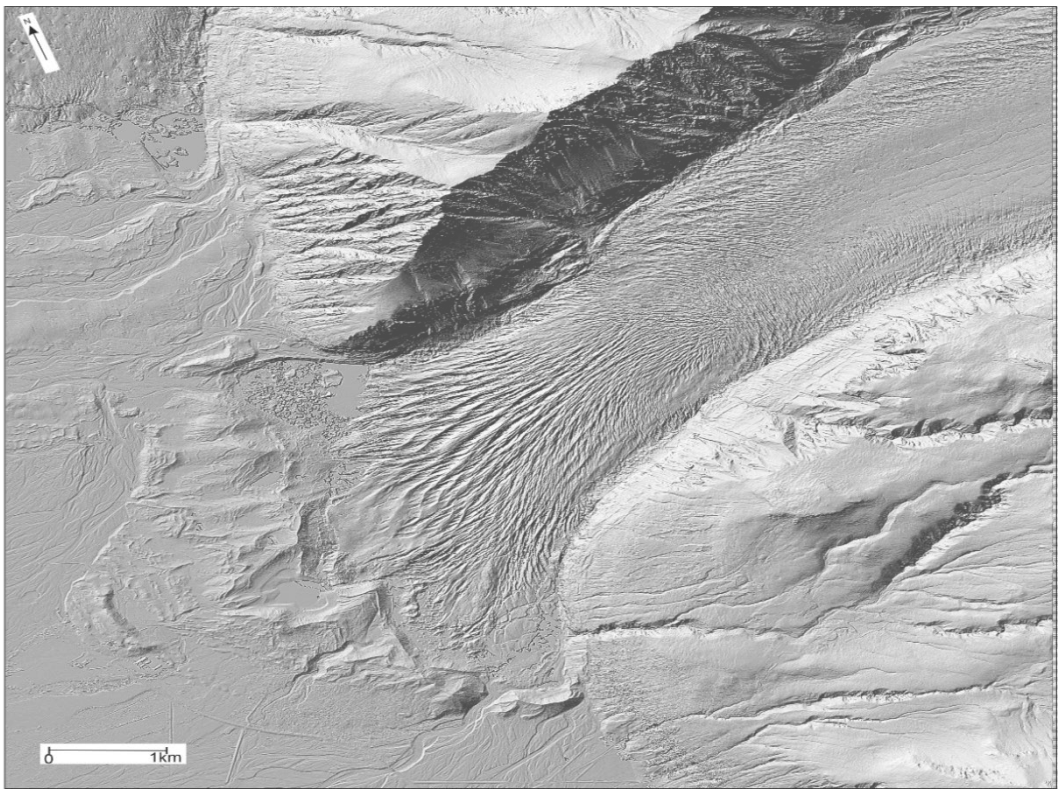

Figure 5.3: High-resolution LiDAR image of Svínafellsjökull and foreland used for landform mapping. LiDAR Image generated by Johannesson et al. (2013).

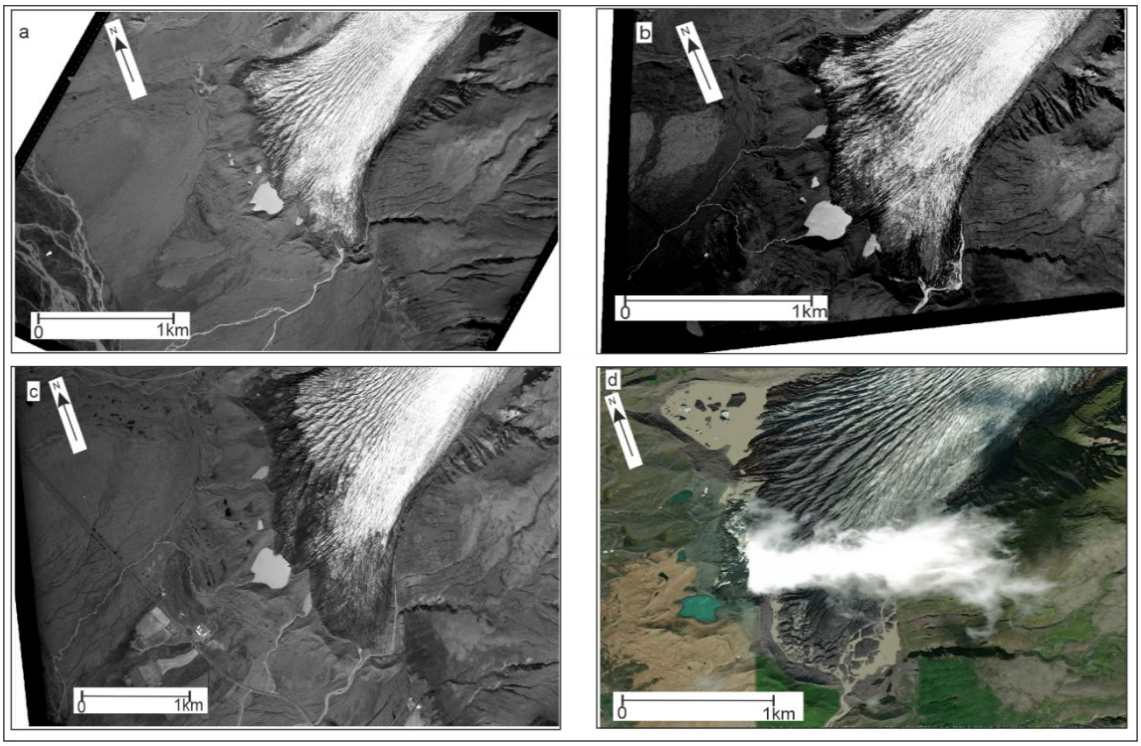

Figure 5.4: High-resolution scans of aerial photographs for the years of: a) 1952; b) 1988; c) 1992. The scans have a resolution of 0.41 m ground sampled; d) foreland of Svínafellsjökull in 2012 using image taken from the Esri World Image Basemap layer (Source: Esri, Maxar, Earthstar Geographics, and the GIS User Community).

5.4 Results

In order to present details on the characteristics of push moraine assemblages at Svínafellsjökull, the glacier foreland was divided into zones. These zones are comparable to the marginal zones used in Chapter 3 and are classified as the northwestern, central, southern and southeastern zones and are demarcated by distinct patterns in the proglacial geomorphology (Figure 5.5). Four historical ice marginal limits, based on those collated by Gudmundsson *et al.* (2019), are highlighted on the glacial geomorphology map of Svínafellsjökull and relate to the dates of 1870/1890 or the historical LIA maximum, 1904, 1930 and the 1990s (Figure 5.6, Appendix 11).

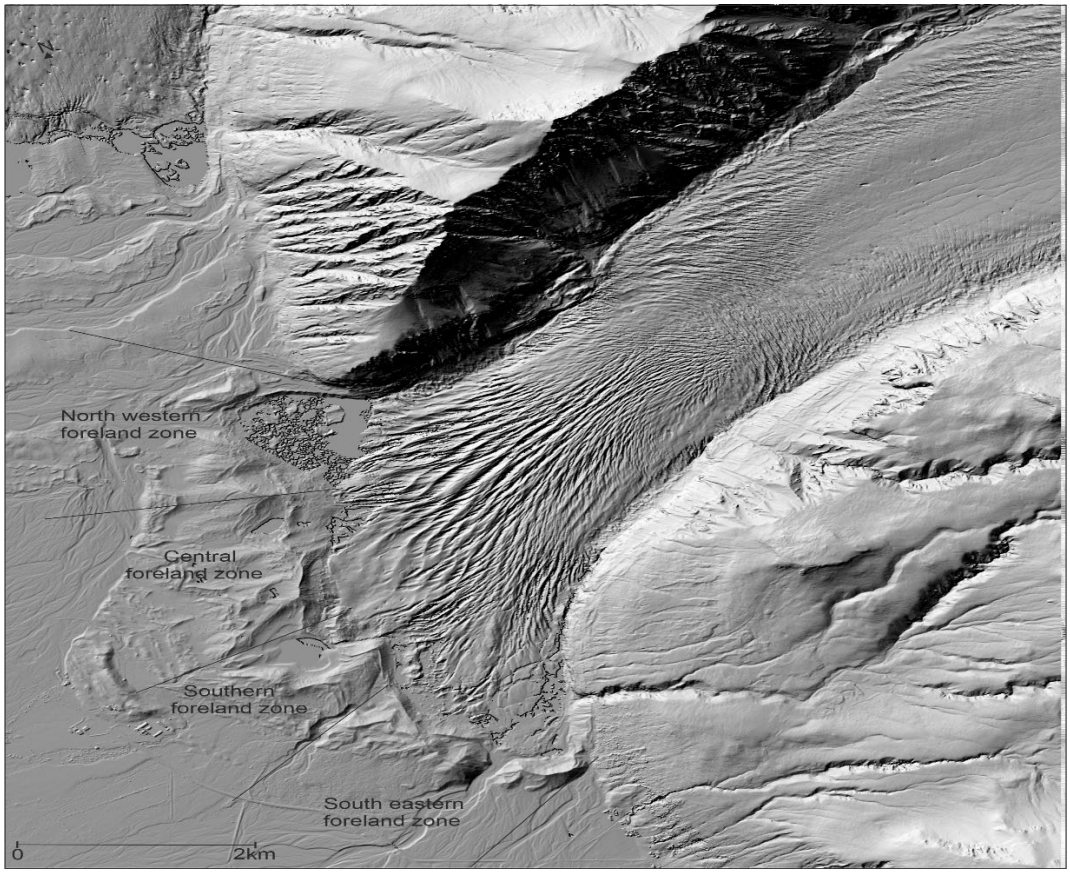

Figure 5.5: High-resolution LiDAR image of Svínafellsjökull and foreland used for landform mapping, with foreland zones used within this study identified. LiDAR Image generated by Johannesson et al. (2013).

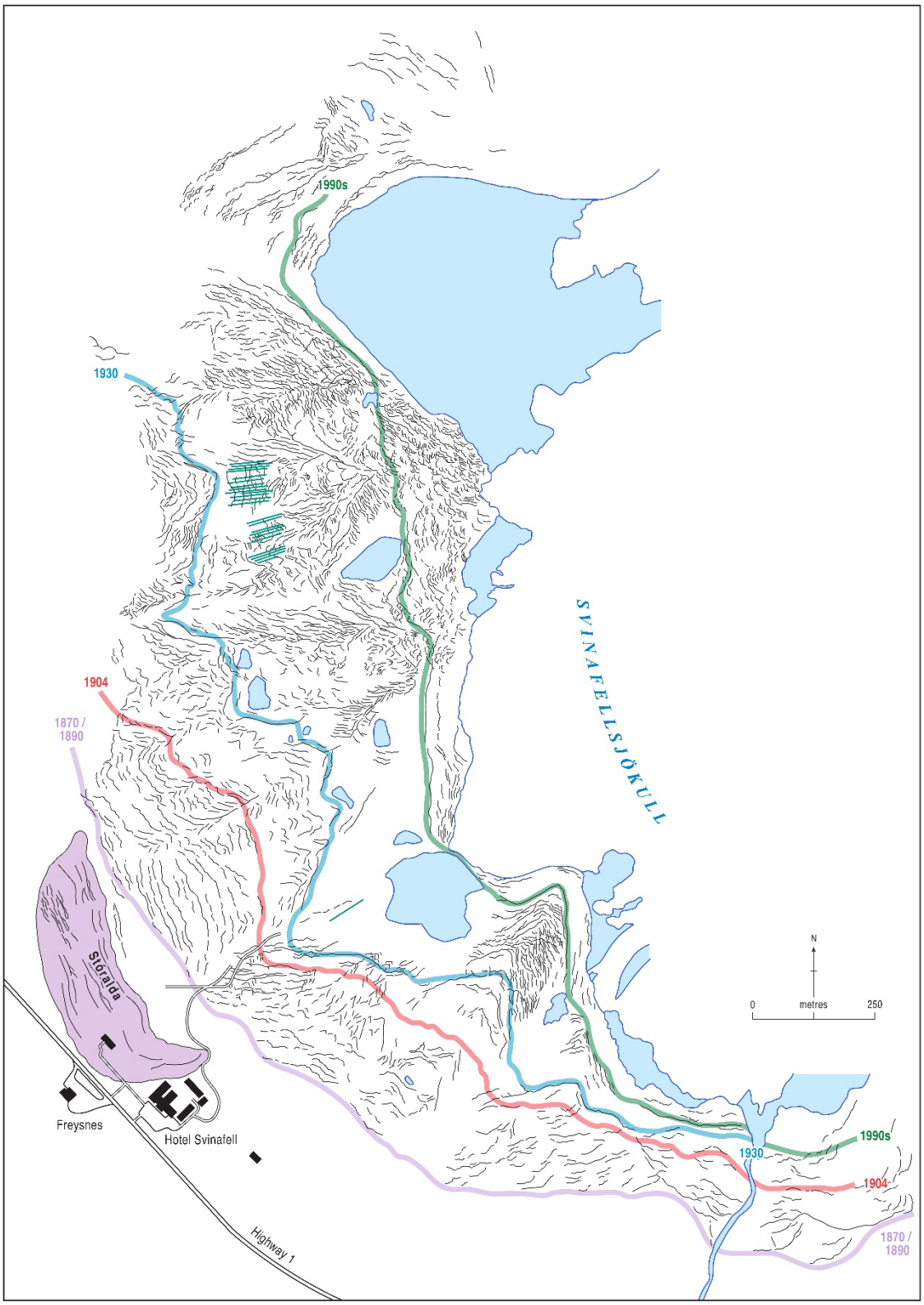

Figure 5.6: Glacial geomorphology map of the Svínafellsjökull foreland, based on LiDAR data (obtained in 2013) as well as field mapping and aerial photograph interpretation. Black lines depict moraine crests, green straight lines show flutings, dated lines are known ice marginal limits complied from Gudmundsson et al. (2019).

5.4.1 Characteristics of push moraine assemblages at Svínafellsjökull

The outermost moraines that stretch across the foreland of Svínafellsjökull form a series of arcuate ridges, the largest and oldest (pre-1362 AD) being named Stóralda (Thorarinsson, 1943; Guðmundsson, 1998; Everest *et al.*, 2017). Stóralda is similar to a number of other older Neoglacial moraine fragments that occur on the outer forelands of the Icelandic south coast glaciers in that it rises well above and beyond the inset sequences of LIA push moraines that demarcate the 1870/1890 ice limit and appears well vegetated in comparison to the younger landforms (Figure 5.2b). Although its surface displays a series of up to five inset minor and relatively straight ridges, its overall morphology comprises an asymmetrical major ridge with steep ice-proximal and shallow ice-distal slopes (Figure 5.6, Appendix 12). A further series of up to nine inset minor ridges occur on the northern part of the distal slope, and these contrast with those on the summit in that they are more closely spaced and are partially overprinted.

Notably Stóralda has been the subject of previous research because of the well-preserved multiple tephra deposits within its internal stratigraphy. Using these deposits to construct a tephrochronology, Thorarinsson (1956) determined the age of the Stóralda moraine to predate 1362 AD or to be of Subatlantic age, the coldest period since the last Glaciation. This was based on the occurrence of the Oraefi 1362 (O1362) tephra on the moraine summit.

Gudmundsson (1998) later identified five major moraine crests on Stóralda. Crests 1, 2, 3 and 5 (Figure 5.7) vary in height from 2-5 m and are composed of matrix supported gravel. Crest 4 was much larger (up to 25 m high), again composed of matrix supported gravel but with occasional boulders (Figure 5.7).

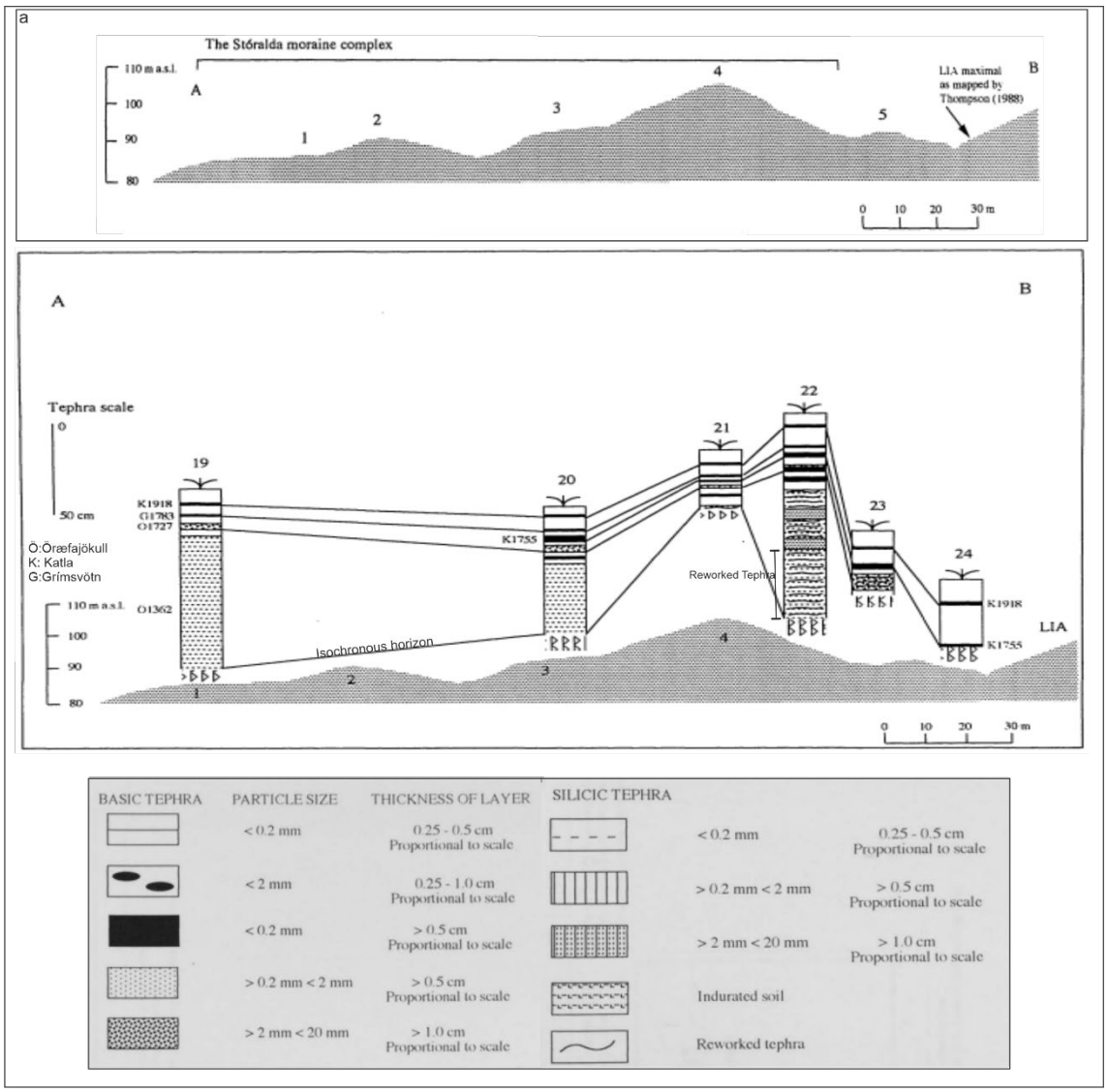

Figure 5.7: Stóralda morphology and stratigraphy, taken from Gudmundsson, (1998); a) Cross profile of the Stóralda moraine complex; b) the tephra stratigraphy of the Stóralda moraine complex, with associated stratigraphy key.

Gudmundsson (1998) regards the five major ridges in the Stóralda moraine complex as a record of multiple ice-marginal positions, which he terms the Stóralda Stage. Stratigraphy profiles 19 – 22 (Figure 5.7) indicate that the moraine complex is older than 1362 AD, as they both contain O1362 tephra at their bases as previously determined by Thorarinsson (1956). In contrast, the O1362 tephra is highly reworked in profile 22, on the proximal side of the largest crest (4), where it is mostly only found as a constituent of the underlying till (Gudmundsson, 1998). Therefore, it is likely that the glacier readvanced to crest 4 after the deposition of the O1362 tephra (Figure

5.7) but prior to 1755, as the K1755 tephra overlies the disturbed deposits containing the O1362 tephra.

Inside Storalda, the inset sequences of minor recessional push moraines display a variety of plan forms, which reflect the characteristics of the glacier snout margin at their time of construction. The moraines dating to the period 1870/1890-1904 occur only in the central, southeastern and southern zones, as they have been removed by proglacial streams towards the north. They are mainly linear and slightly arcuate in plan form in the central zone, with some crenulated or saw-tooth forms occurring in relation to the formation of three re-entrants in the glacier snout (Figure 5.6, Appendix 12). In contrast, more widespread sawtooth forms appear to have developed in the southern zone between 1870/1890 and 1904. Notably the moraines within the 1870/1890-1904 area are generally evenly spaced and hence the lack of localised overprinting, especially in the central zone, allows some quantification of ice-marginal recession rates. Between 18 and 24 individual moraine ridges can be identified in the central zone and these developed over a maximum period of 34 years (minimum = 14 years depending on the age of the outermost LIA moraine). This strongly suggests that the largely evenly spaced moraines were constructed annually and over a maximum distance of 280 m (central zone), thereby indicating maximum and minimum steady recession rates of 20 m^{-a} and 8.2 m^{-a} in the central zone. The moraines of the southern zone are distinctly different to those of all the other zones, from the LIA maximum up to the present day, in that they are fewer in number and lack any crenulated or sawtooth plan forms (Figure 5.4). In the 1870/1890-1904 area of the southern zone, only 10 push moraines occur over a distance of 180 m. This narrower foreland area indicates that maximum and minimum recession rates at the southern part of the snout were 12.9 m^{-a} and 5.3 m^{-a}, respectively, but variable moraine spacing, and some overprinting (Figure 5.6, Appendix 12) indicates that recession was not steady and hence these figures are strictly averages.

More complex, sawtooth or crenulated planforms are evident between 1904 and 1930 (Figure 5.6, Appendix 12). Notably there appear to be less moraine ridges located at the southeastern

(~ 25) and southern (~38) margins compared to the central margin during this time period. Also notable are the more fragmented nature of moraines within this time period compared to the moraine ridges dating from 1870/1890 to 1904, probably due to the variability in intra-moraine crest height. There is variable moraine spacing in all foreland zones between 1904-1930, again indicating recession during this time was not stable and a degree of overprinting of landforms is present. Within the central marginal zone, the distance between the 1904 and 1930 limit ranges from 25m in the most eastern corner of the central zone, to ~250m at the north western edge of the central zone, with the whole zone comprising ~26 moraine crests, again with variable moraine spacing, the largest spacing between moraine crests is 120m and the smallest is 10m. Moraines within the central zone are mostly fragmented in nature and again this could be due to the variability in intra-moraine crest heights. Moraines located at around the 1930s ice margin mimic the large re-entrants of the 1930 snout. Within the northwestern marginal zone there are only 20 moraine crests present between 1904 and 1930. These are less saw-tooth in form compared to the moraines formed within the central zone during this time period. The moraines are also much more evenly spaced within the northwestern marginal zone. Spacing between the moraines here is around 30 m, suggesting these are annual push moraines.

Within the area demarcated by the 1930 and 1990s limits, a number of proglacial lakes developed on the ice-proximal slopes of the outer moraine amphitheatre, which continued to be overprinted with smaller recessional push moraines with the exception of the southern and southeastern foreland zones, where there are a distinct lack of moraines surrounding the largest lake-filled depression (60 and 29 moraine crests in the southern and southeastern zones, respectively). Within the southern marginal zone there is an area of moraines whose broad scale plan forms very closely mimic the indented nature of the receding glacier margin (Figure 5.8). Moraines in the northwestern zone are closely spaced and highly fragmented with significant amounts of overprinting. Although the overall pattern of minor recessional push moraine ridges mimic the large re-entrant of the ice margin within the northwestern zone there is a marked increase in crenulated or sawtooth plan forms at the smaller scale, which is indicative of complex

pecten along the glacier snout. Within the 1930-1990s area of the northwestern and central zones, the till surfaces associated with the recessional push moraines are clearly fluted (Figure 5.9), a common attribute of the foreland zones of active temperate glaciers (Evans and Twigg, 2002).

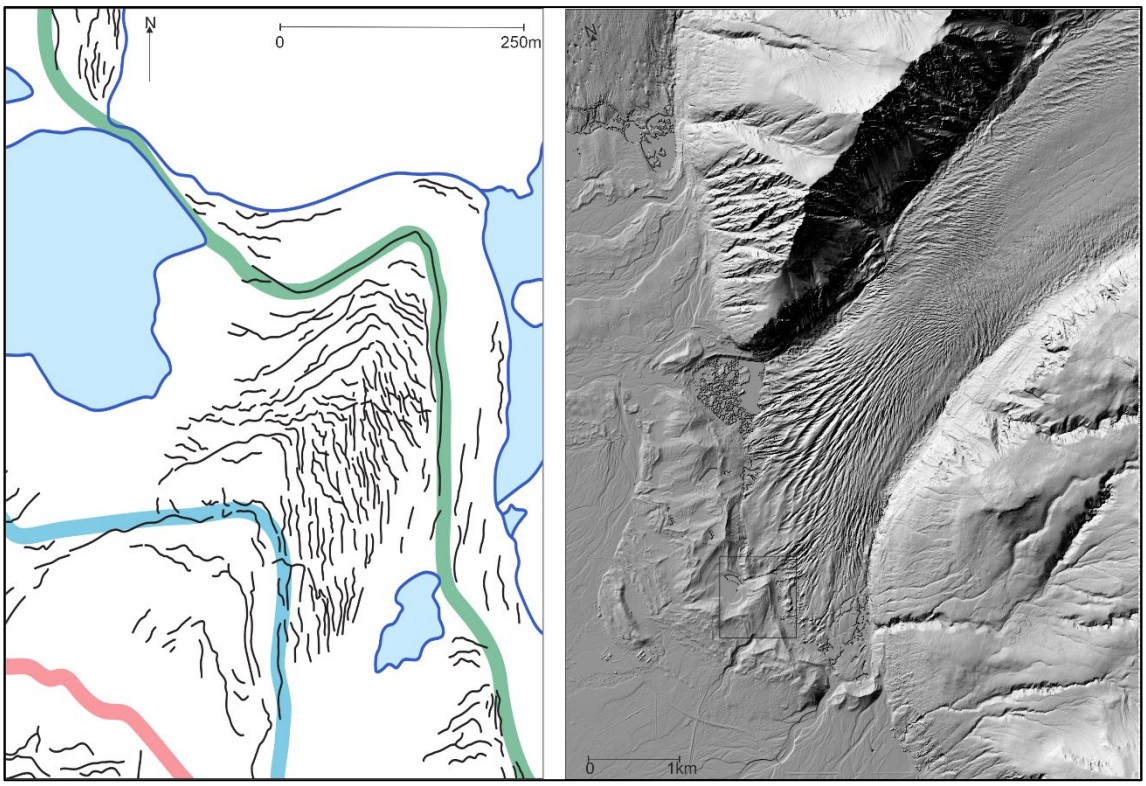

Figure 5.8: Area of saw-toothed moraines which are very closely spaced, situated between the central and south-eastern zone.

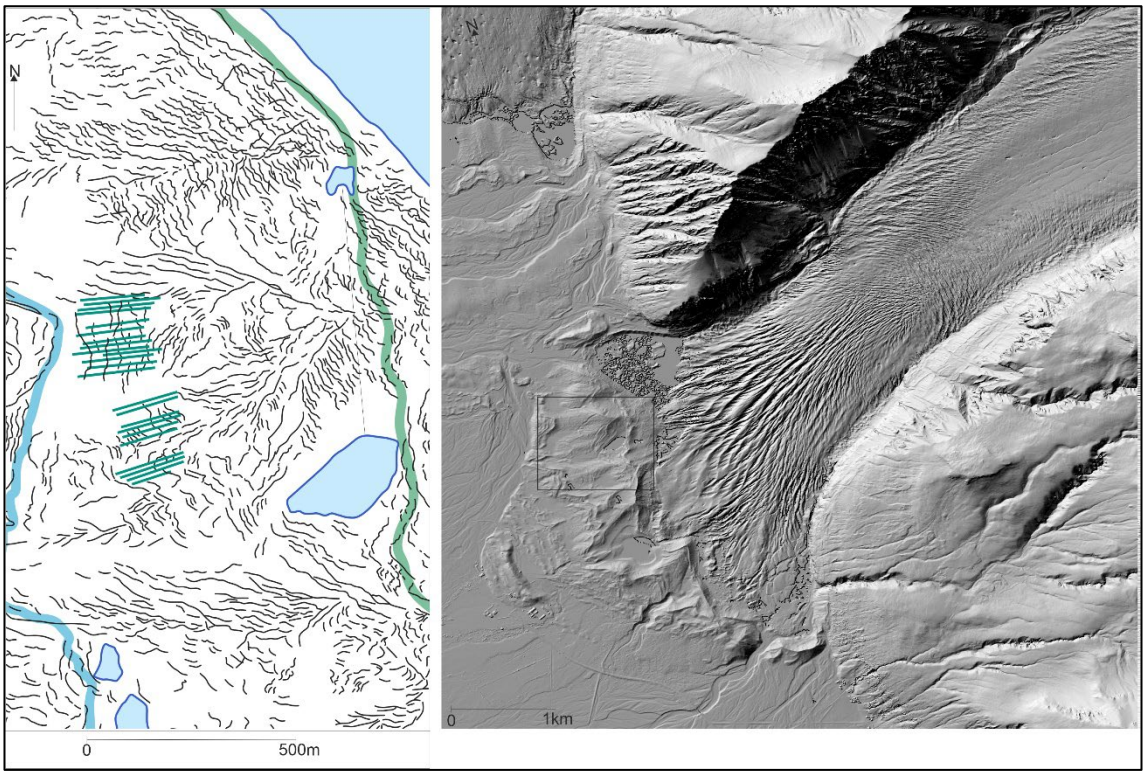

Figure 5.9: Clipped LiDAR and landform map of the northwestern margin with closely spaced, fragmented, saw-toothed moraines, and flutes (green lines).

The most complex and densely spaced minor recessional push moraines occur between the 1990s readvance limit and the present-day ice margin. They exhibit highly complex planform geometries, with extremely sawtooth (or 'hairpin shaped') ridges. Localized superimposition and cross-cutting creates a fragmented appearance to individual ridges. In several cases, the sawtooth moraines continue as, or are connected to, long ridge limbs that are orientated obliquely and sub-parallel to ice flow; this gives rise to moraine limbs that resemble the long arms of hairpins (see Figure 5.6, Appendix 12). Detailed mapping of these landforms reveals that they correspond to narrow blades of ice separated by open crevasses (pecten) marking the presence of large longitudinal fractures within the glacier (Figure 5.10). Significantly, in terms of landform development, over the period from the late 1990s to around 2012, the glacier snout developed strong longitudinal crevassing and associated ice marginal pecten (Figure 5.10). Detailed analysis of the structural architecture of the glacier margin (Chapter 3) indicates that these longitudinal fractures (crevasses) are the dominant deformation structure within the

marginal zone of Svínafellsjökull. Such changes in structural glaciology have been identified at a number of sites around southern Iceland where they are manifest over longer periods of time in changes to push moraine morphology. Chapter 4 presented clast characteristics of recently formed moraine assemblages at this study site and have demonstrated that there are multiple factors involved in the formation of push moraines on the foreland of Svínafellsjökull. The range of clast shape characteristics reported in Chapter 4 indicates a variety of glacial transport pathways to the sub-marginal zone and concluded that it is more appropriate to acknowledge a combination of processes operating on a spatio-temporal continuum around terminal overdeepenings and that sub-marginal entrainment via supercooling contributes only partially to moraine construction, specifically through the melt-out of debris-charged ice (cf. Evans and Hiemstra, 2005; Chandler *et al.*, 2020b).

Figure 5.10: Landform and ice characteristics around Svínafellsjökull Marginal area; a) field photograph from 2016 showing ice splines and open crevasses overriding annual push moraines; b) field photograph from 2016 showing view from northwest margin, looking up ice. Black box depicts ice axe for scale; c) field photograph from 2016 showing view looking north showing ice spline overriding moraine. Black box shows person for scale; d) 2012 air photograph showing small scale features recently formed at the margin of Svínafellsjökull; e) Recently formed crevasse squeezed ridge.

5.4.2 Glacier marginal changes

Marginal fluctuations at Svínafellsjökull are shown in Figure 5.11, highlighting that the margin was relatively stable between 1954 and 2016, with only minor fluctuations. This figure also highlights that up to 1992 the shape of the margin was non-indented. However, after 1992 the shape of the margin became progressively more complex (indented), in particular between 1992 and 2016, reflecting the increasing influence of longitudinal crevasses (open fractures) on the ice margin morphology, which could be mainly a response to mid-1990's re-advance followed by subsequent (post 1990's) surface ablation. Also, the northern and southern margins exhibited the most obvious retreat, with the position of the middle section of the glacier margin remaining relatively stable. There seems to have been a small re-advance of this middle section of the glacier between 2007 and 2012, during which the margin became less indented (Figure 5.11 and 5.12). However, sawtooth moraines had started to appear before snout margin indentation developed, specifically in 1904 with the exception of the southeast zone. Therefore, the period 1904-1992 was characterised by structural glaciological changes that initiated longitudinal re-entrants and marginal crevassing in the glacier snout.

The historical sequence of aerial photographs records changes in proglacial lake extents and subglacial drainage. Two proglacial ice-contact lakes are presently located immediately adjacent to the snout on the northwestern and southeastern margins. The lake waters penetrate into the heavily crevassed and indented glacier snout, and hence they appear to be partly supraglacial (Figure 5.13 a,b, and c). Aerial photography reveals that these lakes initially formed as Svínafellsjökull retreated from its 1990s readvance limit and have been impounded by the large moraine amphitheatre. The ice proximal side of this moraine forms the adverse topographic slope along the south-eastern glacier margin. Rapid recession of Svínafellsjökull since ~2000, has been associated with the formation of lakes at the northern and southeastern parts of the terminus. Gudmundsson *et al.* (2019) suggest that the lowest parts of these areas of the terminus appear to be afloat and conclude that the size of the lakes has grown sporadically from

approximately 0.01 km^2 in 2000 to 0.38 km^2 in 2018, or on average by ~0.02 $km^{2\ a\ -1}$. Gudmundsson *et al.* (2019) also suggest that the area of these lakes was slightly reduced in 2017 by a temporary advance of the terminus. Radio-echo sounding measurements (Magnússon *et al.,* 2012) and soundings of water depth showed that the northwestern lake was 60–70 m deep at its deepest point near the ice margin and the volume of the lakes was ~10×10^6 m^3 in 2018. It was concluded by Gudmundsson *et al.* (2019) that if or when the glacier retreats out of the ~6 km long subglacial trough shown by Magnússon *et al.* (2012), a >300 m deep lake with an area of ~5 km^2 will be formed in the depression. During fieldwork in April 2017, there was an observed fall (over an estimated period of around 24 hours) in the water-level of the largest lake on the north-western side of the glacier, leaving small icebergs and brash-ice stranded on the shallow proximal moraine slopes. Although this lake has previously drained through one of three breaches in the moraine amphitheatre on the western foreland, it now only drains through this breach when the lake reaches its maximum level. Chapter 3 presents 2 theories of the impact this periodic drainage on the structure of the ice and subsequently the drainage pathways (Chapter 3, Figure 3.24).

The subglacial footprint of the Svínafellsjökull foreland has significantly altered during this study period, and therefore examining the changes in the proglacial drainage pathways is important to understand the linkages between these changes and changes in the marginal ice structures, which in turn have effects on moraine morphology. In 1952 a river emerged from the southern margin of the glacier and was connected to an englacial/subglacial conduit, which appears to be the main drainage outlet for the glacier (Figure 5.14a). The conduit was located at the end of a series of relatively closely spaced arcuate/longitudinal fractures, suggesting that there may be a structural control on drainage (Figure 5.14 a). In 1952 there was one relatively small proglacial lake present, whereas in 1988, instead of a single meltwater drainage outlet emerging from the southern margin of the glacier, there is an additional outlet between the southern valley side and the glacier. In terms of drainage in 1992, the only significant changes appear to be a significant reduction in discharge in the stream draining the northern margin and the

appearance of an additional stream draining the front of the glacier. Between 1992 and 2012 the proglacial lake located towards the centre of the glacier had reduced in size and the shorelines can be traced on the adjacent slopes. The two proglacial lakes adjacent to the northern and southern margins of the glacier had started to form. Also, the streams located at the centre of the snout (south of the small proglacial lake) and draining the northern side of the glacier had both ceased flowing (c.f insets in Figure 5.12).

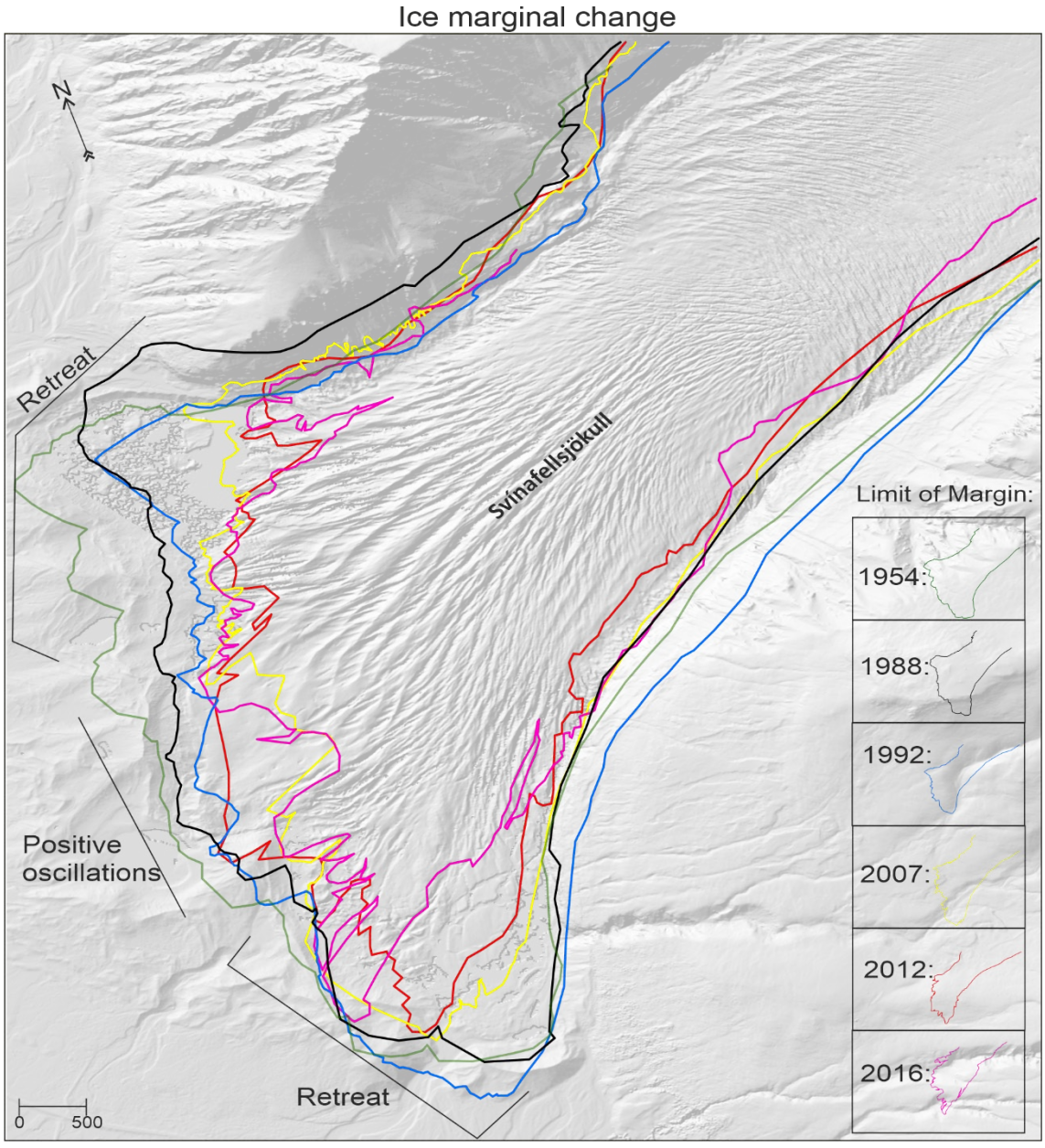

Figure 5.11: The changing position and morphology of the margin of Svínafellsjökull for the years of 1954, 1988, 1992, 2007, 2012 and 2016.

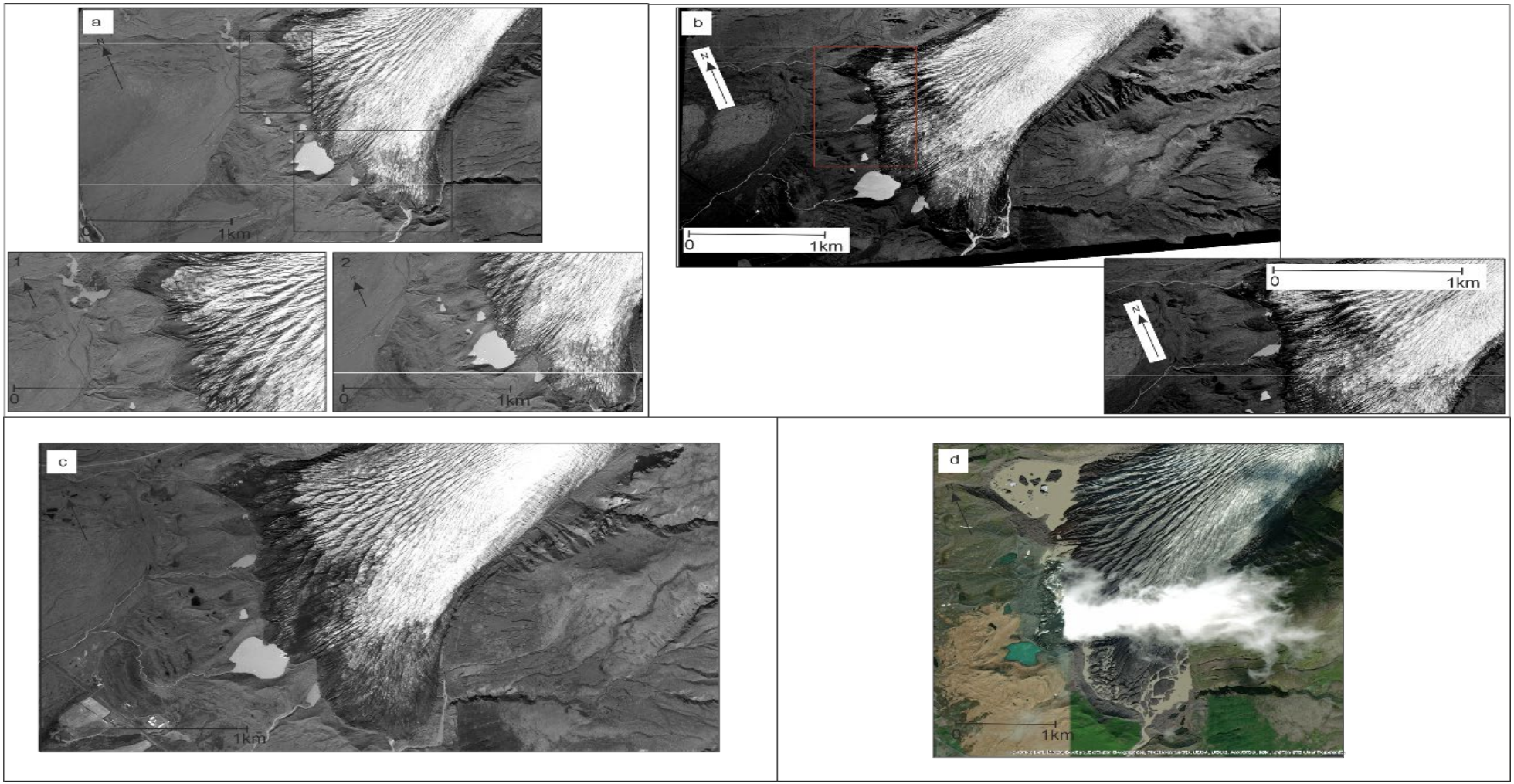

Figure 5.12: Extracts from aerial photographs showing the marginal area of Svínafellsjökull: a) 1952 margin. Inset 1 shows northwest marginal area and inset 2 shows southeastern margin; b) 1988 margin, with red box highlighting inset image of north-western margin; c) 1992 marginal area; d) 2012 marginal area.

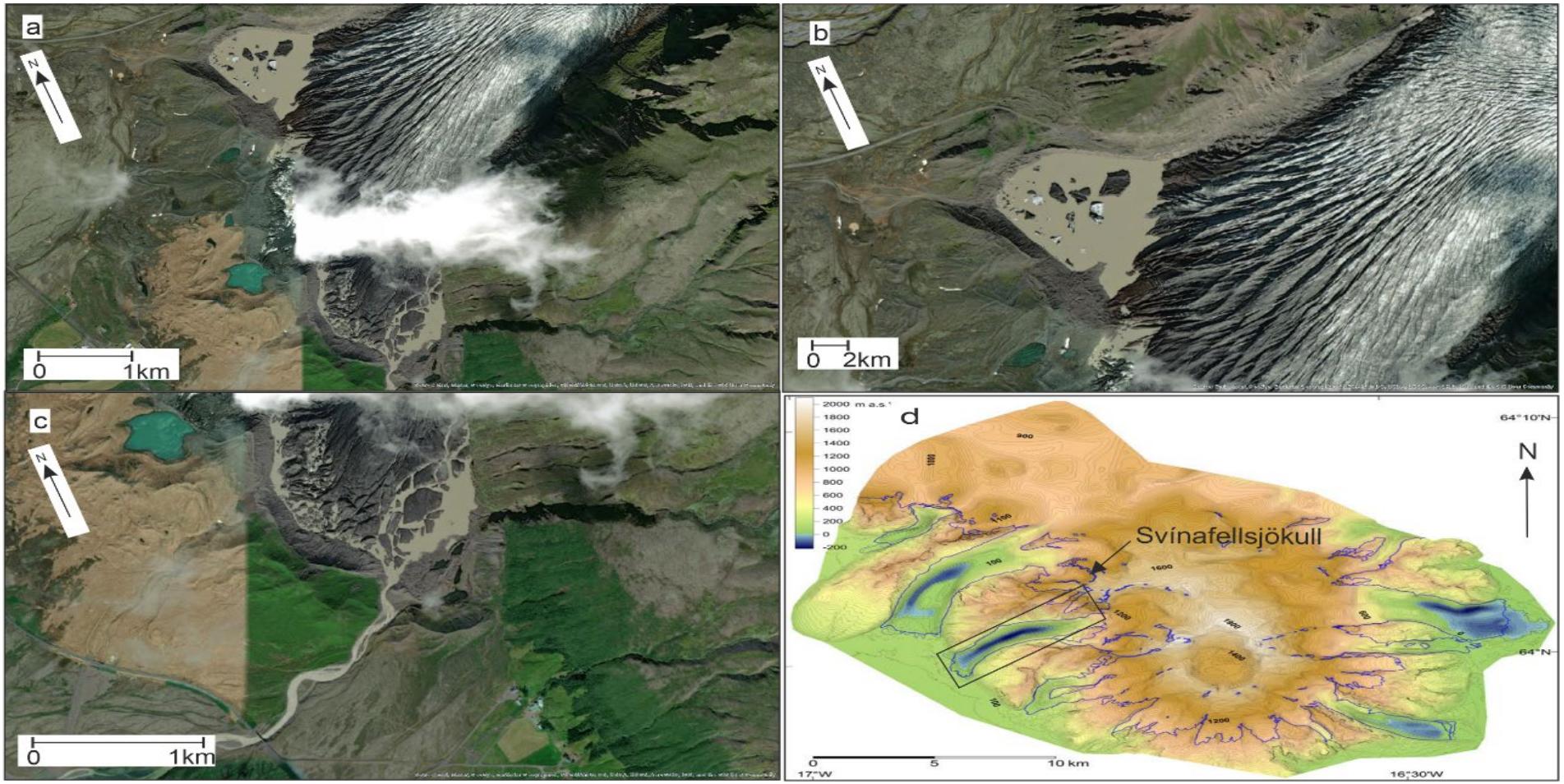

Figure 5.13: Proglacial lakes and emerging topography: a) 2012 aerial photograph showing proglacial lakes; b) proglacial Lake located on the northern margin of Svínafellsjökull; c) proglacial Lake located on the southwestern margin of Svínafellsjökull; d)) Svínafellsjökull's overdeeping mapped by Magnusson et al. (2012) outlined by the black box.

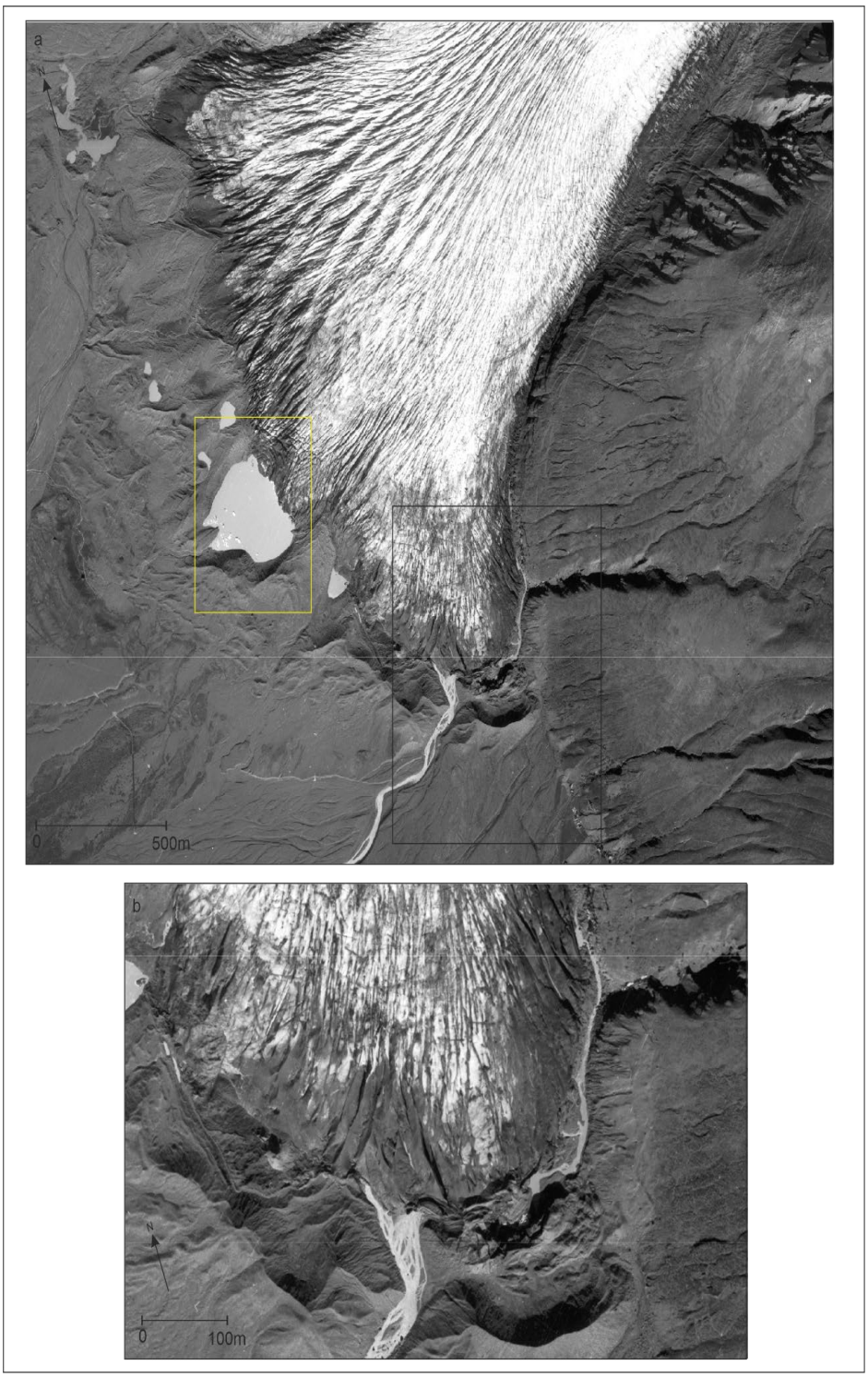

Figure 5.14: 1952 Proglacial drainage at Svínafellsjökull; a) Yellow box highlighting proglacial lake; b) clipped image from the 1952 air photograph showing on ice longitudinal fractures directly up ice of main drainage route.

5.5 Interpretations

Stóralda, the highest and oldest moraine complex on the foreland of Svínafellsjökull, is significant when examining the longer-term evolution of the glacial landsystem. Specifically, the moraine record in front of Svínafellsjökull has been interpreted to date historical advances commencing in the Medieval times and terminating in the late 19th century (e.g. Gudmundsson, 1998). During this time, the glacier advanced ca. 1 km onto the sandur plain and formed moraines of differing morphologies.

One interpretation of Stóralda is that it could be a thrust mass with minor push moraines over-printed upon it. Similar features have been identified in this region of Iceland (e.g. the overridden thrust mass known as Brennhola-alda on the foreland of Breiðamerkurjökull; Evans and Twigg, 2002) and are characterised by multiple, straight-crested ridges overlain by smaller amplitude push moraines. For example, the unusually large size and linearity of the largest ridges (crests 2, 3 and 4, Figure 5.7) in particular, when compared with the standard morphologies of the moraines on the rest of the foreland, could be thrust blocks. If correct, this would have implications for the use of tephrochronology, because the 1362 tephra would be located in thrust material, thereby suggesting that the moraine was constructed after 1362. Importantly, however, Stóralda is comparable in size to the moraine amphitheatre that lies inside it on the foreland, but which is greatly modified (smoothed) by ice overriding and draped with recessional push moraines (moraines found in the 1870/1890-1904 limits). The possibility that such large moraine complexes might simply reflect periods of increased glacier debris loads, for example due to active phases of rock slope failure (incremental stagnation), should also be entertained (c.f. Eyles, 1979, 1983; Bennett and Evans, 2012; Reznichenko *et al.,* 2016). Within the confines of this moraine amphitheatre (from 1904 onwards) there is a change in the morphology and patterns of push moraines found within the foreland.

The results of the geomorphological mapping enables the reconstruction of the changing characteristics of push moraine assemblages at Svínafellsjökull from the LIA maximum to the present day. Moraines formed since the early 1900s are characterized by the initiation and development of distinctive sawtooth and then hairpin-shaped planforms, the latter relating to crevasse squeezing of moraine limbs. Also developing over this time period is a decrease in moraine spacing distances and increasing levels of overprinting. The most complex and densely spaced moraines occur near the present-day ice margin, with the exception of the southeastern marginal zone. Changes to the architecture of the longitudinal crevasses over successive seasonal cycles, together with fluctuations of the actively retreating glacier margin, result in the development of this highly complex zone of moraine superimposition and crevasse-squeeze ridge development (cf. Chandler *et al.,* 2020a).

The change in the morphology of the recessional moraines from relatively smooth arcuate features, to more complex sawtooth, can partly be explained as recording a marked change in the shape of the ice margin. This change in the shape of the ice margin reflects the opening of the longitudinal fractures in response to increased surface ablation and preferential melting/erosion along these pre-existing ice structures. This preferential melting/erosion along pre-existing ice structures which are opening at the margin occurs due to meltwater exploiting these open fractures, along with these open fractures providing more surface ice to be subjected to melting, In turn changing drainage pathways at the margin. This suggests that the morphology of the recessional moraines developed within the forefield of Svínafellsjökull can be used as a proxy for recording significant changes in the glacier margin, due to accelerated rates of surface ablation in response to climate change. However, the indented nature of the margin did not become pronounced until 1992 and, therefore, this cannot fully explain the marked change in moraine morphology occurring immediately after 1904.

Notably moraines constructed before 1904 were arcuate, sinuous and of considerable height, and the sawtoothed moraine construction occurred on the proximal slopes of this moraine

amphitheatre composed of Stóralda and other larger overridden moraines constructed before 1904 (Figure 5.15). The adverse proximal slope of this moraine amphitheatre has affected the morphology of moraines, by not only impounding drainage during the time of moraine formation, but also by limiting the extent of marginal fluctuations of the glacier snout to form partial moraine superimposition (Figure 5.15). This partial superimposition, coupled with the formation of strong radial crevassing and marginal pecten since 1992, has given rise to extremely complex moraine crenulation. The linkage between the evolution of such crevasse architecture and proglacial drainage patterns has recently been discussed by Evans *et al.* (2019) in the study of Hoffellsjökull, SE Iceland, where the additional influence of an overdeepening on increasingly restricted proglacial drainage pathways during snout recession has been demonstrated.

The geomorphological mapping and analysis of aerial photography presented in this thesis indicates that minor push moraines have been formed sub-annually also at Svínafellsjökull, specifically between the early 1990s and the present day. This has been calculated by counting the number of moraine crests occurring laterally over a known time period, for example between 1990 and 2013 if sub-annual moraine formation was occurring there would be more than 23 moraine crests laterally between the marginal limits. Phases of (sub-)annual moraine formation have been associated with periods of above-average summer temperatures in Iceland, where the spacing between individual moraines is primarily controlled by variations in the summer temperature signal from year to year (e.g. Boulton, 1986a, 1986b; Krüger, 1995; Bradwell, 2004; Bradwell *et al.,* 2013; Chandler *et al.,* 2016a, 2016b). An important factor to consider when examining phases of (sub-)annual moraine formation at Svínafellsjökull is the impact of the northwestern proglacial lake draining events. As discussed in Chapters 3 and 4 during September 2018, 24 to 48 hours after a lake draining event, water was observed to be flowing under the ice (See Chapter 3, Figure 3.15b). Observations by glacier tour guides suggest that periodic draining of this lake happens throughout the summer months each year and the periods between lake drainage events can be as short as 24 hours. This water which was observed to be flowing back under the ice, could lubricate the ice at the ice-bed interface enough

to allow the ice to flow forward and oscillate as the ice rides up the adverse slope of the moraine amphitheatre. This motion would cause sub-annual push moraine construction to occur through bulldozing or other processes depending on the ice/bed interface characteristics.

The key finding that can be drawn these interpretations and from the conclusions surrounding moraine clast morphology outlined in chapter 4, is the influence of changing ice marginal drainage on moraine formation. From this key finding a model can be proposed for the evolution of the landsystem signature at Svínafellsjökull in relation to the temporal and spatial changes in glacier marginal conditions and topography. The main steps within this model are (Figure 5.15):

i. Moraine amphitheatre is constructed by the formation of Stóralda and also large linear to arcuate moraines formed during the late 1800s.
ii. This moraine amphitheatre impedes drainage and causes constriction of the ice and results in the ice overriding the moraines and allows them to be greatly modified (smoothed) by ice overriding and draped with recessional push moraines (moraines found in the 1870/1890-1904 limits)
iii. The change in drainage and constriction of the ice allows sub-annual push moraines to be formed on the proximal slope of this moraine amphitheatre.
iv. The constriction caused by the moraine amphitheatre, change in proglacial drainage caused by the moraine amphitheatre, increasing structural complexity of the glacier margin (from the early 1900s), as well as warming temperatures allows the formation and characteristics of push moraines to alter and become much more complex/ sawtoothed. This complexity in the formation and morphology of the moraines increases during retreat creating the signatures that can be seen on the foreland presently.

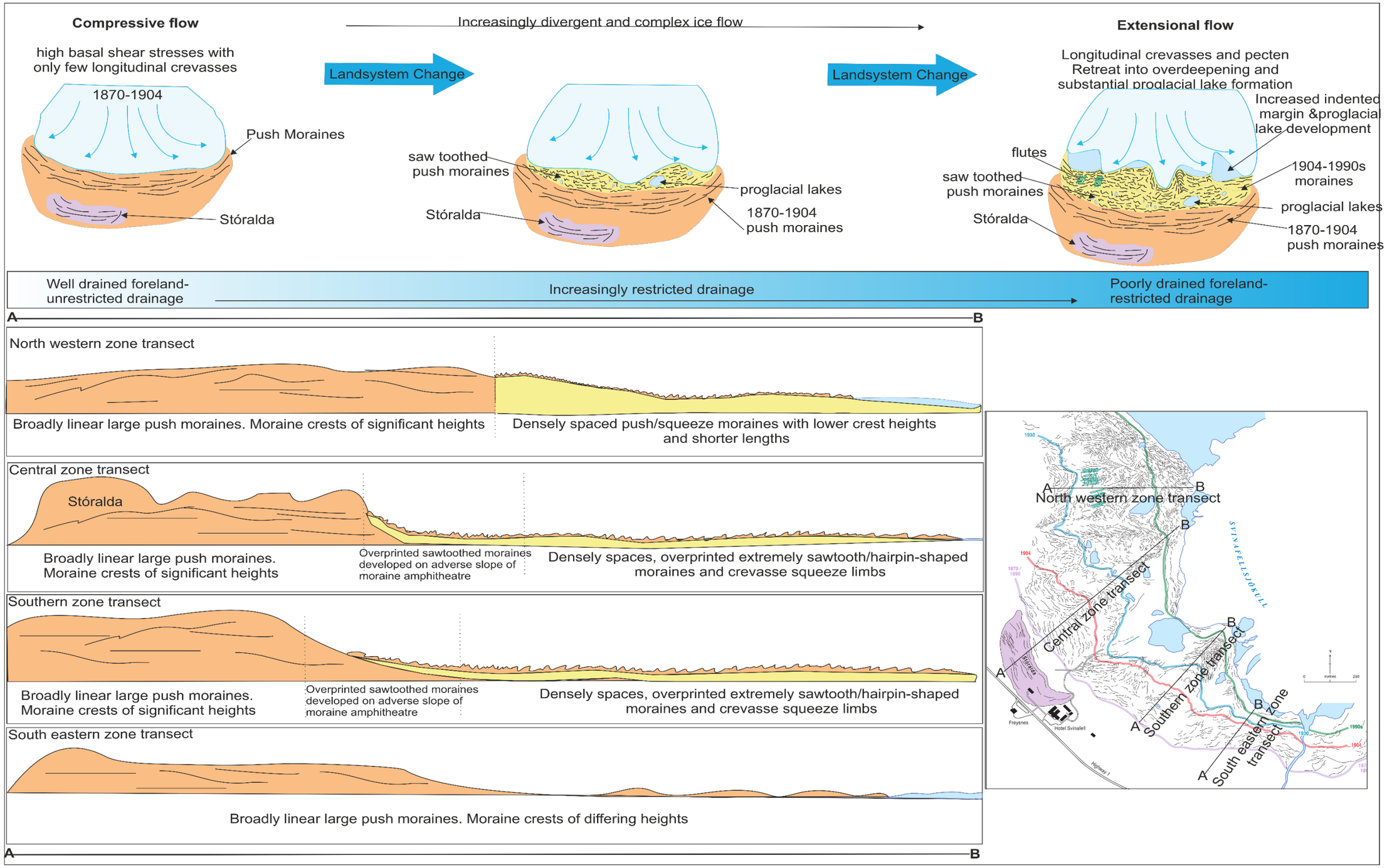

Figure 5.15: Conceptual model depicting the evolution of the landsystem signature at Svínafellsjökull in relation to the temporal and spatial changes in glacier marginal conditions and topography.

5.6 Discussion- Structural drivers of change in moraine development during current glacial retreat at Southeast Iceland

The moraine amphitheatre found at Svínafellsjökull is not unusual when examining glaciers on the southeast coast of Iceland. For example, neighbouring Kvíárjökull is surrounded by a large Holocene latero-frontal moraine ridge similar to that found at Svínafellsjökull (Evans *et al.,* 1999a; Spedding and Evans, 2002; Evans, 2009; Bennett *et al.,* 2010). This moraine comprises two prominent ridges, the Kviarmýrarkambur (150 m a.s.l.) on the southern side of the glacier and Kambsmýrarkambur (129 m a.s.l.) to the north. The unusually large latero-frontal moraine and the supraglacial debris cover of the lower snout have been central to attempts at interpreting debris transport pathways and landform production. Eyles (1979) proposed that a large volume of debris was transported along passive pathways after rockfall events had introduced it to the glacier surface, thereby producing 'supraglacial morainic till' and constructing the large moraine by 'incremental stagnation'. It is known that the valley sides surrounding Svinafellsjokull provides rockfall debris as a source of debris to the glacier. There are well documented accounts of rockfalls within the valley in 2007 and 2013, and presently there is rockfall debris on the glacier surface and ablation beneath the debris deposits has been reduced resulting in up to a 35 m difference between the debris-free and the debris-covered ice (measured in 2020) (Ben-Yehoshua *et al.,* 2022). This gives one explanation as to how the morphology of the moraines produced in 1870/1890-1904 have formed a large amphitheatre at Svínafellsjökull.

The pattern of moraine distribution found on the Svínafellsjökull foreland between 1904 to present day is not unlike other active temperate forelands in SE Iceland and reflects spatio-temporal change in moraine forming processes dictated by changes in a combination of proglacial drainage characteristics and structural glaciology and/or crevasse architecture. This is manifest in the change from more linear and broadly arcuate moraines of the early post-LIA period to increasingly till squeeze-dominated and sawtooth/hairpin plan forms since the mid-twentieth Century. This is evidently a product of a switch from well-drained to increasingly

poorly drained settings, as proglacial drainage became more constrained between emerging overridden moraine arcs that form the moraine amphitheatre, as well as the development of increasingly stronger radial crevassing (Chapter 3).

Chandler *et al.* (2020a) have suggested that drainage conditions are likely to be important factors influencing the nature and frequency of moraine formation. This is based on the foreland of Fjallsjökull, where the development of a large number of push moraines, developing on sub-annual timescales at the southern glacier margin are located on a reverse depositional slope (Evans *et al.,* 2018b) located around the margins of a substantial overdeepening (cf. Magnússon *et al.,* 2012; Dell *et al.,* 2019). This emerging subglacial topography locally impedes drainage, leading to highly saturated subglacial/submarginal sediments and high porewater pressures. Combined with other factors, the poor drainage conditions imparted by the basal topography provide favourable conditions for ice marginal squeezing. Such case studies clearly demonstrate that basal topography and ice-marginal drainage conditions are important influences on the nature and frequency of moraine formation at active temperate glaciers in Iceland, especially where snout morphologies have changed to more divergent flow with stronger radial crevassing in response to overall thinning. The results of the research presented above verifies Chandler *et al.* (2020a) suggestion that changes in drainage conditions are important factors to consider in terms of moraine formation, specifically where local topography impedes drainage. Furthermore, the influence of Svinafellsjokull's basal topography on the glacier's dynamic and structural regime appears to have increased throughout the study period, as the glacier has thinned due to recent climatic warming (see Chapter 3). Additionally, poor draining can result in enhanced basal sliding, bed deformation and forward motion, this could potentially lead to the destabilisation of margin of Svínafellsjökull and collapse of ice into the overdeepening.

The changes within the structural architecture of Svínafellsjökul between 1952 and 2012 clearly has had an impact on snout drainage (see Chapter 3). Significantly, in terms of landform development, over the period of mapping presented here, the glacier snout developed strong

longitudinal crevassing and associated ice marginal pecten. Push moraines on the foreland of Svínafellsjökull are now developing with extreme sawtooth or hairpin plan forms in response to its structural regime. This indicates that snout morphological changes and structural glaciological responses to climate warming can be clearly recorded in the push moraine characteristics over time. Chandler *et al.* (2020a) refers to changes in structural regime to be a factor leading to changes in the morphology and formation of push moraines. The longitudinal fractures within the ice at Svínafellsjökull are a fundamental feature of the structural architecture of the glacier (Chapter 3). The opening of these longitudinal fractures to form crevasses is the process which leads to the formation of the pecten or blades of ice separated by re-entrants. Opening of the fractures at the margin could occur in response to the radial spreading of the ice within the piedmont lobe, or due to differential erosion/melting of the ice along the fractures which capture any surface drainage, further amplifying the effect of this differential melting/erosion. Meltwater flow becomes increasingly concentrated along the open fractures with the angular margins of the crevasses forming the focus for increased/enhanced melting.

Additionally, sawtooth moraine overprinting has developed more recently due to sub-annual moraine construction and short periods of ice-marginal readvance, the latter exemplified by the 1990s regional readvance event (Evans and Hiemstra, 2005; Sigurðsson *et al.*, 2007; Evans *et al.*, 2016, 2017b). Phillips *et al.* (2017) indicate that a short readvance event in 2013-2015 at Kviárjökull occurred and (Einarsson and Sigurðsson, 2015) was recorded only locally in the moraine overprinting record, due to the preferential forward displacement of splines of snout ice whose shapes were pre-conditioned by radial crevasse construction during pre-advance snout thinning over an uneven subglacial topography (see Chapter 3 for details). Observations made during field work at Svínafellsjökull in August-September 2017 clearly demonstrate that an area of the margin was overriding a small-scale (c. 1 to 1.5 m high) push moraine composed of poorly sorted sands and gravels (Figure 5.16). This moraine formed during the previous winter (2016-17) readvance/oscillation, consistent with an overall pattern of active glacial retreat.

However, the continued forward motion and overriding of this recessional push moraine in August 2017 indicates that this marginal area of Svínafellsjökull continued to move forward during the summer months (see Chapter 3 Figure 3.19). In September 2020 it was also observed that Svínafellsjökull was producing sub-annual moraines and that the formation of these moraines was saw-toothed and mirroring the indented shape (and shape of the individual pectin) of the margin (Figure 5.16 a, b , c). This observation is compatible with the proposal of Chandler *et al.* (2020a, 2020b) that push moraines in this part of Iceland have recently been constructed at a rate of more than one per year.

As stated, the present day landsystem signatures of many active temperate glaciers in Iceland are characterized by the creation of increasingly complex, closely spaced, sawtooth or hairpin-shaped moraine sequences over the past ~30 years (e.g. Chandler *et al.,* 2016a, 2016b; 2020 and 2020b; Evans *et al.,* 2016a, 2017b, 2018b, 2019; Evans and Ewertowski, 2018), much like the landforms mapped from the early 1990s at Svínafellsjökull and have been associated with marginal-thickening till wedges (cf. Evans and Hiemstra, 2005; Evans *et al.,* 2018a; Chandler *et al.,* 2020a and 2020b). Chandler *et al.* (2020b) established that the moraines form by (i) submarginal deformation and squeezing of subglacial till or (ii) pushing of extruded tills. It is also noted that glaciofluvial sediments are also incorporated within the moraines during pushing. The authors conclude that these moraines formed sub-annually and Chandler *et al.* (2020b) go on to present a conceptual model for sub-annual moraine formation at Fjallsjökull. This proposes the sawtooth moraine sequence comprises (i) sets of small squeeze moraines formed during melt-driven squeeze events and (ii) larger push moraines formed during winter re-advances. The development of this process-form regime is linked to a combination of higher temperatures, high surface meltwater fluxes to the bed and emerging basal topography (due to an overdeepening). These factors result in highly saturated subglacial sediments and high porewater pressures, which induces submarginal deformation and ice-marginal squeezing during the melt season. Strong glacier recession during the summer, driven by elevated temperatures, allows several squeeze moraines to be emplaced. This process-form regime may

be characteristic of active temperate glaciers receding into overdeepenings during phases of elevated temperatures, especially where their englacial drainage systems allow efficient transfer of surface meltwater to the glacier bed near the snout margin. It is known meltwater is being delivered back under the glacier, and possibly reaching the bed, from the periodic drainage of the proglacial lake situated at the northwestern margin of Svínafellsjökull, this in turn may enhance submarginal deformation and ice-marginal squeezing during the melt season at this location and aid the development of sub-annual moraine construction (Chapter 3). However, increased meltwater at the ice-bed interface could result in the decoupling of the ice leading to enhanced basal sliding with moraine formation.

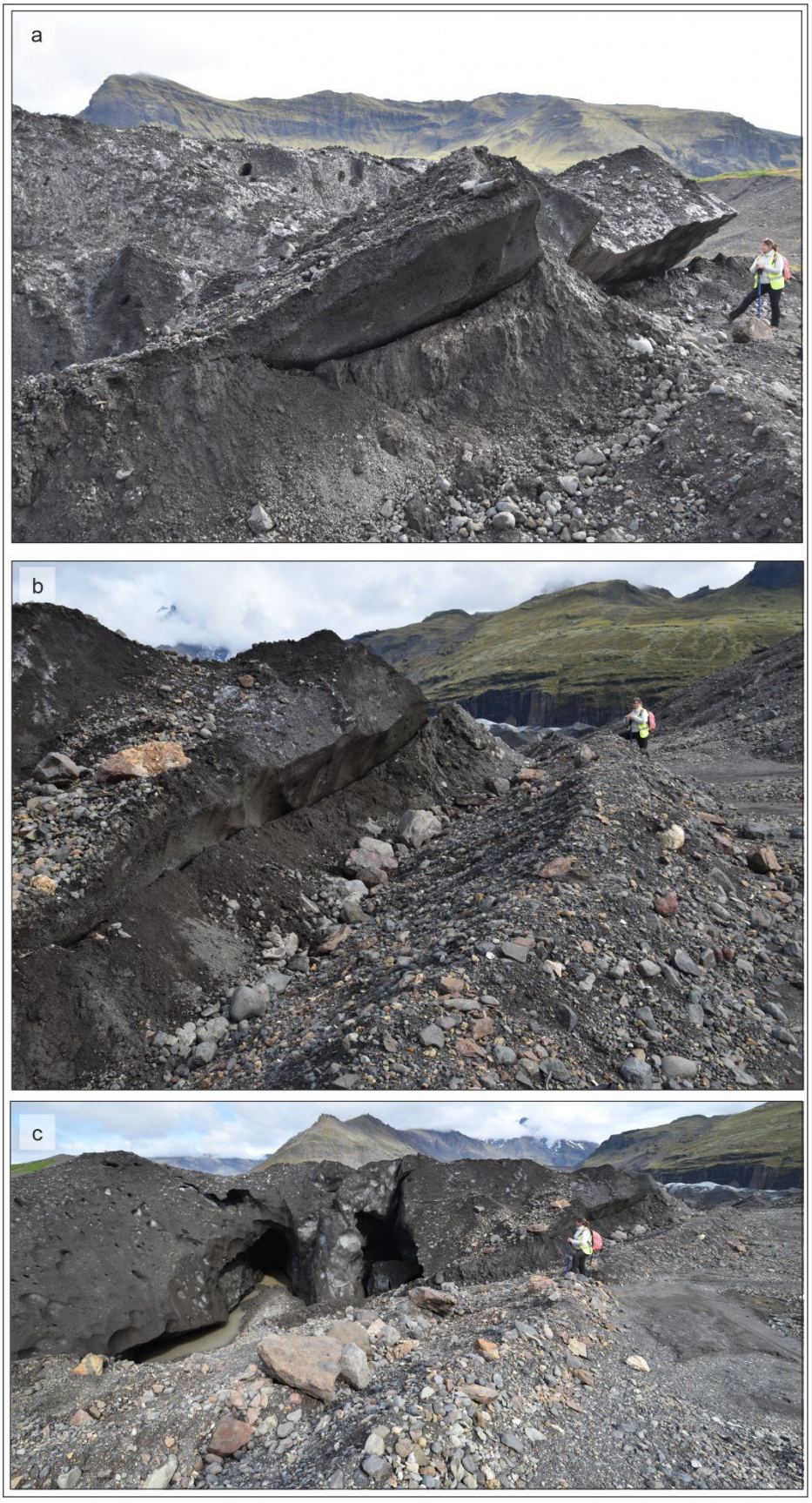

Figure 5.16: Sub-annual saw-toothed push moraines at Svínafellsjökull September 2020.

5.7 Conclusions

Thorough examination of the characteristics of the landforms on the forefield of the Svínafellsjökull glacier allows the idea that landsystems can be used as an indicator of process form relationships. A number of factors, including glacier characteristics and local topography (significantly the presence of an overdeepening and depositional features), contribute to the outcome of landsystem characteristics.

Changes in the structural configuration of the lower reaches of Svínafellsjökull, especially the development of radial crevasses, have impacted upon the landform record preserved within the foreland of the glacier. The most recently formed moraines at Svínafellsjökull display a distinct saw tooth or crenulated pattern in plan form. Geomorphological mapping of the forefield is presented and reveals that the pre-Little Ice Age limits are arcuate in shape with the switch to a saw tooth pattern of moraine crests having occurred during the early 1900s (c.f. Everest *et al.*, 2017). This research demonstrates that the landform record within the foreland at Svínafellsjökull reflects changes in the structural architecture of the marginal zone of the glacier and changes in drainage conditions due to a moraine amphitheatre causing drainage and moraine construction to be restricted/impeded. This has implications for the interpretation of the landform records preserved during deglaciation. These implications include the use of Tephrochronology within moraine construction, and importantly highlight that these complex landsystem models enable landform assemblages in ancient glacial landscapes to be used as proxies for factors such as palaeoglaciological and palaeoclimatic indicators.

The model proposed for the evolution of the landsystem signature at Svínafellsjökull in relation to the temporal and spatial changes in glacier marginal conditions and topography shows that the recently formed moraines at Svínafellsjökull comprise of extremely sawtooth/hairpin moraines, which have been constructed on a sub-annual basis since the early 2000s. This change in both the production of landforms and their characteristics can be attributed to; (a) a change in drainage due to a change from unconfined proglacial drainage to progressively poorly drained

and constrained conditions, and (b) the development of radial crevassing which becomes increasingly pronounced due to accelerated ablation. Importantly, the key control on drainage conditions can be both the emerging proglacial topography constructed by the glacier itself,and/ or the bedrock topography. Similar process form regime changes have been identified in other glaciers in the region and thus it appears that they are a diagnostic characteristic of the active temperate glacial landsystems and should be considered for further research.

6 Conclusions and Implications

6.1 Key conclusions

This research utilises multidisciplinary techniques in order to achieve a detailed understanding of the structural glaciological evolution of Svínafellsjökull and explores the implications for debris entrainment and landform development.

The structure of Svínafellsjökull has been impacted in recent years by a warming climate and this has initiated passive retreat of the glacier. Since this initiation of passive retreat, the glacier has undergone accelerated recession and pronounced thinning over an overdeepening. Chapter 3 investigates the structural glaciological response, both spatially and temporally, to this recession and accompanying thinning of the terminal zone. A combination of remotely sensed data, in particular variation in the orientation, density and morphology of fractures within the ice (crevasses) and field based observations have been used to divide the glacier into two main zones: (i) an extensive upper zone which exhibits a relatively simple radiating/down ice fan-shaped fracture pattern, a locally well-developed network of supraglacial meltwater channels and prominent light and dark coloured ogive bands; and (ii) a structurally more complex lower terminal zone which can be divided into three areas displaying lobate frontal margins. Although initial results suggest that the structure of the upper part of Svínafellsjökull is consistent with the traditional 'plug flow' model, the structural complexity of its multi-lobate marginal zone cannot be explained as the product of the simple radiating crevasses typically associated with the spreading, radial flow of a piedmont lobe over a gently sloping foreland. Significantly the structural evolution of the lower reaches of this glacier is more complex. A multi-lobate structure at the margin occurs due to the focussing of recent flow associated with one or two re-advances within the central marginal zone, along with increases in snout thinning and a concomitant change in snout drainage. Overall, historical mapping indicates that the structures of both the north-western and southern marginal areas of the glacier remained relatively unchanged between 1952 and 2012. This suggests that the north and south margins are largely static and

that flow from the upper reaches of the glacier is being concentrated in the central unit. The change from a conventional "plug flow" mechanism in the upper reaches of Svínafellsjökull to this multi lobate structure is rooted in Domain 2, which is thought to be an area of instability, possibly related to the concentration of subglacial drainage or even ponding of meltwater within the overdeepened trough. Furthermore, it is argued that the spatial complexities of the concentrated flow regime (within the central unit) are governed by the bed topography that underlies the glacier. The influence of this bed topography on the glacier's dynamic and structural regime appears to have increased throughout the study period, as the glacier has thinned. It is proposed that Domain 2 represents an area of instability or constriction within the ice which occurs immediately above the down-ice opening of the narrow axial trough within the bed of Svínafellsjökull (Magnusson *et al.,* 2012). Alternatively, Domain 2 could represent the surface expression of a topographic constraint within the bed (i.e. the trough identified by Magnusson *et al.,* 2012) which, as the glacier progressively thinned, caused the increased funnelling of the ice through this constriction, resulting in preferential concentration of flow along the central axis of the glacier. The detailed mapping of the structure of the marginal zone of Svínafellsjökull presented in Chapter 3 clearly indicates that this is not a recent phenomenon but has been established for at least the past 10 to 15 years. Consequently, it is unlikely that changes in the structures within Domain 2 are associated solely with the thinning of the ice during the recent period of accelerated retreat. The development of this structural evolution within the marginal area of Svínafellsjökull in turn influences the debris entrainment and transport pathways at play.

Complex debris transfer processes in temperate overdeepened systems in Iceland are apparent in the nature of the deposits that comprise large frontal moraine systems, as well as the emergence of downwasting glacier snouts with supraglacial debris of mixed transport origin, thick debris-rich basal ice sequences, debris-lined englacial thrusts and englacial eskers. Understanding the mechanisms involved in the entrainment and transfer of debris along these various pathways is essential to quantifying rates of subglacial erosion in active temperate

glaciers and their role in longer term landscape change. In addition, glacial sedimentary deposits are key to understanding ice dynamics, thermal regime and, in turn, palaeoclimate in Quaternary and ancient glacial systems. Debris transfer within glacial systems occurs via a complex and varied range of pathways that reflect different entrainment sources and processes, referred to as the debris cascade by Benn and Evans, (2010). The number and type of active pathways influences the overall capacity of sediment transport within a system, the volume of material being transported, and the sedimentological and geomorphological nature of resultant deposits and landforms. Chapter 4 provides a critical examination of the Swift *et al.* (2018) debris cascade model, through the analysis of clast shape data collected from the debris-rich ice facies in the marginal zone of Svínafellsjökull and from exposures through the basal ice at the foot of the icefall at neighbouring Falljökull. Additionally, clast shape data collected from the recent moraines constructed around the margin of Svínafellsjökull allow an assessment of the role of englacial transport pathways in the construction of recessional push moraines in terminal overdeepenings. As a result of this analysis and critical examination, a transport process model for Svínafellsjökull and Falljökull has been proposed within Chapter 4. The key proposed debris-rich glacial ice formation processes, debris transport pathways, and their glaciological controls are:

1) entrainment of debris into basal folds and surface crevasses at the ice fall (shown by the data from Falljökull);

2) deformation below the ice fall further elevates basal material into dark-ogive bands and includes relationships between faulting and the pattern of englacial drainage during the ice-margin collapse;

3) longitudinal flow compression at the base of the ice fall produces thrusting along ogive-band foliation, whilst ablation reveals some closely spaced bands that may represent separate fold arms inherited from open folds formed at the base of the icefall;

4) ablation of the ice surface of the lower snout reveals subglacially entrained and englacial channel infill sediments, locally augmented by supercooling, the patterns of which reflect debris transfer processes and their influence in the development of ice-marginal sediments and landforms.

This research also supports the overall theory that debris entrainment is influenced very strongly by the presence of a terminal overdeepening, which promotes deposition of sediment from subglacial fluvial transport pathways, inhibits the flushing of subglacial sediment by fluvial processes, promotes the formation of thick sequences of basal ice that may be thickened by flow along the adverse slope of an overdeepening, and promotes active transport of basal ice and debris to the glacier surface partly along thrust planes. An assessment of the role of englacial transport pathways in the construction of recessional push moraines in terminal overdeepenings has been made from the data obtained at Svínafellsjökull. Alternative genetic models of push moraine formation have been considered and it is concluded that multiple processes are operating on a spatio-temporal continuum in the construction of recessional push moraines at Svínafellsjökull. This is supported by recent push moraine morphology at Svínafellsjökull changing from more linear to increasingly sawtooth plan form, and this has been associated with till squeezing into ice-marginal pecten.

Debris pathways and their effect on delivering sediment to the foreland have changed through time as can be seen from the change in morphologies and characteristics of moraines found on the foreland of Svínafellsjökull. Stóralda and other large linear to arcuate moraines formed during the late 1800s are much larger than those moraines forming presently and some of this difference may be attributed to change in debris load, however as Chapter 5 concludes, there are various factors to consider when examining the changes in moraine morphology both spatially and temporally. Changes in the structural configuration of the lower reaches of Svínafellsjökull, especially the opening of radial crevasses, have impacted upon the landform record preserved within the foreland of the glacier. The recently formed moraines at

Svínafellsjökull comprise of extremely sawtooth/hairpin moraines, which have been constructed on a sub-annual basis since the early 2000s. This change in both the production of landforms and their characteristics can be attributed to; (a) a change in drainage due to a change from unconfined proglacial drainage to progressively poorly drained and constrained conditions, and (b) the development of radial crevassing which becomes increasingly pronounced. Importantly, the key control on drainage conditions can be both the emerging proglacial topography constructed by the glacier itself, and/ or the bedrock topography.

From the interpretations discussed in Chapter 5 a model is proposed for the evolution of the landsystem signature at Svínafellsjökull in relation to the temporal and spatial changes in glacier marginal conditions and topography. The main steps within this model are:

i. A moraine amphitheatre is constructed by the formation of Stóralda and also large linear to arcuate moraines formed during the late 1800s.

ii. This moraine amphitheatre impedes drainage and causes constriction of the ice and results in the ice overriding the moraines and allows them to be greatly modified (smoothed and streamlined) by ice overriding and subsequently draped with recessional push moraines (moraines found in the 1870/1890-1904 limits)

iii. The change in drainage and constriction of the ice allows sub-annual push moraines to be formed on the proximal slope of this moraine amphitheatre

iv. The constriction caused by the moraine amphitheatre, change in proglacial drainage caused by the moraine amphitheatre, increasing structural complexity of the glacier margin (from the early 1900s), as well as warming temperatures allows the formation and characteristics of push moraines to become much more complex and saw-toothed. This complexity in the formation and morphology of the moraines increases during retreat creating the signatures that can be seen on the foreland presently.

Through examination of the characteristics of the landforms on the forefield of the Svínafellsjökull glacier it can be shown that landsystems can be used as an indicator of process from relationships. A number of factors, including glacier characteristics, bedrock type and local topography (significantly the presence of an overdeepening) and proglacial drainage changes contribute to the outcome of landsystem characteristics.

This chapter of this thesis allows linkages between structural glaciological changes, debris transfer pathways and landform developments and explores the relationships between each of these factors. It is imperative to have a full understanding of a glacial landsystem and research linking these factors must be incorporated in any models of spatial and temporal change in structural glaciology and landsystem development. This will facilitate the development of more robust palaeoglaciological models/interpretations of the landform and sedimentary record of Quaternary glacier-climate relations. Overall, these conclusion addresses the research question posed in Section 1.2 and in the sections which follow, future work that will build on the findings of this study is highlighted.

6.2 Implications and further work

6.2.1 Implications

This research highlights the importance of examining multiple aspects of a glacial landsystem in order to achieve a full understanding of the process-from relationships, which are shaping the landscape and enable landform assemblages in ancient glacial landscapes to be used as proxies for factors such as palaeoglaciological and palaeoclimatic indicators. The methods used within this research highlight the need for a multidisciplinary approach to the study of glacial landsystems. Using a geostatistical approach has utility for assessing changes in glacier dynamics through time, by analyzing historical air photographs to quantify changes in crevasse-related surface patterns. However, care must be taken using these approaches, as there are limitations which should be acknowledged. For example, resolution differences in imagery and snow cover being hard to interpret (in terms of snow filled crevasses). Moreover, field-based observations

made during this study, in combination with the use of Digital Elevation Models, aerial photography and LiDAR imagery, have been used to "ground truth" any observations from remotely sensed data, thereby eliminating some of the uncertainty inherent in maps/outputs derived from remotely sensed data alone. With improvements in technology, high-resolution (ground resolution < 0.5 m per pixel) digital copies of aerial photographs have become widely available and used for both the mapping of changes in glacier dynamics and glacial geomorphological mapping.

The research presented within the previous chapters and indeed in the work citied throughout this research, show that these methods are extremely useful when applied to piedmont fronted glaciers located in Southeast Iceland. However, these methods can be applied to temperate maritime glaciers throughout the world to aid the understanding of structural responses to the recent phase of accelerated retreat due to warming climate and, further, assess the implications of such responses on debris transfer and landform development at their retreating margins.

6.2.2 Structural glaciological controls on the incorporation and transport of debris in glacial systems

Highlighting and quantifying the potential complexity of glacial debris transfer pathways are critical to developing a full understanding of glacial debris cascades and their implications for glacial landsystem evolution and the Quaternary record. This research indicates that a large number of active transport pathways should be considered when examining valley glaciers, and that mixing of debris between transport pathways is significant. This research also supports the overall theory that debris entrainment is influenced strongly by the presence of a terminal overdeepening, which promotes deposition of sediment from subglacial fluvial transport pathways, inhibits the flushing of subglacial sediment by fluvial processes, promotes the formation of thick sequences of basal ice that may be thickened by flow along the adverse slope of an overdeepening, and promotes active transport of basal ice and debris to the glacier surface partly along thrust planes. This research also highlights that there are structural controls on the

incorporation and transfer of sediment within glacier landystems. Understanding the mechanisms involved in the entrainment and transfer of debris is essential to quantifying rates of subglacial erosion in active temperate glaciers and their role in longer term landscape change. As piedmont lobes and valley glaciers continue to downwaste and retreat into overdeepenings, the structural of the ice will become increasingly more complex as the overdeepening influences deformation rates and in turn the incorporation, transportation and deposition of debris. Basal ice will also be impacted by this retreat and therefore an understanding of both the structural evolution and how that influences debris entrainment is essential when assessing longer term landscape change.

6.2.3 Glacial Landforms- records of Quaternary glacier-climate relations

This research has addressed the lack of understanding concerning the relationship between ice structures and landform morphology to enable a complete understanding of glacial landsystems and the processes shaping these. This will facilitate the development of more robust palaeoglaciological models/interpretations of the landform and sedimentary record of Quaternary glacier-climate relations.

Awareness is growing on the significance of landforms in glacial systems. However, a complete understanding of the formation within landsystems where overdeepenings are present is still lacking, meaning observations of the location and morphometry of the landforms are required to motivate process understanding further. Cook and Swift (2012) have argued that the glaciological significance of the reverse-bed gradient that occurs in the presence of such landforms is one which a complete understanding of landform formations and morphologies is essential, and the results of the research presented this thesis highlights the need for this understanding and adds to understanding the critical ice-bed processes and can be used to inform predictions of past and present ice-mass behaviour.

The examination of the characteristics of the landforms on the forefield of Svínafellsjökull allows the idea that landsystems can be used as an indicator of process form relationships. A number of factors, including glacier characteristics and local topography (significantly the presence of an overdeepening and depositional features), contribute to the outcome of landsystem characteristics. This research demonstrates that the landform record within the foreland at Svínafellsjökull reflects changes in the structural architecture of the marginal zone of the glacier and changes in drainage conditions due to a moraine amphitheatre causing drainage and moraine construction to be restricted/impeded. This has implications for the interpretation of the landform records preserved during deglaciation. These implications include the use of Tephrochronology within moraine construction, and importantly highlight that these complex landsystem models enable landform assemblages in ancient glacial landscapes to be used as proxies for factors.

6.2.4 Further work and Concluding remarks

To build on the findings of this study further work would strengthen the analysis of the understanding of structural responses to the recent phase of accelerated retreat due to warming climate and, assess the implications of such responses for debris transfer through these glaciers and landform development at their retreating margins. For example, in order to fully understand the impact of the proglacial lake draining events that take place on the north western margin of Svínafellsjökull and the frequency of these events, time lapse photography would be a very useful addition. This repeat photography of the proglacial lake will allow the frequency of these events to be established along with where the water drains to and the effect this has on collapse of marginal pectin around Svínafellsjökull. Also, a repeat survey, with additional ice radar points, similar to that carried out by Magnusson *et al.* (2012), would help establish a more detailed map of the overdeepening and would develop a more robust set of relationships between bed topography and the control/influence that has on the surface structures. This suggested further research would aid the understanding of glacial landsystems, however in Iceland in particular

work must be done to protect these landsystems from impacts such as tourism and educate authorities such as national parks as to why these landscapes should be protected from these impacts and why these landscapes are sites of scientific interest.

Approximately a quarter of all glacier tour enterprises in Iceland provide tours on or in the direct vicinity of the different outlet glaciers of the Vatnajökull icecap (Welling and Abegg, 2021). The Vatnajökull region contains several outlet glaciers which have been exploited for recreational purposes on a regular basis. Svínafellsjökull is used for sightseeing, glacier hikes and ice-climbing and in the year of 2018 195,358 visitors used Svínafellsjökull for recreational purposes (Welling and Abegg, 2021). The large number of visitors impact the landscape both directly and indirectly, for example trampling over recently formed moraines, destruction of moraines to construct paths and car parks and litter. However, in 2019 tour companies were restricted from using Svínafellsjökull for tours due to the apparent imminent threat of a large scale rockfall. A fracture in the mountainside of Svínafellsheiði threatens to cause between 60 and 100 million m^3 of rock to fall onto the glacier below (Matti and Ögmundardóttir, 2021). Increasing melt of glaciers results in a higher risk of natural hazards (e.g. lake outburst floods and rock falls) and an improved understanding of natural hazards is essential to the sustainability of the tourism industry, given the importance of glacier-related tourism in local and regional economies. An ongoing multidisciplinary approach that combines research on changes to the physical environment, with expectations and perceptions of people working, living and visiting these environments, is essential to enable communities and policy makers to adapt to climate-related change, make decisions about the future and protect the environment. Scientists can assist adaptation by contributing knowledge to the development and review of environmental policy. As climate change is a pressing social and environmental topic, quantitative and scientific data need to be utilised to allow policy makers to make informed decisions in relation to national parks and glacier-tourism. Therefore, future research should assist adaptation by partly focusing glaciological research on shorter temporal scales and contributing knowledge to the development and review of environmental policy.

7.1 Appendix 1 Structural map of Svínafellsjökull for the year of 2012 with associated rose diagrams

N

Domain 14
N
N=194

Domain 15
N
N=60

Domain 13
N
N=43

Domain 12
N
N=367

Domain 11
N
N=44

Domain 10
N
N=1579

Domain 9
N
N=1708

Domain 8
N
N=395

Domain 7
N
N=3092

Domain 16
N
N=43

Slope failure
N

Domain 17
N
N=43

Domain 18
N
N=19

Domain 2
N
N=510

Ogive banding
N
N=1977

Domain 19
N
N=75

Domain 1
N
N=300

Domain 3
N
N=553

Domain 5a
N
N=2785

Domain3a
N
N=310

Domain 5
N
N = 247

Domain 5c
N
N=330

Domain 4a
N
N=1036

Domain 4
N
N = 621

Domian5e
N
N = 781

N=177

0 500m

Domains 1to19- Structural Domains (see text for details)

Coloured lines, linear features identified on glacier surface
(including open and closed fractures etc.)

Limit of mapped area

7.2 Appendix 2 Structural maps of Svínafellsjökull for 1954, 1988, 1992, 2007 and 2012

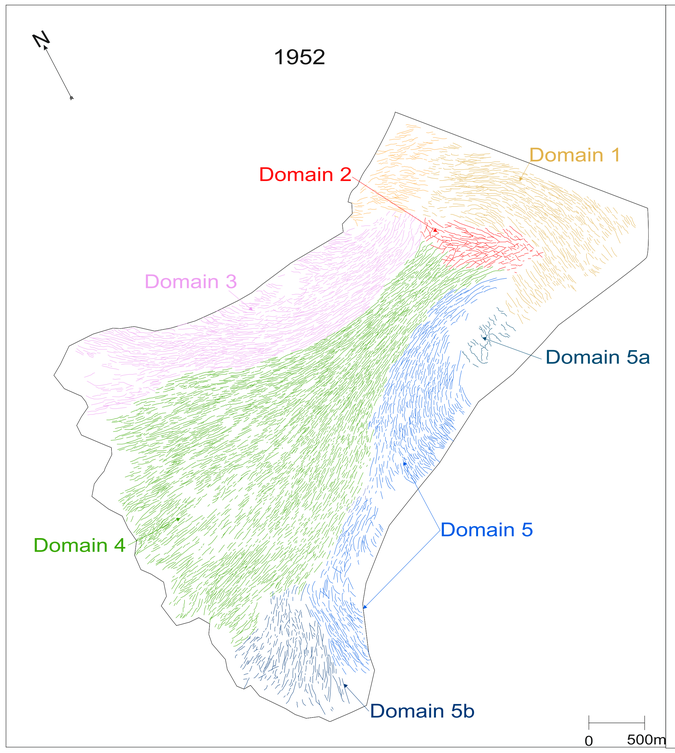

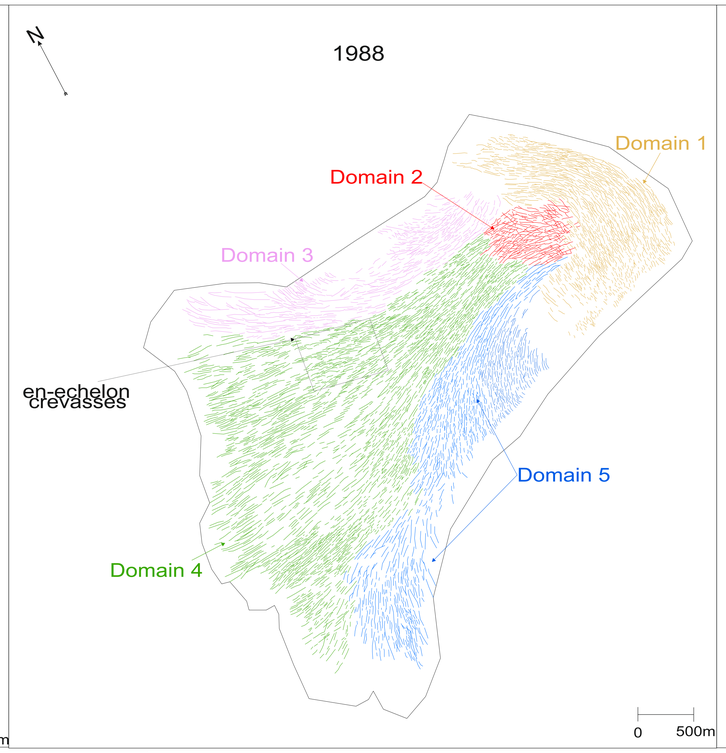

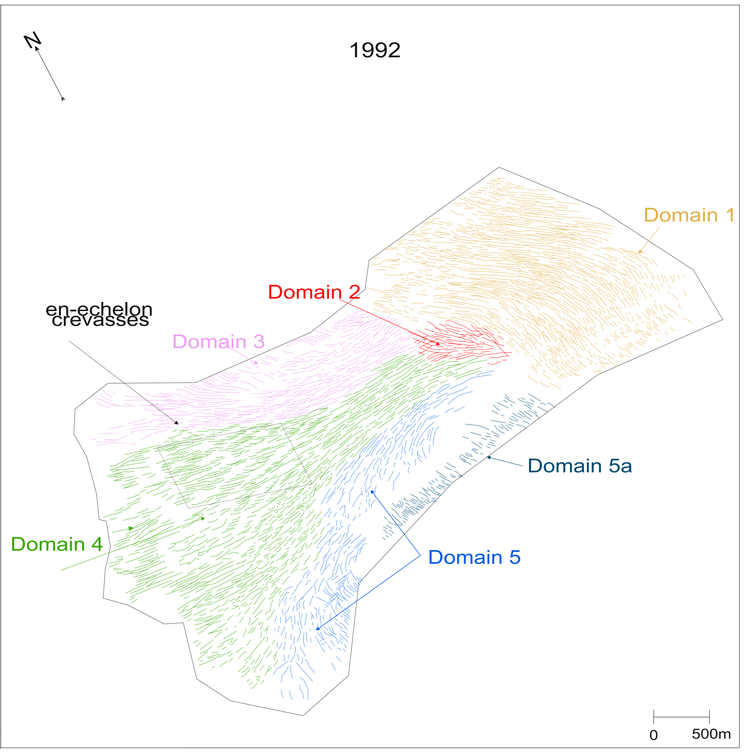

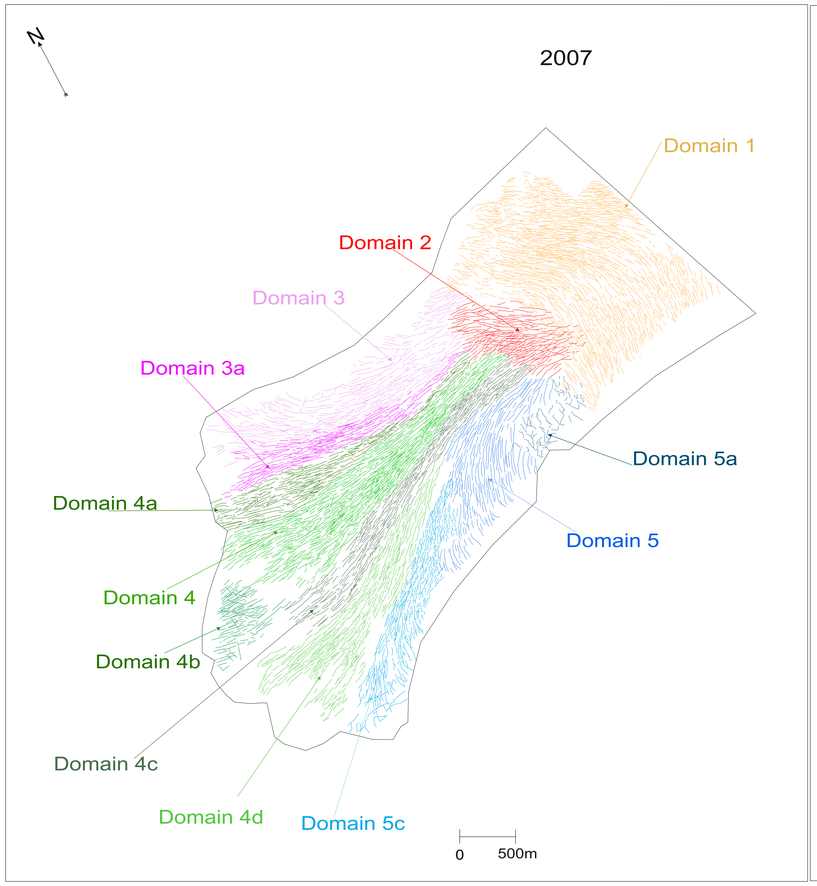

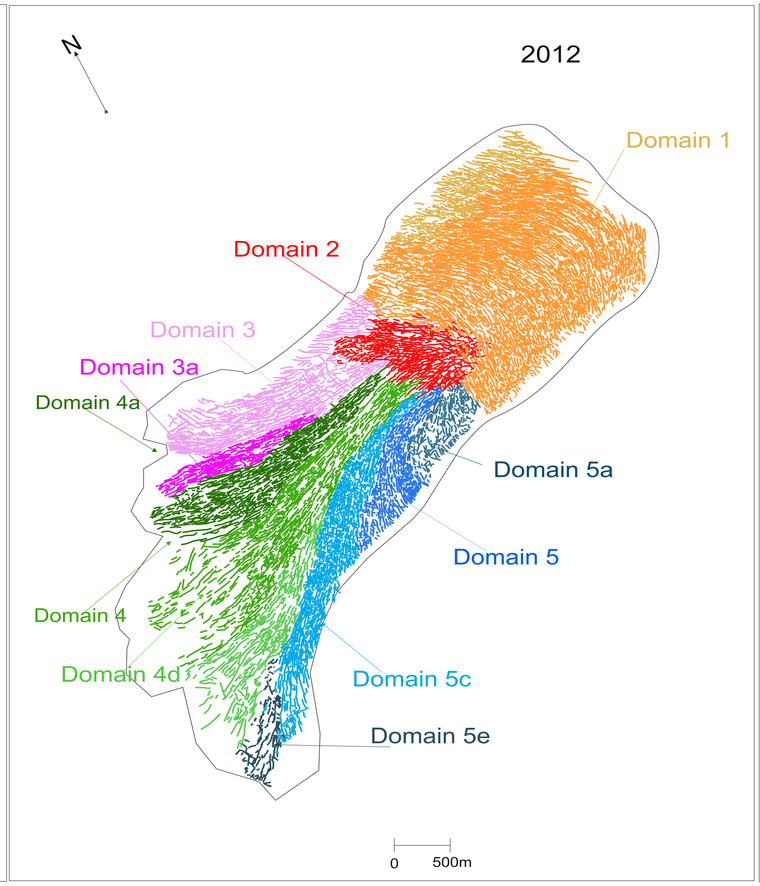

Domains 1-5d- structural domains
Pink coloured domains- North-western marginal zone
Green coloured domains- Central marginal zone
Blue coloured domains- South-eastern marginal zone

Coloured lines- linear features of glacier surface (including open and closed fractures)

Limit of mapped area

1952 Structural map

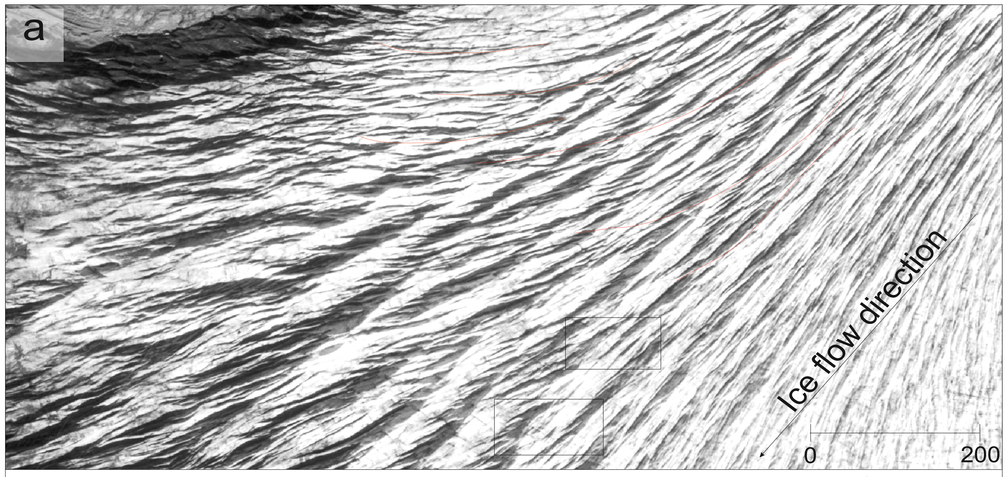

Truncation of fractures in Domain 4 by those in Domain 3

longitudinal fractures, which curved towards the NW margin of the glacier

N

Domain 1

Domain 2

Domain 3

Longitudinal fractures

Truncation of fractures in Domain 4 by those in Domain 3

Domain 5a

Domain 4

Domain 5

Domain 5b

0
500

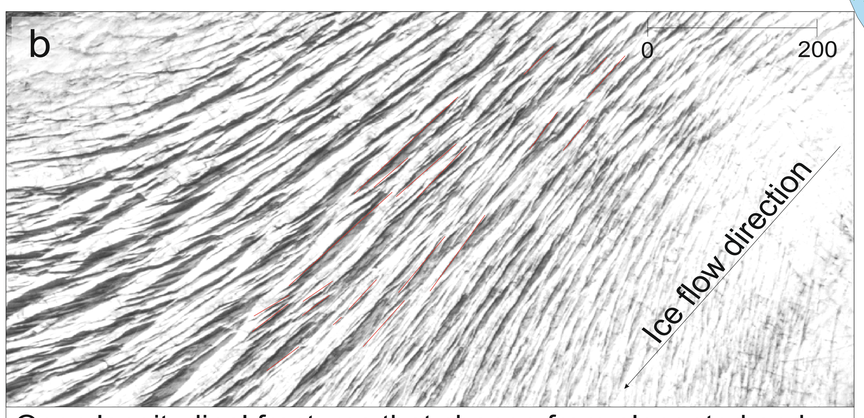

Open longitudinal fractures that change from elongated and continuous to short longitudinal features

Truncations of the SSW-SSE-trending fractures identified within Domains 5 and 5b by those structures mapped as Domain 4.

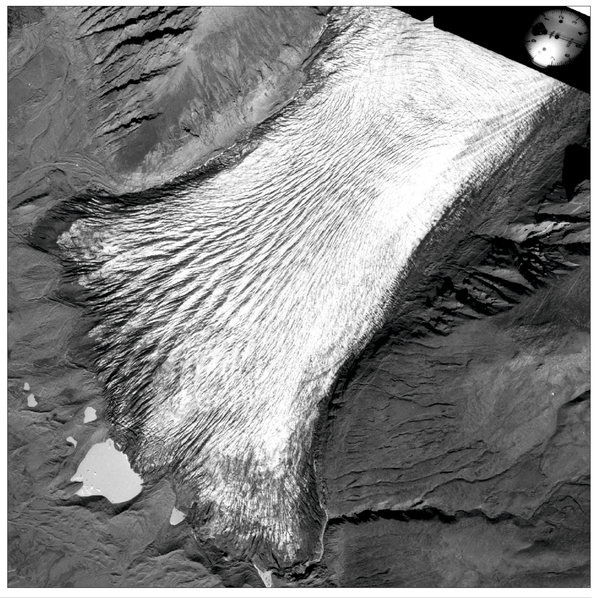

Domains 1 to 5b- Structural Domains (see text for details)

Coloured lines, linear features identified on glacier surface (including open and closed fractures etc.)

Limit of mapped area

1988 Structural map

Domains 1to 5- Structural Domains (see text for details)

Coloured lines, linear features identified on glacier surface (including open and closed fractures etc.)

Limit of mapped area

N

Domain 1

Domain 2

Domain 3

Domain 4

Domain 5

en-echelon crevasses

0 500

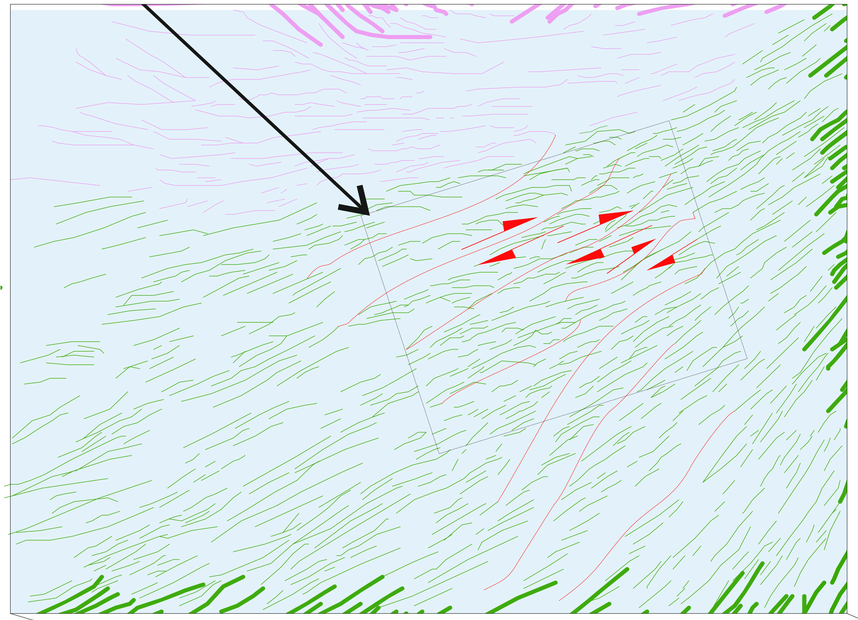

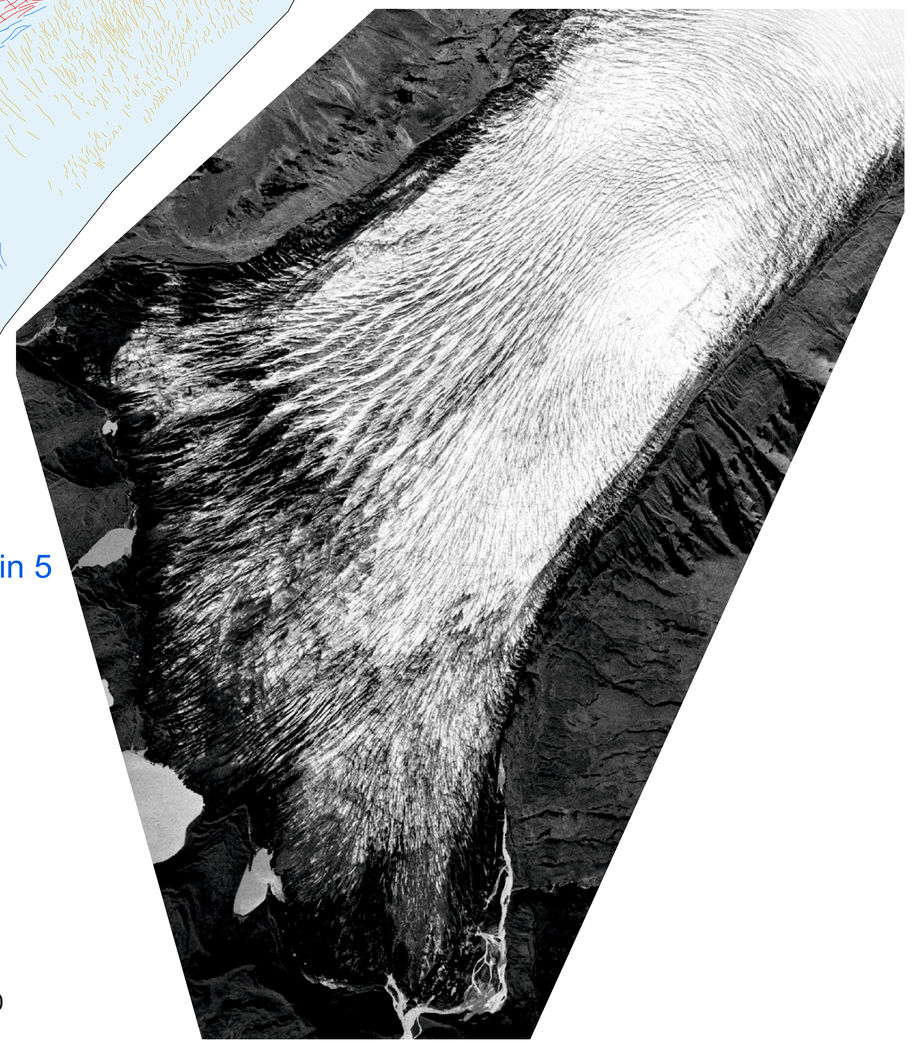

1992 Structural map

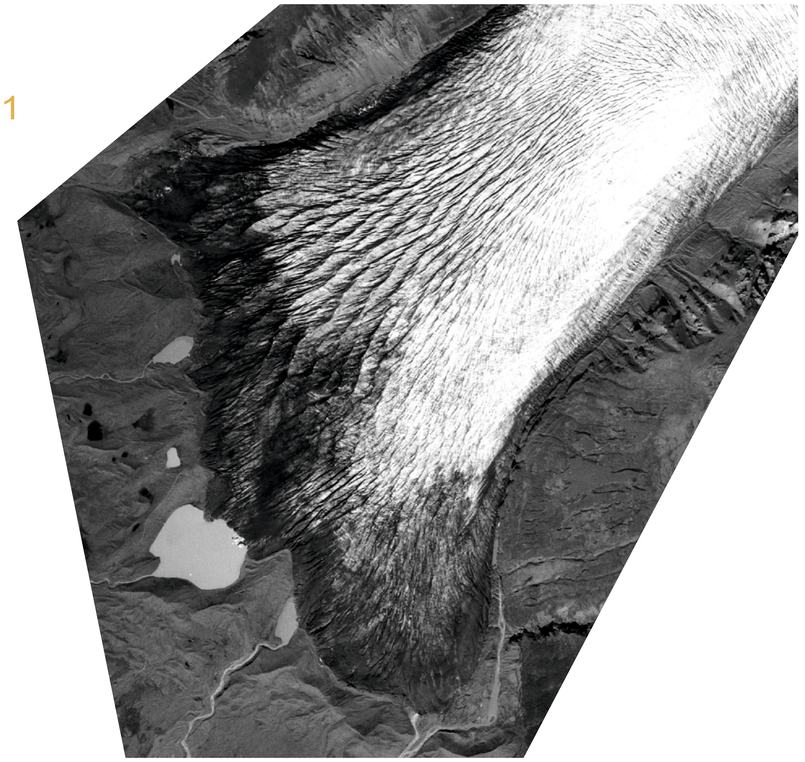

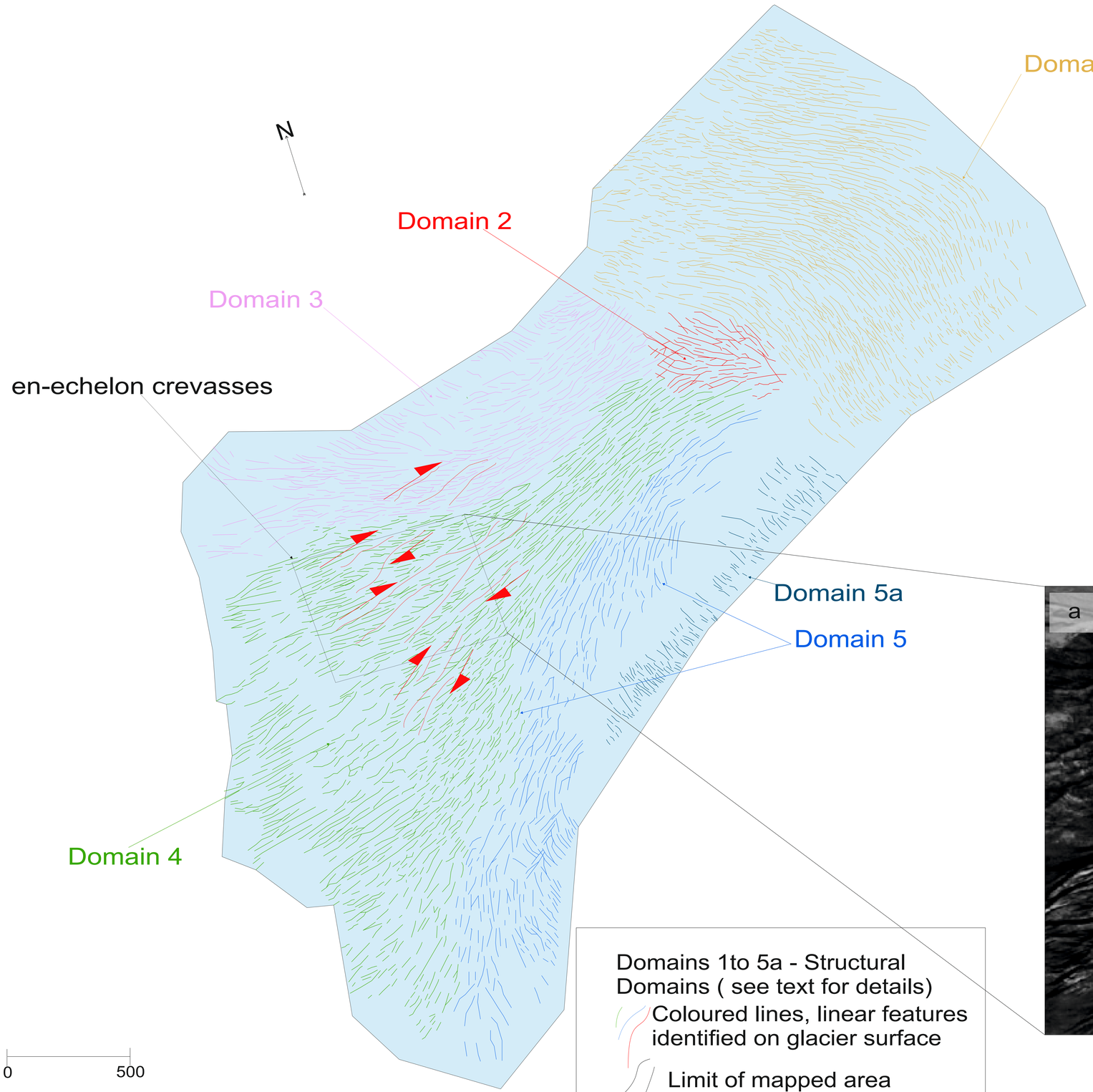

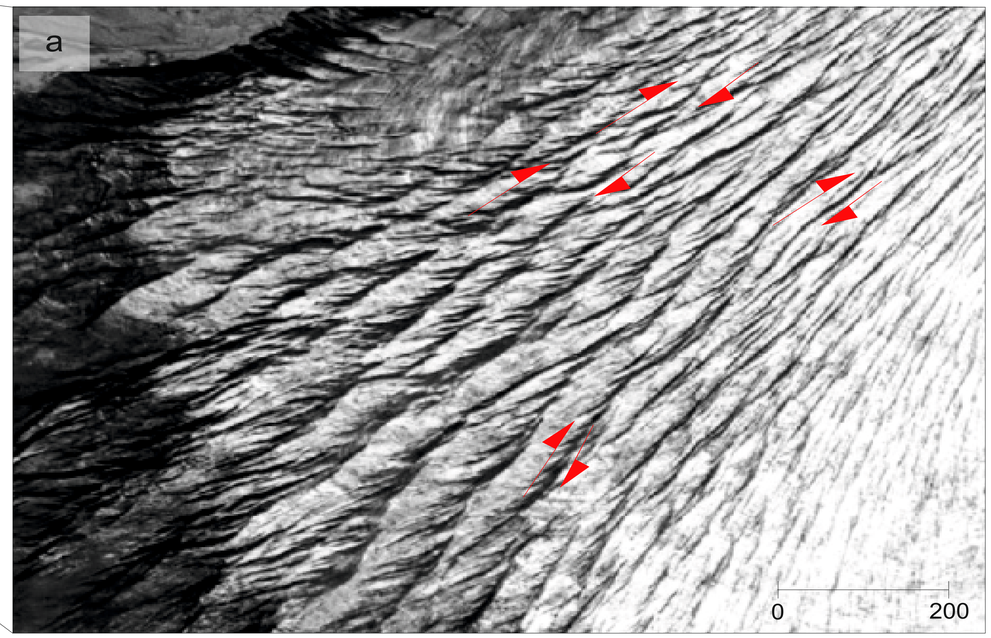

Domains 1to 5a - Structural Domains (see text for details)

Coloured lines, linear features identified on glacier surface

Limit of mapped area

2007 Structural map

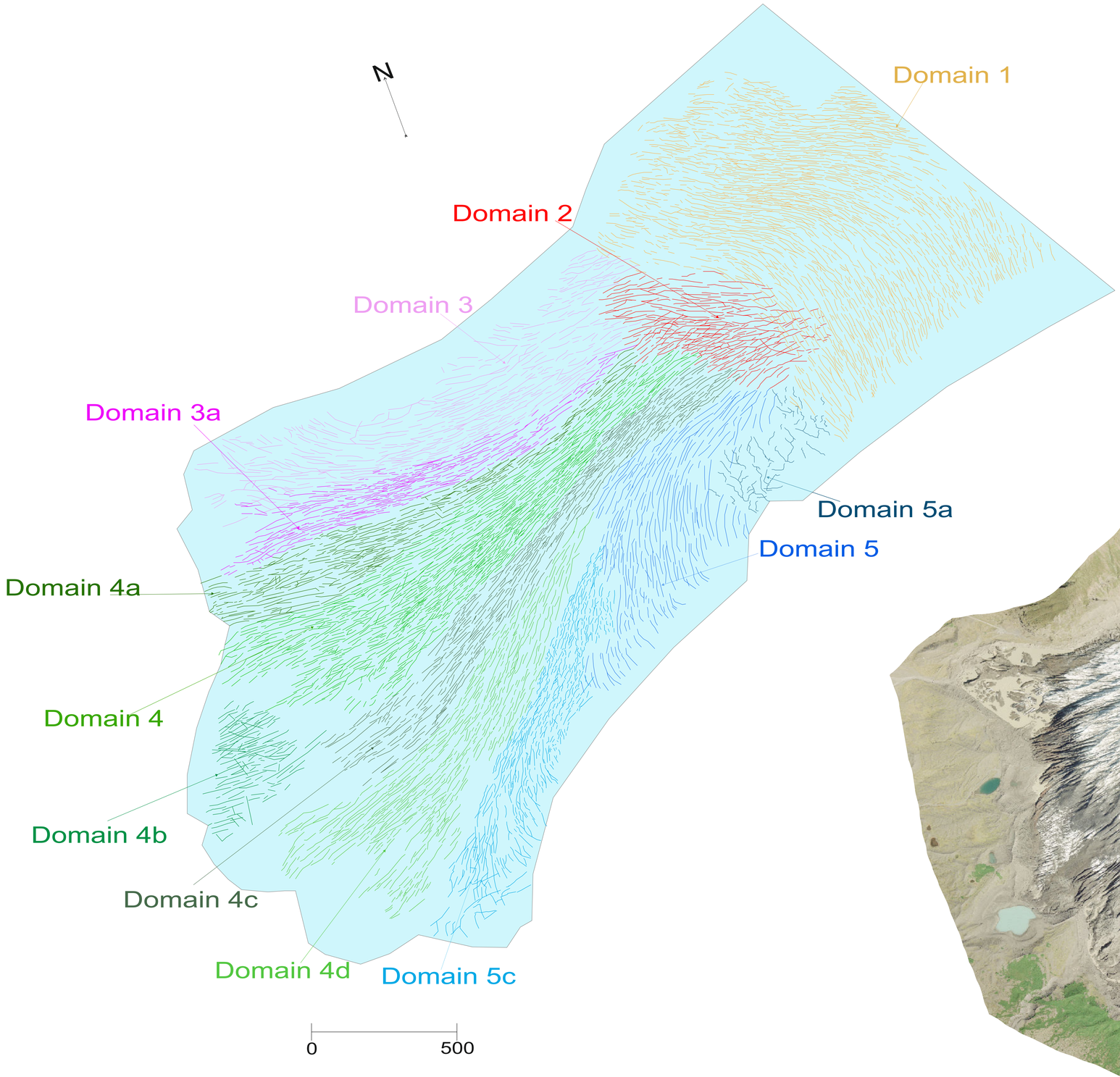

Domains 1to 5d- Structural Domains (see text for details)

Coloured lines, linear features identified on glacier surface (including open and closed fractures etc.)

Limit of mapped area

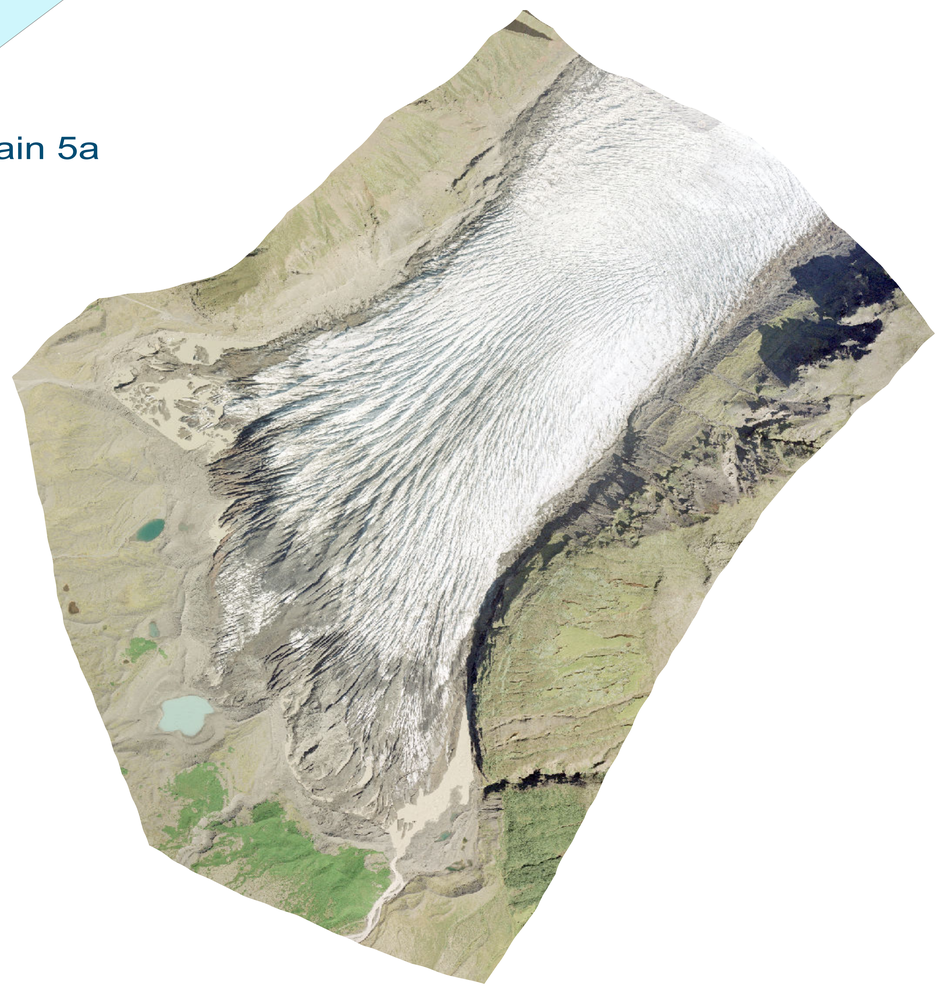

2012 Structural map

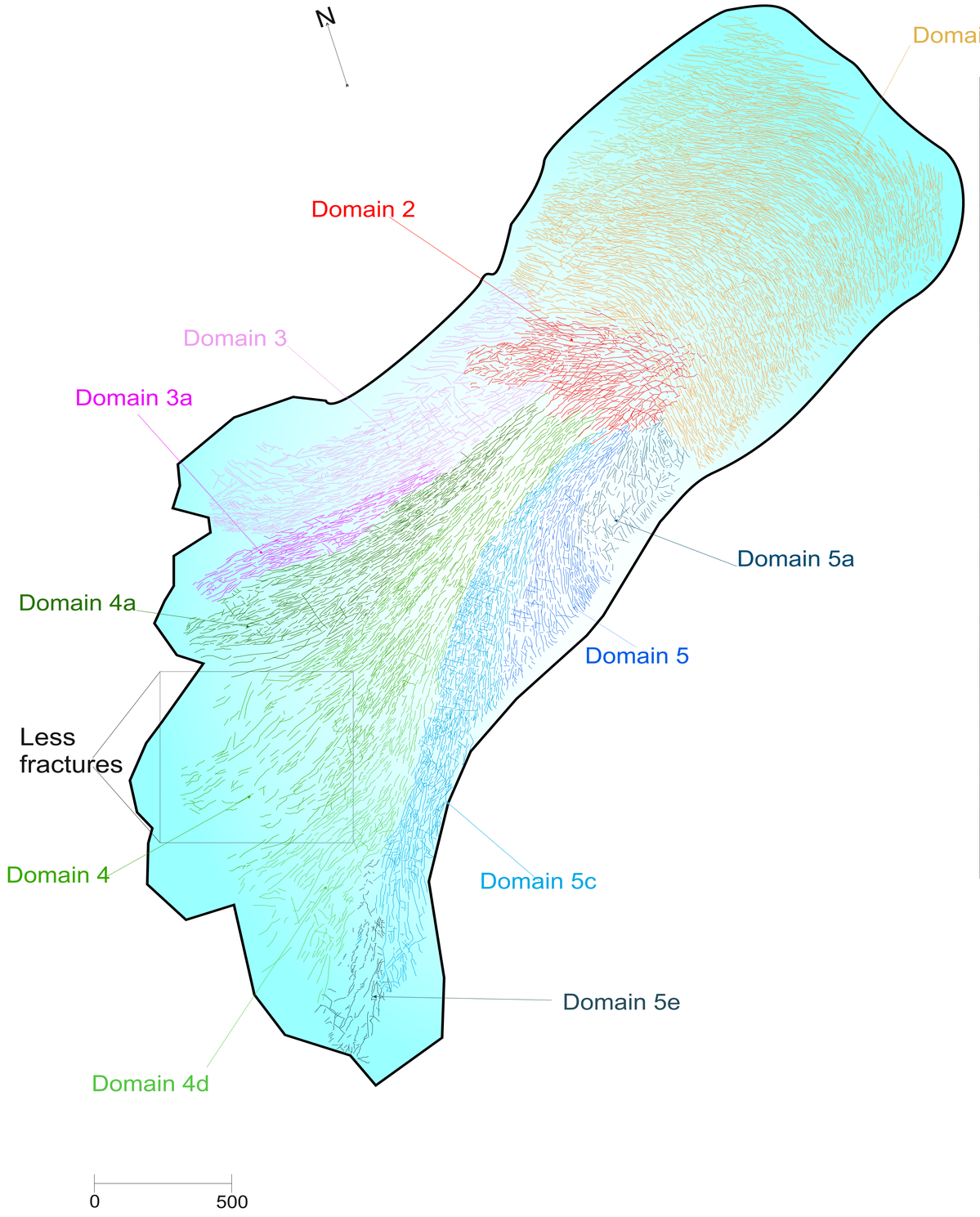

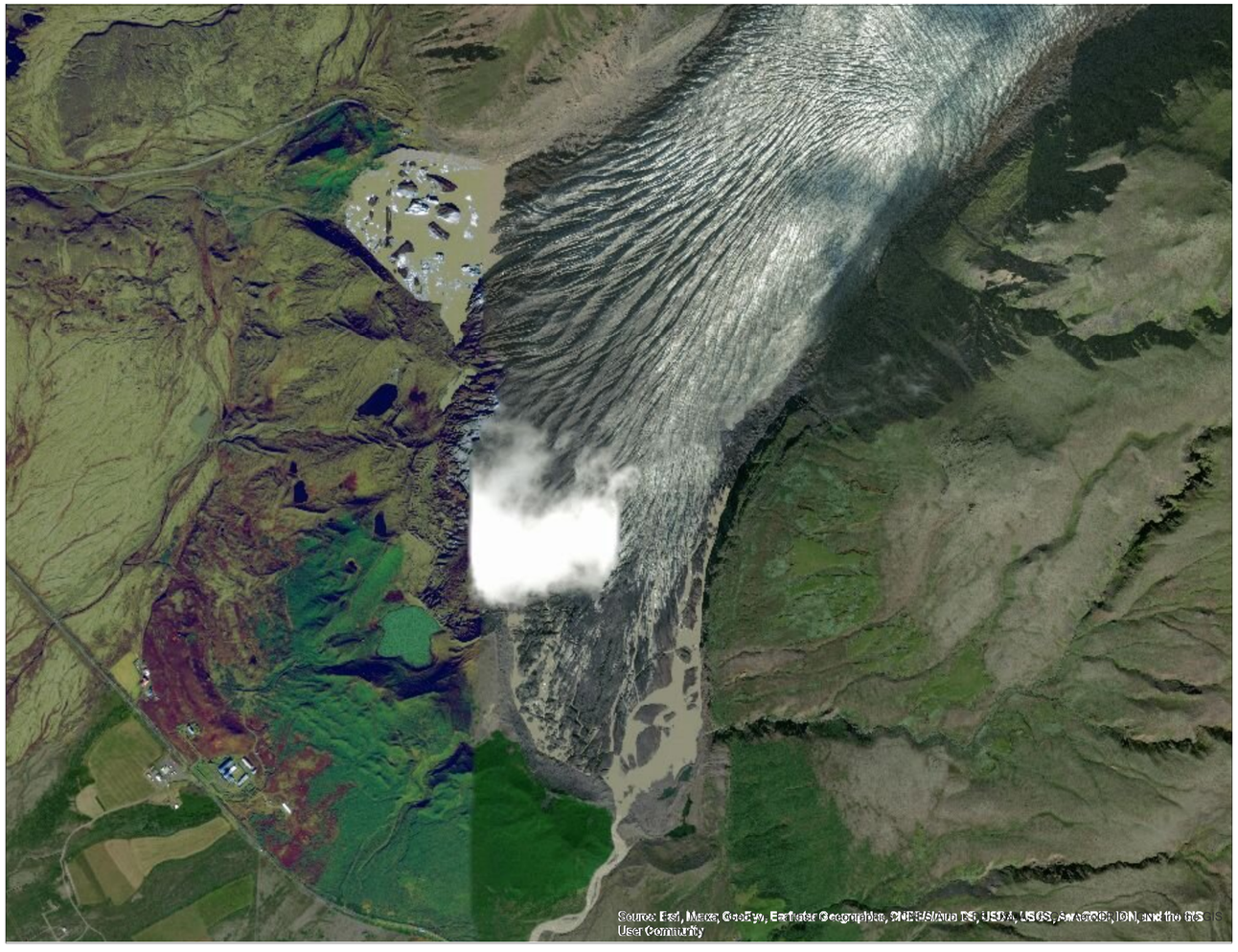

Domains 1to 5e- Structural Domains (see text for details)

Coloured lines, linear features identified on glacier surface (including open and closed fractures etc.)

Limit of mapped area

7.8 Appendix 8 Overarching sample map of on and off-glacier sample sites

On ice sample sites

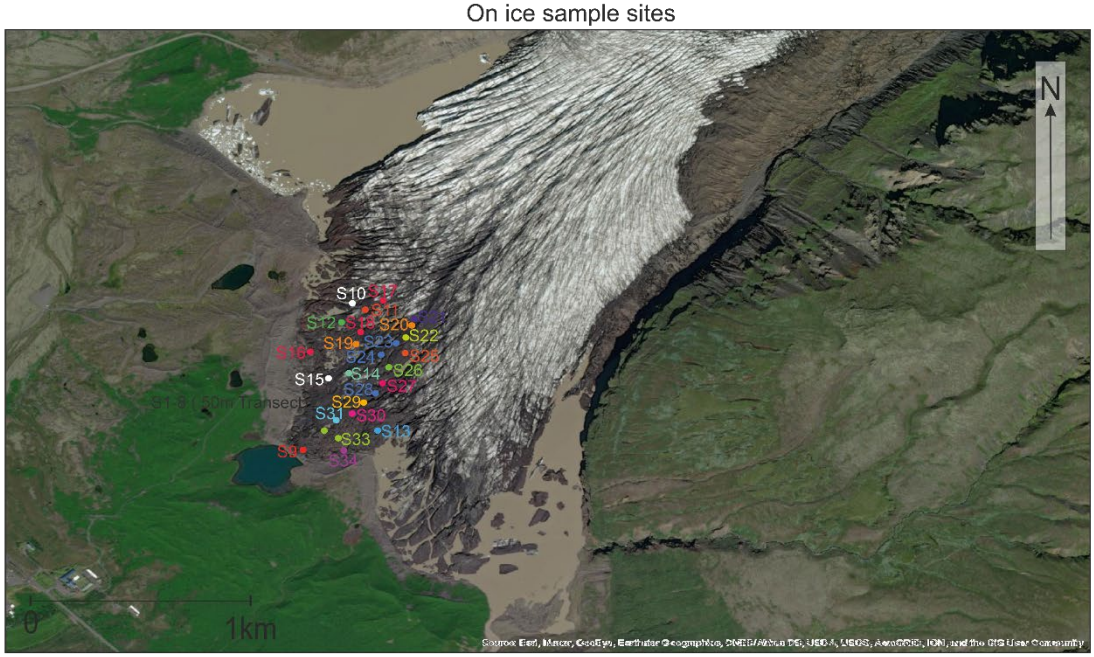

Contemporary sub-marginal push moraine sample sites

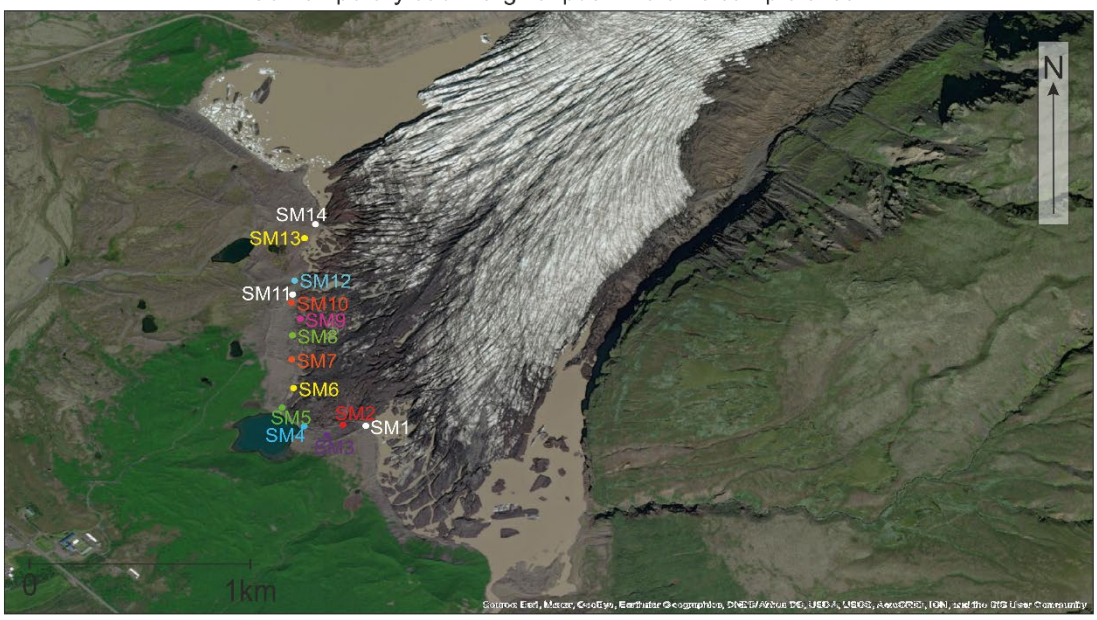

7.9 Appendix 9 Debris samples site located on Ice at Svínafellsjökull

S9

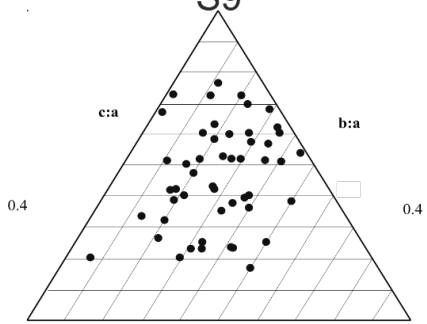

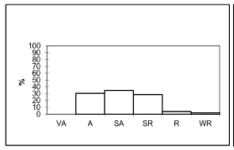

C40	63
RA	30.61
RWR	**6.12**
AvR	**2.12**
% striated	36
% faceted	4

S10

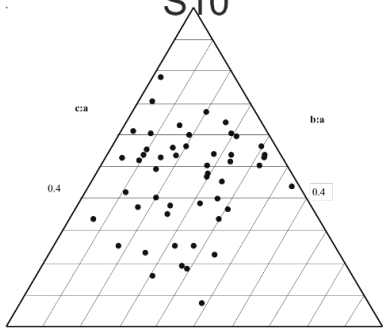

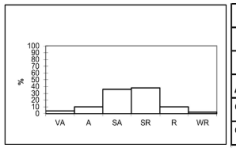

C40	36
RA	14
RWR	**12.00**
AvR	**2.50**
% striated	10
% faceted	28

S11

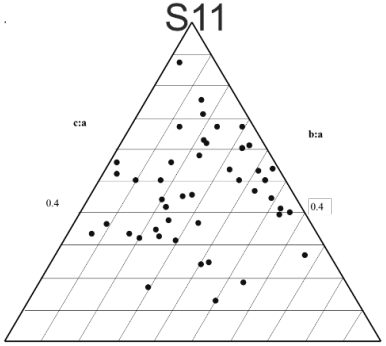

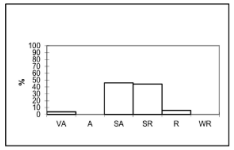

C40	34
RA	4
RWR	**6.00**
AvR	**2.52**
% striated	40
% faceted	36

S12

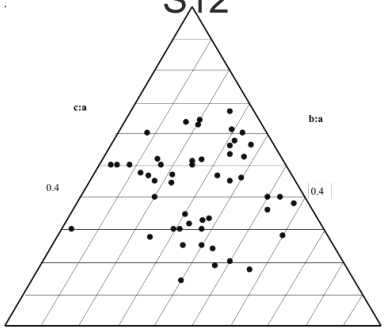

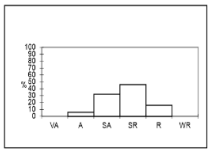

C40	44
RA	4
RWR	**16.00**
AvR	2.72
% striated	60
% faceted	26

S13

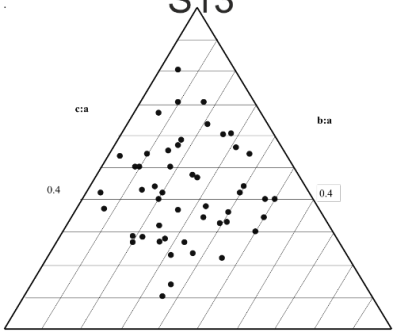

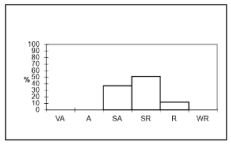

C40	50
RA	0
RWR	**12.00**
AvR	**2.75**
% striated	36
% faceted	18

S14

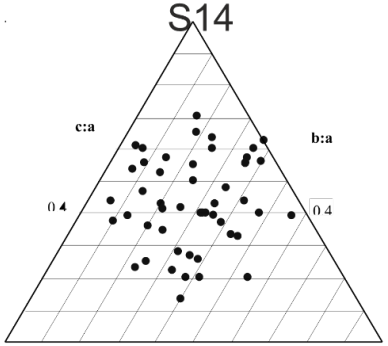

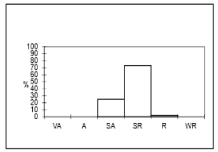

C40	47
RA	0
RWR	**2.00**
AvR	**2.77**
% striated	62
% faceted	36

S15

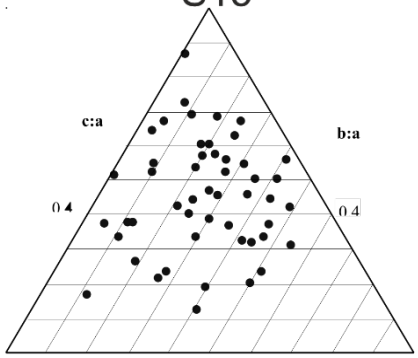

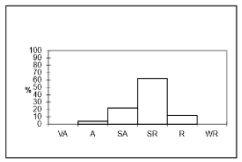

C40	42
RA	4
RWR	**12.00**
AvR	**2.82**
% striated	82
% faceted	24

S16

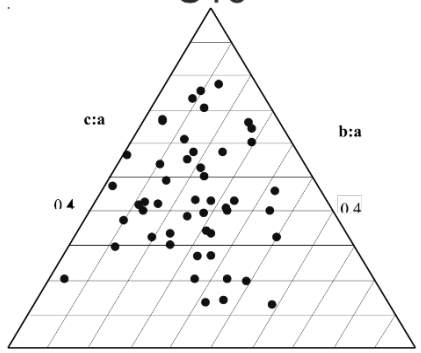

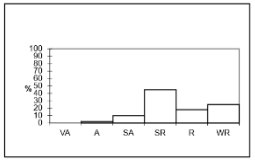

C40	45
RA	2
RWR	**43.00**
AvR	**3.50**
% striated	72
% faceted	10

S17

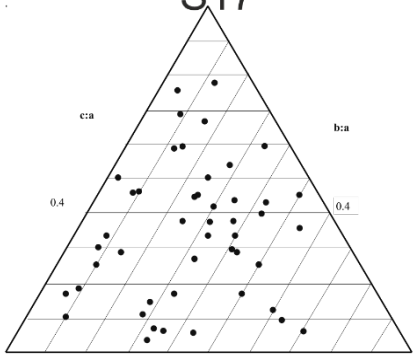

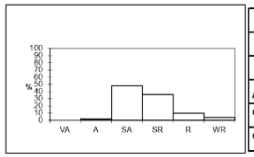

C40	40
RA	2
RWR	**14.00**
AvR	**2.66**
% striated	78
% faceted	26

S18

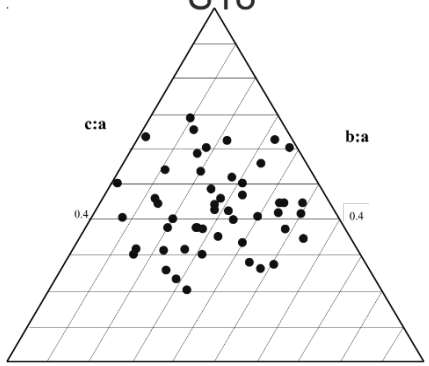

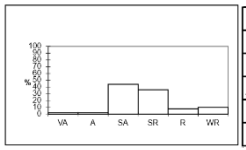

C40	42
RA	4
RWR	**18.00**
AvR	**2.82**
% striated	76
% faceted	22

S19

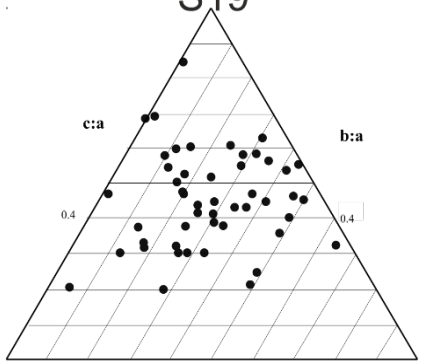

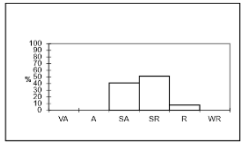

C40	3 37
RA	0
RWR	**8.00**
AvR	**2.67**
% striated	86
% faceted	36

S20

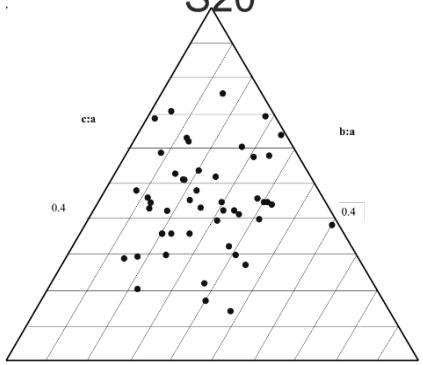

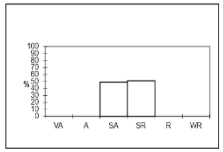

C40	35
RA	0
RWR	**0.00**
AvR	**2.51**
% striated	62
% faceted	28

S21

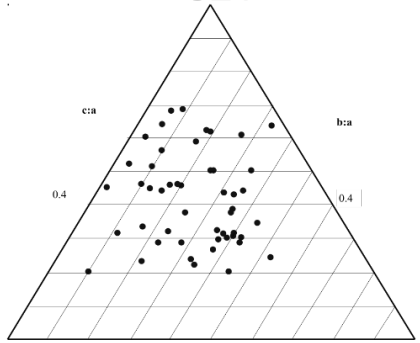

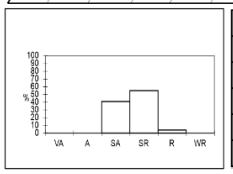

C40	49
RA	0
RWR	**4.00**
AvR	**2.63**
% striated	39
% faceted	26

S22

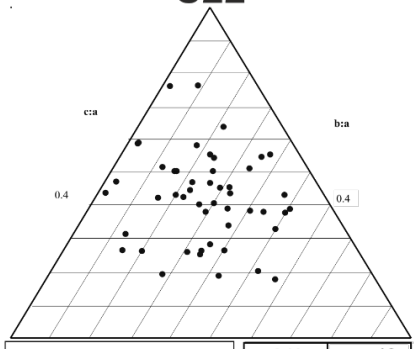

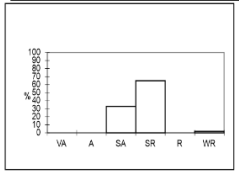

C40	43
RA	0
RWR	**2.00**
AvR	**2.71**
% striated	100
% faceted	62

S23

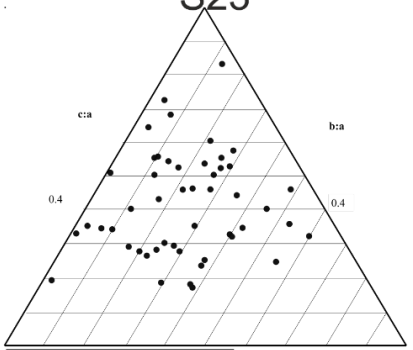

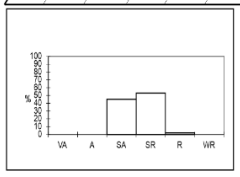

C40	53
RA	0
RWR	**2.00**
AvR	**2.57**
% striated	78
% faceted	66

S24

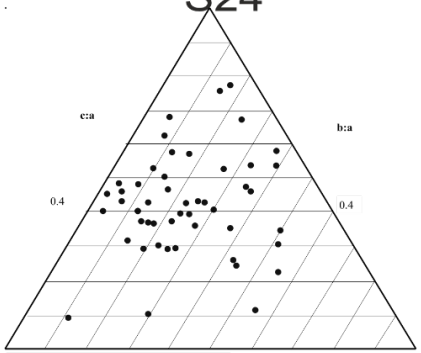

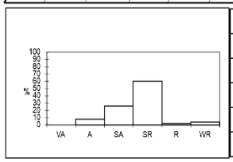

C40	48
RA	8
RWR	**6.00**
AvR	**2.68**
% striated	74
% faceted	58

S25

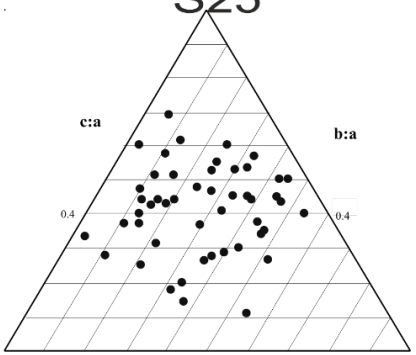

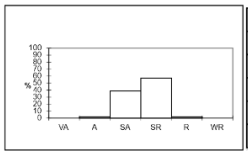

C40	43
RA	2
RWR	**2.00**
AvR	**2.59**
% striated	76
% faceted	62

S26

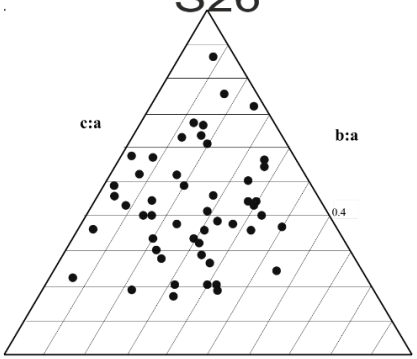

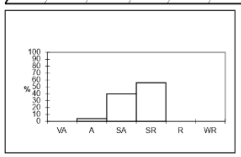

C40	50
RA	4
RWR	**0.00**
AvR	**2.52**
% striated	78
% faceted	56

S27

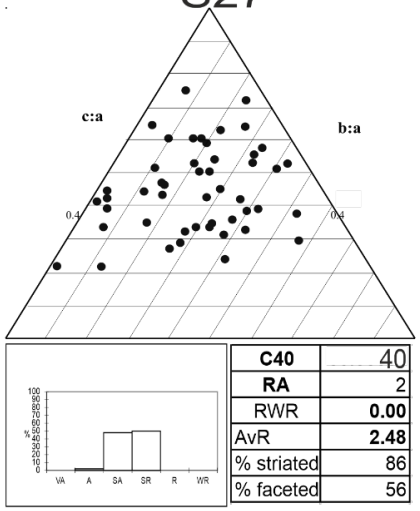

C40	40
RA	2
RWR	**0.00**
AvR	**2.48**
% striated	86
% faceted	56

S28

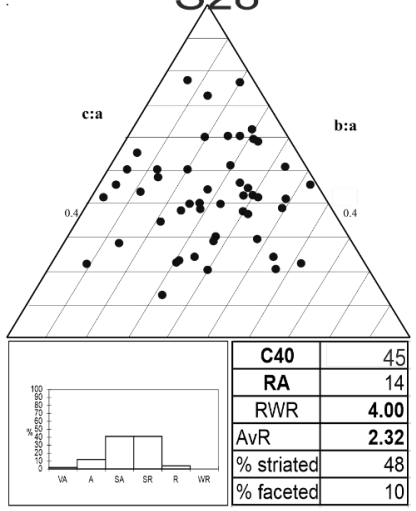

C40	45
RA	14
RWR	**4.00**
AvR	**2.32**
% striated	48
% faceted	10

S29

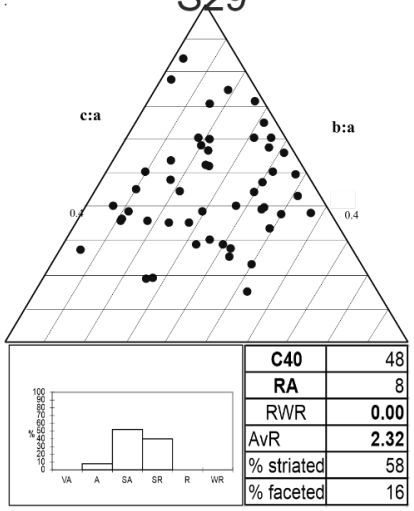

C40	48
RA	8
RWR	**0.00**
AvR	**2.32**
% striated	58
% faceted	16

S30

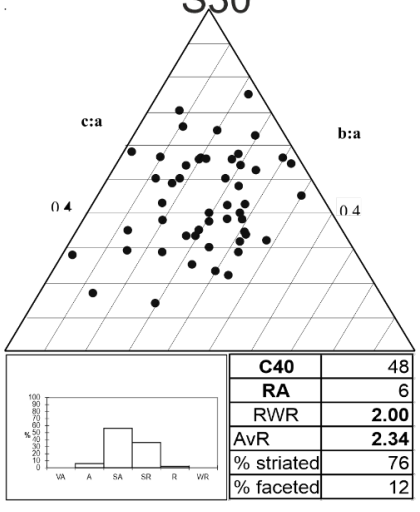

C40	48
RA	6
RWR	**2.00**
AvR	**2.34**
% striated	76
% faceted	12

S31

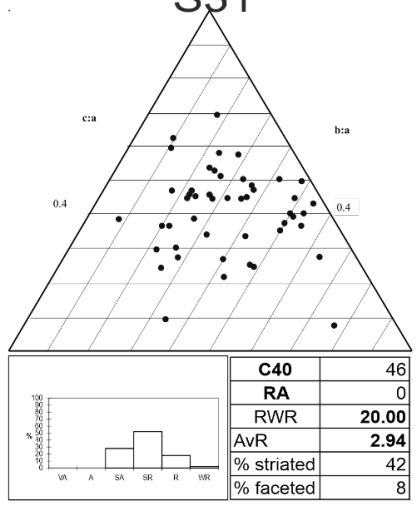

C40	46
RA	0
RWR	**20.00**
AvR	**2.94**
% striated	42
% faceted	8

S32

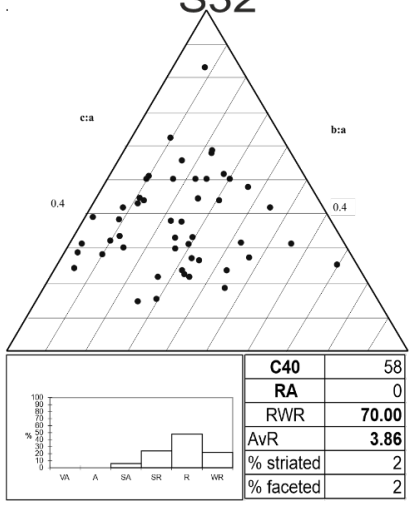

C40	58
RA	0
RWR	**70.00**
AvR	**3.86**
% striated	2
% faceted	2

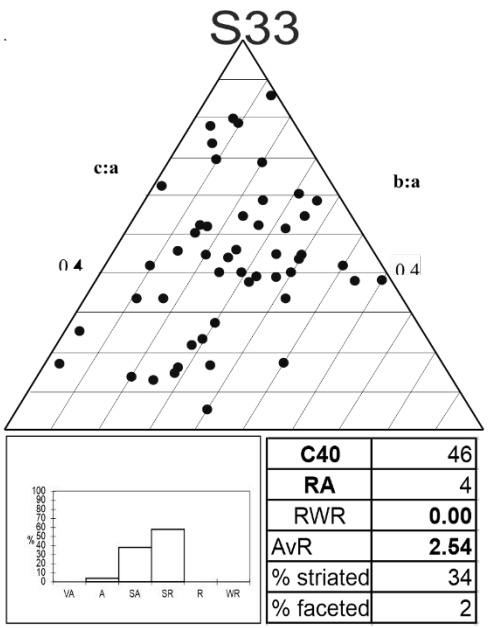

C40	46
RA	4
RWR	**0.00**
AvR	**2.54**
% striated	34
% faceted	2

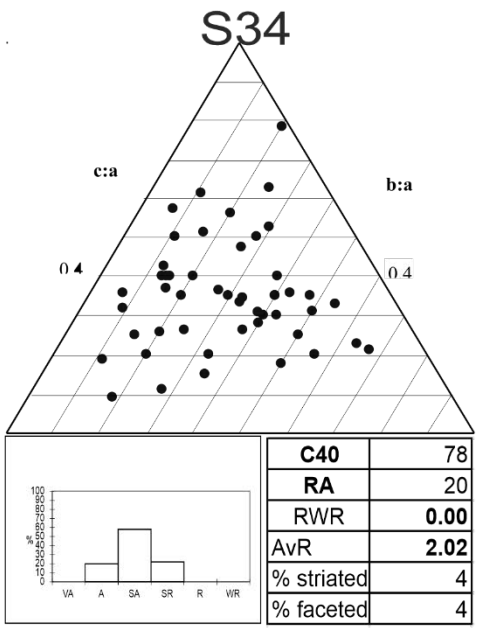

C40	78
RA	20
RWR	**0.00**
AvR	**2.02**
% striated	4
% faceted	4

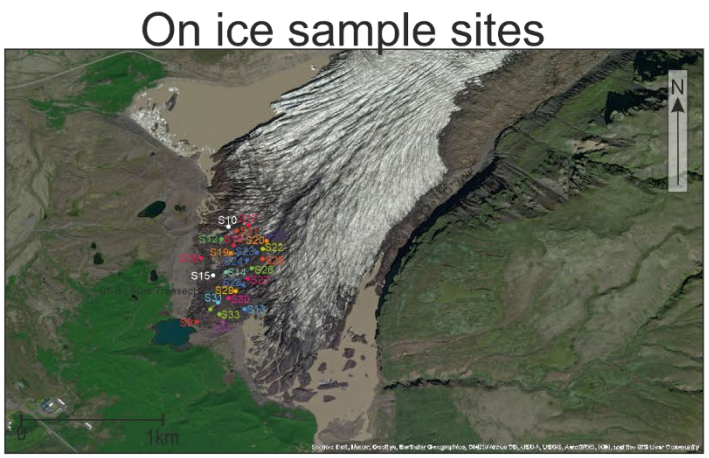

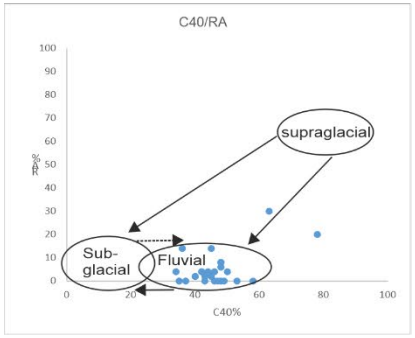

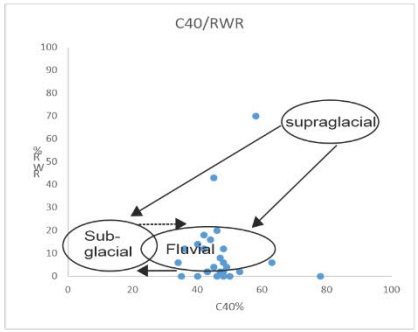

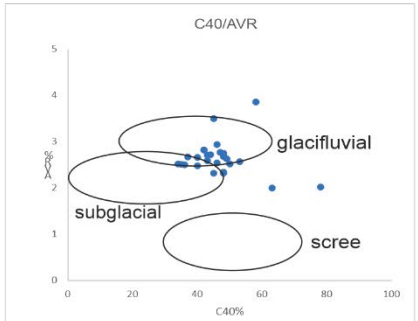

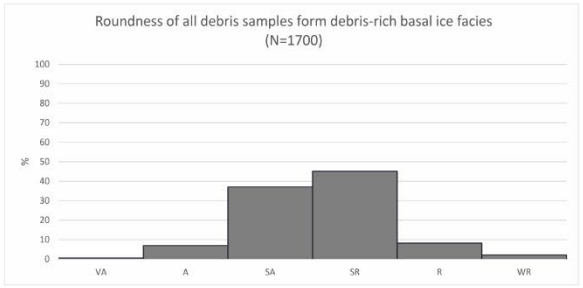

7.10 Appendix 10 Debris samples of a 50m transect on ice at Svínafellsjökull

S1

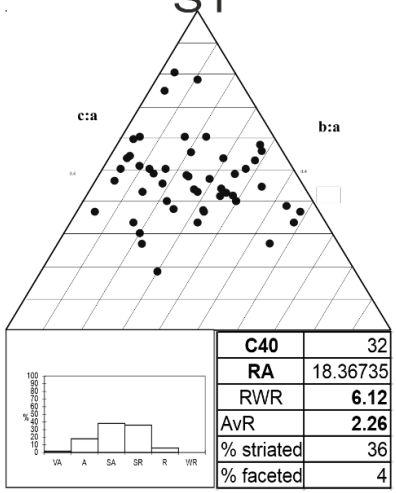

C40	32
RA	18.36735
RWR	**6.12**
AvR	**2.26**
% striated	36
% faceted	4

S2

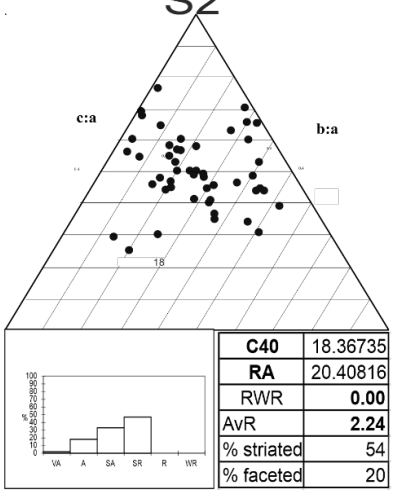

C40	18.36735
RA	20.40816
RWR	**0.00**
AvR	**2.24**
% striated	54
% faceted	20

S3

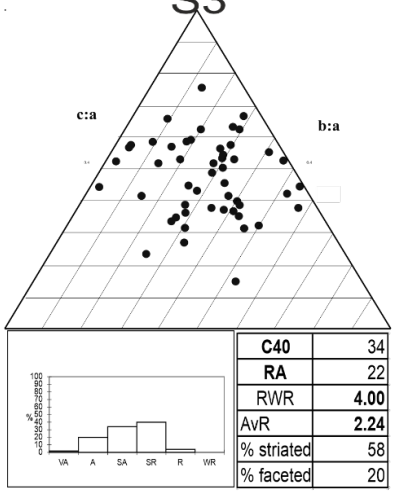

C40	34
RA	22
RWR	**4.00**
AvR	**2.24**
% striated	58
% faceted	20

S4

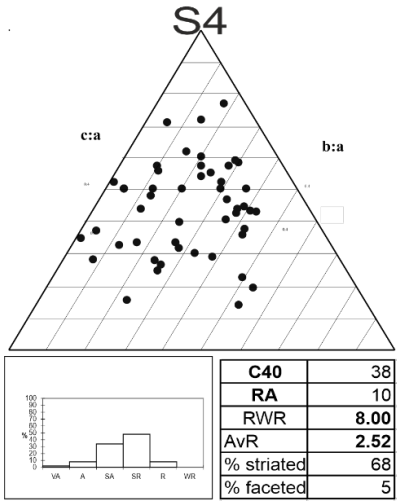

C40	38
RA	10
RWR	**8.00**
AvR	**2.52**
% striated	68
% faceted	5

S5

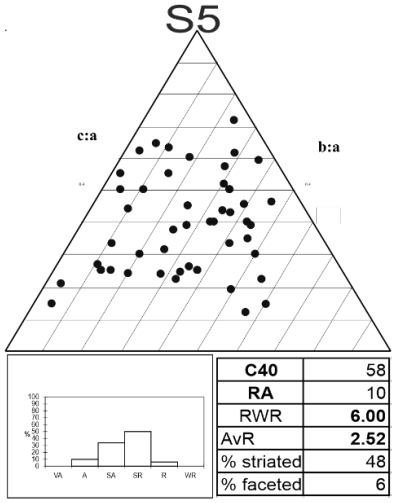

C40	58
RA	10
RWR	**6.00**
AvR	**2.52**
% striated	48
% faceted	6

S6

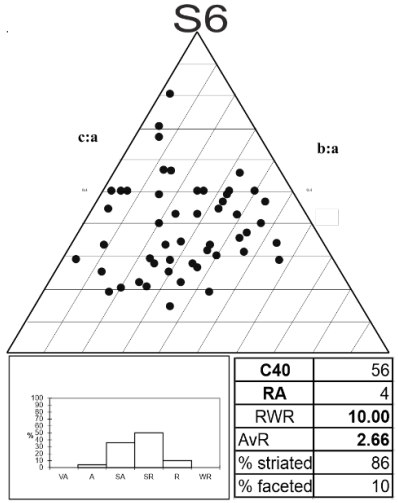

C40	56
RA	4
RWR	**10.00**
AvR	**2.66**
% striated	86
% faceted	10

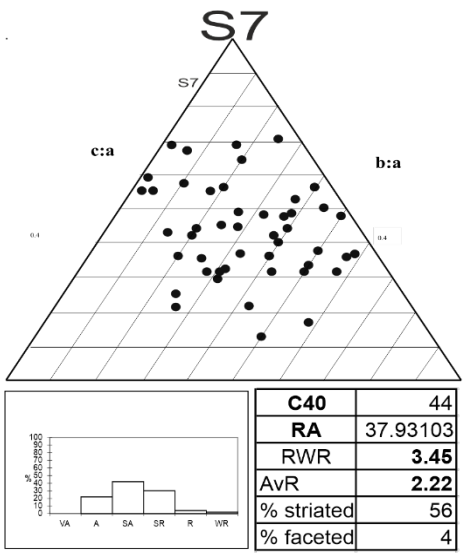

C40	44
RA	37.93103
RWR	**3.45**
AvR	**2.22**
% striated	56
% faceted	4

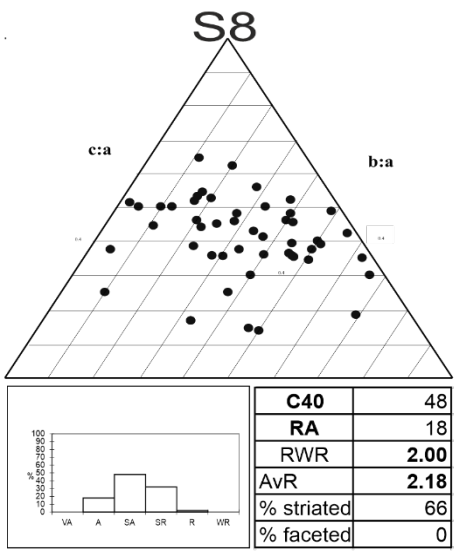

C40	48
RA	18
RWR	**2.00**
AvR	**2.18**
% striated	66
% faceted	0

On ice 50m transect

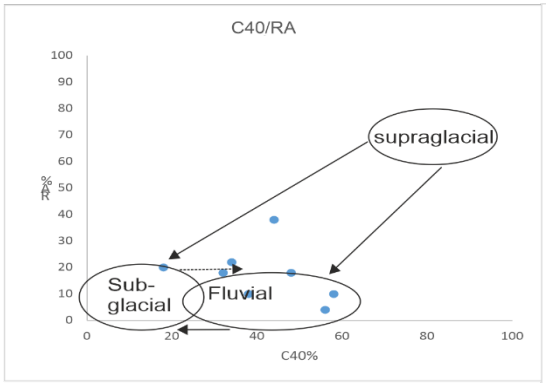

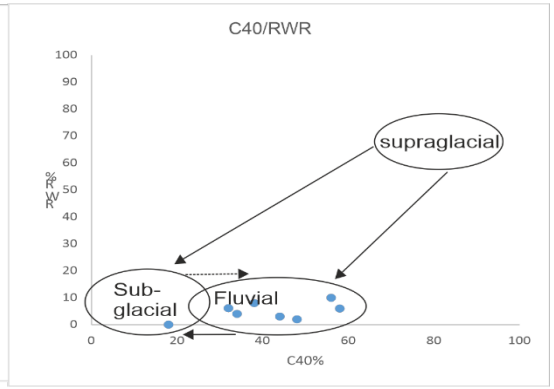

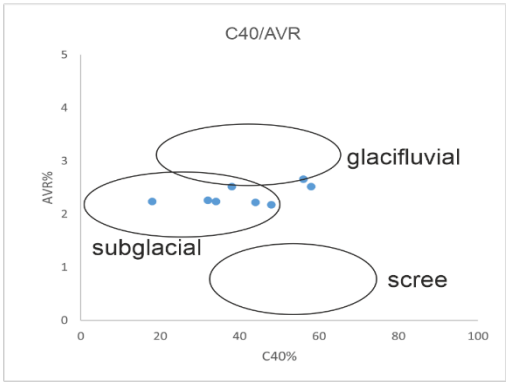

7.11 Appendix 11 Debris samples on marginal sediments at Svínafellsjökull

SM1

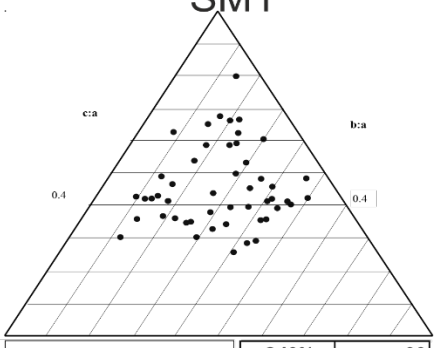

C40%	38
RA%	2
RWR%	8.00
AvR	2.62
% striated	32
% faceted	11

SM2

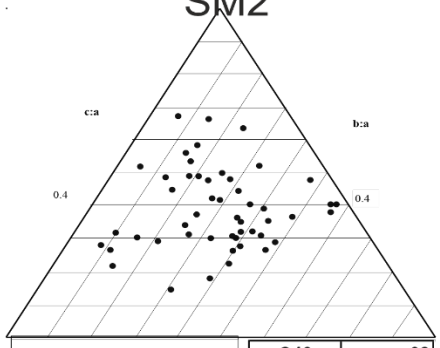

C40	62
RA	2
RWR	4.00
AvR	2.50
% striated	94
% faceted	24

SM3

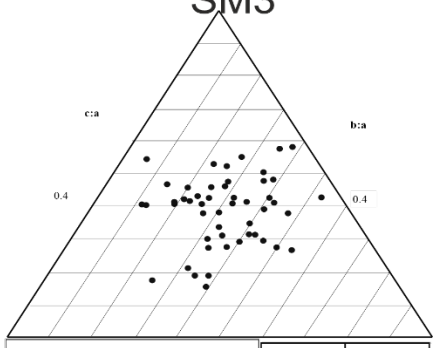

C40	44
RA	2
RWR	10.00
AvR	2.48
% striated	58
% faceted	6

SM4

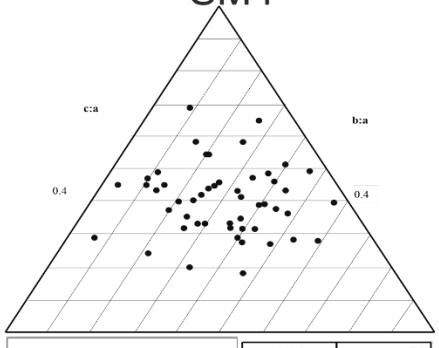

C40	52
RA	0
RWR	4.00
AvR	2.56
% striated	74
% faceted	24

SM5

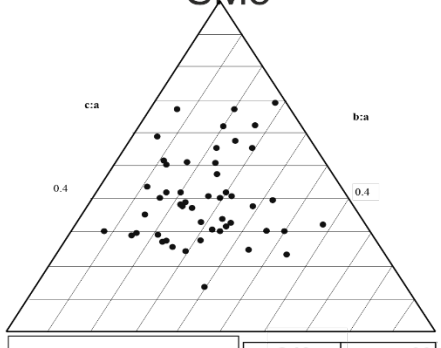

C40	60
RA	2
RWR	6.00
AvR	2.50
% striated	62
% faceted	36

SM6

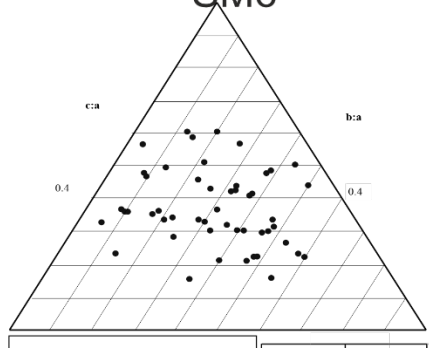

C40	60
RA	2
RWR	2.00
AvR	2.30
% striated	86
% faceted	32

SM7

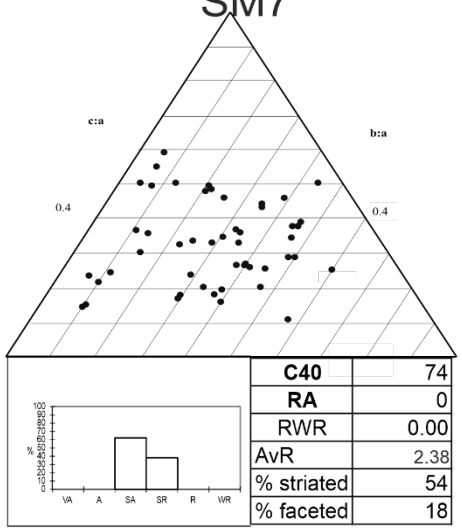

C40	74
RA	0
RWR	0.00
AvR	2.38
% striated	54
% faceted	18

SM8

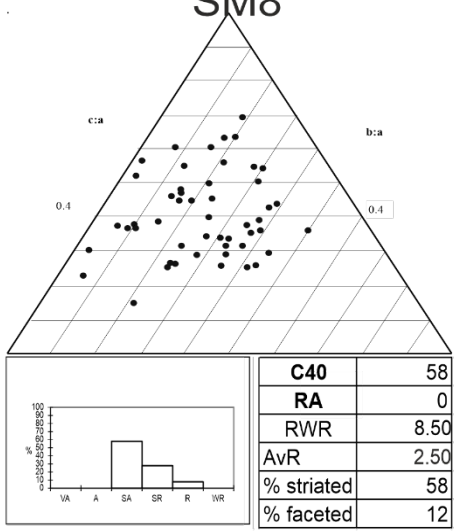

C40	58
RA	0
RWR	8.50
AvR	2.50
% striated	58
% faceted	12

SM9

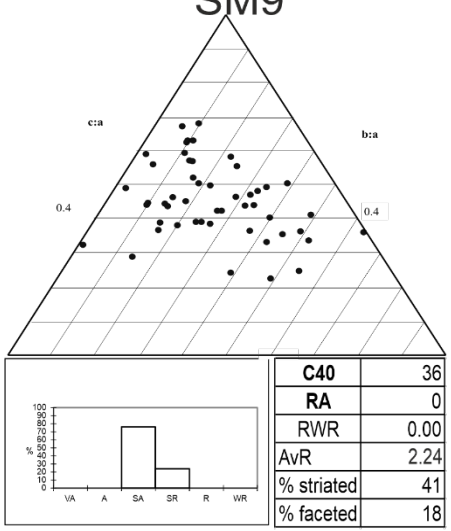

C40	36
RA	0
RWR	0.00
AvR	2.24
% striated	41
% faceted	18

SM10

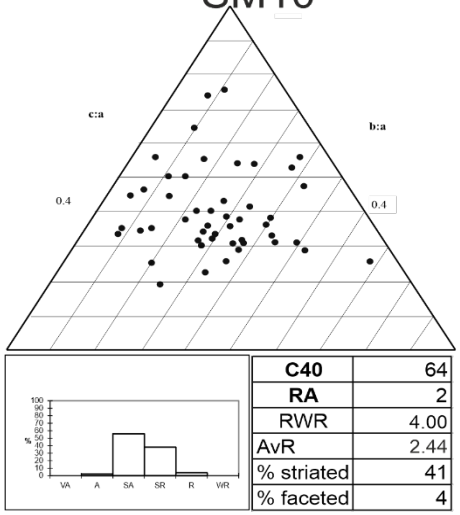

C40	64
RA	2
RWR	4.00
AvR	2.44
% striated	41
% faceted	4

SM11

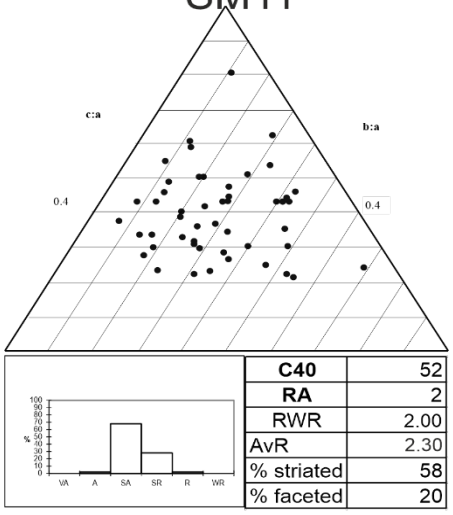

C40	52
RA	2
RWR	2.00
AvR	2.30
% striated	58
% faceted	20

SM12

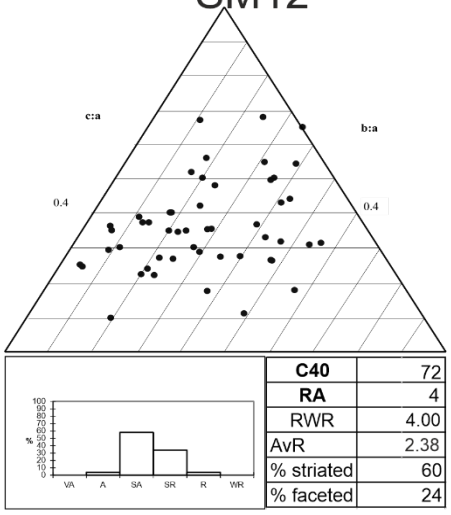

C40	72
RA	4
RWR	4.00
AvR	2.38
% striated	60
% faceted	24

SM13

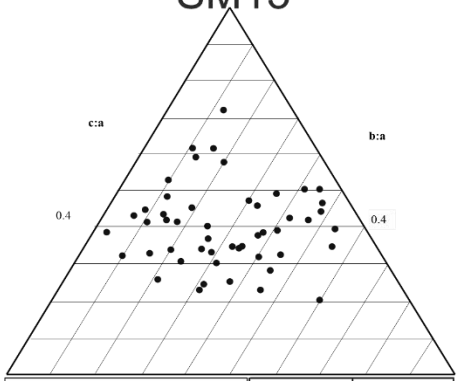

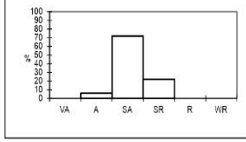

C40	54
RA	6
RWR	0.00
AvR	2.16
% striated	62
% faceted	18

SM14

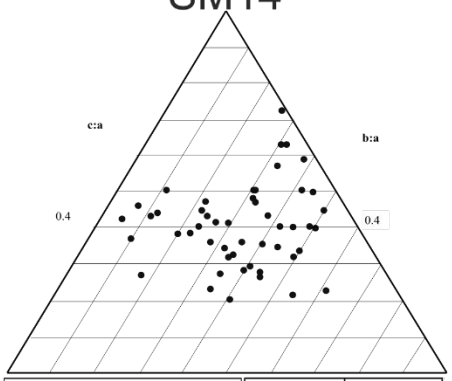

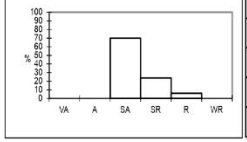

C40	54
RA	0
RWR	6.00
AvR	2.36
% striated	64
% faceted	24

Contemporary sub-marginal push moraines

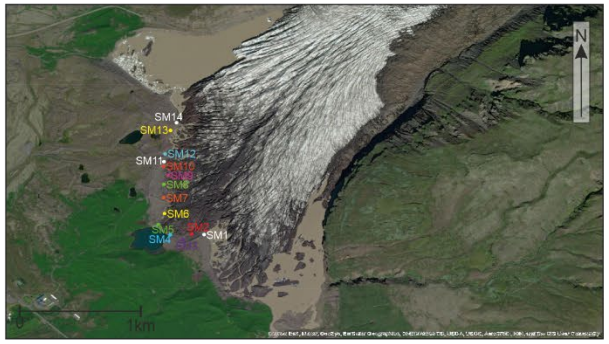

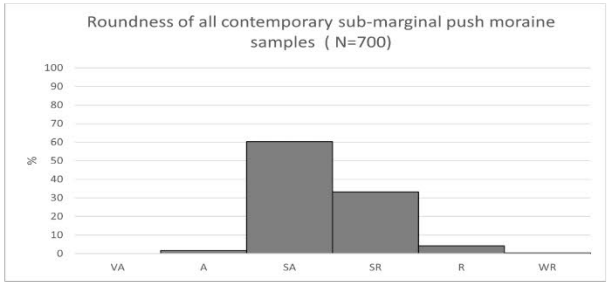

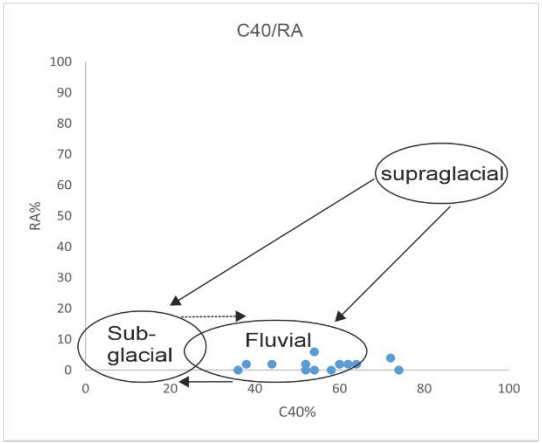

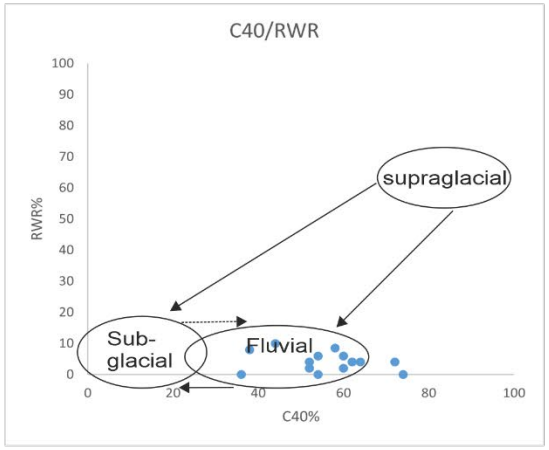

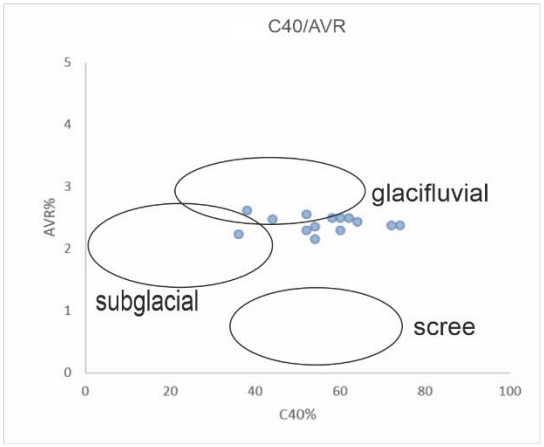

7.12 Appendix 12 Geomorphological map of Svínafellsjökull

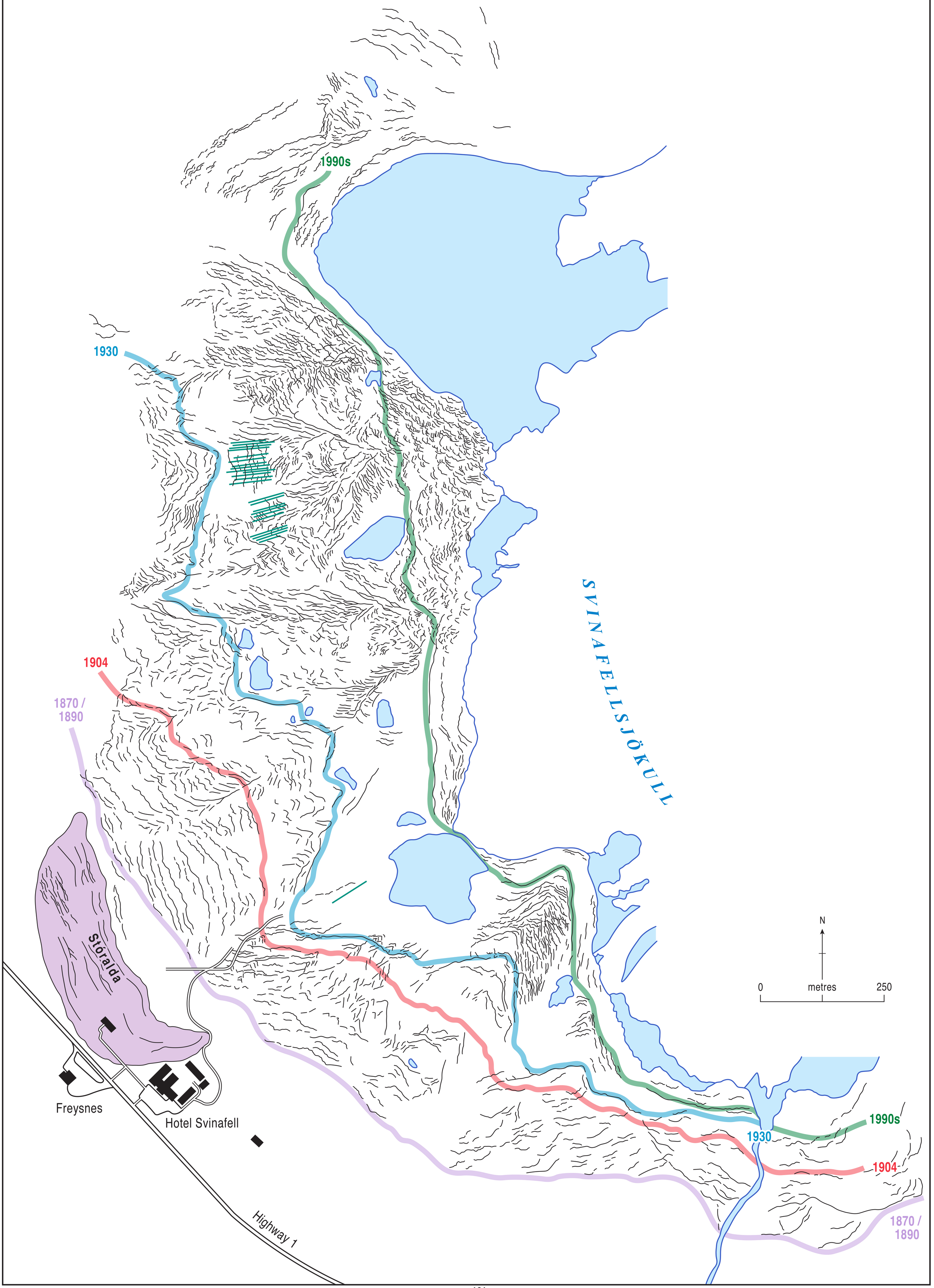

8 References

Allen, C.R., Kamb, W.B., Meier, M. F., Sharp, R. P. (1960). Structure of the Lower Blue Glacier, Washington. *Journal of Geology*, 68, 601–625.

Alley, N.F. and Frakes, L.A. (2003). First known cretaceous glaciation: Livingston tillite member of the cadna-owie formation, South Australia. *Australian Journal of Earth Sciences*, *50*(2), 139-144.

Alley, R.B., Cuffey, K.M., Evenson, E.B., Strasser, J.C., Lawson, D.E., Larson, G.J. (1997). How glaciers entrain and transport basal sediment: physical constraints. *Quaternary Science Reviews*, 16, 1017-1038.

Anderson, R.S. (2000). A model of ablation-dominated medial moraines and the generation of debris-mantled glacier snouts. *Journal of Glaciology* 46, 459–469.

Appleby, J.R., Brook, M.S., Vale, S.S., MacDonald-Creevey, A.M. (2010). Structural glaciology of a temperate maritime glacier: Lower Fox Glacier, New Zealand. *Geografiska Annaler*, Series A, 92, 451-467.

Aylsworth, J.M. and Shilts, W.W. (1989). Bedforms of the Keewatin ice sheet, Canada. *Sedimentary Geology*, 62, 407-428.

Ballantyne, C.K. (1982). Aggregate clast form characteristics of deposits at the margins of four glaciers in the Jotunheimen Massif, Norway. *Norsk Geografisk Tidsskrift,* 36,103–113.

Barr, I., Dokukin, M., Kougkoulos, I., Livingstone, S., Lovell, H., Małecki, J., Muraviev, A. (2018). Using Arctic DEM to Analyse the Dimensions and Dynamics of Debris-Covered Glaciers in Kamchatka, Russia. *Geosciences,* 2018, 8, 216.

Beedle, M.J., Menounos, B., Luckman, B.H., Wheate, R. (2009). Annual push moraines as climate proxy. *Geophysical Research Letters,* 36, L20501. http://dx.doi.org/10.1029/ 2009GL039533.

Benediktsson, I. O., Möller, P., Ingölfsson, O., Van der Meer,J. J. M., Kjær, K. H., Krüger, J. (2008). Instantaneous end moraine and sediment wedge formation during the 1890 glacier surge of Brúarjökull, Iceland. *Quaternary Science Reviews*, 27, 209–234.

Benn, D.I. (1989). Debris transport by Loch Lomond Readvance glaciers in northern Scotland, basin form and the within-valley asymmetry of lateral moraines. *Journal of Quaternary Science* 4, 243–254.

Benn, D.I. (1992). The genesis and significance of 'hummocky moraine': evidence from the Isle of Skye, Scotland. *Quaternary Science Reviews,* 11 781–799.

Benn, D.I. (1995). Fabric signature of subglacial till deformation, Breidamerkurjökull, Iceland. *Sedimentology*, *42*, 735-747.

Benn D.I. (2004). Clast morphology. In A Practical Guide to the Study of Glacial Sediments, Evans D.J.A, Benn D.I (eds). Arnold, London; 78–92.

Benn, D.I. (2007). Clast form analysis. In Encyclopedia of Quaternary Science, Elias SA (ed). *Elsevier*, Amsterdam, 904–909.

Benn, D.I., and Ballantyne, C.K. (1993). The description and representation of particle shape. *Earth Surface Processes and Landforms,* 18, 665–672.

Benn, D.I., and Ballantyne, C.K. (1994). Reconstructing the transport history of glacigenic sediments: a new approach based on the co-variance of clast shape indices. *Sedimentary Geology*, 91, 215–227.

Benn, D.I., and Evans, D.J.A. (2010). Glaciers and Glaciation. Routledge, London.

Benn, D. I., and Lukas, S. (2006). Younger Dryas glacial landsystems in northwest Scotland: an assessment of modern analogues and palaeoclimatic implications. *Quaternary Science Reviews* 25, 2390-2408.

Benn, D.I., and Lukas, S. (2021). Clast shape. In: Evans, D.J.A., Benn, D.I. (Eds.), A Practical Guide to the Study of Glacial Landforms, Second edition. QRA, London, 107–124.

Bennett, G.L.B., Evans, D.J.A., Carbonneau, P., Twigg, D.R. (2010). Evolution of a debris charged glacier landsystem, Kviárjökull, Iceland. *Journal of Maps*, 40-67.

Bennett, M. R., and Evans, D.J.A. (2012). Glacier retreat and landform production on an overdeepened glacier foreland: the debris-charged glacial landsystem at Kviárjökull, Iceland. *Earth Surface Processes and Landforms* 37, 1584–1602. DOI: 10.1002/esp.3259.

Bennett, M. R., Huddart, D., and Waller, R. I. (2000). Glaciofluvial crevasse and conduit fills as indicators of supraglacial dewatering during a surge, Skeiðarárjökull, Iceland. *Journal of Glaciology*, 46, 25–34.

Bennett, M.R., Hambrey, M.J., and Huddart, D. (1997). Modification of clast shape in high-arctic glacial environments. *Journal of Sedimentary Research,* 67, 550–559.

Bennett, M.R., Hambrey, M.J., Huddart, D., Ghienne, J.F. (1996). The formation of geometrical ridge networks ('crevasses-fill' ridges), Kongsvegen, Svalbard. *Journal of Quaternary Science* 11, 430–438.

Ben-Yehoshua, D., Sæmundsson, Þ., Helgason, J.K., Belart, J.M., Sigurðsson, J.V. and Erlingsson, S. (2022). Paraglacial exposure and collapse of glacial sediment: The 2013 landslide onto Svínafellsjökull, southeast Iceland. *Earth Surface Processes and Landforms*, 47, 2612-2627.

Björnsson, H., and Pálsson, F. (2008). Icelandic glaciers. *Jokull,* 58, 365–386.

Björnsson, H., Pálsson, F., Guðmundsson, S., Magnússon, E., Aðalsgeirsdóttir, G., Jóhannesson, T., Thorsteinsson, T. (2013). Contribution of Icelandic ice caps to sea level rise: Trends and variability since the Little Ice Age. *Geophysical Research Letters*, 40, 1546–1550.

Boston, C. M. (2012). A glacial geomorphological map of the Monadhliath Mountains, Central Scottish Highlands. *Journal of Maps*, 8,4, 437–444. doi:10.1080/17445647. 2012.743865.

Boulton, G.S. (1967). The development of a complex supraglacial moraine at the margin of Sorbreen, Ny Friesland, Vestspitzbergen. *Journal of Glaciology* 6, 717–736.

Boulton, G.S. (1978). Boulder shapes and grain-size distributions of debris as indicators of transport paths through a glacier and till genesis. *Sedimentology* 25,773–799.

Boulton, G. S. (1986a). A paradigm shift in glaciology? Nature, 322, 18.

Boulton, G.S. (1986b). Push moraines and glacier contact fans in marine and terrestrial environments. Sedimentology 33, 677-698.

Boulton, G.S. (1996). Theory of glacial erosion, transport and deposition as a consequence of subglacial sediment deformation. *Journal of glaciology* 42, 43-62.

Boulton, G. S. and Eyles, N. (1979). Sedimentation by valley glaciers: a model and genetic classification, In Schluchter, C., (ed.) *Moraines and Varves,* vol. 33, Balkema, Rotterdam, 11–23.

Boulton, G.S. and Hindmarsh, R.C.A. (1987). Sediment deformation beneath glaciers: rheology and geological consequences. *Journal of Geophysical Research: Solid Earth*, *92*, 9059-9082.

Boulton, G.S., Dobbie, K.E. and Zatsepin, S. (2001). Sediment deformation beneath glaciers and its coupling to the subglacial hydraulic system. *Quaternary International*, *86*, 3-28.

Bradwell, T. (2004). Annual moraines and summer temperatures at Lambatungnajökull, Iceland. *Arctic, Antarctic and Alpine Research* 36, 502–508.

Bradwell, T., Sigurðsson, O., and Everest, J. (2013). Recent, very rapid retreat of a temperate glacier in SE Iceland. *Boreas*, 42,4, 959–973. doi:10.1111/bor.12014.

Brook, M.S. and Lukas, S. (2012). A revised approach to discriminating sediment transport histories in glacigenic sediments in a temperate alpine environment: a case study from Fox Glacier, New Zealand. *Earth Surface Processes and Landforms*, *37*, 895-900.

Brown, V. H., Evans, D. J. A., and Evans, I. S. (2011). The glacial geomorphology and surficial geology of the South-West English Lake district. *Journal of Maps*, 7,1, 221–243. doi:10.4113/jom.2011.1187.

Brynjólfsson, S., Schomacker, A., and Ingólfsson, Ó. (2014). Geomorphology and the little ice age extent of the Drangajökull ice cap, NW Iceland, with focus on its three surge-type outlets. *Geomorphology*.

Chandler, B. M. P., Evans, D. J. A., and Roberts, D. H. (2016 a). Recent retreat at a temperate Icelandic glacier in the context of the last ~80 years of climate change in the North Atlantic region. *Arktos* 2, 24, doi:10.1007/s41063-016-0024-1.

Chandler, B.M., Boston, C.M., Lukas, S., Lovell, H. (2021). Re-interpretation of 'hummocky moraine'in the Gaick, Scotland, as erosional remnants: Implications for palaeoglacier dynamics. *Proceedings of the Geologists' Association*, *132*, 506-524.

Chandler, B.M.P., Evans, D.J.A., Roberts, D.H., Ewertowski, M.W., Clayton, A.I. (2015). Glacial geomorphology of the Skálafellsjökull foreland, Iceland: A case study of 'annual' moraines. *Journal of Maps*, doi: http://dx.doi.org/10.1080/17445647.2015.1096216.

Chandler, B.M.P., Evans, D., J., Roberts, D., H., Ewertowski, M.W., Clayton, A., I. (2016 b). Glacial geomorphology of the Skálafellsjökull foreland, Iceland: A case study of 'annual' moraines. *Journal of Maps*, 12,5, 904-916, DOI: 10.1080/17445647.2015.1096216.

Chandler, B.M.P., Evans, D.J.A., Chandler, S.J.P., Ewertowski, M.W., Lovell, H., Roberts, D.H., Schaefer, M. (2020 b). The glacial landsystem of Fjallsjökull, Iceland: spatial and temporal evolution of process-form regimes at an active temperate glacier. *Geografiska Annaler*.

Chandler, B.M.P., Chandler, S.J.P., Evans, D.J.A., Ewertowski, M.W., Lovell, H., Roberts, D.H., Schaefer, M., Tomczyk, A.M. (2020a). Sub-annual moraine formation at an active temperate Icelandic glacier. *Earth Surface Processes and Landforms*.

Chandler, B.M.P., Lovell, H., Boston, C.M., Lukas, S., Barr, I.D., Benediktsson, Í.Ö., Benn, D.I., Clark, C.D., Darvill, C.M., Evans, D.J.A., Ewertowski, M.W., Loibl, D., Margold, M., Otto, J.-C., Roberts, D.H., Stokes, C.R., Storrar, R.D., Stroeven, A.P. (2018). Glacial geomorphological mapping: a review of approaches and frameworks for best practice. *Earth-Science Reviews,* 185, 806–846.

Christoffersen, P. and Tulaczyk, S. (2003). Signature of palaeo-ice-stream stagnation: Till consolidation induced by basal freeze-on. *Boreas*, *32*,114-129.

Christoffersen, P., Tulaczyk, S., Carsey, F.D. and Behar, A.E., (2006). A quantitative framework for interpretation of basal ice facies formed by ice accretion over subglacial sediment. *Journal of Geophysical Research: Earth Surface*, *111*.

Clark, P.U. (1987). Subglacial sediment dispersal and till composition. *The Journal of Geology*, *95*, 527-541.

Colgan, W., Rajaram, H., Abdalati, W., McCutchan., Mottram, R., Moussavi, M. S., Grigsby, S. (2016). Glacier crevasses: Observations, models, and mass balance implications. *Reviews of Geophysics*, 54, doi:10.1002/2015RG000504.

Cook, A., Vaughan, D., Luckman, A., and Murray, T. (2014). A new Antarctic Peninsula glacier basin inventory and observed area changes since the 1940s. *Antarctic Science*, 26, 614-624. doi:10.1017/S0954102014000200.

Cook, S.J., Graham, D.J., Swift, D.A., Midgley, N.G., Adam, W.G. (2011a). Sedimentary signatures of basal ice formation and their preservation in ice-marginal sediments. *Geomorphology*, *125*, 122-131.

Cook, S.J., Knight, P.G., Waller, R.I., Robinson, Z.P., Adam, W.G. (2007). The geography of basal ice and its relationship to glaciohydraulic supercooling: Svínafellsjökull, southeast Iceland. *Quaternary Science Reviews,* 26, 2309-2315.

Cook, S. J., Robinson, Z. P., Fairchild, I. J., Knight, P. G., Waller, R. I., Boomer, I. (2009). Role of glaciohydraulic supercooling in the formation of stratified facies basal ice: Svínafellsjökull and Skaftafellsjökull, southeast Iceland. *Boreas*, 10.1111/j.1502-3885.2009.00112. x. ISSN 0300-9483.

Cook, S.J., Robinson, Z.P., Fairchild, I.J., Knight, P.G., Waller, R.I., Boomer, I. (2010). Role of glaciohydraulic supercooling in the formation of stratified facies basal ice: Svínafellsjökull and Skaftafellsjokull, southeast Iceland. *Boreas*, 39,1, 24–38.

Cook, S.J., Swift, D.A. (2012). Subglacial basins: their origin and importance in glacial systems and landscapes. *Earth Science Reviews*, 115, 332–372.

Cook, S. J., Waller, R. I. and Knight, P. G. (2006). Glaciohydraulic supercooling: The process and its significance. *Progress in Physical Geography,* 30, 577–588.

Cook.S.J., Swift.D.A., Graham.D.J., Midgley.N.G. (2011b). Origin and significance of 'dispersed facies' basal ice: Svınafellsjokull, Iceland. *Journal of Glaciology*, Vol. 57 No. 204.

Cuffey, K.M. and Paterson, W.S.B. (2010). The physics of glaciers. Academic Press.

Dąbski, M., Fabiszewski, B. and Pękalska, A. (1998). Marginal zone of Flajòkull (Iceland). Initial results of research. *Miscellanea Geographica. Regional Studies on Development*, *8*, 47-54.

Darvill, C. M., Stokes, C. R., Bentley, M. J., Lovell, H. (2014). A glacial geomorphological map of the southernmost ice lobes of Patagonia: The Bahía Inútil – San Sebastián, Magellan, Otway, Skyring and Río Gallegos lobes*. Journal of Maps,* 10,3, 500–520. doi:10.1080/ 17445647.2014.890134

Darvill, C.M., Stokes, C.R., Bentley, M.J., Evans, D.J. and Lovell, H. (2017). Dynamics of former ice lobes of the southernmost Patagonian Ice Sheet based on a glacial landsystems approach. Journal of Quaternary Science, 32,857-876.

De Angelis, H. and Skvarca, P. (2003). Glacier surge after ice shelf collapse. *Science*, 299,5612, 1560–1562. *German and Austrian Alpine Club,* 1,1, 1–112.

Deline, P. and Orombelli, G. (2005). Glacier fluctuations in the western Alps during the Neoglacial, as indicated by the Miage morainic amphitheatre (Mont Blanc massif, Italy). *Boreas*, 34, 456-467.

Dell, R., Carr, R., Phillips, E., Russell, A.J. (2019). Response of glacier flow and structure to proglacial lake development and climate at Fjallsjökull, south-east Iceland. *Journal of Glaciology,* 65, 321–336.

Derbyshire, E., Cooper, R.G., Page, L.W.F. (1979). Recent Movements on the Cliff at St Mary's Bay, Brixham, Devon. *Geographical Journal*,86-96.

Dredge, L.A. and Cowan, W.R. (1989). Quaternary geology of the southwestern Canadian Shield.

Drewry, D.J. (1972). A quantitative assessment of dirt-cone dynamics. *Journal of Glaciology* 11,63, 431–446.

Dugmore, A.J. (1987). Holocene glacier fluctuations around Eyjafjallajokull, south Iceland: a tephrochronological study. University of Aberdeen (United Kingdom).

Dyke, A.S., Morris, T.F., Green, D.E.C. and England, J. (1992). Quaternary geology of Prince of Wales Island, Arctic Canada. Geological Survey of Canada Memoir 433.

Egholm, D.L., Pedersen, V.K., Knudsen, M.F., Larsen, N.K. (2012). Coupling the flow of ice, water, and sediment in a glacial landscape evolution model. *Geomorphology,* 141-142, 47-66.

Einarsson, B. and Sigurðsson, O. (2015). Glacier changes, 1930-1970, 1970-1995, 1995-2013 and 2013-2014. *Jökull,* 65, 91-96.

Ensminger, S.L., Alley, R.B., Evenson, E.B., Lawson, D.E., Larson, G.J. (2001). Basal crevasse-fill origin of laminated debris bands at Matanuska Glacier, Alaska, USA. *Journal of Glaciology*, 47, 412-422.

Etienne, J.L., Glasser, N.F. and Hambrey, M.J. (2003). Proglacial sediment—landform associations of a polythermal glacier: Storglaciären, Northern Sweden. *Geografiska Annaler: Series A, Physical Geography*, *85*, 149-164.

Evans, D. J. A. (1989). The nature of glacitectonic structures and sediments at sub-polar glacier margins, northwest Ellesmere Island, Canada. *Geografiska Annaler: Series A, Physical Geography*, *71*,113-123.

Evans, D. J. A. (1999). Glacial debris transport and moraine deposition: a case study of the Jardalen cirque complex, SognogFjordane, western Norway. *Period for geomorphology,* 43, 203–234.

Evans, D. J. A. (2003). Glacial Landsystems. Arnold: London.

Evans, D. J. A. (2009). Controlled moraines: Origins, characteristics and paleoglaciological implications. *Quaternary Science Reviews* 28, 183–208.

Evans, D. J. A. (2010). Controlled moraine development and debris transport pathways in polythermal plateau icefields: examples from Tungnafellsjökull, Iceland. *Earth Surface Processes and Landforms* 35, 1430–1444.

Evans, D. J. A. (2013). The glacial and periglacial research- geomorphology and retreating glaciers. In Shroder, J., Giardino, R., Harbor, J. (eds.): Treatise on Geomorphology, Volume 8, *Glacial and Periglacial Geomorphology*, 460–478.

Evans, D. J. A. (2018). Till: a glacial process sedimentology. Chichester, Wiley-Blackwell.

Evans, D.J.A. (2000). A gravel outwash/deformation till Continuum, Skalafellsjokull, Iceland. *Geografiska Annaler*, 82, 499-512. https://doi.org/10.1111/j.04353676.2000.00137.x.

Evans, D. J. A., Archer, S. and Wilson, D.J.H. (1999a). A comparison of the lichenometric and Schmidt hammer dating techniques based on data from the proglacial areas of some Icelandic glaciers. *Quaternary Science Reviews*, 18, 13–41.

Evans, D. J. A., and Benn, D.I. (2014). A practical guide to the study of glacial sediments. Routledge.

Evans, D.J.A, and Ewertowski, M.W. (2018). The glacial landsystem of the Fláajökull north lobe. In Glacial Landsystems of Southeast Iceland – Quaternary Applications: Field Guide, Evans DJA (ed). Quaternary Research Association: London; 243–258.

Evans, D. J. A., Ewertowski, M., and Orton, C. (2015). Fláajökull (north lobe), Iceland: Active temperate piedmont lobe glacial landsystem. *Journal of Maps*, doi:10. 1080/17445647.2015.1073185.

Evans, D. J. A., Ewertowski, M., and Orton, C. (2016). Fláajökull (north lobe), Iceland: active temperate piedmont lobe glacial landsystem. *Journal of Maps*, 777-789, DOI: 10.1080/17445647.2015.1073185.

Evans, D. J. A., Ewertowski, M., Orton, C. (2017a). Skaftafellsjökull, Iceland: glacial geomorphology recording glacier recession since the Little Ice Age. *Journal of Maps*, 13,358–368.

Evans, D. J. A., Ewertowski, M.W., and Orton, C., (2017b). The glaciated valley landsystem of Morsárjökll, southeast Iceland. *Journal of Maps*, *13*, 909-920.

Evans, D. J. A., Ewertowski, M.W., and Orton, C. (2019). The glacial landsystem of Hoffellsjökull, SE Iceland: contrasting geomorphological signatures of active temperate glacier recession driven by ice lobe and bed morphology. *Geografiska Annaler*. 101:3, 249-276, DOI: 10.1080/04353676.2019.1631608.

Evans, D. J. A., Ewertowski, M.W., Orton, C., Graham, D.J. (2018a). The Glacial Geomorphology of the Ice Cap Piedmont Lobe Landsystem of East Mýrdalsjökull, Iceland. *Geosciences* 2018, 8, 194.

Evans, D. J. A., and Hiemstra, J. F. (2005). Till deposition by glacier submarginal, incremental thickening. *Earth Surface Processes and Landforms*, 30, 1633–1662.

Evans, D. J. A., Lemmen, D.S., and Rea, B.R. (1999b). Glacial landsystems of the southwest Laurentide Ice Sheet: modern Icelandic analogues. *Journal of Quaternary Science,* 14, 673–691.

Evans, D. J. A., and Orton, C. (2015). Heinabergsjökull and Skálafellsjökull, Iceland: Active temperate piedmont lobe and outwash head glacial landsystem. *Journal of Maps* 11, 415-431.

Evans, D. J. A. and Rea, B. (2003). Surging glacier landsystem, In EVANS, D. J. A., (ed.*) Glacial Land- systems*, Arnold, London, 259–288.

Evans, D. J. A., Shand, M., and Petrie, G. (2009). Maps of the snout and proglacial landforms of Fjallsjökull, Iceland (1945, 1965, 1998). *Scottish Geographical Journal*, 125, 304–320.

Evans, D. J. A. and Twigg, D. R. (2002). 'The active temperate glacial landsystem: a model based on Breiðamerkurjökull and Fjallsjökull, Iceland.', *Quaternary science reviews*, 21, 2143-2177.

Evans, D. J. A., Young, N. J. P., and Ó Cofaigh, C. (2014). Glacial geomorphology of terrestrial-terminating fast flow lobes/ice stream margins in the Southwest Laurentide ice sheet. *Geomorphology*, 204, 86–113. doi:10.1016/j.geomorph.2013.07.031.

Evans, D.J., Nelson, C.D. and Webb, C. (2010). An assessment of fluting and “till esker” formation on the foreland of Sandfellsjökull, Iceland. *Geomorphology*, *114*, 453-465.

Evans, D.J., Roberts, D.H., Hiemstra, J.F., Nye, K.M., Wright, H., Steer, A. (2018b). Submarginal debris transport and till formation in active temperate glacier systems: the southeast Iceland type locality. *Quaternary Science Reviews*, *195*, 72-108.

Evans, D.J.A., Phillips, E.R., Hiemstra, J.F., Auton, C.A. (2006). Subglacial till: formation, sedimentary characteristics, and classification. *Earth-Science Reviews*, *78*, 115-176.

Evenson, E.B., Lawson, D.E., Strasser, J.C., Larson, G.J., Alley, R.B., Ensminger, S.L., Stevenson, W.E. (1999a). Field evidence for the recognition of glaciohydrologic supercooling. *Special Paper of the Geological Society of America*, *337*, 23-35.

Everest, J., Bradwell, T., Jones, L., Hughes, L. (2017). The geomorphology of Svínafellsjökull and Virkisjökull-Falljökull glacier forelands, southeast Iceland. *Journal of Maps*, 13, 936-945, DOI: 10.1080/17445647.2017.1407272.

Ewertowski, M.W., Tomczyk, A.M., Evans, D.J., Roberts, D.H. and Ewertowski, W. (2019). Operational framework for rapid, very-high resolution mapping of glacial geomorphology using low-cost unmanned aerial vehicles and structure-from-motion approach. *Remote Sensing*, 11, 65.

Eyles, N. (1979). Facies of supraglacial sedimentation on Icelandic and Alpine temperate glaciers. *Canadian Journal of Earth Sciences.* 16, 1341-1361.

Eyles, N., Eyles, C.H. and Miall, A.D. (1983). Lithofacies types and vertical profile models; an alternative approach to the description and environmental interpretation of glacial diamict and diamictite sequences. *Sedimentology*, *30*, 393-410.

Eyles, N. and Rogerson, R.J. (1978). Sedimentology of medial moraines on Berendon Glacier, British Columbia, Canada: implications for debris transport in a glacierized basin. *Geological Society of America Bulletin*, *89*, 1688-1693.

Fountain, A.G., and Walder, J.S. (1998). Water flow through temperate glaciers. *Reviews of Geophysics,* 36, 299-328.

Fulton, I.M., Guion, P.D. and Jones, N.S. (1995). Application of sedimentology to the development and extraction of deep-mined coal. Geological Society, London, Special Publications, 82, 17-43.

Gardner, A. S., Fahnestock, M. A. and Scambos, T. A. (2019). ITS_LIVE Regional Glacier and Ice Sheet Surface Velocities. Data archived at National Snow and Ice Data Center; doi:10.5067/6II6VW8LLWJ7.

Gardner, A. S., Moholdt, G. Scambos, T. Fahnstock, M. Ligtenberg, S. van den Broeke, M. (2018). Increased West Antarctic and unchanged East Antarctic ice discharge over the last 7 years. *Cryosphere*, 12, 521–547, doi:10.5194/tc-12-521-2018.

Glasser, N.F., Bennett, M.R. and Huddart, D. (1999). Distribution of glaciofluvial sediment within and on the surface of a high Arctic valley glacier: Marthabreen, Svalbard. *Earth Surface Processes and Landforms. 24*, 303-318.

Glasser, N.F., and Ghiglione, M., C. (2009). Structural, tectonic and glaciological controls on the evolution of fjord landscapes. *Geomorphology*, Volume 105, Issues 3–4, ISSN 0169-555X, https://doi.org/10.1016/j.geomorph.2008.10.007.

Glasser, N.J., Hambrey, M.J., Etienne, J.L., Jansson, P., Pettersson, R. (2003). The origin and significance of debris-charged ridges at the surface of Storglaciären, northern Sweden. *Geography Annaler*, 85, 127–147.

Glasser, N.F., Jansson, K., Mitchell, W.A., Harrison, S. (2006). The geomorphology and sedimentology of the 'Témpanos' moraine at Laguna San Rafael, Chile. *Journal of Quaternary Science: Published for the Quaternary Research Association*, *21*, 629-643.

Glasser, N.F. and Scambos, T.A. (2008). A structural glaciological analysis of the 2002 Larsen B ice-shelf collapse. *Journal of Glaciology*, 54, 3-16.

Glen, J. W. (1995). The creep of polycrystalline ice. *Proceedings of the Royal Society A- London*, 228, 519-538, 1955.

Goodsell, B., Hambrey, M.J., and Glasser, N.F. (2002). Formation of band ogives and associated structures at Bas Glacier d'Arolla, Valais, Switzerland. *Journal of Glaciology*, 48, 287-300.

Goodsell, B., Hambrey, M.J., Glasser, N.F., Nienow, P., Mair, D. (2005). The structural glaciology of a temperate valley glacier: Haut Glacier d'Arolla, Valais Switzerland. *Arctic, Antarctic and Alpine Research*, 37, 218-232.

Gordon, J. E., and Sharp, M. (1983). Lichenometry in dating recent glacial landforms and deposits, southeast Iceland. *Boreas*, 12, 191–200. doi:10.1111/j.1502-3885.1983. tb00312.x.

Graham, D.J., Bennett, M.R., Glasser, N.F., Hambrey, M.J., Huddart, D., Midgley, N.G. (2007). Comment: a test of the englacial thrusting hypothesis of; hummocky'moraine formation. *Boreas*, *36*, 103-107.

Graham, D.J. and Midgley, N.G. (2000). Graphical representation of particle shape using triangular diagrams: an Excel spreadsheet method. *Earth Surface Processes and Landforms*, *25*, 1473-1477.

Gudmundsson, H. J. (1998). Holocene glacier fluctuations and tephrochronology of the Öraefi district, Iceland. (Unpublished PhD thesis). University of Edinburgh.

Guðmundsson, S. and Evans, D.J.A (2022). Geomorphological map of Breiðamerkursandur 2018: the historical evolution of an active temperate glacier foreland. Geografiska Annaler: Series A, Physical Geography, 104, 298-332.

Guðmundsson, S., Björnsson, H., Pálsson, F., Magnússon, E., Sæmundsson, Þ. and Jóhannesson, T. (2019). Terminus lakes on the south side of Vatnajökull ice cap, SE-Iceland. Jökull, 69, 1-34.

Hallet, B., Hunter, L., and Bogen, J. (1996). Rates of erosion and sediment evacuation by glaciers: a review of field data and their implications. *Global and Planetary Change,* 12, 213–235.

Hambrey, M.J. (1977). Foliation, minor folds and strain in glacier ice. *Tectonophysics,* 391–3, 397–416.

Hambrey, M.J., Bennett, M.R., Dowdeswell, J.A., Glasser, N.F., Huddart, D. (1999). Debris entrainment and transfer in polythermal valley glaciers. *Journal of Glaciology* 45, 69–86.

Hambrey, M.J., Dowdeswell, J.A., Murray, T., Porter, P.R. (1996). Thrusting and debris-entrainment in a surging glacier, Bakaninbreen, Svalbard. *Annals of Glaciology* 22, 241–248.

Hambrey, M.J., and Glasser, N.F. (2012). Discriminating glacier thermal and dynamic regimes in the sedimentary record. *Sediment Geology*, 251-252, 1-33.

Hambrey, M. J., Huddart, D., Bennet, R., Glasser, N., F. (1997). Gcnesis of "humocky moraines" by thrusting in glacier ice: evidence from Svalbard and Britain. *The Geological Society of London,* 153,623 632.

Hambrey, M.J., and Lawson, W.J. (2000). Structural styles and deformation fields in glaciers: a review. In: Maltman, A.J., Hubbard, B., Hambrey, M.J. (Eds.), Deformation of Glacial Materials: *Geological Society Special Publication*, 176, 59-83.

Hambrey, M.J., and Milnes, A.G. (1977). Structural geology of an Alpine glacier (Griesgletcher, Valais, Switzerland). *Swiss Journal of Geoscience*, 70, 667-684.

Hambrey, M.J., Milnes, A., and Siegenthaler, H. (1980). Dynamics and structure of Griesgletscher, Switzerland, *Journal of Glaciology*, 25, 215–228.

Hambrey, M.J., and Müller, F. (1978). Structures and ice deformation in the White Glacier, Axel Heiberg Island, Northwest Territories, Canada. *Journal of Glaciology,* 20, 41–66.

Hambrey, M. J., Murray, T., Glasser, N. F., Hubbard, A., Hubbard, B., Stuart, G., Hansen, S., Kohler, J. (2005). Structure and changing dynamics of a polythermal valley glacier on a centennial timescale: Midre Lovenbreen, Svalbard. *Journal of Geophysical Research*, 110, F01006, doi:10.1029/2004JF000128.

Hannesdóttir, H., Björnsson, H., Pálsson, F., Aðalgeirsdóttir, G., Guðmundsson, S. (2015a). Variations of southeast Vatnajökull ice cap (Iceland) 1650–1900 and reconstruction of the glacier surface geometry at the little Ice Age maximum. *Geografiska Annaler:* Series A, Physical Geography, 97, 237–264.

Hannesdóttir, H., Björnsson, H., Pálsson, F., Aðalgeirsdóttir, G., Guðmundsson, S. (2015b). Changes in the southeast Vatnajökull ice cap, Iceland, between ∼1890 and 2010. *The Cryosphere*, 9, 565–585.

Hart, J. K., Rose, K. C. and Martinez, K. (2011). Subglacial till behaviour derived from in situ wireless multi-sensor subglacial probes: rheology, hydro-mechanical interactions and till formation. *Quaternary Science Reviews,* 30, 234–247.

Herbst, P., Neubauer, F., and Schopfer, M.P.J. (2006). The development of brittle structures in an alpine valley glacier: Pasterzenkees, Austria, 1887-1997. *Journal of Glaciology*, 52, 128-136.

Herzfeld, U., Clarke, G., Mayer, H., and Greve, R. (2004). Derivation of deformation characteristics in fast moving glaciers. *Computer Geoscicience*, 30,291–302.

Herzfeld, U., and Zahner, O. (2001). A connectionist-geostatistical approach to automated image classification, applied to the analysis of crevasse patterns in surging ice. *Computer Geoscience*, 21, 499–512.

Hodgson, D.A., Vincent, J.S., and Fyles, J.G. (1984). Quaternary geology of central Melville Island, Northwest Territories. In: Geological Survey of Canada, 83-16.

Hooke, R.L. (1973). Structure and flow in the margin of the Barnes Ice Cap, Baffin Island, NWT, Canada. *Journal of Glaciology*, *12*, 423-438.

Hooke, R.L. (2019). Principles of glacier mechanics. Cambridge university press.

Hooke, R., and Hudleston, P. (1978). Origin of Foliation in Glaciers. *Journal of Glaciology, 20*, 285-299. doi:10.3189/S0022143000013848.

Hubbard, B., Cook, S., and Coulson, H. (2009). Basal ice facies: a review and unifying approach. *Quaternary Science Reviews*, 28, 1956-1969.

Hubbard, B., Glasser, N., Hambrey, M., Etienne, J. (2004). A sedimentological and isotopic study of the origin of supraglacial debris bands: kongsfjorden, Svalbard. *Journal of Glaciology*, 50, 157-170.

Hubbard, B., and Sharp, M.J. (1989). Basal ice formation and deformation: a review. *Physical Geography*, 13, 529-558.

Hubbard, B., and Sharp, M.J. (1993). Weertman regelation, multiple refreezing events and the isotopic evolution of the basal ice layer. *Journal of Glaciology,* 39, 275-291.

Hudleston, P.J. (1976). Recumbent folding in the base of the Barnes ice cap, Baffin Island, northwest Territories, Canada. *Geological Society of America Bulletin*, *87*, 1684-1692.

Hudleston, P. J. (1989). The association of folds and veins in shear zones. *Journal of Structural Geology*. 11, 949-957.

Hudleston P.J. (2015). Structures and fabrics in glacial ice: a review. *Journal of Structural Geology* 81, 1–27.

Huddleston, P.J., and Hooke, R. L. (1980). Cumulative deformation in the Barnes Ice Cap and implications for the development of foliation, *Tectonophysics*, 66, 127–146.

Jennings, S.J. and Hambrey, M.J. (2021). Structures and deformation in glaciers and ice sheets. *Reviews of Geophysics*, *59*.

Jennings, S.J.A., Hambrey, M.J., and Glasser, N.F. (2013). Ice flow-unit influence on glacier structure, debris entrainment and transport. *Earth Surface Processes and Landforms,* 39.10, 1279-1292.

Jennings, S.J., Hambrey, M.J., and Glasser, N.F. (2014). Ice flow-unit influence on glacier structure, debris entrainment and transport. *Earth Surface Processes and Landforms*, 39, 1279-1292.

Jennings, S.J.A., Hambrey, M.J., Moorman, B.J., Holt, T.O., Glasser, N.F. (2022). Upscaling ground-based structural glaciological investigations via satellite remote sensing to larger-scale ice masses: Bylot Island, Canadian Arctic. *Earth Surface Processes and Landforms*, 1–21. https://doi.org/10.1002/esp.5367.

Johannesson, T., Björnsson, H., Magnusson, E., Guðmundsson, S., Palsson, F., Sigurðsson, O., Thorsteinsson, T. and Berthier, E. (2013). Ice-volume changes, bias estimation of mass-balance measurements and changes in subglacial lakes derived by lidar mapping of the surface of Icelandic glaciers. Annals of Glaciology, 54, 63-74.

Jóhannesson, T. and Sigurðsson, O. (1998). Interpretation of glacier variations in Iceland 1930-1995. *Jökull*, 45, 27-33.

Jónsson, S. A., Schomacker, A., Benediktsson, Í. Ö., Ingólfsson, Ó., and Johnson, M. D. (2014). The drumlin field and the geomorphology of the Múlajökull surge-type glacier, central Iceland. *Geomorphology*, 207, 213–220. doi:10.1016/j. geomorph.2013.11.007.

Kellerer-pirklbauer, A., Lieb, G.K., Avian, M., and Gspurning, J. (2008). The response of partially debris-covered valley glaciers to climate change: the example of the Pasterze Glacier (Austria) in the period 1964 to 2006. *Geografiska Annaler: Series A, Physical Geography*, *90*, 269-285.

Kirkbride, M. P. (2000). Ice marginal geomorphology and Holocene expansion of debris-covered Tas- man Glacier, New Zealand, In Nakawo, M., Raymond, C. And A. Fountain, A., (eds.) Debris- Covered Glaciers, *IAHS Publication* 264, 211–217.

Kirkbride, M.P. and Warren, C.R. (1999). Tasman Glacier, New Zealand: 20th-century thinning and predicted calving retreat. *Global and Planetary Change*, *22*, 11-28.

Kjær, K.H., and Krüger, J. (2001). The final phase of dead-ice moraine development: processes and sediment architecture, Kotlujokull. Iceland. *Sedimentology* 48, 935–952.

Kleman, J. and Stroeven, A.P. (1997). Preglacial surface remnants and Quaternary glacial regimes in northwestern Sweden. Geomorphology, 19, 35-54.

Knight, P.G. (1987). Observations at the edge of the Greenland ice sheet: Boundary condition implications for modellers. In: Symposium at Vancouver 1987-The Physical Basis of Ice Sheet Modelling. *IAHS Publications*, 170, 359-366.

Knight, P.G. (1994). Two-facies interpretation of the basal layer of the Greenland ice sheet contributes to a unified model of basal ice formation. *Geology,* 22, 971-974.

Knight, P.G. (1997). The basal ice layer of glaciers and ice sheets. *Quaternary Science Reviews*, 16, 975-993.

Knight, P.G. and Knight, D.A. (2005). Laboratory observations of debris-bearing ice facies frozen from supercooled water. *Journal of Glaciology*, *51*, 337-339.

Knight, P.G., Sugden, D.E., and Minty, C.D. (1994). Ice flow around large obstacles as indicated by basal ice exposed at the margin of the Greenland ice sheet. *Journal of Glaciology*, *40*, 359-367.

Krüger, J. (1979). Structures and textures in till indicating subglacial deposition. *Boreas*, *8*(3), 323-340.

Krüger, J. (1987). The development of a glacial landscape on the northern edge of Myrdalsjökull, Iceland. *Danish Geological Society*, 1986, 49–65.

Krüger, J. (1994). Glacial processes, sediments, landforms and stratigraphy in the terminus region of Myrdalsjokull, Iceland. *Folia Geographica Danica,* 21, 1–233.

Krüger, J. (1995). Origin, chronology and climatological significance of annual-moraine ridges at Myrdalsjökull, Iceland. *The Holocene*, 5,420–427. doi: 10.1177/095968369500500404.

Larsen, N.K., Piotrowski, J.A. and Kronborg, C. (2004). A multiproxy study of a basal till: a time-transgressive accretion and deformation hypothesis. *Journal of Quaternary Science: Published for the Quaternary Research Association*, *19*, 9-21.

Larson, G.J., Lawson, D.E., Evenson, E.B., Alley, R.B., Knudsen, Ó., Lachniet, M.S., Goetz, S.L. (2006). Glaciohydraulic supercooling in former ice sheets? *Geomorphology*, *75*, 20-32.

Larson, G.J., Lawson, D.E., Evenson, E.B., Knudsen, O., Alley, R.B., Phanikumar, M.S. (2010). Origin of stratified basal ice in outlet glaciers of Vatnajokull and Oræfajokull. *Boreas* 39, 459-470.

Lawson, D.E. (1979). Sedimentological Analysis of the Western Terminus Region of the Matanuska Glacier, Alaska. *Cold Regions Research and Engineering Laboratory*, Report 79-9, 6-27.

Lawson, D.E., Strasser, J.C., Evenson, E.B., Alley, R.B., Larson, G.J., Arcone, S.A. (1998). Glaciohydraulic supercooling: a freeze-on mechanism to create stratified, debris-rich basal ice: I. Field evidence. *Journal of Glaciology*, 44, 547-562.

Lawson, W. (1996). Structural evolution of variegated Glacier, Alaska, USA, since 1948. *Journal of Glaciology*, 42, 261–270.

Lawson, W., Sharp, M.J., and Hambrey, M.J. (1994). The structural glaciology of a surge-type glacier. *Journal of Structural Geology*, 16, 1447–1462.

Lovell, H., Fleming, E.J., Benn, D.I., Hubbard, B., Lukas, S., Rea, B.R., Noormets, R., Flink, A.E. (2015). Debris entrainment and landform genesis during tidewater glacier surges. *Journal of Geophysical Research: Earth Surface*, *120*, 1574-1595.

Lukas, S. (2005). A test of the englacial thrusting hypothesis of 'hummocky'moraine formation: case studies from the northwest Highlands, Scotland. *Boreas*, *34*, 287-307.

Lukas, S. (2007). 'A test of the englacial thrusting hypothesis of "hummocky" moraine formation: case studies from the northwest Highlands, Scotland': Reply to comments. *Boreas*, *36*(1),108-113.

Lukas, S. (2012). Processes of annual moraine formation at a temperate alpine valley glacier: insights into glacier dynamics and climatic controls. *Boreas* 41, 463–480.

Lukas, S. and Benn, D.I. (2006). Retreat dynamics of Younger Dryas glaciers in the far NW Scottish Highlands reconstructed from moraine sequences. *Scottish Geographical Journal*, *122*, 308-325.

Lukas, S., Benn, D. I., Boston, C.,I., Brook, M., S., Coray, S., Evans, D.J.A., Graf, A., Kellerer-Pirklbauer-Eulenstein, A., Kirkbride, M.P., Krabbendam, K., Lovell, H., Machiedo, M., Mills, S., C., Nye, K., Reinardy, B.T.I., Ross, F.H., Signer, M. (2013). Clast shape analysis and clast transport paths in glacial environments: a critical review of methods and the role of lithology. *Earth-Science Review*., 121, 96-116.

Lukas, S., and Lukas, T. (2006). A glacial geological and geomorphological map of the far NW highlands, Scotland. Part 1. *Journal of Maps*, 2, 43–55. doi:10.4113/jom.2006.50.

Lukas, S., Spencer, J.Q., Robinson, R.A., Benn, D.I. (2007). Problems associated with luminescence dating of Late Quaternary glacial sediments in the NW Scottish Highlands. *Quaternary Geochronology*, *2*, 243-248.

Magnússon, E., Pálsson, F., Björnsson, H., Guðmundsson, S. (2012). Removing the ice cap of Öræfajökull central volcano, SE-Iceland: Mapping and interpretation of bedrock topography, ice volumes, subglacial troughs and implications for hazards assessments. *Jökull*, 62, 131-150.

Maltman, A.J., Hubbard, B., and Hambrey, M.J. (2000). Deformation of Glacial Materials: *Geological Society, London, Special Publications,* 176.

Marren, P. M. (2002). Glacier margin fluctuations, Skaftafellsjökull, Iceland: Implications for sandur evolution. *Boreas*, 31, 75–81.

Matthews, J.A. (1987). Regional variation in the composition of Neoglacial end moraines, Jotunheimen, Norway: an altitudinal gradient in clast roundness and its possible palaeoclimatic significance. *Boreas.* 16, 173–188.

Matthews, J.A., and Petch, J.R. (1982). Within-valley asymmetry and related problems of Neoglacial lateral moraine development at certain Jotunheimen glaciers, southern Norway. *Boreas.* 11, 225–247.

Matti, S. and Ögmundardóttir, H. (2021). Local knowledge of emerging hazards: Instability above an Icelandic glacier. International Journal of Disaster Risk Reduction, 58, 102-187.

Meier, M. F., Conel, J. E., Hoerni, J. A., Melbourne, W. G., Pings, C. J., Walker, P. T. (1960). Preliminary study of crevasse formation, blue ice valley, Greenland*, in SPIRE* Rep. 28, 1957.

Meier, M.F., Lundstrom, S., Stone, D., Kamb, B., Engelhardt, H., Humphrey, N., Dunlap, W.W., Fahnestock, M., Krimmel, R.M., Waters, R. (1994). Mechanical and hydrological basis for rapid motion of a large tidewater glacier. *Journal of Geophysics*, 99(B9): 15,219-15,229.

Mills, S.C., Grab, S.W., and Carr, S.J., 2009. Recognition and palaeoclimatic implications of late Quaternary niche glaciation in eastern Lesotho. *Journal of Quaternary Science: Published for the Quaternary Research Association*, *24*, 647-663.

Monz, M.E., Hudleston, P.J., Cook, S.J., Zimmerman, T., Leng, M.J. (2022). Thrust faulting in glaciers. Re-examination of debris bands near the margin of Storglaciären, Sweden. *Boreas*, *51*, 78-99.

Moore, P.L., Iverson, N.R., and Cohen, D. (2010). Conditions for thrust faulting in a glacier. *Journal of Geophysics*, 115.

Mottram, R.H. and D.I. Benn. (2009). Testing crevasse-depth models: a field study at Breiðamerkurjokull, Iceland. *Journal of Glaciology*. 55, 746–752.

Nye, J. F. (1953). The flow law of ice from measurements in glacier tunnels, laboratory experiments, and the Jungfraufirn borehole experiment. *Proceedings of the Royal Society of London*, 1, 219, 477-489.

Nye, J. F. (1957). The distribution of stress and velocity in glaciers and ice-sheets. *Proceedings of the Royal Society of London*, Vol. 239, 113-33.

Nye, J. F. (1967). Plasticity solution for a glacier snout. *Journal of Glaciology*, 6, 695-715.

Owen, L. A. and Derbyshire, E. (1989). The Karakoram glacial depositional system. *Journal of Geomorphology*, 76, 33–73.

Pearce, D., Rea, B. R., Bradwell, T., McDougall, D. (2014). Glacial geomorphology of the Tweedsmuir Hills, Central Southern Uplands, Scotland. *Journal of Maps*, 10, 457–465. doi:10.1080/17445647.2014.886492

Petricca, P., Carminati,E., Doglioni, C., Riguzzi, F. (2018). Brittle-ductile transition depth versus convergence rate in shallow crustal thrust faults: Considerations on seismogenic volume and impact on seismicity. *Physical Earth Planet Interiors*, 284, 72-81, 10.1016/j.pepi.2018.09.002

Phillips, E., Everest, J., Evans, D.J.A., Finlayson, A., Ewertowski, M., Guild, A., Jones, L. (2017). Concentrated, 'pulsed' axial glacier flow: structural glaciological evidence from Kviárjökull in SE Iceland. *Earth Surface Processes and Landforms*. DOI: 10.1002/esp.4145.

Phillips, E., Finlayson, A., Bradwell, T., Everest, J., Jones, L. (2014). Structural evolution triggers a dynamic reduction in active glacier length during rapid retreat: Evidence from Falljökull, SE Iceland, *Journal of Geophysical Research: Earth Sciences*, 119, doi:10.1002/2014JF003165.

Phillips, E., Finlayson, A., Jones, L. (2013). Fracturing, block faulting, and moulin development associated with progressive collapse and retreat of a maritime glacier: Falljökull, SE Iceland. *Journal of Geophysical Research: Earth Surface*, Vol. 118, 1–17.

Powers, M. C. (1953). A new roundness scale for sedimentary particles*. Journal of Sediment Research*, 10.1306/D4269567-2B26-11D7-8648000102C1865D, 117–119.

Price, R.J. (1969). Moraines, sandar, kames and eskers near Breidamerkurjökull, Iceland. Transactions of the Institute of British Geographers, 17-43.

Price, R. J. (1970). Moraines at Fjallsjökull, Iceland. *Arctic and Alpine Research*, 2, 27–42.

Pritchard, H. D., and Vaughan, D. G. (2007). Widespread acceleration of tidewater glaciers on the Antarctic Peninsula. *Journal of Geophysics Research*, 112, F03S29, doi:10.1029/2006JF000597.

Ramsay, J.G. (1963). Structural investigations in the Barberton Mountain Land, eastern Transvaal. *Geological Society.* 66, 353-398.

Reinardy, B. T. I., Leighton, I., and Marx, P. J. (2013). Glacier thermal regime linked to processes of annual moraine formation at Midtdalsbreen, southern Norway. *Boreas*, 42, 896–911. doi:10.1111/bor.12008.

Reznichenko, N.V., Davies, T.R. and Winkler, S. (2016). Revised palaeoclimatic significance of Mueller Glacier moraines, Southern Alps, New Zealand. Earth Surface Processes and Landforms, 41, 196-207.

Roberson, S. (2008). Structural composition and sediment transfer in a composite cirque glacier: Glacier de St. Sorlin, France. *Earth Surface Processes and Landforms,* 33, 1931–1947.

Roberts, D.H., Yde, J.C., Knudsen, N.T., Long, A.J., Lloyd, J.M. (2009). Ice marginal dynamics during surge activity, Kuannersuit Glacier, Disko Island, West Greenland. *Quaternary Science Reviews*, *28*. 209-222.

Roberts, M.J., Russell, A.J., Tweed, F.S. and Knudsen, Ó. (2000). Ice fracturing during jökulhlaups: implications for englacial floodwater routing and outlet development. *Earth surface processes and landforms*, *25*, 1429-1446.

Roberts, M.J., Tweed, F.S., Russell, A.J., Knudsen, O., Lawson, D.E., Larson, G.J., Evenson, E.B., Björnsson, H. (2002). Glaciohydraulic supercooling in Iceland. *Geology* 30, 439–442.

Rutter, N.W. (1965). Foliation pattern of Gulkana Glacier, Alaska Range, Alaska. *Journal of Glaciology*, *5*, 711-718.

Salt, K.E., and Ballantyne, C.K. (1997). The structure and sedimentology of relict talus, Knockan, Assynt. *Scottish Geographical Magazine,* 113, 82–89.

Scambos, T.A., Bohlander, J.A., Shuman, C.A., Skvarca, P. (2004). Glacier acceleration and thinning after ice shelf collapse in the Larsen B embayment, Antarctica. *Geophysical Research Letters,* 31(18), L18402. 10.1029/2004GL020670.

Schomacker, A. and Kjær, K.H. (2008). Quantification of dead-ice melting in ice-cored moraines at the high-Arctic glacier Holmströmbreen, Svalbard. Boreas, 37, 211-225.

Schomacker, A., Benediktsson, Í. Ö. and Ingólfsson, Ó. (2014). The Eyjabakkajökull glacial landsystem, Iceland: Geomorphic impact of multiple surges. *Journal of Geomorphology*, 218, 98–107.

Shakesby, R.A. (1989). Variability in neoglacial moraine morphology and composition, Sortbreen, Jotunheimen, Norway: within-moraine patterns and their implications. *Geografiska Annaler,* 71, 17–29

Sharp, M. (1982). Modification of clasts in lodgement tills by glacial erosion. *Journal of Glaciology* 28, 475–481.

Sharp, M. (1984). Annual moraine ridges at Skálafellsjökull, southeast Iceland. *Journal of Glaciology* 30, 82–93.

Sharp, M. (1988). Surging glaciers – behaviour and mechanisms. *Progress in Physical Geography* 12, 349–370.

Sharp, M., Lawson, W. and Anderson, W. (1988). Tectonic processes 468 in a surge type glacier. *Journal of Glaciology*, 40, 327-340.

Sharp, M.J., Jouzel, J., Hubbard, B., and Lawson, W. (1994). The character, structure and origin of the basal ice layer of a surge-type glacier. *Journal of Glaciology,* 40, 327-340.

Shaw, J. (1977b). Sedimentation in an alpine lake during deglaciation, Okanagan Valley, British Columbia, Canada. *Geografiska Annaler: Series A, Physical Geography*, *59*, 221-240.

Shaw, J. (1977a). Till body morphology and structure related to glacier flow. *Boreas*, *6*, 189-201.

Sigurðsson, O. (1998). Glacier variations in Iceland 1930–1995: From the database of the Iceland Glaciological Society. *Jökull*, 45, 3–25.

Sigurðsson, O., Jónsson, T. and Jóhannesson, T. (2007). Relation between glacier-termini variations and summer temperatures in Iceland since 1930. *Annals of Glaciology*, 42, 395-401.

Small, R.J. (1983). Lateral moraines of Glacier de Tsidjiore Nouve: form, development and implications. *Journal of Glaciology,* 29, 250–259.

Sneed, E.D., and Folk, R.L. (1958). Pebbles in the lower Colorado River, Texas, a study in particle morphogenesis. *Journal of Geology*, 66, 114–150.

Spedding, N. (1997). On growth and form in geomorphology. Earth Surface Processes and Landforms: The Journal of the British Geomorphological Group, 22, 261-265.

Spedding, N., and Evans, D.J.A. (2002). Sediments and landforms at Kvıarjökull, southeast Iceland: A reappraisal of the glaciated valley landsystem. *Sedimentary Geology,* 149, 21–42.

Sugden, D.E., Marchant, D.R., Lorrain, R., Tison, J.L., Jouzel, J. (1987). Evidence for two zones of debris entrainment beneath the Greenland ice sheet. *Nature*, 328, 238-241.

Sutherland, J.L., Carrivick, J.L., Evans, D.J., Shulmeister, J. and Quincey, D.J. (2019). The Tekapo Glacier, New Zealand, during the Last Glacial Maximum: An active temperate glacier influenced by intermittent surge activity. Geomorphology, 343, 183-210.

Swift, D.A. (2011). Basal Sediment Evacuation by Subglacial Drainage Systems. In: Singh, V.P., Singh, P., Haritashya, U.K. (eds) *Encyclopedia of Snow, Ice and Glaciers. Encyclopedia of Earth Sciences Series.* Springer, Dordrecht. https://doi.org/10.1007/978-90-481-2642-2_473.

Swift, D.A., and Cook, S.J. (2018). Glaciological processes associated with the terminal overdeepening at Svínafellsjökull. In Evans, D. (Ed.), Glacial Landsystems of Southeast Iceland: Quaternary Applications (pp. 124-136). London: Quaternary Research Association.

Swift, D.A., Cook, S.J., Graham, D.J., Midgley, N.G., Fallick, A.E., Storrar, R., Toubes Rodrigo, M., Evans, D.J.A. (2018). Terminal zone glacial sediment transfer at a temperate

overdeepened glacier system. *Quaternary Science Reviews*, Vol 180, 111-131, ISSN 0277-3791.

Swift, D.A., Evans, D.J.A., and Fallick, A.E. (2006). Transverse englacial debris-rich ice bands at Kvíárjökull, southeast Iceland. *Quaternary Science Reviews,* 25, 1708-1718.

Swift, D.A and Jones, A.H. (2018). Going against the flow: testing the hypothesis of pulsed axial glacier flow. *Earth Surface Processes and Landforms*, 43, 2754–2761.

Swift, D.A., Tallentire, G.D., Farinotti, D., Cook, S.J., Higson, W.J., Bryant, R.G. (2021). The hydrology of glacier-bed overdeepenings: sediment transport mechanics, drainage system morphology, and geomorphological implications. *Earth Surface Processes and Landforms*, *46*, 2264-2278.

Thompson, A. (1988). Historical development of the proglacial landforms of Svínafellsjökull and Skaftafellsjökull, Southeast Iceland. *Jökull*, 38, 17–30.

Thompson, A. and Jones, A. (1986). Rates and causes of proglacial river terrace formation in southeast Iceland: an application of lichenometric dating techniques. Boreas, 15, 231-246.

Thorarinsson, S. (1943). Vatnajökull, scientific results of the Swedish-Icelandic investigations 1936-37-38. Part XI oscillations of the Icelandic glaciers in the last 250 years*. Geografiska Annaler*, 25, 1–25.

Thorarinsson S. (1956). On the variations of Svinafellsjökull, Skaftafellsjökull, and Kviarjökull in Oraefi. Jökull 6, 1–15.

Tweed, F.S., Roberts, M.J., and Russell, A.J. (2005). Hydrologic monitoring of supercooled meltwater from Icelandic glaciers. *Quaternary Science Reviews*, 24(22), 2308–2318.

Waller, R.I., Russell, A.J., Van Dijk, T.A.G.P., Knudsen, O. (2001). Jökulhlaup-related ice fracture and supraglacial water release during the November 1996 jökulhlaup,Skeiðarárjökull, Iceland. *Geografiska Annaler: Series A, Physical Geography*, *83*,29-38.

Waltham, T. (2009). Foundations of Engineering Geology, Third Edition. CRC Press, London.

Weertman, J. (1961). Mechanism for the formation of inner moraines found near the edge of cold ice caps and ice sheets. *Journal of Glaciology*, 3, 965-978

Welling, J. and Abegg, B. (2021). Following the ice: Adaptation processes of glacier tour operators in Southeast Iceland. International Journal of Biometeorology, 65, 703-715.

Woodward, J., Murray, T., and McCraig, A. (2002). Formation and reorientation of structure in surge-type glacier Kongsvegen, Svalbard. *Journal of Quaternary Science Reviews*, 17, 201–209.

Woodward, J., Murray, T., and McCaig, A. (2003). Reply to Glasser *et al.*, 2003. *Journal of Quaternary Science*, 18, 99-100.